POLITECHNIKA KRAKOWSKA im. T. Kościuszki
Wydział Mechaniczny
Instytut Pojazdów Samochodowych i Silników Spalinowych

Kierunek studiów: Mechanika i Budowa Maszyn
Specjalność: Silniki Spalinowe

STUDIA STACJONARNE

PRACA DYPLOMOWA

MAGISTERSKA

Michał Gałka

INTEGRATION AND ENGINEERING STUDIES OF THE UPSTREAM TRACKER DETECTOR FOR THE LHCb EXPERIMENT AT CERN

BADANIA INTEGRACYJNE I INŻYNIERSKIE DETEKTORA UPSTREAM TRACKER DLA EKSPERYMENTU LHCb W CERN

Promotor:
Dr inż. **Ryszard Kantor**

Kraków, rok akad. 2018/2019

Autor pracy: **Michał Gałka**

Nr pracy: **……………………………………………**

OŚWIADCZENIE O SAMODZIELNYM WYKONANIU PRACY DYPLOMOWEJ

Oświadczam, że przedkładana przeze mnie praca dyplomowa magisterska/~~inżynierska~~* została napisana przeze mnie samodzielnie. Jednocześnie oświadczam, że ww. praca:

1) nie narusza praw autorskich w rozumieniu ustawy z dnia 4 lutego 1994 r. o prawie autorskim i prawach pokrewnych (Dz.U. z 2006 r. Nr 90, poz. 631 z późn. zm.) oraz dóbr osobistych chronionych prawem cywilnym, a także nie zawiera danych i informacji, które uzyskałem/~~am~~* w sposób niedozwolony,

2) nie była wcześniej podstawą żadnej innej procedury związanej z nadawaniem tytułów zawodowych, stopni lub tytułów naukowych.

Jednocześnie przyjmuję do wiadomości, że w przypadku stwierdzenia popełnienia przeze mnie czynu polegającego na przypisaniu sobie autorstwa istotnego fragmentu lub innych elementów cudzej pracy, lub ustalenia naukowego, właściwy organ stwierdzi nieważność postępowania w sprawie nadania mi tytułu zawodowego (art. 193 ustawy z dnia 27 lipca 2005 r. Prawo o szkolnictwie wyższym, Dz.U. z 2012 r. poz. 572, z późn. zm.).

………………………………
data i podpis

* niepotrzebne skreślić

Uzgodniona ocena pracy: ……………………………………………………………..

....
podpis promotora

....
podpis recenzenta

Acknowledgments

Many thanks to Burkhard Schmidt, who kindly selected me for a CERN contract at a very beginning and made my CERN adventure possible. I thank him for guiding me through my first steps at CERN.

Great thanks to Joao Carlos Batista Lopes, who helped me to stay at CERN even longer. I thank him for his exceptional support.

Finally, I would like to thank Ryszard Kantor from the Cracow University of Technology very much, for arranging all formalities related to my contracts at CERN, as well as, for promotion of this master thesis.

I would like to write separate acknowledgments to my beloved girlfriend – Paulina Jordan, who always believed in me and supported me greatly through all these years at CERN.

TABLE OF CONTENT

1. **Purpose and scope of thesis**

The purpose of this thesis is to describe complex and challenging integration studies performed at CERN, in order to design the Upstream Tracker detector for LHCb experiment.

This thesis has been divided for 3 main chapters.

First chapter is a brief introduction about what is CERN (its mission and experiments), the LHC project , what LHCb experiment is looking for, and what are its sub-detectors.

Second chapter is focused on detailed description of Upstream Tracker detector (UT) and several key components, of which it consists. This chapter will describe the requirements and constraints which are the basis for the design and integration.

Third chapter focuses on prototype construction details, which is built in order to check the integration of UT critical areas. With information why we need a mock-up and description what we learned from building it, this will be the last main chapter of thesis.

The issues encountered during integration and engineering studies will be summarized in thesis conclusions.

Scope of thesis, in which the author was directly involved, includes:

- Thesis author responsibilities at CERN was integration work, based on parts designed by large interdisciplinary collaboration. Thesis author, was person involved in the integration of different solutions and was responsible for preparing large assemblies consisted from various components. Thesis author, integrated several UT detector areas, like: integration inside UT detector box (in the initial phase) (Chapter 3.5.4), peripheral electronics (PEPI) mechanics and integration (Chapter 3.7), service bays crate (SBC) mechanics and integration (Chapter 3.9.1), service bays rack (SBR) mechanics and integration (Chapter 3.9.2).
- An important task, in thesis author responsibilities at CERN, was to design mechanical elements supporting electronics, for example: DCB cooling interface or LVR heat sink.
- Moreover, thesis author was involved in prototype construction of the UT detector critical areas. In this matter, thesis author responsibilities, was to prepare elements adapted to 3D printing, and to perform 3D printing using FDM 3D printer. Some of this work is described and illustrated in Chapter 4, for example page 99. Additionally, thesis author had to design mechanical support for pathfinder test (Chapter 4.2.1).
- The author of this thesis performed several analytical calculations, as well as several FEM analyzes of the designed elements and structures, in order to estimate their usefulness and strength. For example: stave support thermal contraction/expansion (Chapter 3.5.4.2), water pipe clamp assessment (Chapter 3.7.6.8), heat pipe clamp assessment (Chapter 3.7.6.8) and service bays rack assessment (Chapter 3.9.2.5).

In addition, at the end of this thesis, an Appendix containing several production drawings of Upstream Tracker detector components, prepared by thesis author, will be presented.

2. **Introduction**

CERN is the European Council for Nuclear Research. Its acronym comes from French name of the organization *Conseil Européen pour la Recherche Nucléaire*. It was founded in Paris in December 1951. From the beginning CERN laboratory was planned as an international collaboration, where scientists from around the world can meet, work, exchange ideas and make great strides in fundamental research and stretch the limits of our technology and imagination. Today, our understanding of matter goes much deeper than the nucleus, and CERN's main area of research is particle physics. Because of this, the laboratory operated by CERN is often referred to as the European Laboratory for Particle Physics [12].

2.1. CERN accelerator complex

CERN labolatory consists of several different types of accelerators, Figure 2.1.

Before being injected into largest 27 km LHC loop, particles need to be accelerated in several smaller accelerators. Starting their journey from Linear Accelerator – LINAC, which brings their energy to 50 MeV, through Proton Synchrotron (PS) with circumference of 628 meters and final particles energy of 25 GeV, followed by the Super Proton Synchrotron (SPS), which measures nearly 7 kilometers in circumference and increases particles energy to the range of 450 GeV, particles are finally being injected into LHC, where their energy is accelerated up to 7 TeV.

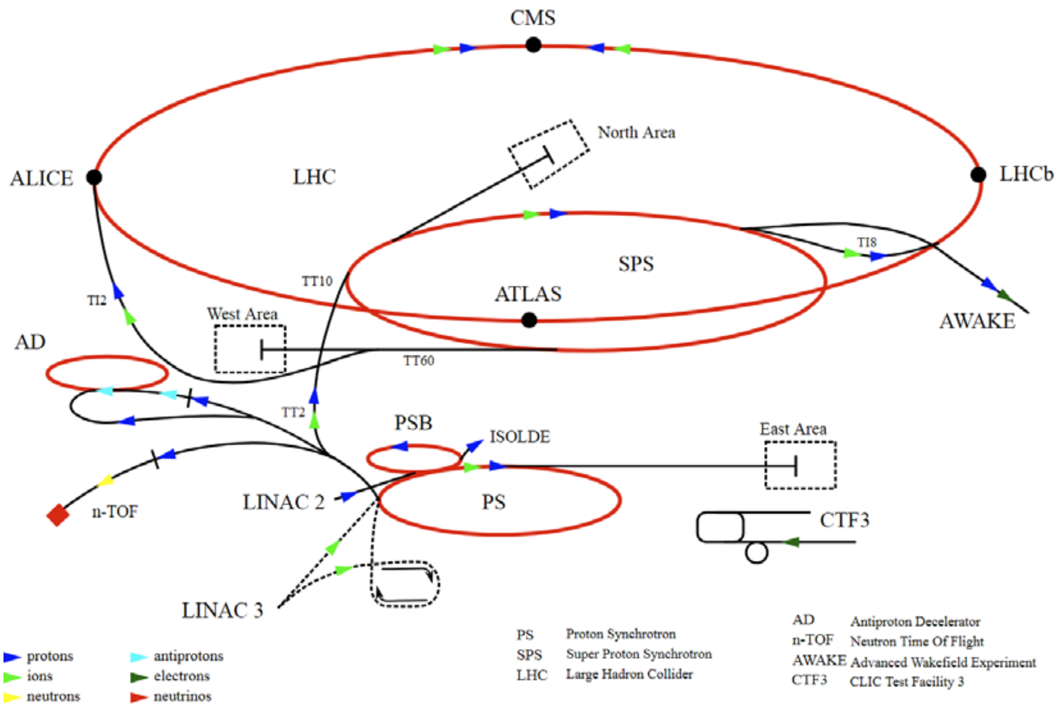

Figure 2.1 Scheme of the CERN accelerator complex [16]

Rysunek 2.1 Schemat kompleksu akceleratorów w CERN [16]

2.2. CERN LHC

LHC – (Large Hadron Collider) – is the biggest and the most powerful particle accelerator on the world. The LHC consists of a 27-kilometre ring of superconducting magnets with a number of accelerating structures to boost the energy of the particles along the way. Large Hadron Collider machinery is located in an underground tunnel, Figure 2.2.

Inside the accelerator, two high-energy particle beams travel at close to the speed of light before they are made to collide. The beams travel in opposite directions in separate beam pipes – two tubes kept at ultrahigh vacuum. They are guided around the accelerator ring by a strong, 8.7 tesla, magnetic field maintained by superconducting electromagnets. The electromagnets are built from coils of special electric cable (Niobium-titanium (Nb-Ti) wire) that operates in a superconducting state, efficiently conducting electricity without resistance or loss of energy. This requires chilling the magnets to −271.3°C (1.9 K) – a temperature colder than outer space. It is achieved by connecting much of the accelerator structure to a distribution system of liquid helium, which cools the magnets, as well as to other supply services [15]. In LHC, magnets shapes and focus the beam, while electric field is used to accelerate the particles.

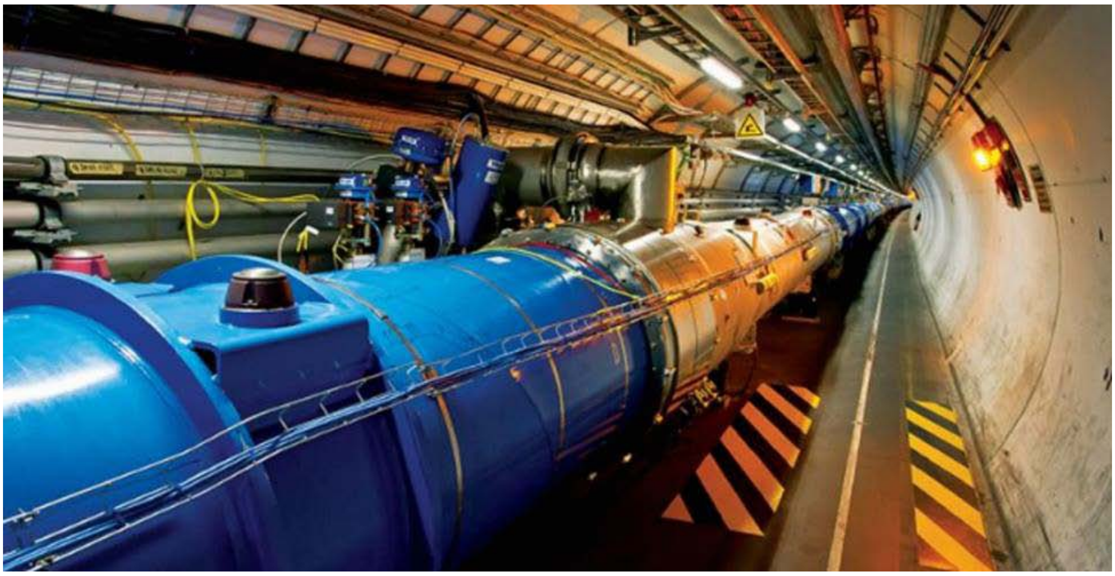

Figure 2.2 Accelerator tunnel [13]
Rysunek 2.2 Tunel akceleratora [13]

The ultra high vacuum in LHC accelerator is used for several different purposes:

1. Inside the accelerator beam pipes, in which, particle beams travel. The reason for this is to avoid particles collisions with ambient air molecules, which would make LHC operational impossible. That is why, the air needs to be pumped out and high-energy particle beams has to travel in vacuum.
2. Inside the cryo-magnets and the liquid helium distribution lines, the vacuum serves a different purpose. Here, it acts as a thermal insulator, to reduce the amount of heat that penetrates from the surrounding room-temperature environment into the cryogenic parts, which are kept at 1.9 K (–271.3°C) [15].

Figure 2.3 shows the complexity of the accelerator tube, as well as different components of which it consists.

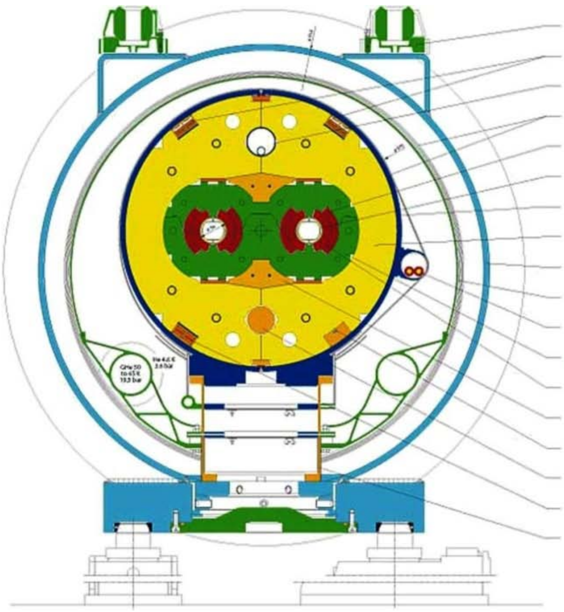

Figure 2.3 Inside the LHC [14]
Rysunek 2.3 Wewnątrz LHC [14]

2.2.1. Why LHC is located underground?

The LHC machine is located underground, in a tunnel, inherited from previous CERN experiment – LEP (Large Electron–Positron Collider). There are several reasons for burring device like this underground:

- Earth's crust provides good shielding against radiation;
- thick layer of soil provides shielding for both, surrounding environment against stray particles, as well as for accelerator itself against changing environment conditions on the surface. For example, vibrations coming from industry and people's daily life (commuting) as well as sunlight, would interfere with the precise experiments conducted at LHC, if located on surface;
- maintaining clean, reliable and temperature controlled environment, required to sustain a stable particle path, as well as uninterrupted work of a series of superconducting magnets, is much easier in an underground tunnel;
- boring a tunnel ensures its flatness. Which is not necessarily the case for the soil on surface;
- underground, the delicate and sensitive machinery of the accelerator is protected against elements;
- building such an enormous structure on the surface requires purchasing a vast piece of land, which would be very expensive and could not be used for any other purposes. CERN does not own or control most of the land under which the LHC is built.;
- building underground also prevents interference with natural landscape.

2.2.2. What is luminosity?

Luminosity – is a rate of collisions (events) inside the accelerator. In more detailed definition, luminosity is the number of collisions per square centimeter and per second cm^{-2} s^{-1}. In other words, the quantity that measures the ability of a particle accelerator to produce the required number of interactions is called the luminosity [10].

The more collisions there occurs, the more scientific data can be obtained, and new breakthroughs in particle physics can be established. Hence, LHC operators makes constant effort to increase accelerator luminosity. In 2017 the operators managed to obtain up to 60 collisions at each bunch crossing, with each bunch containing 100 billion particles.

The revolution frequency in LHC machine is 11.2 kHz. It means that beams travel around accelerator ring 11 200 times per second. Taking into account around 60 collisions per passage, we obtain about 672 000 events per second.

2.2.3. High-Luminosity LHC (HL–LHC)

The High-Luminosity Large Hadron Collider (HL-LHC) project, is an upgrade of the LHC machine, in order to increase its luminosity (rate of collisions) by a factor of ten beyond existing accelerator design value. Higher rate of collisions increase chances to observe rare events, which are of the most interest for physicists, hence the desire to increase the luminosity.

After five years of design study and R&D, this challenging project requires now about ten years of developments, prototyping, testing and implementation. Hence, operation is expected to start in the middle of the next decade. The timeline of the project is dictated by the fact that, at the beginning of the next decade, many critical components of the accelerator will reach the end of their lifetime due to radiation damage and will thus need to be replaced. The upgrade phase is therefore crucial not only for the full exploitation of the LHC physics potential, but also to enable operation of the collider beyond 2025 [11].

In order to extend its discovery potential, the upgraded LHC machine, will be equipped with several of key innovative technologies, representing exceptional technological challenges, such as cutting-edge 11–12 tesla superconducting magnets, very compact superconducting cavities for beam rotation with ultra-precise phase control, new technology for beam collimation and 300-meter-long high-power superconducting links with negligible energy dissipation [11].

2.3. CERN experiments

Inside the Large Hadron Collider loop particles travel in opposite directions and collide, in four CERN largest experiments located on the ring, with energy of 14 TeV.

Each experiment was developed in order to study different filed of particle physics.

2.3.1. ALICE

ALICE (A Large Ion Collider Experiment) – is a heavy-ion detector on the Large Hadron Collider (LHC) ring. It is designed to study the physics of strongly interacting matter at extreme energy densities, where a phase of matter called quark-gluon plasma forms. It is believed that, this state of matter have formed just after the big bang [17].

2.3.2. ATLAS

ATLAS (A Toroidal LHC ApparatuS) – is one of two general-purpose detectors at the Large Hadron Collider (LHC). It investigates a wide range of physics, from the search for the Higgs boson to extra dimensions and particles that could make up dark matter. It shares the same scientific goals as the CMS experiment, but uses different technical solutions and a different magnet-system design [18].

2.3.3. CMS

CMS (Compact Muon Solenoid) – is a general-purpose detector at the Large Hadron Collider (LHC). It has a broad physics programme ranging from studying the Standard Model (including the Higgs boson) to searching for extra dimensions and particles that could make up dark matter. Although it has the same scientific goals as the ATLAS experiment, it uses different technical solutions and a different magnet-system design [19].

2.3.4. LHCb

LHCb (Large Hadron Collider beauty) experiment – specializes in investigating the slight differences between matter and antimatter by studying a type of particle called the "beauty quark", or "b quark". It was designed in order to find an answer on a question why we live in a universe that appears to be composed almost entirely of matter, but no antimatter [20].

Unlike ATLAS and CMS detectors, which surrounds completely their interaction points, LHCb experiment uses a series of sub-detectors to detect mainly forward particles – those thrown forwards by the collision in one direction. The first sub-detector is located close to the collision point, with the others following one behind the other over a length of 20 meters, Figure 2.4 [20].

LHCb detector is 21 meters long, 10 meters high and 13 meters wide, and weights 5600 tones, it is situated 100 meters below the ground near the village of Ferney-Voltaire in France, and Geneva airport in Switzerland.

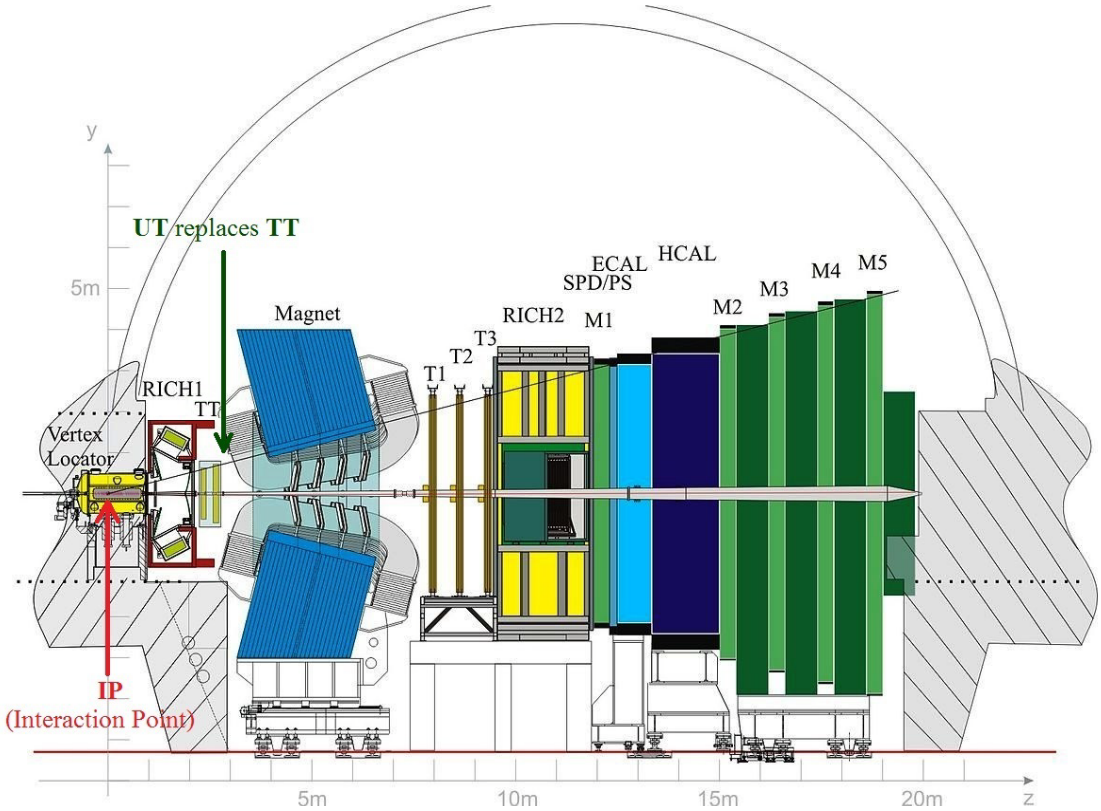

Figure 2.4 LHCb detector [21]

Rysunek 2.4 Detektor LHCb [21]

The LHCb detector consists of several separate sub-detectors situated in series along the beam line one after another, starting from interaction point (IP). Each one of them is responsible for detecting different types of particles or unique particles properties.

Starting with the Vertex Locator (VELO), a silicon strip device that surrounds the proton-proton interaction region and is positioned with its sensitive area 8 mm from the beam during collisions. It provides precise locations for primary *pp* interaction vertices, the locations of decays of long-lived particles, and contributes to the measurement of track momentum [22].

First RICH (Ring-Imaging Cherenkov) detector is located behind VELO, and a second one in front of muon station. They serves to identify charged hadrons.

When a charged particle travels faster than light does through a given medium, it emits Cherenkov radiation at an angle that depends on its velocity. The particle's velocity can be calculated from this angle. Velocity can then be combined with a measure of the particle's momentum to determine its mass, and therefore its identity [23].

Trigger Tracker (TT) detector is located between RICH1 and a 4 Tm dipole magnet. It consists of a large area silicon strip sensors and is used for tracking particles paths.

Tracking devices reveal the paths of electrically charged particles as they pass through and interact with suitable substances. Most tracking devices do not make particle tracks directly visible, but record tiny electrical signals that particles trigger as they move through the device. A computer program then reconstructs the recorded patterns of tracks [23].

A 1500 tones 4 Tm dipole magnet located in LHCb cavern provides magnetic field required to curve particles paths.

Physicists can calculate the momentum of a particle – a clue to its identity – from the curvature of its path: particles with high momentum travel in almost straight lines, whereas those with very low momentum move forward in tight spirals inside the detector [23].

Further downstream an Electromagnetic Calorimeter (ECAL) is used for photon detection and electron identification, followed by a Hadron Calorimeter (HCAL).

Calorimeters measures the energy a particle loses as it passes through. It is usually designed to stop entirely or “absorb” most of the particles coming from a collision, forcing them to deposit all of their energy within the detector [23].

Electromagnetic calorimeters measure the energy of electrons and photons as they interact with the electrically charged particles in matter. Hadronic calorimeters sample the energy of hadrons (particles containing quarks, such as protons and neutrons) as they interact with atomic nuclei. Calorimeters can stop most known particles except muons and neutrinos [23].

At the end of sub-detectors chain a MUON system is located. Described as M1–M5 in the Figure 2.4. It is an apparatus consisting of alternating layers of iron and chambers – MPWC (Multi-Wire Proportional Chambers) together with triple-GEM (Gas Electron Multiplier) sensors that distinguishes muons from hadrons.

Muons are the particles, which interacts very little with matter – they can travel through meters of dense material before they are finally stopped. For this reason, muon chambers – tracking devices specialized for detecting muons – are usually arranged as outermost layer of a detector.

2.3.4.1. LHCb upgrade for LS2

The LHCb detector is planned to be upgraded in years 2019 – 2021, during long shutdown 2 (LS2). It is necessary to improve read out rate and prepare the detector to operate with about 5 times higher luminosities. Several sub-detectors will also be upgraded, or replaced, in order to meet new requirements and implement new technologies available.

Implementing the 40 MHz read-out for the upgrade will require replacing all the front-end electronics. The VELO sensors will also have to be replaced, due to the increased radiation dose expected in the upgrade. For the RICH detectors, the vessels will be reused, but since the front-end electronics is encapsulated within the current photon detectors (HPDs) they will need to be replaced. Replacement of the silicon tracking stations is also required, since the front-end electronics is attached to the sensors [22].

One of the silicon tracking stations, which is going to be removed, is the Trigger Tracker (TT), it will be replaced by the new Upstream Tracker (UT), Figure 2.4. They both serve the same purpose, which is to reconstruct charged particle tracks with high spatial resolution. The TT was designed to withstand an integrated luminosity of approximately $10fb^{-1}$ ($1fb^{-1}$ is equal to approximately 100 trillion proton-proton collisions), which is not sufficient for the post-upgrade LHC. The new UT have been designed to withstand an integrated luminosity of at least $50fb^{-1}$ [8].

A computer generated 3D model of the LHCb detector can be seen in Figure 2.5.

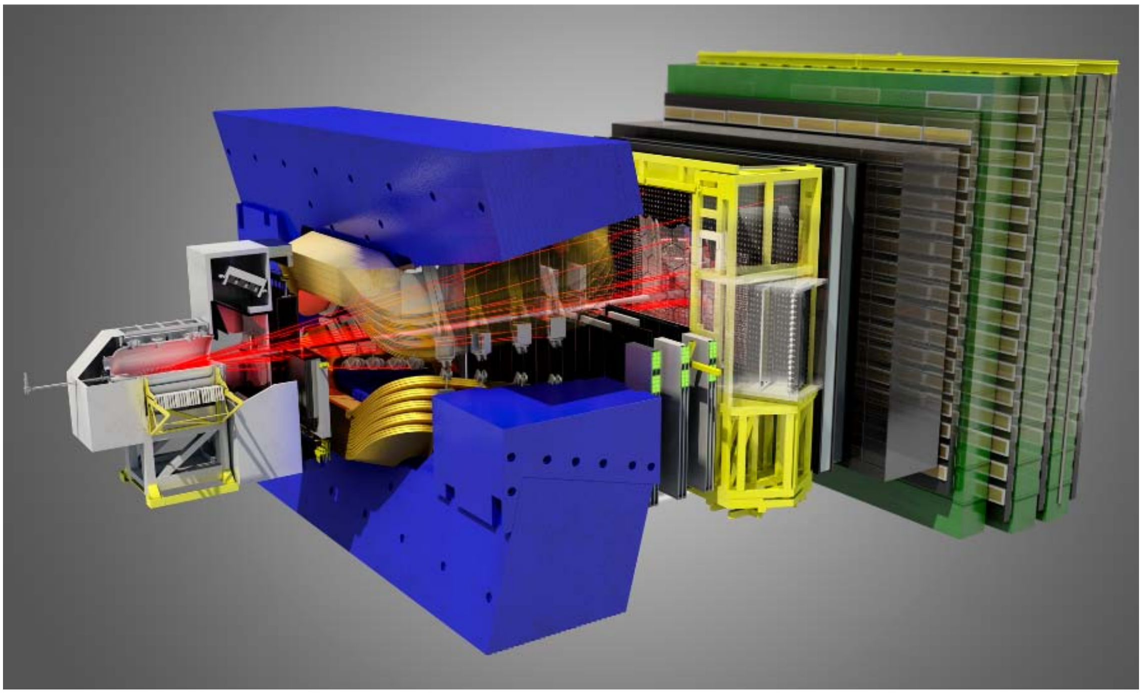

Figure 2.5 Computer generated 3D model of the LHCb detector [24]
Rysunek 2.5 Komputerowo wygenerowany model detektora LHCb [24]

A reconstruction of an actual particles collision event can be seen in Figure 2.6.

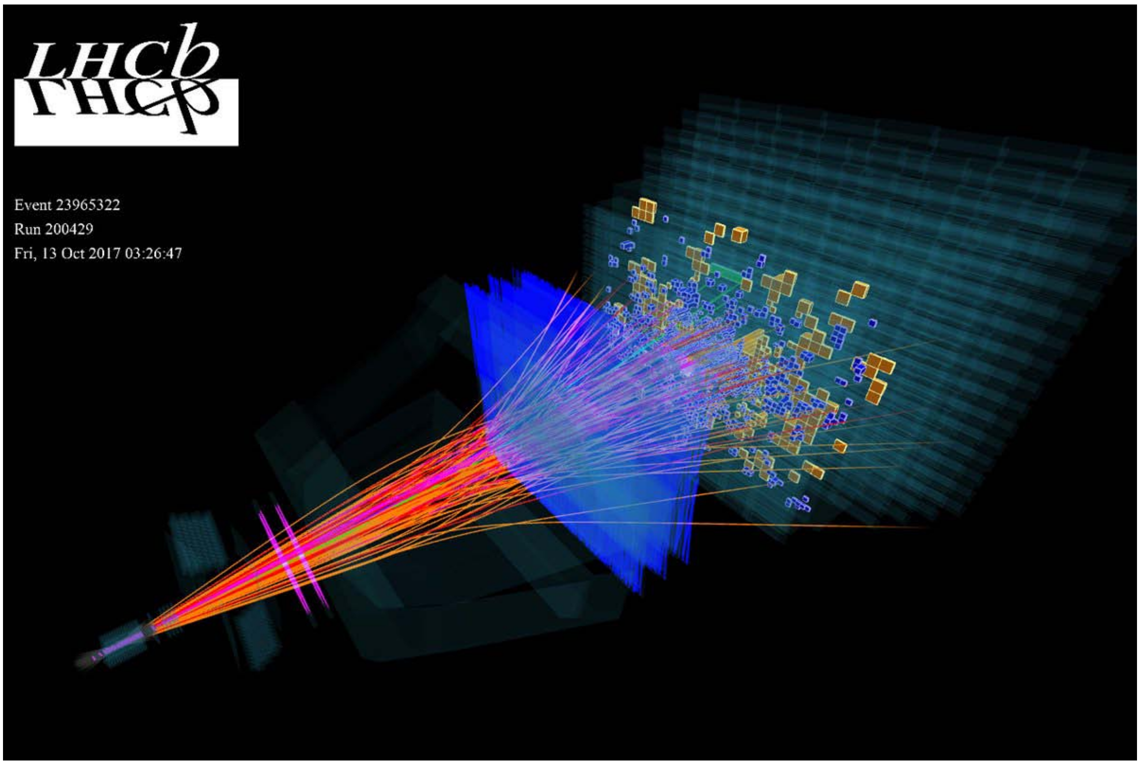

Figure 2.6 Reconstruction of the event [25]
Rysunek 2.6 Rekonstrukcja zderzenia cząstek w detektorze [25]

2.3.4.1. LHCb Collaboration

LHCb experiment is a large international collaboration composed of 1255 members, from 74 institutes in 16 countries. Status by day 15 June 2018 [43].

For example Upstream Tracker detector collaboration consists of following institutes:

- AGH University of Science and Technology, Krakow, Poland;
  - SALT hybrids,
- Zurich University, Zurich, Switzerland;
  - electronics,
  - cabling,
- University of Milan, Milan, Italy;
  - CO_2 cooling,
- ITEP Institute for Theoretical and Experimental Physics, Moscow, Russia;
  - PEPI cooling,
  - SBC cooling,
- Syracuse University, Syracuse, United States;
  - UT stave,
- University of Maryland, Maryland, United States;
  - PEPI electronics (backplane, DCB),
- Center for High Energy Physics, Tsinghua University, Beijing, China

Each institute design and manufacture a part of the UT detector. At CERN, coordination and integration of work done by all institutes is performed.

At CERN Catia V5 R2017 CAD software is used for 3D modeling, integration studies and making technical documentation (production drawings). For Catia files management tool CERN uses SmarTeam software, which allows team work within the project.

External institutes, often use other CAD software, which is not compatible with Catia. It leads for exchanging STEP files, which are not editable, and makes integration studies even more challenging.

ANSYS software is used at CERN for FEM analysis.

3. **Upstream Tracker detector (UT) mechanics and integration**

Upstream Tracker detector (UT) – is one of tracking sub-detectors in LHCb machine, located approximately 2.5 meters downstream from LHCb's interaction point (upstream of dipole magnet), Figure 2.4. It consists of 68 modules (called "Staves") equipped with single sided silicon micro-strip sensors. The UT silicon sensors are solid state detectors. When a charged particle with high energy travels through solid state sensor, it creates a small current flow in the semiconductor chip. This current is then seen as a signal, which can be translated into coordinates for the particle track. Staves are arranged in 4 consecutive layers, forming 4 curtains of measuring area – UTaX, UTaU, UTbV and UTbX. Layers UTaU and UTbV are 5 degrees inclined with respect to beam line, each one in opposite direction. The orientation and dimensions of the curtains are shown in Figure 3.1.

The replacement of the existing Trigger Tracker (TT) by UT is driven by the fact that, the front-end electronics is embedded in the sensors, Figure 3.17 b, c. In order to provide a read-out on the level of 40MHz, instead of 1MHz in existing detector design, all front-end electronics is required to be exchanged. The new detector is also going to have sensors of higher granularity and will be more radiation resistant, in order to withstand higher radiation levels associated with higher luminosity.

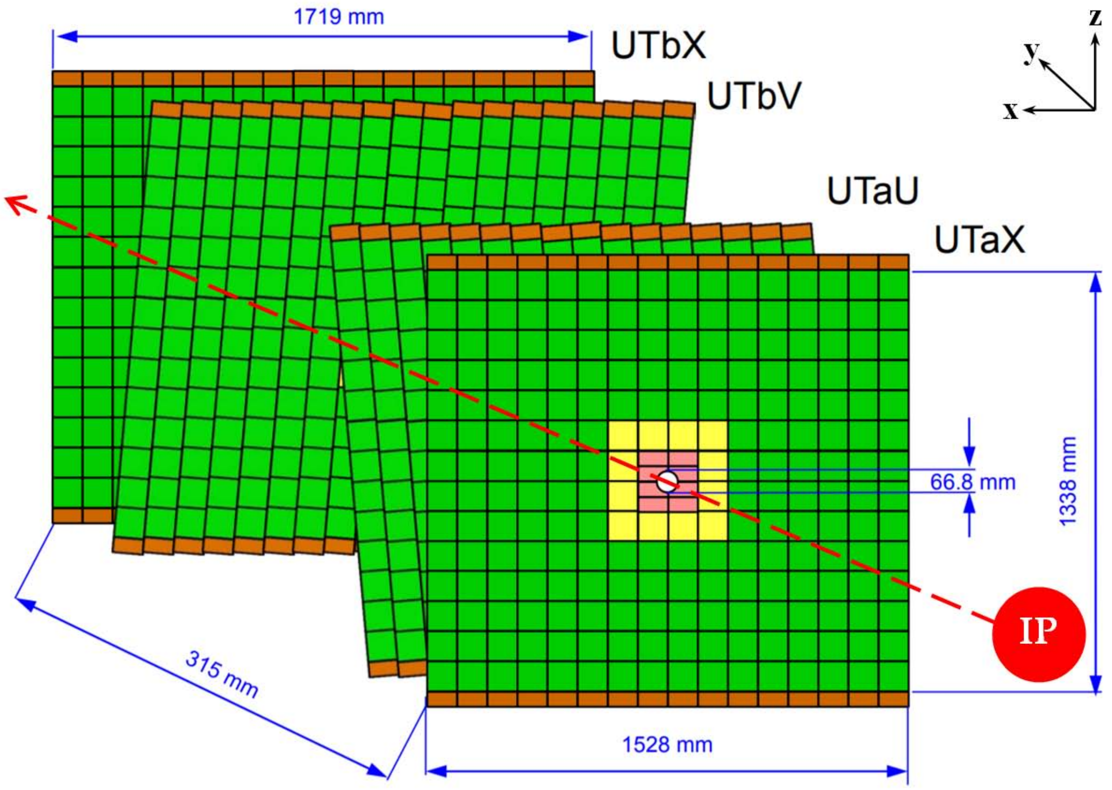

Figure 3.1 UT staves curtains geometries looking downstream [21]
Rysunek 3.1 Geometria kurtyn czujników UT patrząc w dół strumienia cząstek [21]

3.1. UT detector layout

The Upstream Tracker detector consists of several subsystems, which work together, in order to fulfill several different detector requirements. UT detector is made of two halves, called A-side (access side) and C-side (cryo side), closed over a Beryllium beam pipe. Each half contains necessary components to support 34 staves.

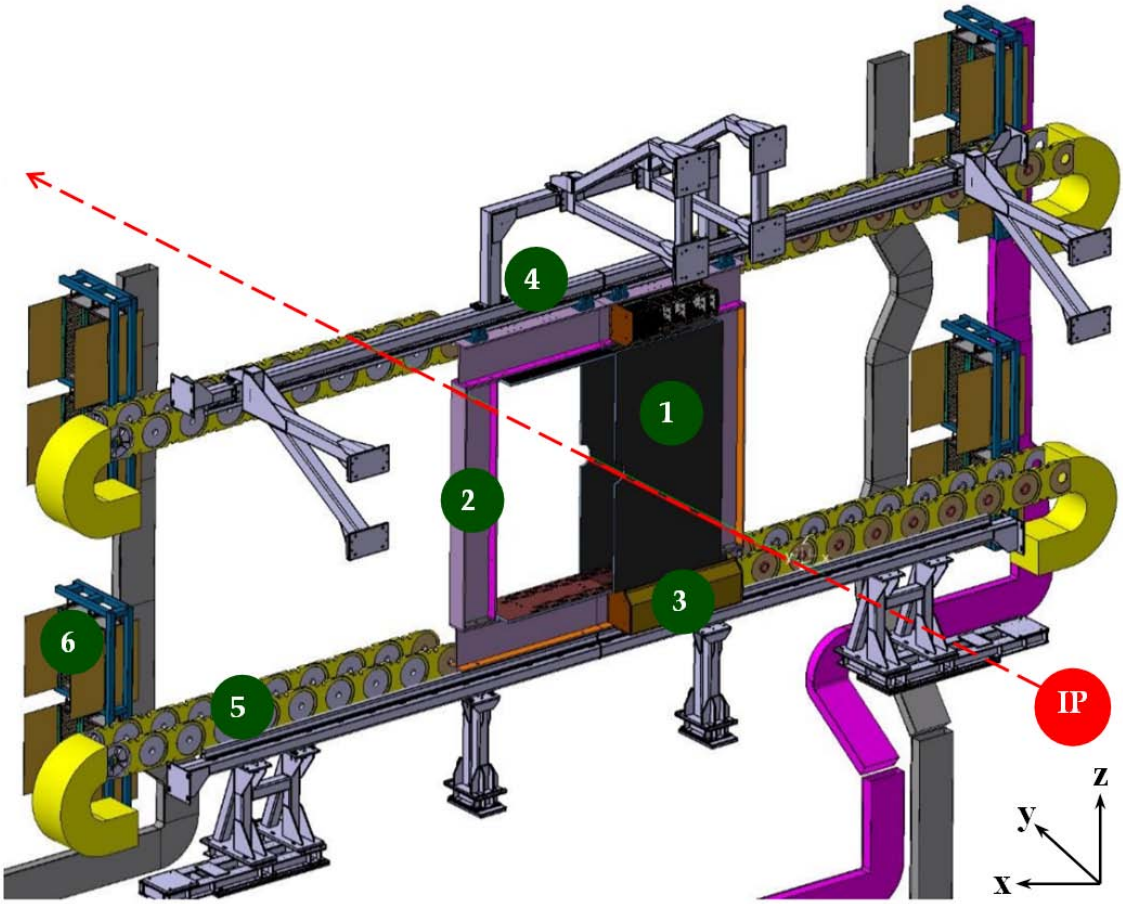

Figure 3.2 UT detector layout [26]
Rysunek 3.2 Układ detektora UT [26]

In the Figure 3.2, following components of the UT detector complex can be distinguished:

1. Detector box (UT box) – contains all the staves with silicon sensors, protects them against the surrounding environment and provides required working conditions – Chapter 3.5.
2. C-Frame – provides positioning and support for UT detector box, as well as for cable chain (from one side), patch panels, local CO_2 cooling box and PEPI electronics – Chapter 3.6.
3. PEPI electronics (called PEPI volume or PEPI chassis) – contains all the necessary electronics needed to read-out signals from the detector sensors – Chapter 3.7.
4. Rails – supply guidance and support for the detector C-Frame, on which the UT box is situated. Rails also allow the UT detector box halves to open and close.
5. Cable chain – hosts all the cables outgoing from detector electronics – Chapter 3.8.
6. SBC – service bays provides intermediate connection between cables inside cavern and cables going out / coming in, to / from surface – Chapter 3.9.

Most of the UT detector components listed in this section, will be described in details, in the following parts of this chapter.

3.2. UT mechanics challenges

Mechanical engineering challenges in a project of this scale are endless. From parts exposed for ultra high vacuum and extremely low temperatures, to elements working in high radiation environment. Different parts of LHC machine has to meet wide variety of different requirements. For example, low radiation length, high radiation resistance (radiation hardness), especially read-out electronics, very low dew point dry air, ultra high precision mechanics providing supports for precise silicon sensors positioning in the detector, and many others… All the components have to withstand their properties with time, very long period of time. Moreover, only minimal maintenance can be provided, because, once assembled, detector becomes very difficult to access and repairs are hard to perform. If mandatory, they take significant time and resources. For example, taking part of detector back on surface, is very challenging, while it is irradiated. That is why, most of CERN's detectors, including the one described in this thesis (Upstream Tracker (UT)), are designed to withstand in harsh experiment environment for at least 10 years.

3.3. LHCb envelope

Envelope – is the maximum volume filled by equipment as described in Figure 3.3. The total envelope includes manufacturing tolerances, assembly tolerances and respects deformations due to operational loads. This scheme applies in any section of the equipment in any direction [42].

Clearance – is defined as space between two adjacent envelopes. The clearance has to be determined by the required space needed for all operations (installation, access, alignment, maintenance, etc.) and uncertainties from fault conditions and unknown or unforeseen loads. This scheme applies in any direction [42].

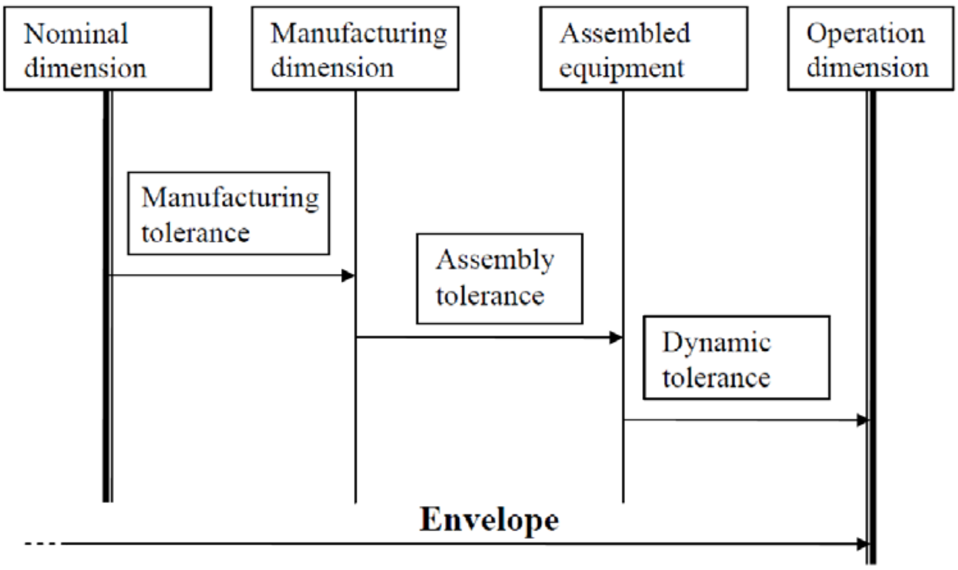

Figure 3.3 Envelope definition [42]
Rysunek 3.3 Definicja koperty [42]

3.4. Coordinate systems in the LHCb cavern

In order to communicate within collaboration correctly and to integrate detector components inside the LHCb cavern in proper manner, several coordinate systems have been developed, agreed and approved by technical board.

3.4.1. Physics

In physics coordinate system with origin in interaction point (IP), Z-axis points downstream along the beam line and is inclined by 3.601 mrad (0.206 degree) with respect to cavern floor. X and Y axes are perpendicular to the Z-axis. Y-axis is vertical and points cavern ceiling, while X-axis lies on the same plane as Z-axis and points outside the LHC ring. The arrangement of the physics coordinate system can be seen in the Figure 3.4.

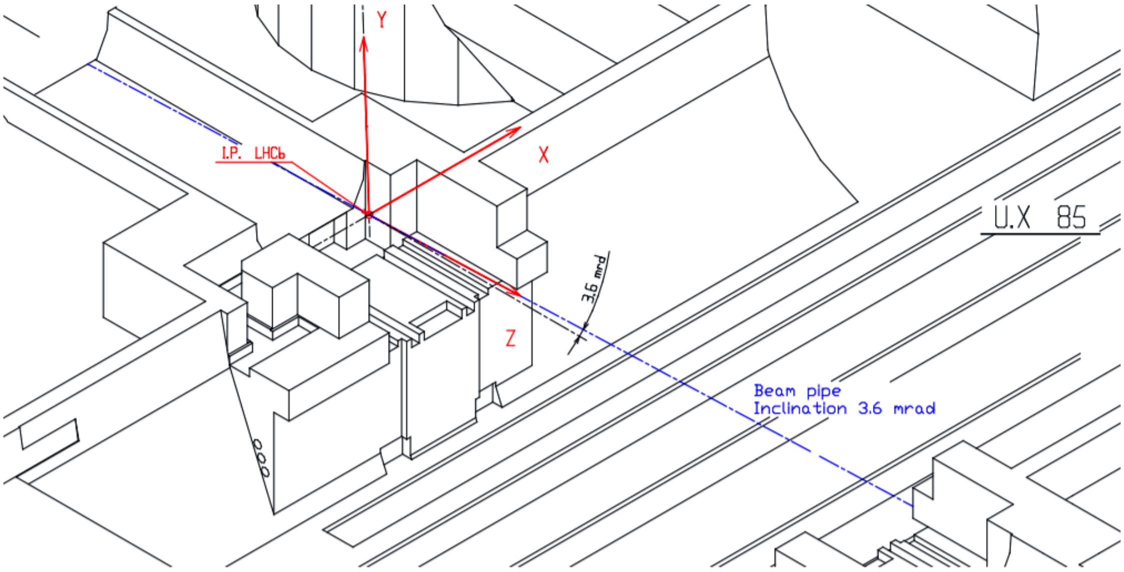

Figure 3.4 LHCb coordinate system (used by physicists) [9]
Rysunek 3.4 Układ współrzędnych LHCb (używany przez fizyków) [9]

3.4.2. Integration

In the integration coordinate system (civil engineering system) with origin in interaction point (IP), X-axis is horizontal, parallel to the cavern floor and points towards the center of the LHC ring. Y-axis is perpendicular to the X-axis, (parallel to the cavern floor), and points downstream of the LHCb experiment. Z-axis is the vertical axis and points cavern ceiling. The arrangement of the integration coordinate system can be seen in the Figure 3.5.

Following thesis treats about integration issues. Therefore, integration axis system will be used throughout all of its chapters.

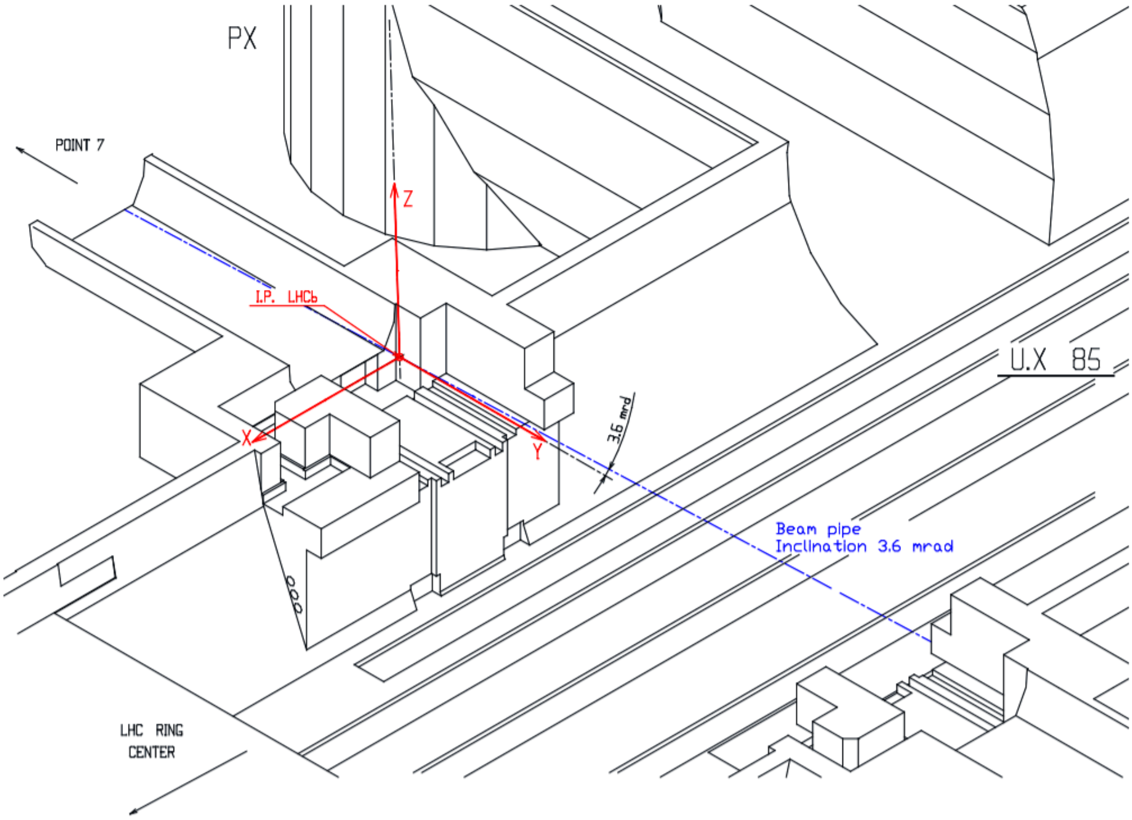

Figure 3.5 Integration coordinate system (civil engineering system) (used by engineers) [9]
Rysunek 3.5 Układ współrzędnych służący do integracji (układ inżynierii lądowej) (używany przez inżynierów) [9]

3.5. UT detector box integration

It is exceptionally important to isolate the detector form its surroundings in order to sustain proper working environment for sensors curtains hosted inside. One of the main reasons, why the detector is enclosed in a box, is the fact that, photons of ambient light would produce signals from the sensors, therefore the detector has to be operated in the dark.

Main systems in the box are: staves, stave supports, evaporative CO_2 cooling manifolds, read-out cables (called "pigtails"), high voltage cables, dry air lines. Each system has to keep its reliability for at least 10 years, maintain its efficiency with time and under harsh environment of cold temperature (–30 degrees Celsius) and under radiation. Moreover, only minimum maintenance is possibly over entire lifetime of the detector, because of very difficult access after detector is put in place. All above mentioned applies not only to the parts kept inside the UT box, but also to the elements in its immediate surroundings, like PEPI or C-Frame.

Every part of detector has to be well integrated in order to fit properly within given volume and ensure well cooperation with neighboring elements.

In this chapter the complexity of the UT detector box will be described.

3.5.1. UT detector box requirements

Main requirements for the UT box are the following:

1. **The UT box has to be light tight.**
   Since the sensitivity of the silicon sensors is very high, light (photons), would trigger signals from the detector. In order to prevent this from happening, detector has to operate in light tight box.

2. **The UT box needs to be gas tight.**
   The UT box will be continuously flushed with dry air or dry nitrogen gas in order to prevent moisture condensation inside the detector, which would damage the staves and the beam pipe. There will be a slight over pressure in the UT box, hence the dry gas will leak out, instead of humid gas leaking in through holes and gaps in the UT box. Small leaks are expected but they have to be limited [8].

3. **The UT box should be built as a Faraday cage.**
   External electromagnetic fields can produce noise and disturb the signals generated by particles of interest. Therefore, the UT box should act as a Faraday cage in order to prevent this from happening [8].

4. **UT box shell provide a good thermal insulation.**
   The ambient temperature in the LHCb cavern is about 20°C. The silicon sensors inside the box have to be kept at a temperature not higher than –5°C, in order to operate correctly. The UT staves are cooled down using evaporative CO_2 cooling system. This cooling system has a capacity of 5kW. 500W is reserved for heat transfer through the box walls. The rest of the power is needed to deal with the heat, which the detector electronics generate. The UT box has to be well thermally insulated. If it is not the case and heat seeps from the surrounding room temperature environment into the box, cooling system might not be able to transfer it away, which could cause temperature raise and sensors failure after irradiation.

5. **The UT box should have low radiation length.**
   The UT box shall be constructed of lightweight material with low radiation length. Radiation length is a material property related to the energy loss of high energy, electromagnetic-interacting particles, when propagating through the material [8].

6. **The UT box must be radiation resistant (radiation hard).**
   The material properties of the UT box must not change under the radiation exposure. A minimum radiation hardness of the UT box has to be on the level of 5×10^7rad.

7. **The force transmitted from the UT box to the LHCb beam pipe has to be limited.**
   The LHCb beam pipe, going through the UT box, is made of Beryllium, because it is almost transparent to the particles, which should be studied (has very low radiation length). Beryllium is very fragile and will break, if too much force is applied. This is a critical requirement, since big force can break the LHCb beam pie. In such case the LHC machine would have to stop. Only a few Newtons of force are allowed to be applied when the box is closed.

8. **The detector should be accessible.**
   In order to simplify detector reparations and future possible upgrades, it should be possible to easily remove UT box from the beam pipe, and to reinstall it without damaging neighboring elements. However, taking into account cavern environment and closeness of other detectors, this is very difficult to achieve, and any access to the detector has to be planned carefully.

3.5.2. UT detector box geometry

In order to fulfill its requirements in terms of accessibility and maintenance, as well as to allow the LHCb beam pipe to pass freely through the middle of the UT staves curtains, Upstream Tracker detector box consists of two separate halves. Outside dimensions of one half of the UT box are the following:

- height (z-axis): 1970 mm,
- width (x-axis): 1025 mm,
- depth (y-axis): 430 mm.

Thickness of the top and bottom walls as well as side wall (walls touching C-Frame) is 25 mm.
Thickness of the downstream and upstream walls is 20 mm.
Positions with respect to the LHCb interaction point (IP) and the dimensions of the detector halves can be seen in the Figure 3.6 and Figure 3.7.
Both halves of the detector enclosed around beam pipe can be seen on Figure 3.8.

The thickness of the UT box walls is dictated by thermal requirements. Walls have to be good thermal insulators to prevent condensation on the outside of the wall.

There is however one more mechanical requirement about thickness of the top and bottom walls of the box, which are attached to the C-Frame. They have to withstand the load of the staves curtains attached to them. They act as an interface between C-Frame supporting the entire detector box, and the staves supports inside the box. The deflection of those plates cannot be too big, because it has an impact on precise sensors positions mounted on the staves. Moreover, top and bottom plates of the box requires several elongated holes Figure 3.8 and Figure 3.11, in order to pass through read-out cables from the staves electronics. It means they are mechanically weaken and need more careful investigation in order to ensure their mechanical integrity.

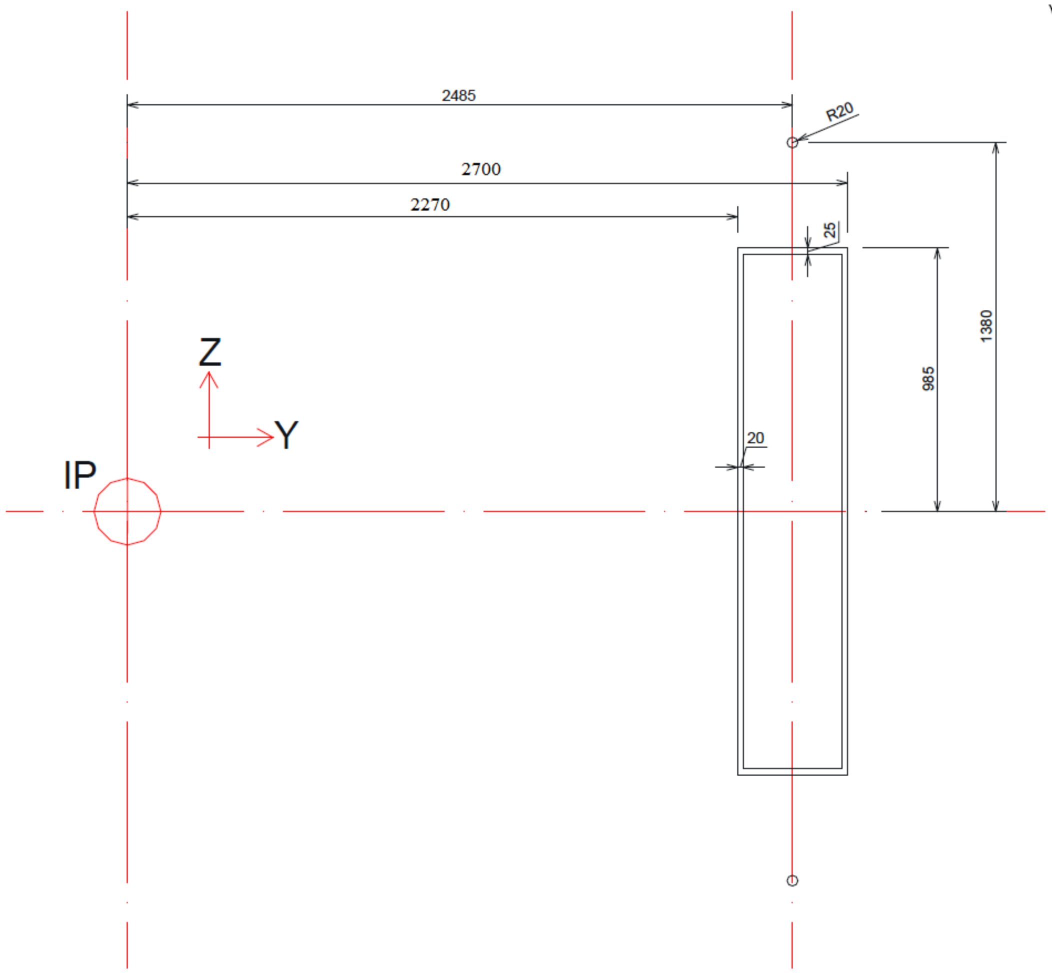

Figure 3.6 UT box position with respect to IP, side view with dimensions and mounting rails [27]
Rysunek 3.6 Pozycja skrzynki detektora UT względem punktu interakcji (IP), widok z boku z wymiarami i szynami montażowymi [27]

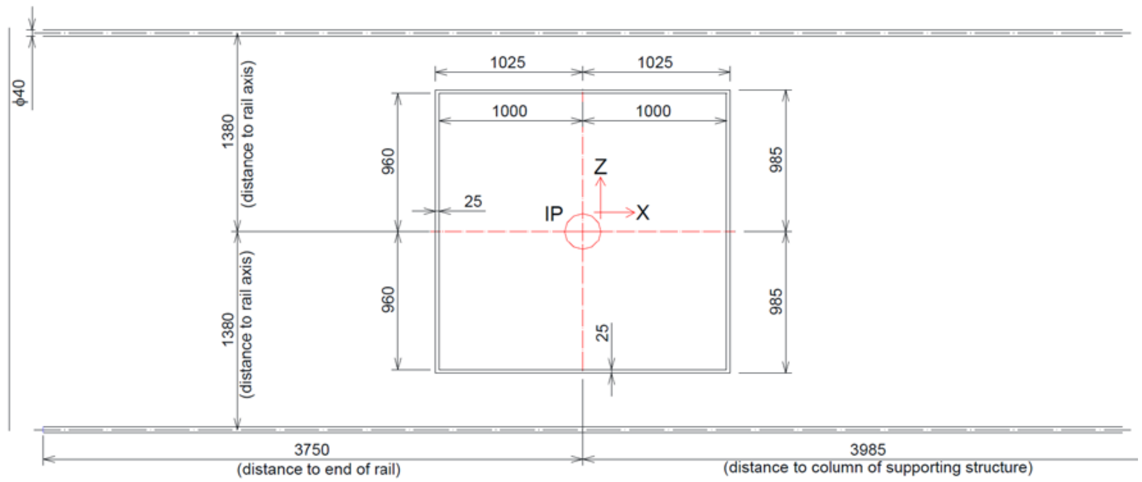

Figure 3.7 UT box front view with dimensions and mounting rails [27]
Rysunek 3.7 Skrzynka detektora UT, widok frontowy z wymiarami i szynami montażowymi [27]

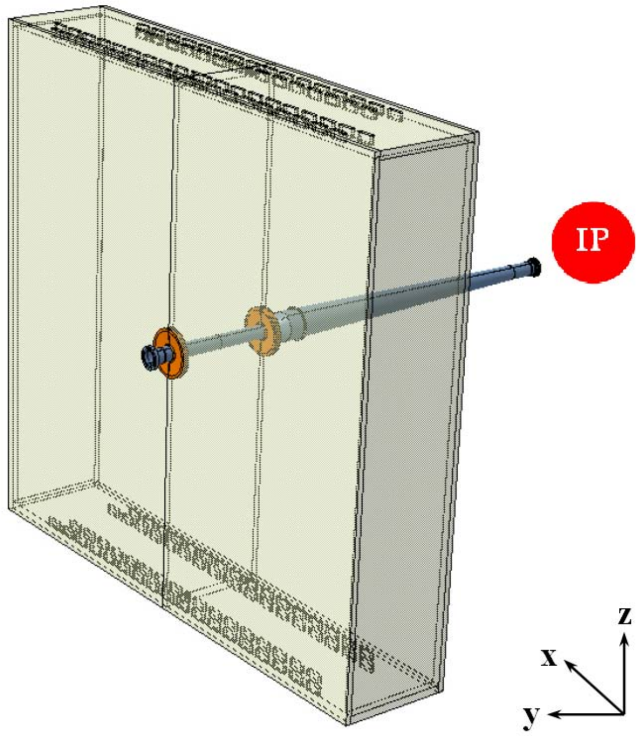

Figure 3.8 Transparent view of empty UT box with beam pipe crossing the box [8]
Rysunek 3.8 Widok przezroczystej i pustej skrzynki detektora UT wraz z rurą, w której krążą wiązki cząstek, przecinającą skrzynkę [8]

The interface between the UT box and the LHCb beam pipe represented in the Figure 3.8 as orange discs where the pipe gets in and goes out from the box, is not a subject of this thesis. More detailed information about this interface can be found in reference [8].

3.5.3. UT detector box material

In order to fulfill its requirements in terms of being lightweight, having good thermal insulation properties, acting as a Faraday cage, being radiation hard and having small radiation length, UT detector box is made of composite sandwich plates consisting of three different materials:

- carbon fiber reinforced polymer,
- Airex foam,
- copper net.

A single composite sandwich plate is built of Airex foam core covered on both sides with several layers of carbon fiber reinforced polymer. In addition to that, a copper net is embedded in one of the carbon fiber reinforced polymer layer, in order to make UT box resistant against external electromagnetic fields (Faraday cage).

A layout of the sandwich components can be seen in the Figure 3.9.

An assembled composite sandwich plate can be seen in the Figure 3.10.

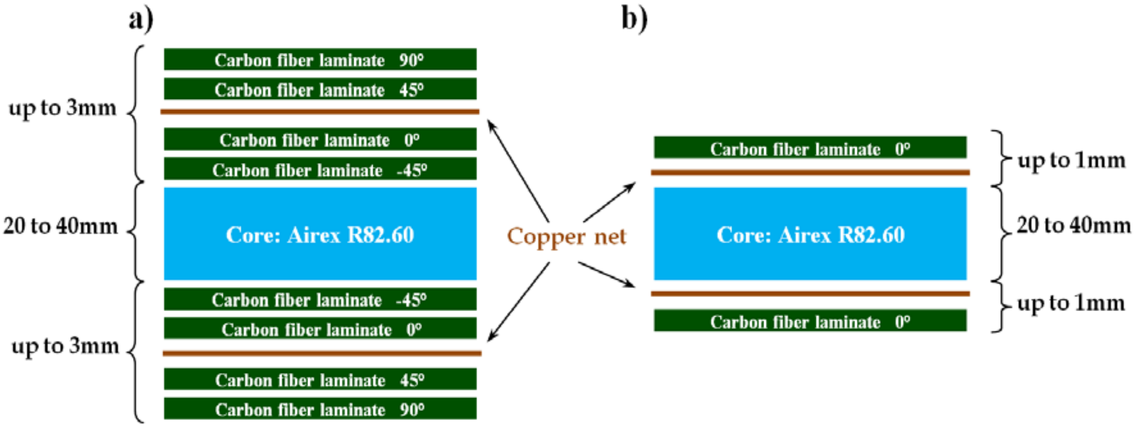

Figure 3.9 a) Layout of the sandwich components for top, bottom and side UT box plates; b) Layout of the sandwich components for front and back UT box plates [30]

Rysunek 3.9 a) Rozkład komponentów kompozytu dla górnej, dolnej i bocznej płyty detektora UT; b) Rozkład komponentów kompozytu dla przedniej i tylniej płyty detektora UT [30]

Carbon fiber reinforced polymer (carbon fiber laminate) is used to ensure structural stability of the UT box walls. Provided by CTMI company (weave twill 2/2, reference 5626-1808S-50/120 [28]). There are different thickness used. For front (downstream) and back (upstream) walls, the maximum thickness of the carbon fiber laminate layer is 1mm, in order to ensure low radiation length Figure 3.9 b. For the top, bottom and side walls, to provide sufficient stability, thickness of the carbon fiber laminate layer can be up to 3mm Figure 3.9 a.

Airex foam (AIREX R82.60 [28]) is an excellent thermal insulator. With thermal conductivity k = 0.036 W/mK, provides good thermal insulation properties for the UT box.

Copper net (Dexmet 2CU6-100FA [28]) embedded between carbon fiber laminate layers, provides shielding against external electromagnetic fields for the UT box construction. The copper net in all panels are connected together to make the Faraday cage. This concept have been tested and validated. The diameter of the holes in this copper net is 2.54mm, and thus electromagnetic radiation with a wavelength superior to this will be blocked. 2.54mm wavelength is in the short end of the microwave region [8].

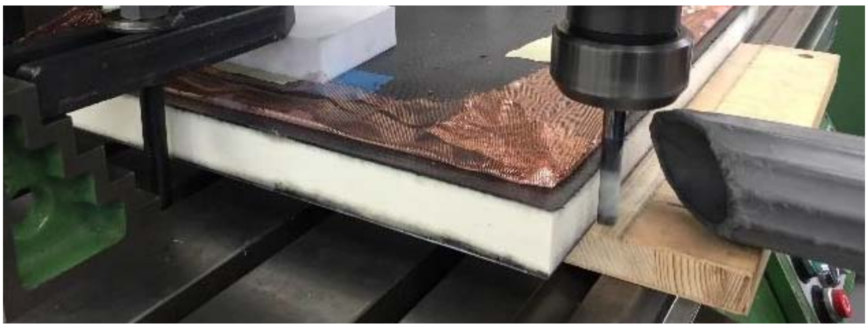

Figure 3.10 Assembled composite sandwich plate [28]

Rysunek 3.10 Złożona kompozytowa płyta [28]

The developed sandwich construction satisfies all thermal, mechanical and electrical requirements of the UT detector box.

The full size top and bottom carbon reinforced UT detector box plate can be seen in Figure 3.11.

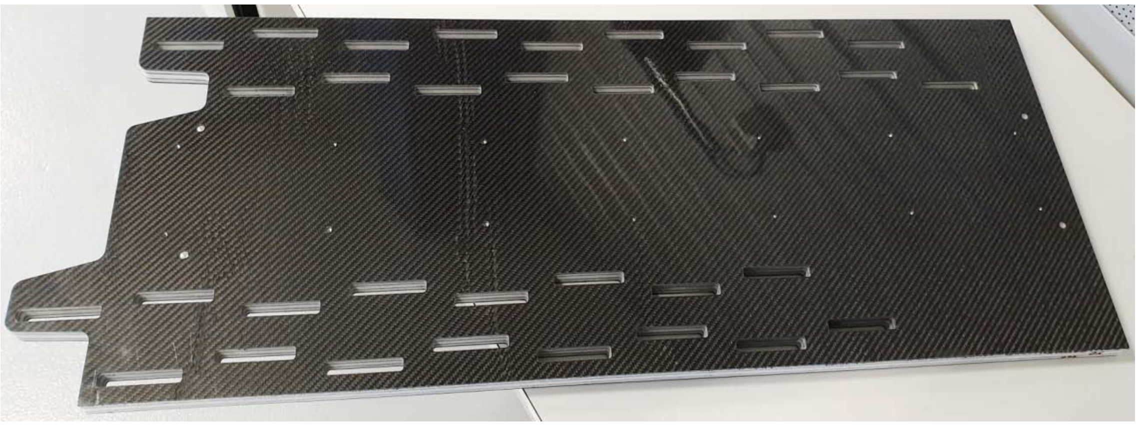

Figure 3.11 Full size top and bottom carbon reinforced plate, (prototype)
Rysunek 3.11 Wzmocniona włóknem węglowym, górna i dolna płyta w pełnym rozmiarze, (prototyp)

A specific shape of the top and bottom UT detector box plate is shown in the Figure 3.12. This shape is a result of the staves inclination in UTaU and UTbV layers. Because staves are inclined, data read-out cables (pigtails) connects to them with the same angle and need more room to go out of the detector box. Some cables from A-Side passes to the C-Side and vice versa. However, pigtails from A-Side has to connect to the PEPI volumes located on A-Side, otherwise opening the detector would not be possible. Hence, top and bottom plates of the detector box must follow the staves inclination and pigtails paths.

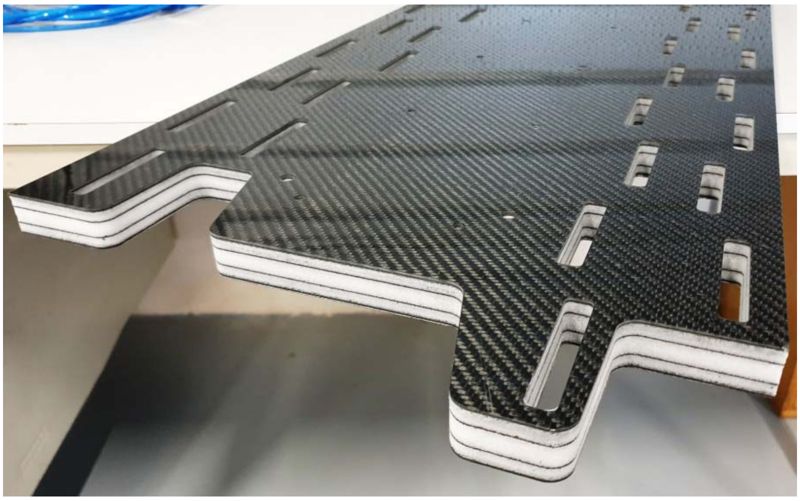

Figure 3.12 Specific shape of the top and bottom UT detector box plate, (prototype)
Rysunek 3.12 Specyficzny kształt górnej i dolnej płyty detektora UT, (prototyp)

From the mechanical engineering point of view, this shape creates a bunch of challenges. From precise machining of such shape in given material, to provide tight sealing of the UT detector box, when two halves are put together. The seal must follow the shape of the box providing gas and light tightness.

3.5.3.1. UT detector box inserts

Because UT detector box is made of Airex foam attaching it to supporting frame (C-Frame), and attaching staves supports as well as cooling manifolds supports to top and bottom plates of the box (inside it) is not a straightforward task. Foam itself is too soft and cannot host thread inside. Drilling it through is also not acceptable (due to gas and light tightness requirements). Moreover, staves supports needs to be precisely positioned. Therefore, a solution satisfying both cases had to be developed.

Inserts had been implemented – Figure 3.13.

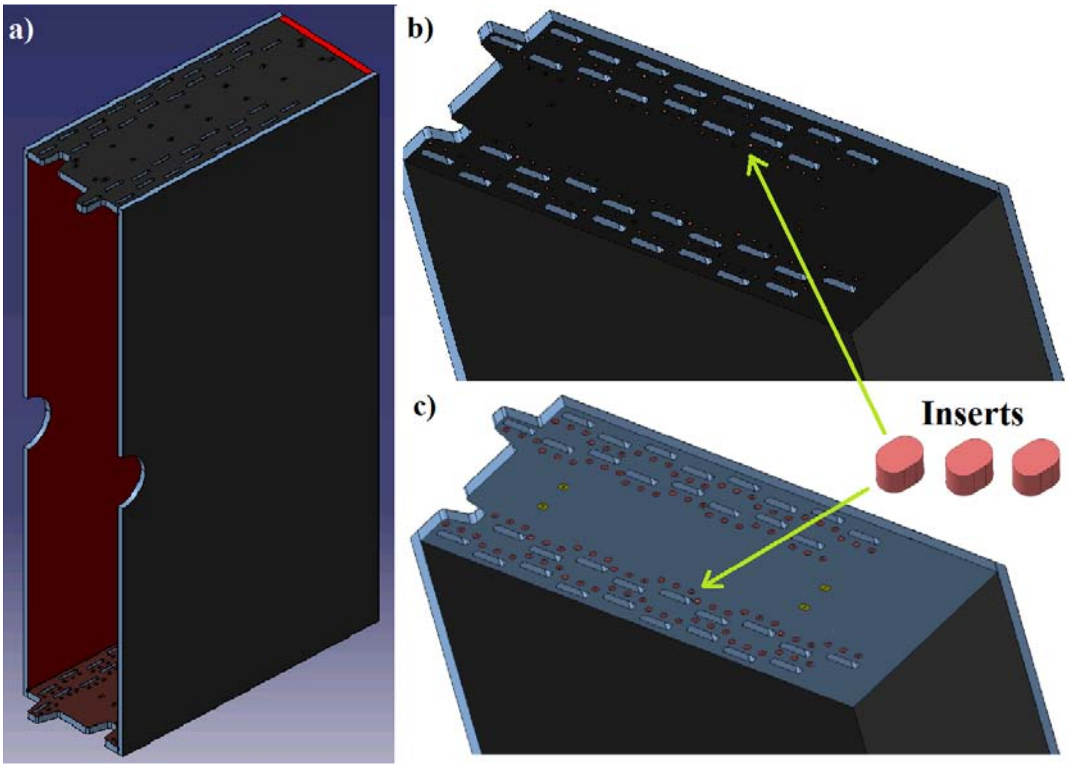

Figure 3.13 a) One half of UT detector box (C-Side); b) Top carbon reinforced sandwich plate of the box (view from inside); c) Airex with inserts inside – top plate (view from inside) [26]
Rysunek 3.13 a) Połowa skrzynki detektora UT (Strona-C); b) Górna płyta ze wzmocnionego włóknem węglowym kompozytu warstwowego (widok od wewnątrz); c) Airex z wkładkami w środku – górna płyta (widok od wewnątrz) [26]

The idea is, to precisely machine edge and openings of plates of the box together with its outer shape, elongated holes for data read-out cables (pigtails), and holes for inserts. Afterwards, plane inserts (without holes), will be glued inside respective holes in Airex foam, using heavy duty glue. For obtaining precision, only after gluing the inserts inside the plate, they will be drilled and tapped using CNC milling machine. The elongated shape of the inserts, shown in Figure 3.13, improves durability and prevents from damaging the inserts when too much torque applied.

In addition, inserts are also used to build the box itself. They are placed on the edge of one plate and connect with respective mounting points on another plate. Furthermore, inserts with dowel pins are used to position detector box on the supporting C-Frame.

3.5.3.2. UT detector box inserts test

In order to be sure inserts are sufficient to support load from staves and will act properly for an interface between the UT detector box and the C-Frame, a tensile test on G10 inserts enclosed in composite sandwich plate was conducted.

The aim of the test was to find out the magnitude of force, under which, inserts might be damaged. Another goal was to learn what kind of damage may occur. To Airex foam, to glue interface or to insert itself.

A graph presenting damaging force can be seen in Figure 3.14.

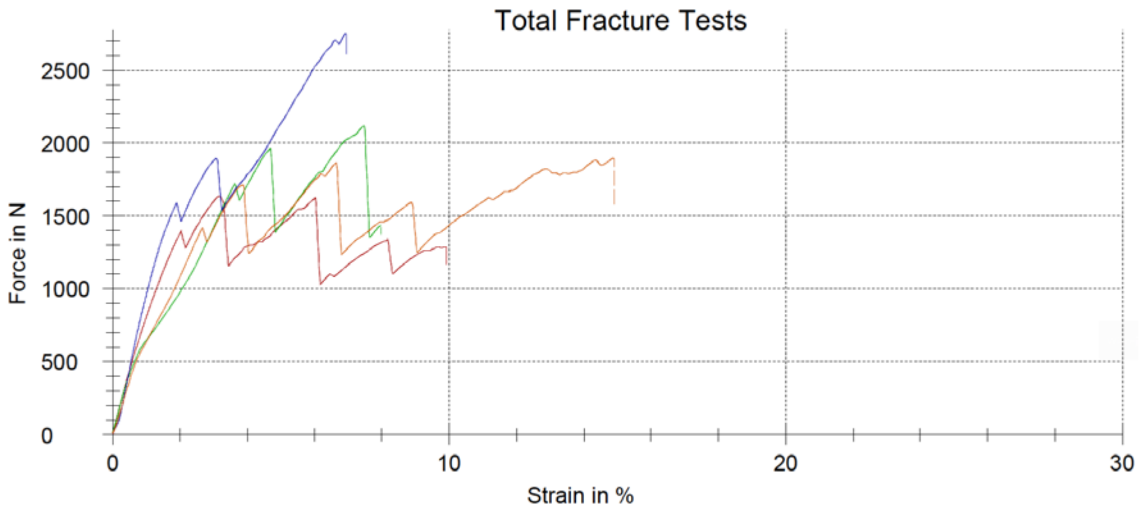

Figure 3.14 Damaging force graph [29]

Rysunek 3.14 Wykres siły niszczącej [29]

A sandwich plate with insert inside prepared for test is presented in Figure 3.15 a, b.

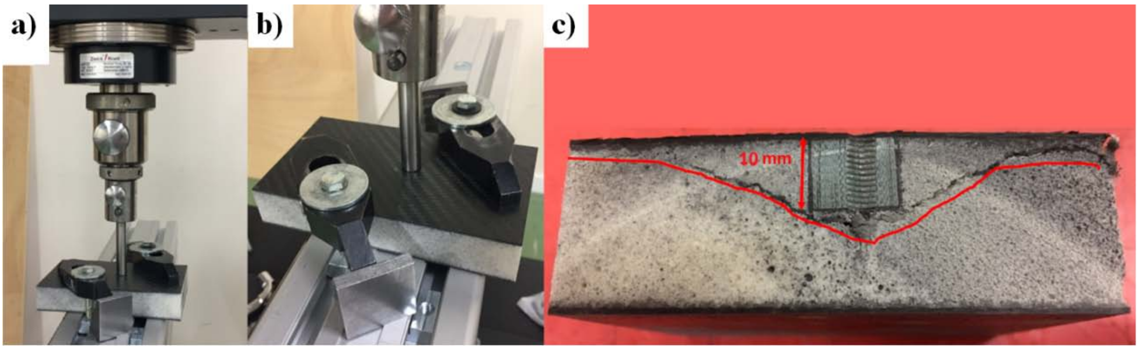

Figure 3.15 a, b) Sandwich plate containing insert prepared to the test;
c) Fractured sandwich plate [29]

Rysunek 3.15 a, b) Płyta kompozytowa zawierająca wkładkę przygotowana do testu;
c) Pęknięta płyta kompozytowa [29]

A conclusion from the test is that sandwich plate begin to fail under the force around 1500N. All the samples show a fracture of the Airex foam (Figure 3.15 c) and not to the glue interface or to the insert.

As a consequence, it was learned, that single insert can withstand a load of about 150kg. Single stave alone weights ~2kg. Together with supports and pigtails on both ends ~5kg. Therefore, inserts are sufficient for supporting staves.

3.5.4. Integration inside the UT detector box

This chapter describes integration studies inside the UT detector box. In the Figure 3.16 there is one quarter of the detector box shown from inside.

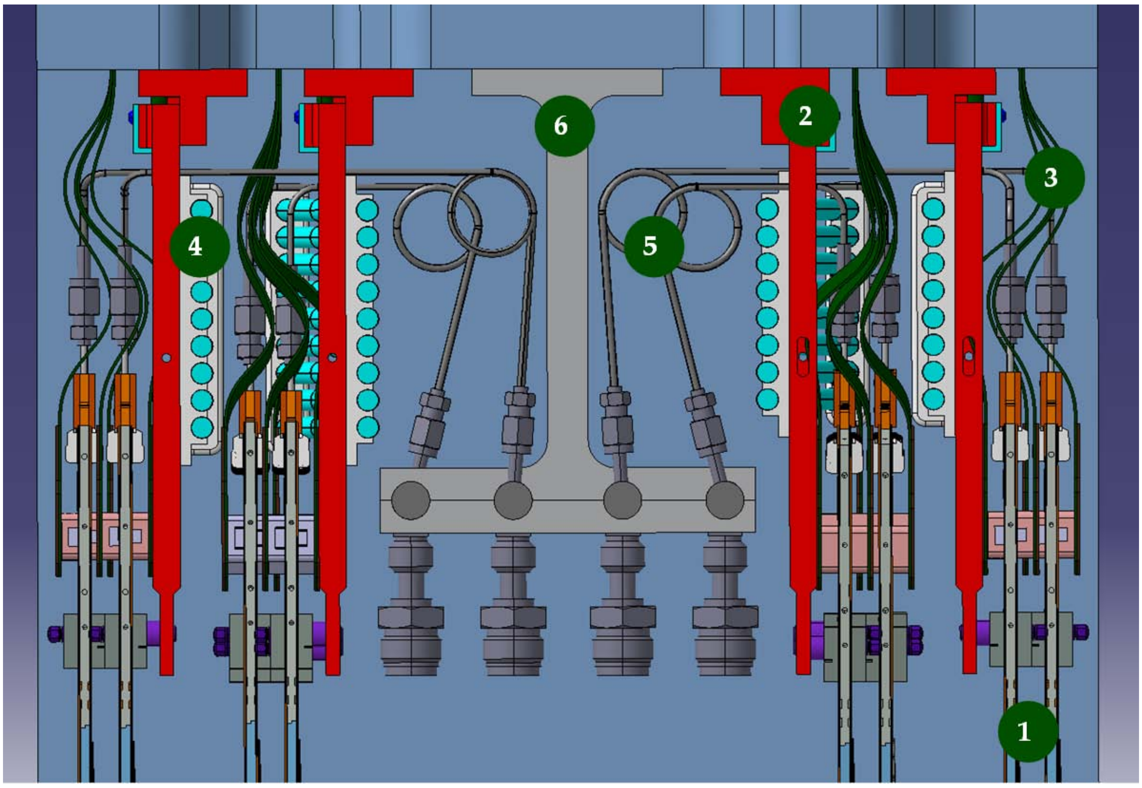

Figure 3.16 An overview of components inside the UT detector box, (looking from the beam pipe)
Rysunek 3.16 Widok elementów wewnątrz detektora UT, (patrząc od strony rury w której krążą wiązki cząstek)

In the Figure 3.16, following components of the UT detector box can be distinguished:

1. Staves – supports silicon sensors and read-out electronics.
2. Staves supports – provides mechanical support for staves.
3. Data read-out cables (Pigtails) – conducts signals from silicon sensors on staves to the peripheral electronics (PEPI) located on a C-Frame above and below the UT box. In addition, provide low voltage power for electronics embedded in staves.
4. High voltage cables – supplies power for silicon sensors.
5. CO_2 cooling manifolds – provides the UT detector box with cooling power.
6. Manifolds supports – provides mechanical support for cooling manifolds.

All UT detector box components listed in this section, will be described in details, in the following parts of this chapter.

3.5.4.1. Stave

There are three different types of UT staves – A (56 staves), B (8 staves) and C (8 staves). A and B are mechanically identical, while C staves (Figure 3.17) have opening in the middle of their length in order to accommodate beam pipe going through the detector. Staves hosts silicon sensors together with the read-out electronics (ASICs – Application-Specific Integrated Circuits (Figure 3.17 b)) as well as titanium cooling pipe (Figure 3.17 a), used to cool down the sensors and electronic chips with CO_2 evaporative cooling system.

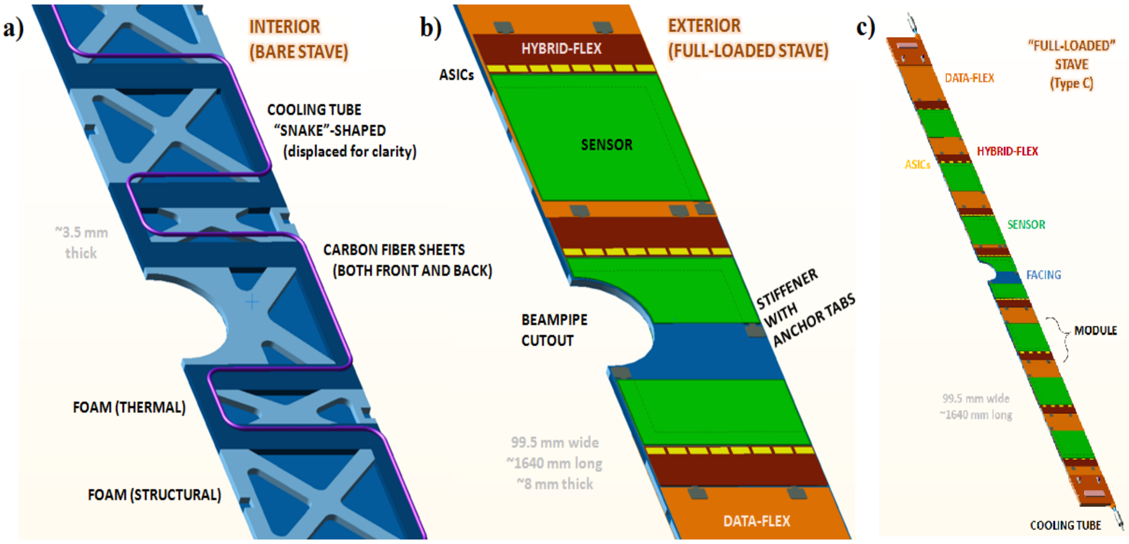

Figure 3.17 a) Bare stave; b) Full-loaded stave; c) Entire stave [31]

Rysunek 3.17 a) Stave – budowa wewnętrzna; b) W pełni wyposażony stave; c) Cały stave [31]

Staves parameters are the following:

- length – 1657.6mm,
- width – 99.5mm,
- thickness of bare stave – ~3.5mm,
- thickness of fully-equipped stave – ~8mm,
- silicon sensor width is 97.5mm – stave is 1mm wider than sensor on each side.

Bare stave is constructed from CFRP (Carbon Fiber Reinforce Polymer) elements. They are glued using epoxy resin to foam core in sandwich structure with embedded cooling tube. The entire part is epoxy glued construction.

There are two different types of foam used in bare stave production. First one is a thermal foam for good heat transfer. It comes with contact with titanium cooling pipe (Figure 3.17 a). Another foam is a structural foam. It provides lightweight and rigidity to the stave sandwich structure (Figure 3.17 a).

Cooling tube is a titanium pipe with 2.275mm of outside diameter and 135um wall thickness. It is formed in "snake" shape and runs under all ASICs and one edge of each sensor.

A purpose of this construction is to keep sensors at a temperature of –5°C or below. Another goal is to achieve uniform ΔT=5°C across sensor and keep ASICs below 40°C (6 mW/channel, 0.768 W/ASIC).

Adjacent staves are overlapped in order to provide continuous curtain of sensors Figure 3.18.

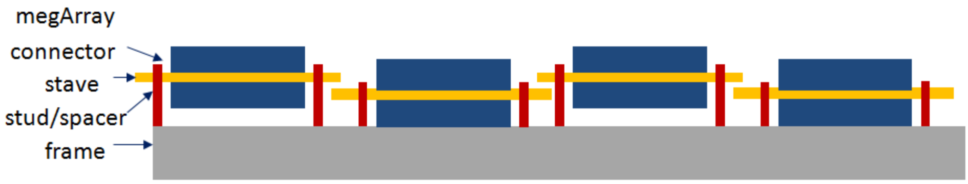

Figure 3.18 Special mounting system providing overlap for adjacent staves [30]
Rysunek 3.18 Specjalny system montażowy zapewniający nakładanie się sąsiadujących stave-ów [30]

The complete view of four staves curtains is shown in Figure 3.1.

3.5.4.2. Stave support

FEM analysis of the stave indicated that thermal transverse contraction under given temperature difference of 50°C is on the magnitude of 0.2mm, while longitudinal contraction is up to 0.8mm. Therefore, fixing and positioning of the staves is another challenge. An appropriate amount of DOF (Degrees of Freedom) must be provided to the stave fixation points in order to avoid over-constraining the system. In addition to this, staves are very long, about 1.65m, it gives large lever-arm for even small displacements. Moreover, staves supports also suffer from thermal contraction themselves. Hence, selection of proper material for supports is crucial to provide correct support for the most delicate elements in the UT detector – staves.

Staves support must provide precise position for staves, which hosts silicon sensors. The accuracy of the detector rely on precise sensors positioning. In addition, as shown in Figure 3.18 and Table 3.1, staves support must be constructed in the way, which provides the adjacent staves overlap.

Table 3.1 Staves positions and overlap values for the right half of all four layers [32]
Tabela 3.1 Pozycje stave-ów i wartości zachodzenia ich na siebie dla prawej połowy, dla wszystkich czterech warstw [32]

Stave	Left edge	Center	Right edge	Overlap [mm]	
1R	-3,55	46,2	95,95	5,5	1L to 1R
2R	91,55	141,3	191,05	4,2	2 to 1
3R	186,65	236,4	286,15	4,2	3 to 2
4R	282,55	332,3	382,05	3,6	4 to 3
5R	378,45	428,2	477,95	3,6	5 to 4
6R	474,35	524,1	573,85	3,6	6 to 5
7R	570,25	620	669,75	3,6	7 to 6
8R	666,15	715,9	765,65	3,6	8 to 7
9R	762,05	811,8	861,55	3,6	9 to 8

In the Table 3.2, there is a list of potential estimated uncertainties associated with staves x-positioning (where staves needs to be overlapped).

Table 3.2 Uncertainties in x-axis staves positioning.
Tabela 3.2 Niepewności w pozycjonowaniu stave-ów w osi x.

Type of uncertainty	**Value [mm]**
Degree Of Freedom (DOF) in X-Axis foreseen on stave supports	0.5
Mistake on precision in position for holes for inserts in carbon box	0.1
Manufacturing tolerance of insert	0.05
Insert gluing procedure mistake	0.1
Machining precision of the stave support	0.05
Machining precision of end of stave region	0.05
Manufacturing tolerance of pins, on which stave hangs	0.05
Tolerance of silicon sensors placement on the stave	0.1
Manufacturing tolerance of entire stave	0.2
Thermal contraction/expansion of stave support in x-axis	0.05
Thermal contraction/expansion of stave itself in x-axis	0.2
Sum:	**1.45**

The overlap of the adjacent staves must be larger than 1.45mm (Table 3.2).

As described in Table 3.1 overlap between adjacent staves in the middle of the detector, (between two detector halves), is the largest, and equals 5.5mm. It must accommodate all the uncertainties of positioning, parts manufacturing and final assembly when two detector halves meets together. In addition to that, for two central staves, it is mandatory to take into account the manufacturing tolerance, of the length, of top and bottom carbon box plates, which is ~0.5mm for each plate. Moreover there will be a seal between the two detector box halves, which will obscure some space. Taking all mentioned elements into account the overlap between central staves must be sufficient for the proper detector operation.

Overlap between the rest of the staves may be smaller, because it is possible to achieve better precision in manufacturing staves supports.

Counting from the Interaction Point (IP) towards the magnet the staves layers are:

- UTaX – 16 staves perpendicular to the beam pipe (Figure 3.19 in blue),
- UTaU – 16 staves 5 degrees inclined with respect to beam pipe (Figure 3.19 in orange),
- UTbV – 18 staves 5 degrees inclined with respect to beam pipe, opposite inclination like UTaU layer (Figure 3.19 in yellow),
- UTbX – 18 staves perpendicular to the beam pipe (Figure 3.19 in green).

Figure 3.19 presents staves positions with respect to the beam line. Each layer is placed in certain distance from interaction point (IP) (Figure 3.20). In addition, staves within single layer are overlapped (staggered by 15mm) with respect to each other, along z-axis. This gives possibility to maintain continuous curtain of silicon sensors.

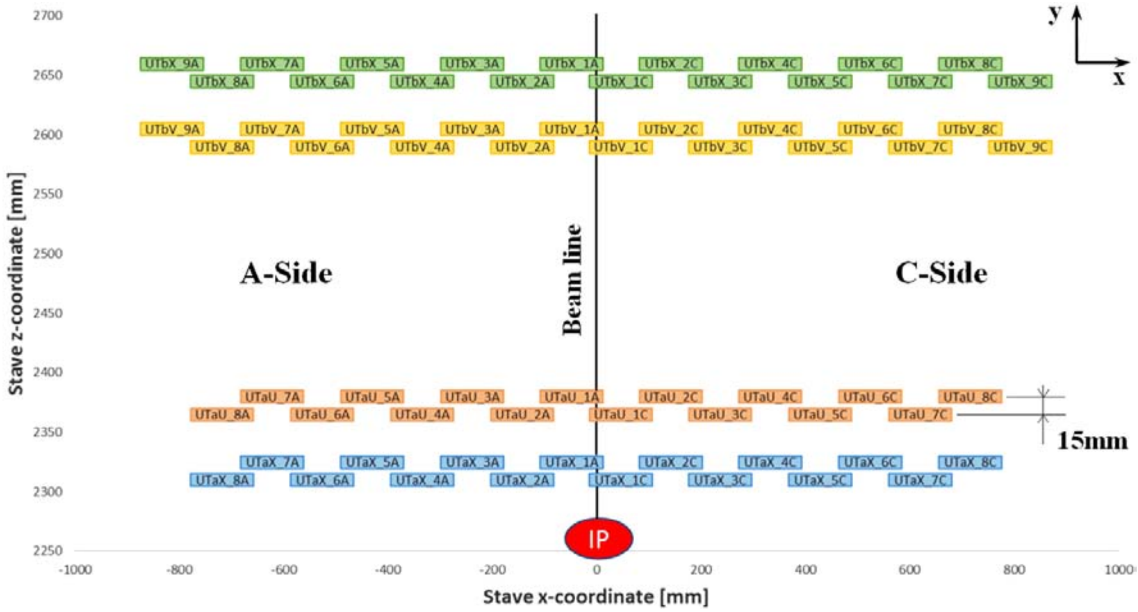

Figure 3.19 UT staves positions with respect to the beam line [26]
Rysunek 3.19 Pozycje stave-ów UT względem rury w której krążą wiązki cząstek [26]

Figure 3.20 shows staves positions with respect to the interaction point (IP).

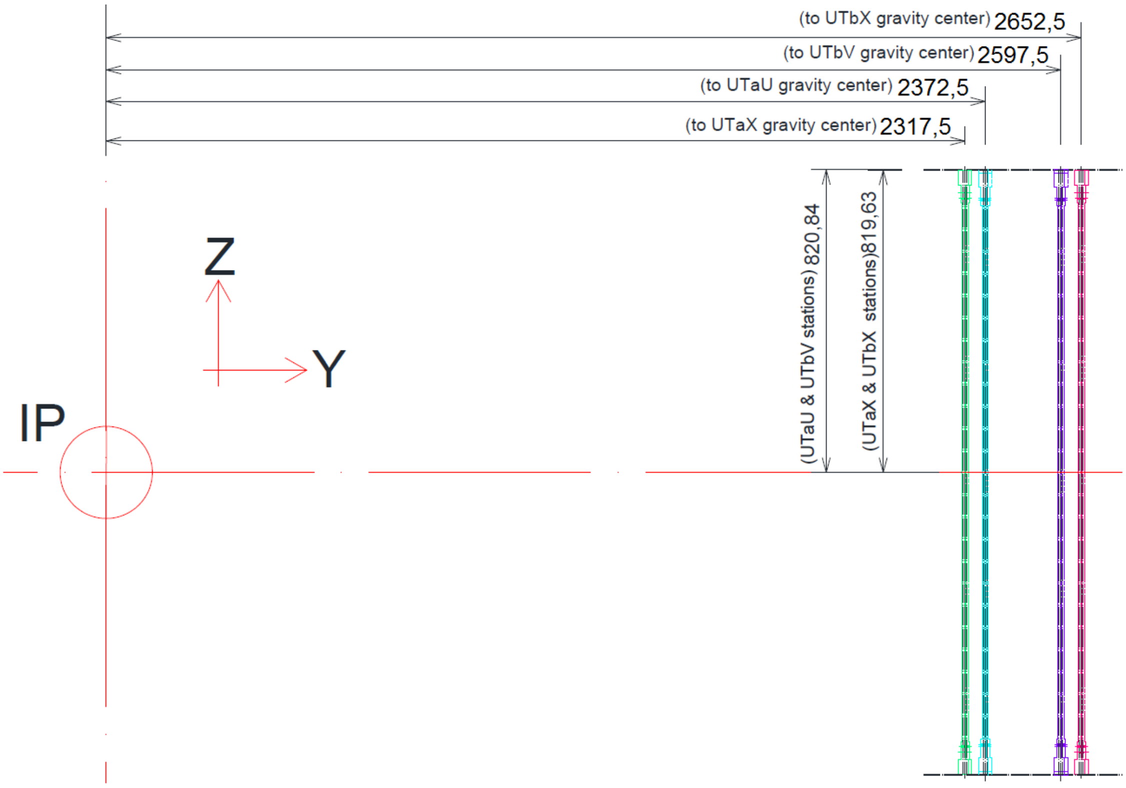

Figure 3.20 UT staves positions with respect to the interaction point [27]
Rysunek 3.20 Pozycje stave-ów UT względem punktu interakcji (punktu zderzenia cząstek) [27]

Stave supports, in the (Figure 3.21 a) described as 'frame', should provide the precise locations for the stave mounts. In addition to that, they should take into account some tolerance, to avoid stressing the stave. To achieve this, the frame should compensate its own thermal and gravitational deformations, as well as, its manufacturing tolerances. Following the requirements, each stave has four mounting points, two on each end. Only one of these points is completely fixed (Figure 3.21 b), in order to provide precise stave positioning. The rest of the mounting points provide possibility to move, in both, x-direction and z-direction (Figure 3.21 b, c), to compensate thermal contraction of frame and stave.

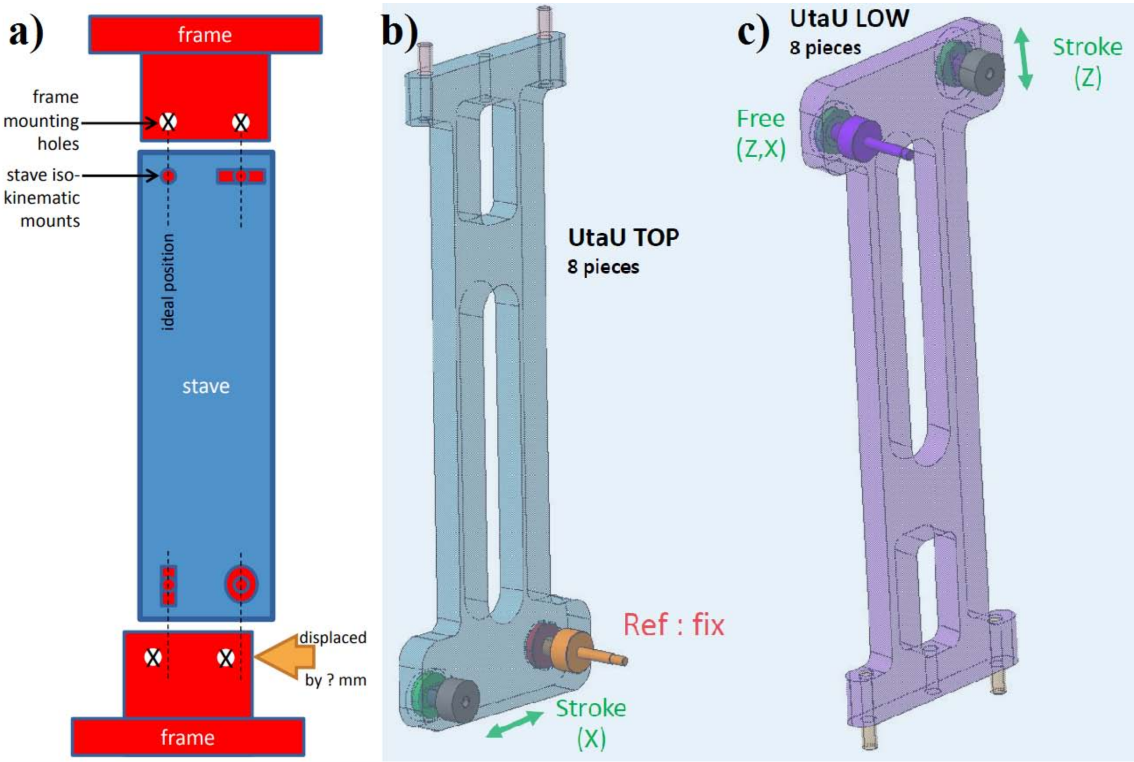

Figure 3.21 a) Iso-kinematic stave mounting system; b) UTaU layer top support (top 'frame'); c) UTaU layer bottom support (bottom 'frame') [26], [33]

Rysunek 3.21 a) Iso-kinematyczny system montowania stav-ów; b) górna podpora warstwy UTaU (górna 'rama'); c) dolna podpora warstwy UTaU (dolna 'rama') [26], [33]

Each stave support is attached to top and bottom plate of the box using two dowel pins at extremities and a screw at a centre (Figure 3.21, b, c). It provides necessary positioning precision with respect to the box.

The single stave weights about 2kg. Therefore, supporting it in terms of mass does not create big difficulties. However, and what is of the most importance, precise positioning is very challenging, due to temperature difference and changes in material dimensions, in low temperatures. Moreover, as described in Chapter 3.5.4.1, staves themselves are constructed from different materials bonded by epoxy resin. End-of-stave-mount, which meets with staves supports inside the UT detector box, is made of aluminum. Staves supports themselves are made of stainless steel. Each different material has its own thermal contraction/expansion coefficient.

All these requirements led to use special iso-kinematic staves mounting system (Figure 3.21 a). In order to provide this kind of mounting system to each staves layer and each separate stave, four different designs of staves supports were needed. Different for top and bottom, as well as, for perpendicular and inclined staves Figure 3.22.

The frames are mounted on carbon fiber plates, which have on its core inserts, which are precisely machined with respect to each other in order to guarantee the precise placement of the frame and subsequently of the staves.

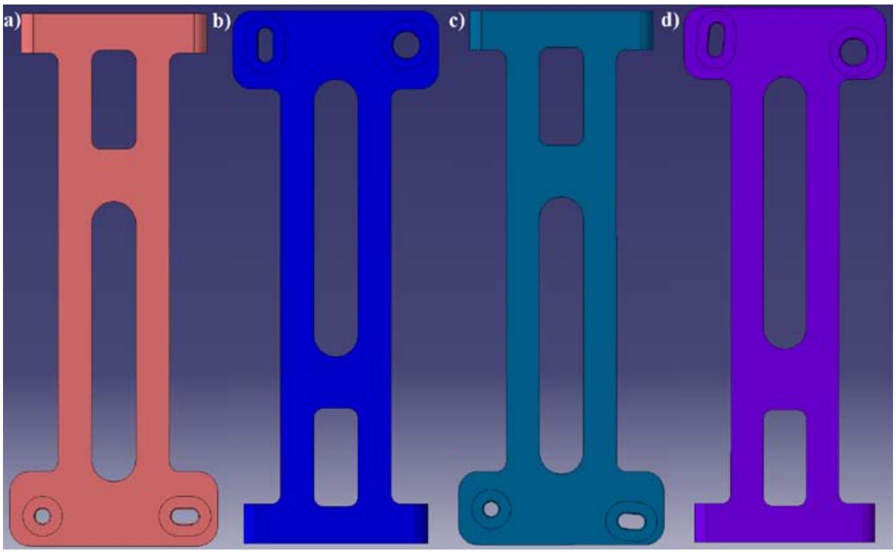

Figure 3.22 a) UTaX and UTbX top stave support; b) UTaX and UTbX bottom stave support; c) UTaU and UTbV top stave support; d) UTaU and UTbV bottom stave support [26]
Rysunek 3.22 a) Górna podpora dla stave-ów w warstwach UTaX i UTbX; b) Dolna podpora dla stave-ów w warstwach UTaX i UTbX; c) Górna podpora dla stave-ów w warstwach UTaU i UTbV; c) Dolna podpora dla stave-ów w warstwach UTaU i UTbV [26]

Staves supports for staves perpendicular to the beam pipe can be seen in Figure 3.22 a, b. Respectively, stave support for staves 5° inclined with respect to the beam pipe can be seen in Figure 3.22 c, d.

Each of four stave mounting points need different staves mounts (pins), using which, staves will be attached to their supports Figure 3.23 and Figure 3.24.

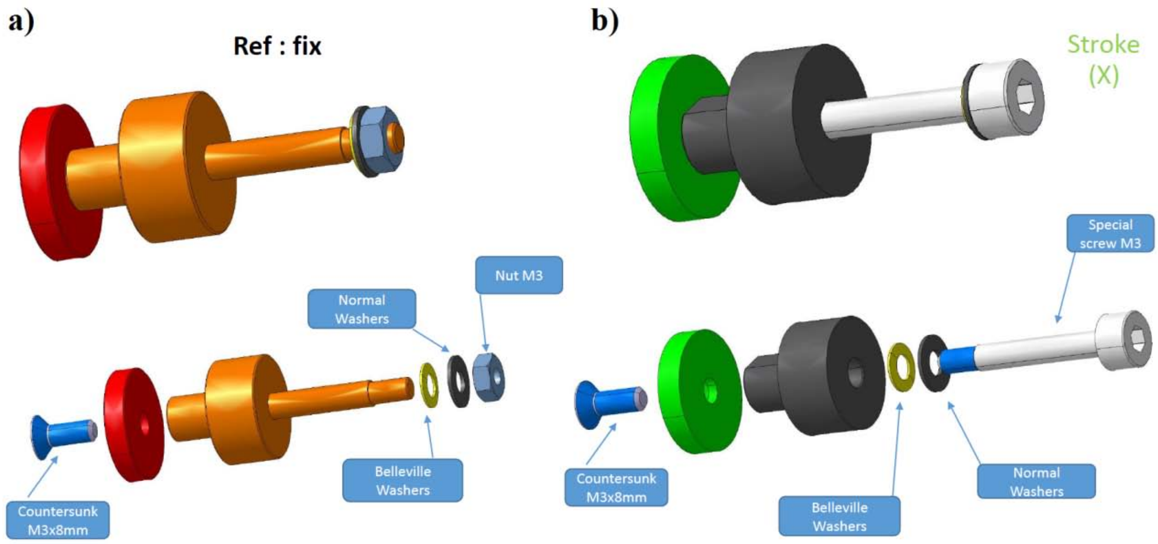

Figure 3.23 a) Pins for top reference (fixed) position; b) Pins for top x-free mount [26]
Rysunek 3.23 a) Piny górnej referencyjnej (ustalonej) pozycji; b) Piny górnej x-luźnej pozycji [26]

Pin design for top reference position (Figure 3.23 a), allows to fix stave in one of its mounting points in order to achieve precise stave positioning. It blocks all stave movements in this point.

Pin design for top x-free mount (x-stroke) (Figure 3.23 b), allows for slight movement along x-direction. Hence, it can compensate transverse thermal contraction/expansion of the stave. In addition, it blocks z-direction stave movement, which prevents stave from twisting.

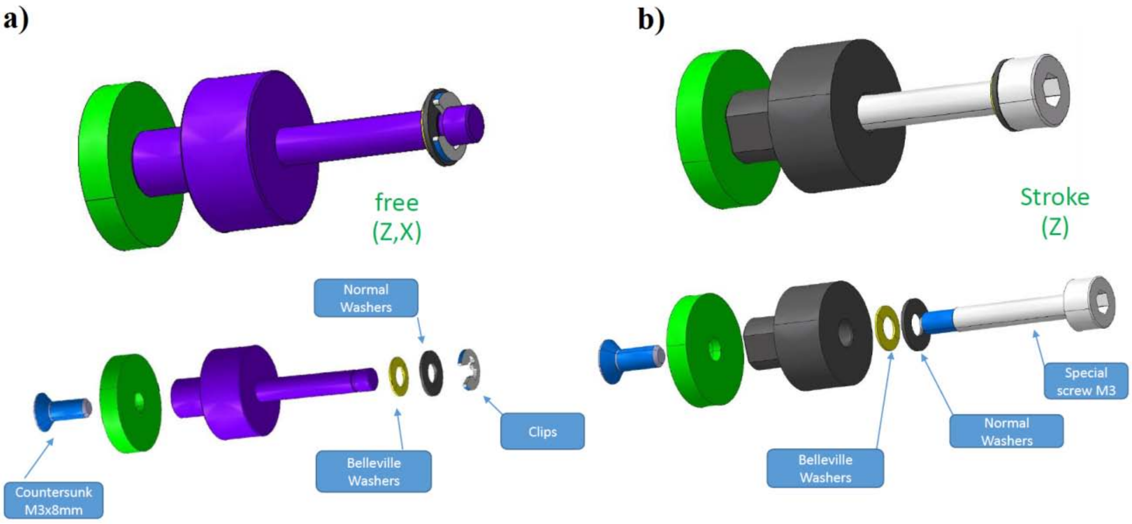

Figure 3.24 a) Pins for bottom x,z-free mount; b) Pins for bottom z-free mount [26]
Rysunek 3.24 a) Piny dolnej x,z-luźnej pozycji; b) Piny dolnej z-luźnej pozycji [26]

Pin design for bottom x,z-free mount (Figure 3.24 a), allows stave to move freely in both x-direction and z-direction. It can compensate both transverse and longitudinal stave contraction/expansion.

Pin design for bottom z-free mount (z-stroke) (Figure 3.24 b), allows for slight movement along z-direction. Hence, it can compensate longitudinal thermal contraction/expansion of the stave. In addition, it blocks x-direction stave movement, which prevents stave from twisting.

Because both bottom stave mounts allow free movement in z-direction, they are able to compensate longitudinal stave contraction/expansion.

- Stave support material

Choosing a material for staves supports was a difficult task. They had to meet several requirements. Among others, the most important one, was small thermal contraction/expansion coefficient. Second very important issue was ability to form (machine) the material in complicated shapes, in order to meet very limited space inside the UT detector box.

Three different materials were carefully considered.

First of them, the best in terms of thermal contraction/expansion coefficient, was carbon fiber reinforced composite. It has an excellent thermal properties, ranging $1.1*10^{-6}\,K^{-1}$. However, its main drawbacks are being hard to form and being expensive.

Second material, was an aluminum. With thermal contraction/expansion coefficient at the level of $23.1*10^{-6}\,K^{-1}$, much higher than carbon fiber, it was also the cheapest option to choose. Additionally, easiest and simplest to machine into whatever shape necessary.

Last material taken into consideration was stainless steel. Its thermal contraction/expansion coefficient equals $10.1*10^{-6}\,K^{-1}$, and is lower than aluminum but still significantly higher than carbon fiber. It is easy to machine, so there is no problem to form it in necessary shape.

Carbon fiber reinforced composite was rejected due to its high price and difficulties with manufacturing.

After further consideration aluminum was rejected as well, due to its high thermal contraction/expansion coefficient. Under 50°C of ΔT the stave mounts would shift significantly, if staves supports were made of aluminum.

Finally, stainless steel was chosen as a material for staves supports.

An equation for calculation a thermal contraction/expansion is presented in Formula 3.1.

$$\Delta L = L * \gamma * \Delta T \qquad \text{Formula 3.1}$$

where:

L – length of the element;

γ – thermal contraction/expansion coefficient;

ΔT – temperature difference;

ΔL – contracted/elongated value.

Stave support mounting points dimensions are shown in Figure 3.25. Longitudinally, from top/bottom box plate to pin mounts equals 203mm. Transverse, between pin mounts equals 57.5mm.

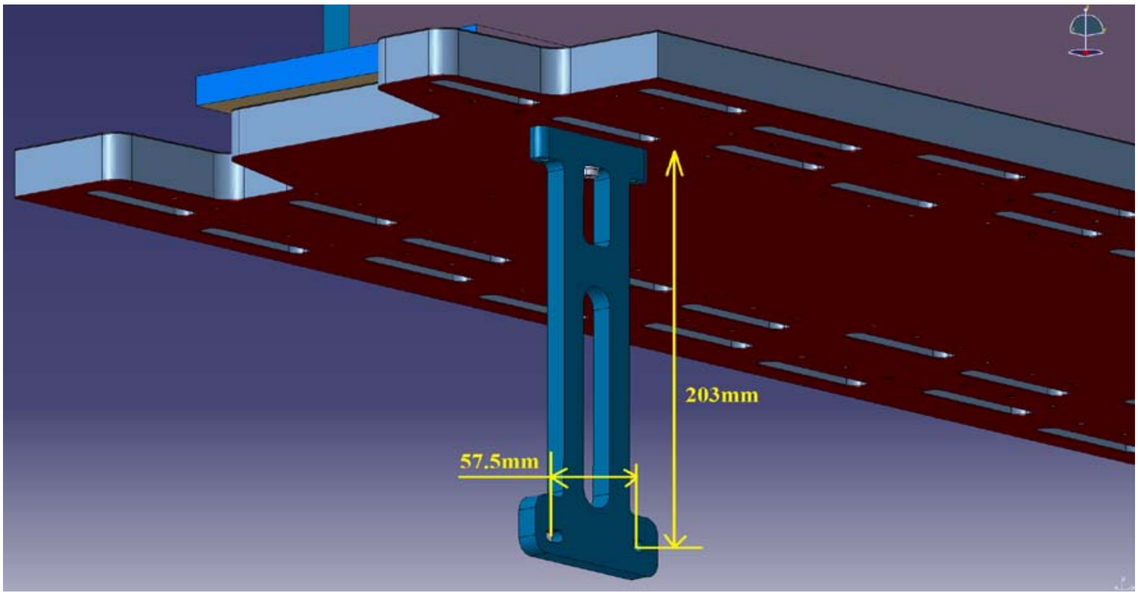

Figure 3.25 Stave support dimensions [26]

Rysunek 3.25 Wymiary podpory dla stave'a [26]

Calculation of different stave support displacement, longitudinally and transverse, depending on different material used, is presented in Table 3.3.

Table 3.3 Different displacement depending on different material used.
Tabela 3.3 Różne przemieszczenie w zależności od rodzaju użytego materiału.

$\Delta T = 50°C$	**Carbon fiber**	**Stainless steel**	**Aluminum**
γ coefficient	$1.1*10^{-6}K^{-1}$	$10.1*10^{-6}K^{-1}$	$23.1*10^{-6}K^{-1}$
Displacement [mm]			
Transverse (57.5mm)	0,003	0,029	0.066
Longitudinal (203mm)	0.011	0.103	0.235

As can be seen from the Table 3.3, changes in material dimensions for stainless steel, under given ΔT is more than half smaller in comparison to aluminum. Therefore, stainless steel was chosen for staves supports inside the UT detector box.

3.5.4.3. CO_2 Cooling manifolds

Because all silicon sensors has to be kept at a temperature below -5°C in order to maintain its long term reliability, as well as, all read-out electronics (ASICs) embedded in staves has to stay below 40°C in order to maintain their stable operation, the UT detector box has to be cooled down, to meet these requirements.

Evaporative CO_2 cooling system was applied in order to keep the UT detector box components within required temperatures. Figure 3.26 shows a coolant distribution system for one half of the box (34 staves).

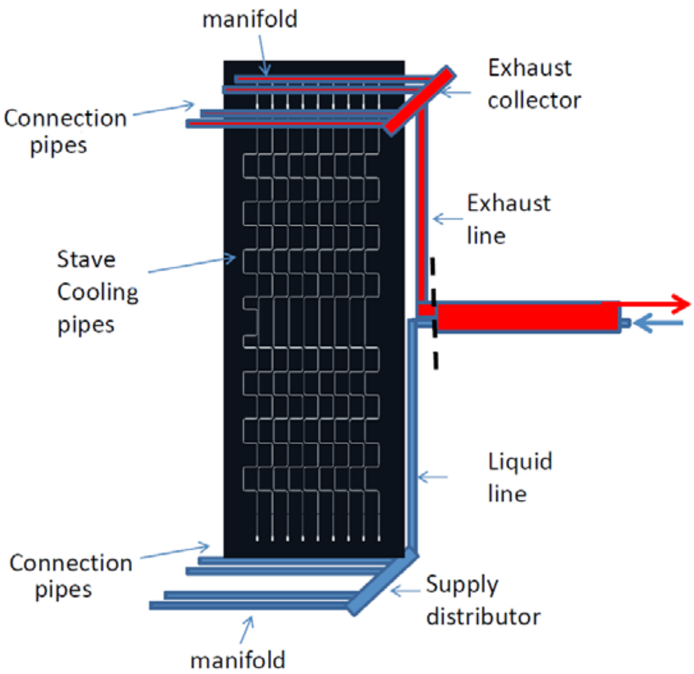

Figure 3.26 CO_2 cooling distribution system [33]
Rysunek 3.26 System dystrybucji chłodziwa CO_2 [33]

Integration of cooling manifold inside the UT detector box is very challenging. Especially due to the fact that, cooling pipes going to extreme staves layers has to pass through internal layers without colliding with their infrastructure. Another issue to solve is the fact that staves in each layer are staggered, so supply cooling pipes has to reach different positions not only between two different layers but also within a single layer. In addition, for inclined staves layers cooling pies has to reach stave connector at a given angle. Moreover pipes needs some flexibility in order to cope with cooling stresses as well as with manufacturing and positioning tolerances. Furthermore, space between end of saves and top and bottom box plates is strictly limited, and cannot be enlarged. 3D model of CO_2 distribution system for one quarter of the UT box can be seen in Figure 3.27. Cooling manifolds can be also seen in the Figure 3.16.

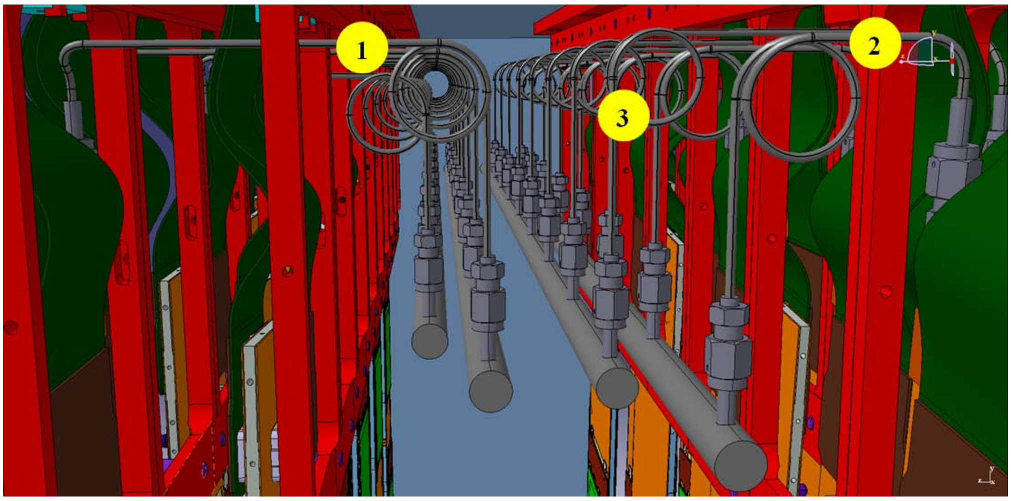

Figure 3.27 CO_2 cooling distribution system 3D model

Rysunek 3.27 Model 3D systemu dystrybucji chłodziwa CO_2

Cooling pipe distributing CO_2 to extreme staves layer is marked as "1" in the Figure 3.27.
Cooling pipe distributing CO_2 to inner staves layer is marked as "2" in the Figure 3.27.
Cooling pipe loop (helix) allowing for its flexibility is marked as "3" in the Figure 3.27.

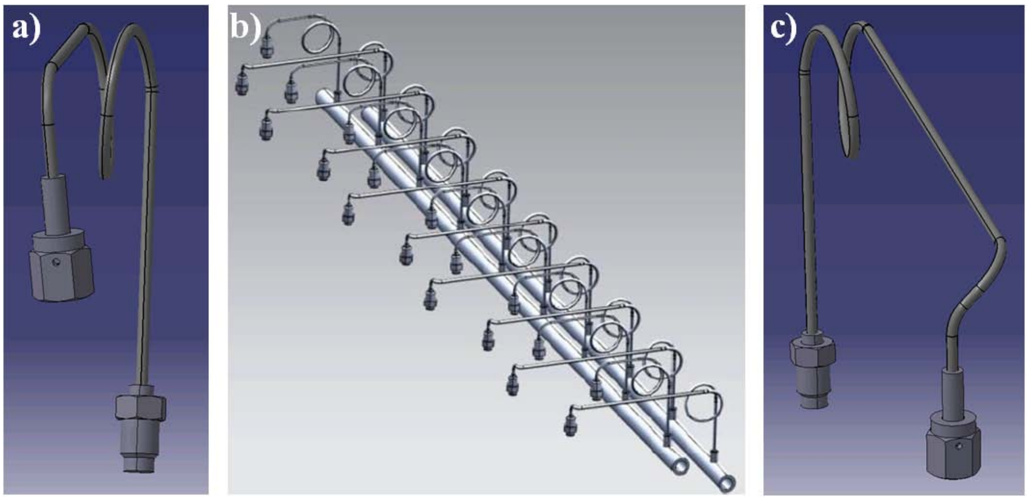

Figure 3.28 a) Inner layer inclined stave pipe; b) Manifold for two adjacent stave curtains; c) Extreme layer perpendicular stave pipe

Rysunek 3.28 a) Rurka stave'a kątowego w warstwie wewnętrznej; b) Kolektor dla dwóch sąsiadujących kurtyn stave-ów; c) Rurka stave'a prostopadłego w warstwie zewnętrznej.

Four different types of cooling pipes connecting staves with manifolds had to be designed in order to meet all the requirements. Two different types, for staves perpendicular to the beam pipe (Figure 3.28 c) and inclined staves (Figure 3.28 a), as well as, two different lengths of each type because of staggering staves in each layer.

Outside diameter of the helix pipes (Figure 3.27 and Figure 3.28) connecting manifold rail with stave connector is 2.5mm. Wall thickness of those pipes is 0.25mm.

In the Figure 3.28 b, there are two cooling manifolds for two adjacent staves layers. Each individual stave is supply from cooling manifold dedicated to its layer. Therefore, there are four manifolds required for CO_2 distribution to all staves. Cooling manifolds are placed in the top and bottom part of the UT detector box, (attached to top and bottom box plates (Figure 3.16)), and in the middle between two sets of staves layers (Figure 3.16 and Figure 3.27).

Cooling manifolds are supplied by single pipe going outside the box Figure 3.29 b.

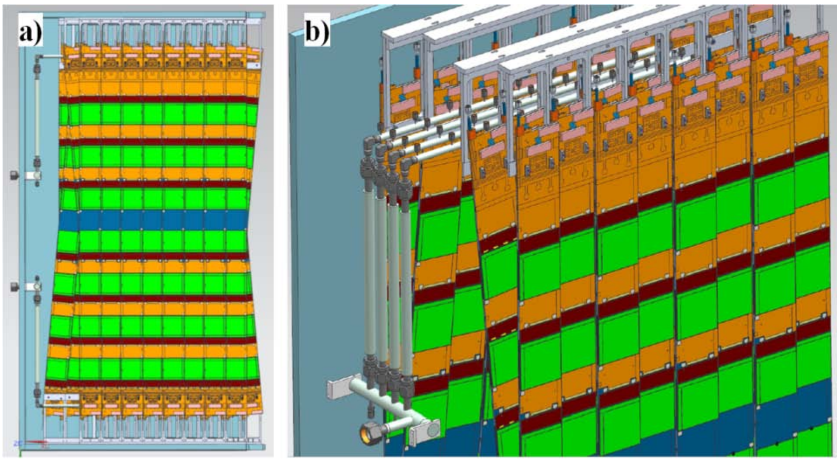

Figure 3.29 a) Cooling manifolds going outside the box; b) Single pipe supply for 4 manifolds [33]
Rysunek 3.29 a) Wyjście kolektorów chłodzących poza skrzynkę detektora; b) Pojedyncze zasilanie 4 kolektorów [33]

Supply pipes for top and bottom (inlet and outlet) manifolds enters the box in the middle of its height Figure 3.29 a. There is a local cooling box foreseen as an intermediate connection between CO_2 supply in the LHCb cavern and manifolds inside the UT detector box.

The main rail manifold pipes supplying coolant for all staves in single layer (8 or 9 staves), (Figure 3.28 b and Figure 3.31) are outside diameter of 12mm and wall thickness of 1mm.

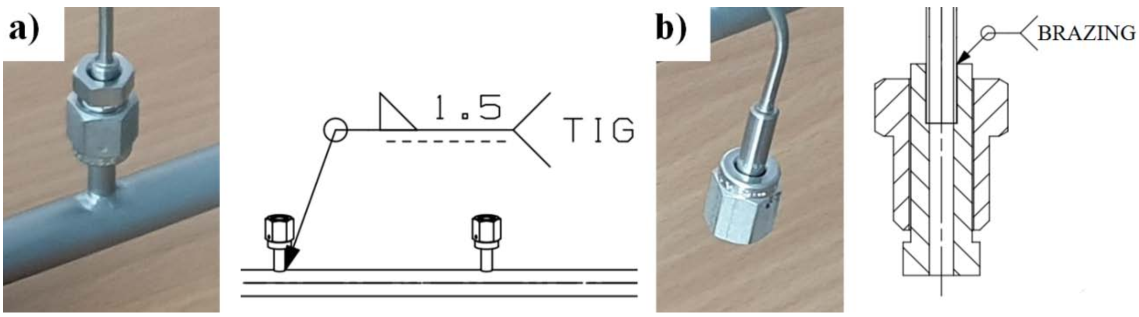

Figure 3.30 a) VCR welded to supply pipe using TIG; b) VCR brazed to helix pipe [33]
Rysunek 3.30 a) VCR przyspawany do rury zasilającej przy użyciu TIG; b) VCR przylutowany do spiralnej rurki [33]

Special VCR connections Figure 3.30 are used in order to connect cooling pipes with supply rail and cooling pipes with stave. The VCR connections are welded using micro TIG to the main manifold rail (Figure 3.30 a) and brazed to the helix pipe (Figure 3.30 b).

The prototype of CO_2 cooling manifold for 9 staves UT detector layer can be seen in Figure 3.31.

Figure 3.31 CO_2 cooling manifold prototype [33]
Rysunek 3.31 Prototyp kolektora chłodzącego CO_2 [33]

The material used for cooling pipes and manifolds is stainless steel 316L.

3.5.4.4. Data read-out cables (Pigtails) inside UT detector box and PEPI volume

In order to read signals generated by silicon sensors special types of cables were implemented. Data read-out cables (called "Pigtails") because they are curved significantly, inside and outside of the box. They are flat, 60mm wide and ~1.4mm thick cables, and consists of about 400 copper paths stacked in several layers. They serves for conducting signals coming from sensors, as well as, provides low voltage power for electronics (ASICs) embedded inside staves.

Pigtails cables connects staves inside the UT detector box and backplane inside the PEPI volume. Each pigtail cable, (from each side of the stave), goes to separate connector on the PEPI backplane Figure 3.32.

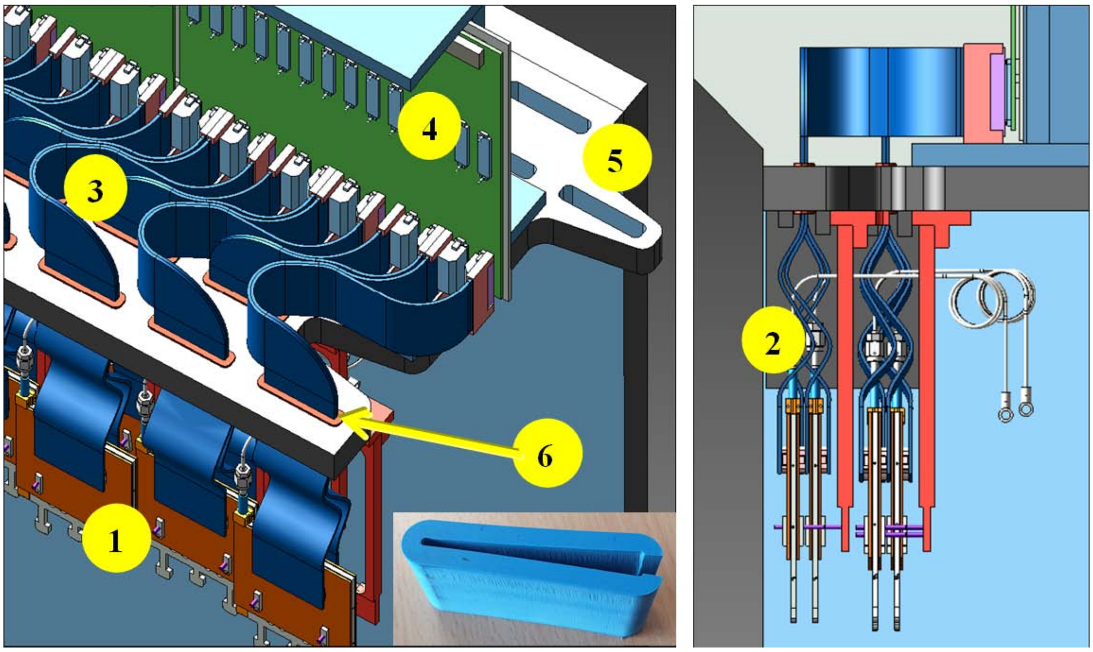

Figure 3.32 UT Pigtails 3D model [36]
Rysunek 3.32 UT Pigtails – model 3D [36]

In the Figure 3.32, following components can be distinguished:

1. Staves inside the UT detector box.
2. Pigtails, inside the UT detector box, attached to staves connectors.
3. Pigtails, inside PEPI volume, making several turns to reach backplane connectors.
4. Backplane, inside PEPI volume, attached to the C-Frame.
5. Top and bottom plates of the UT box with elongated holes for pigtails passing.
6. EPDM rubber seal to maintain the box requirements (light and gas tightness), and preventing moisture from penetrating inside the box.

Two rows of elongated holes on each side of top and bottom plate of the box refers to the 4 staves curtains inside the box. Two staves curtains are placed on the interaction point (IP) side, another two from the magnet side. Two adjacent staves layers are served by 2 PEPI volumes, one on the top of the detector box, another on the bottom, for each end of stave respectively.

To serve its purpose, pigtails has to be tailored into specified shape, in order to fit in very tight and crowded space, as well as, they must perform a specific 90 degrees turn to reach backplane located in PEPI volume – Figure 3.32 right side. Some of them, which serves for inclined staves must in addition be 5 degrees inclined, on the end going inside the UT detector box, in order to fit into the connector on inclined staves.

In order to meet all the requirements, four different pigtails types had been designed.

First, is straight short (XS) Figure 3.33 b. This particular pigtail is made for staves which are perpendicular to the beam pipe (straight). They occur in outer layers. Due to staggering of the staves in each layer some staves are closer to the backplane in PEPI volume some of them are further from it. Straight short pigtails (XS), serves perpendicular staves closer to the backplane.

Second, straight long (XL) Figure 3.33 a. Straight long pigtails (XL) serves perpendicular staves further from the backplane.

Third, stereo short (XS) Figure 3.33 d. This particular pigtail is made for staves which are inclined with respect to the beam pipe (angled/"stereo"). They occur in inner layers. Due to staggering of the staves in each layer some staves are closer to the backplane in PEPI volume some of them are further from it. Stereo short pigtails (XS), serves inclined staves closer to the backplane.

Forth, stereo long (XL) Figure 3.33 c. Stereo long pigtails (XL) serves inclined staves further from the backplane.

Purple dash line in Figure 3.33 represents top and bottom detector box plates, where pigtails passes through, from UT detector box volume into PEPI volume.

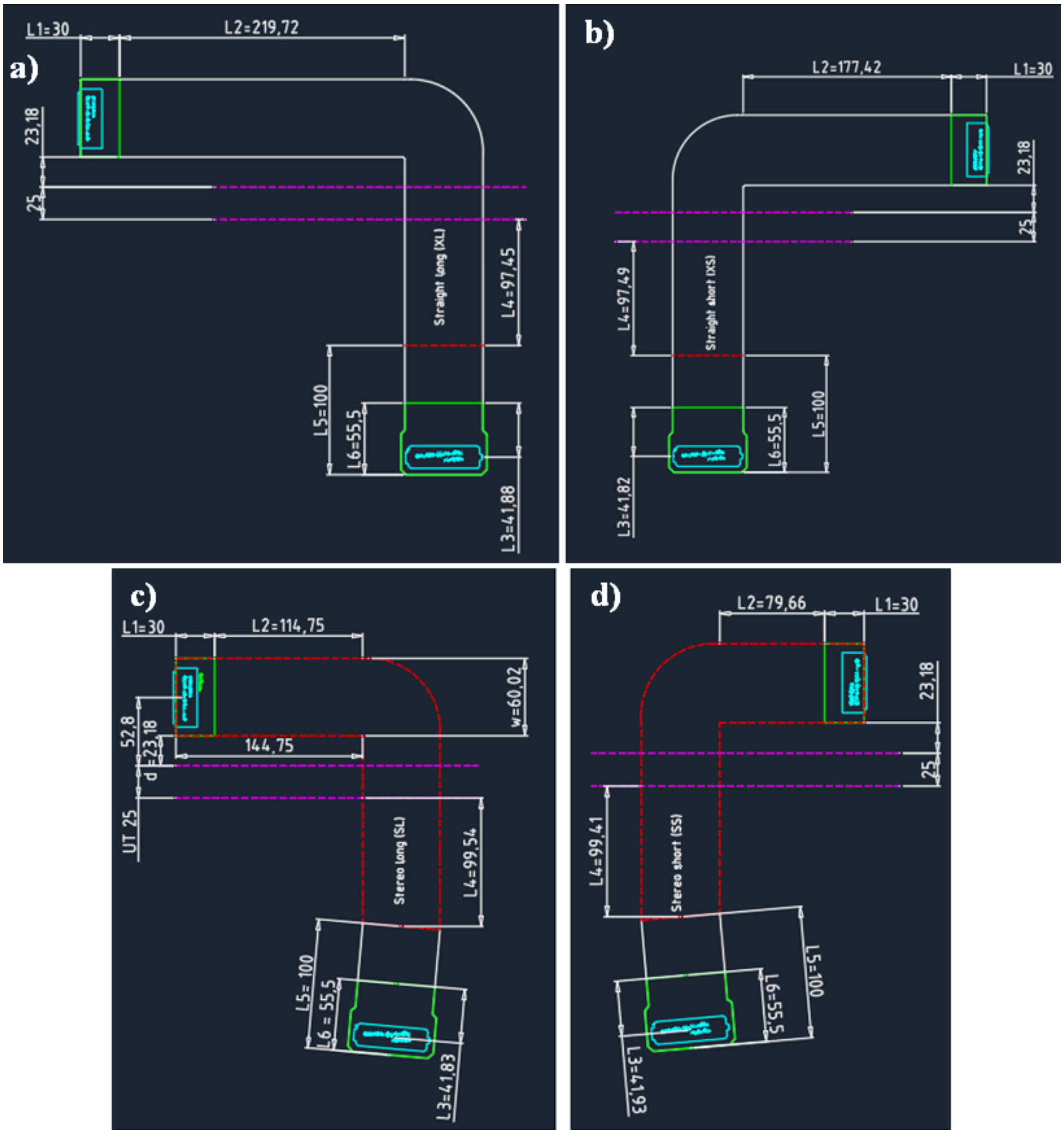

Figure 3.33 Pigtails different types: a) Straight long; b) Straight short; c) Stereo long; d) Stereo short [35]

Rysunek 3.33 Różne typy Pigtails-ów: a) Prosty długi; b) Prosty krótki; c) Kątowy długi; d) Kątowy krótki [35]

As silicon sensors are placed on both sides of the staves, pigtails connectors are placed on both sides of the stave as well – Figure 3.34 a, and on both of stave ends. It leads to the amount of 4 pigtails per stave, and 272 pigtails in total. A model of the pigtail cable is shown in Figure 3.34 b.

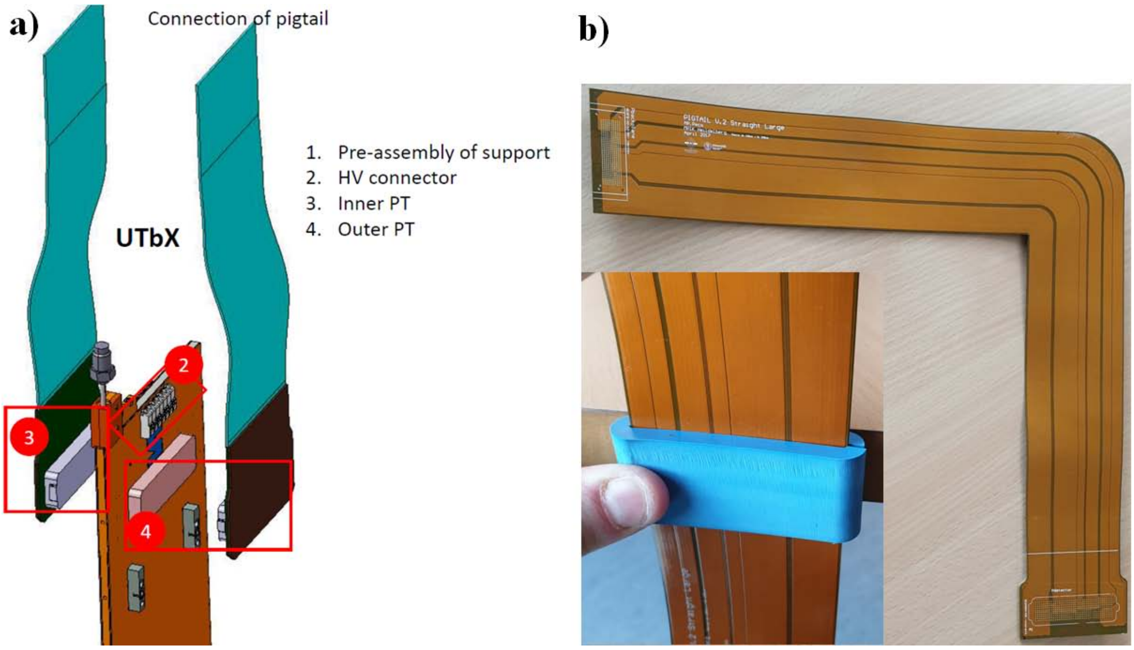

Figure 3.34 a) Two data read-out cables on each end of stave; b) Pigtail cable [26]
Rysunek 3.34 a) Dwa kable odczytu danych na każdym końcu stave'a; b) Kabel Pigtail [26]

Each pigtail has a 1mm thick aluminum stiffener on both of its ends in order to provide necessary stiffness, rigidity and support in the connector area – Figure 3.33 a-d marked in green lines; Figure 3.34 a and Figure 3.35 in brown color.

Because mock-up studies shown that stiffness of the pigtail cable is quite significant and it may cause stave connector to disconnect, special clamps were designed in order to prevent this from happening.

First iteration of the clamp design can be seen in Figure 3.35. The idea is to hold pigtails connectors on both sides simultaneously against each other and against the stave.

The most difficult task is to find the correct shape for the clamp and fit it in very limited space between staves, where they are overlapped – right most view in Figure 3.35.

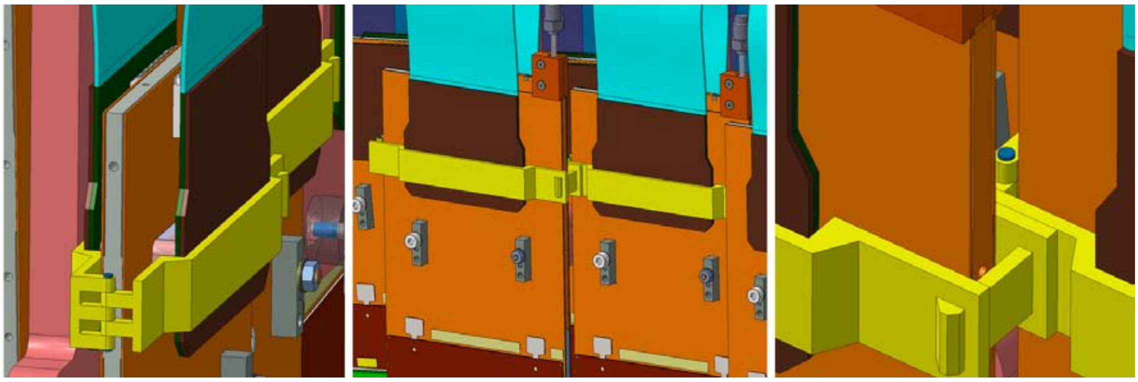

Figure 3.35 Pigtails clamps on stave side
Rysunek 3.35 Klamry pigtails-ów po stronie stave-ów

3.5.4.5. High voltage cables

High voltage cables serves for powering silicon sensors. Silicon sensors must be supplied with certain amount of energy, in order to produce signals when particles flies through them. The magnitude of voltage delivered to each sensor is up to 500V. Due to radiation degradation of silicon sensors with time, the voltage supplied to each individual sensor needs to be increased to maintain sensor performance. From about 80V at the beginning of detector operation, up to 500V at the end of silicon sensor lifetime.

Silicon sensors are placed on staves inside the UT detector box. Hence, high voltage cables must reach each stave inside the box to deliver necessary power. The high voltage connectors are placed on each side of the stave on both its ends Figure 3.34 a number 2. Foreseen connectors are WAGO 2060, with self tightening mechanism [1].

One of the requirements from electronic team, about high voltage cables, was that they must be insulated (shielded) until the very end, where they reach stave connector.

The high voltage cable chosen to be use in UT detector consists of rubber coating, aluminum foil shielding for all wires and each separate wire is wrapped with polymer insulation – CABLE HT 14x0.14mm^2 3kV. An example of this kind of cable, (with 56 wires inside), is presented in Figure 3.36.

Figure 3.36 UT high voltage cable
Rysunek 3.36 Kabel wysokiego napięcia dla detektora UT

Each stave hosts 14-15 silicon sensors. Each half of the stave is equipped with 6-7 sensors, which creates a need to attach 6-7 pairs of high voltage cables to each stave end. Therefore, one big cable containing 14 little high voltage wires is delivered to each end of each stave (Figure 3.37). On the arrival of cable at the end of stave it is peel off and wires are attached to the staves high voltage connectors.

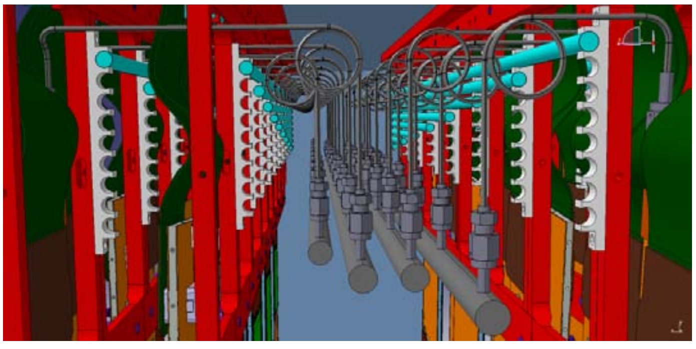

Figure 3.37 High voltage cables attached to staves supports
Rysunek 3.37 Kable wysokiego napięcia przytwierdzone do wsparcia stave-ów

HV cables are attached to the staves supports using plastic or aluminum brackets, shown in white in Figure 3.37.

High voltage cables enter the box through 4 holes in 4 corners of the side plate of the UT detector box – Figure 3.38.

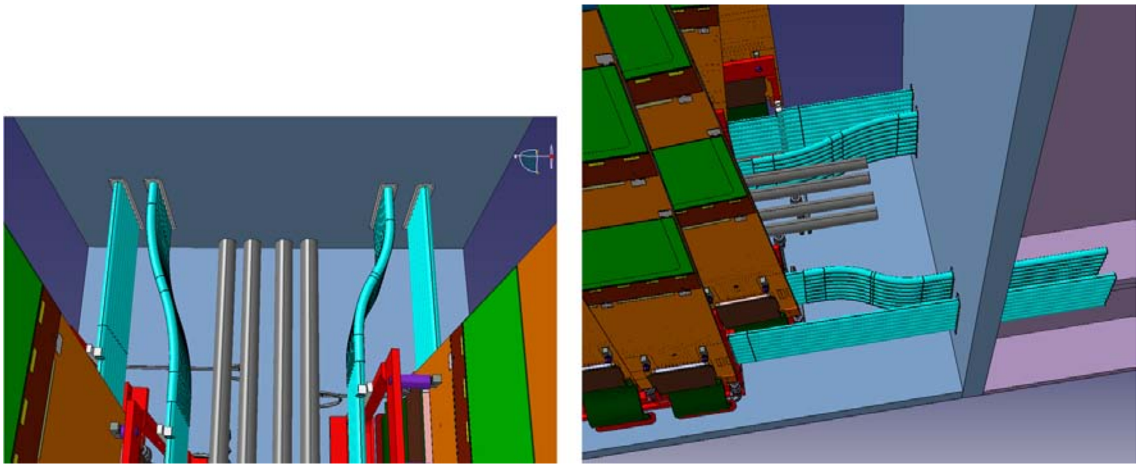

Figure 3.38 High voltage cables entering UT detector box
Rysunek 3.38 Kable wysokiego napięcia wchodzące do skrzynki detektora UT

In order to fulfill box requirements in terms of light and gas tightness, special fit-through system from Roxtec company has been applied, in the areas, where cables entering the UT box. It consists of special aluminum frame Figure 3.39 a, with EPDM rubber blocks inside it, Figure 3.39 b. Rubber elements are cut on half and a hole inside it can be adjusted in diameter to seal different cable sizes. After placing cables in correct position, aluminum frame is tighten around rubber and closes the gaps. The same system can be used for cables, water pipes, dry air pipes as well as for CO_2 cooling pipes.

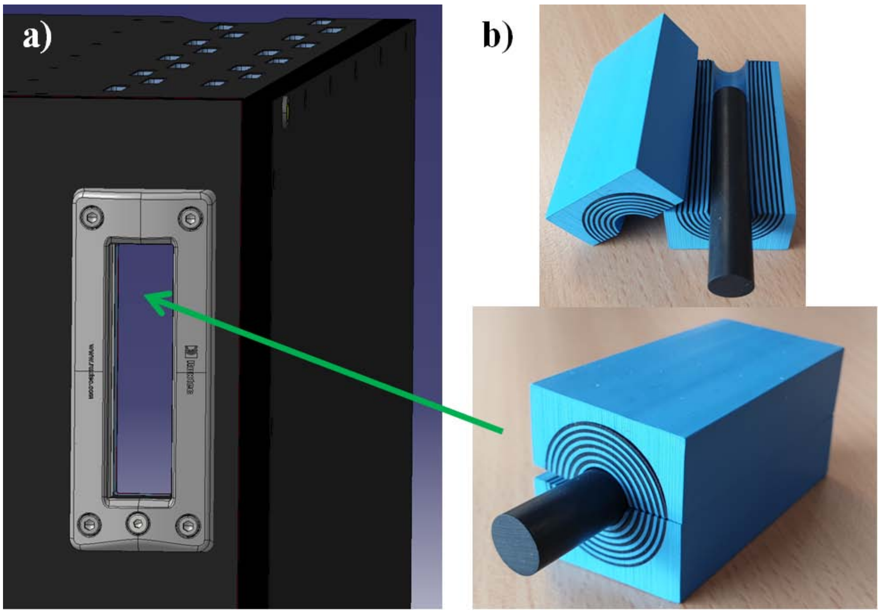

Figure 3.39 a) Roxtec compressible aluminum frame; b) EPDM rubber seal
Rysunek 3.39 a) Zaciskowa aluminiowa rama Roxtec; b) Uszczelka z gumy EPDM

3.5.4.6. Dry air lines

Flushing UT box with dry air, or as is under discussion with dry nitrogen, is vitally important to prevent condensation inside UT detector box. The temperature inside the box is around –30 degrees Celsius. Therefore, dew point of the dry air must be very low, to avoid ice creation on the elements inside the detector box. Using dry nitrogen has one more advantage, which is fire safety. Nitrogen is a neutral gas and flushing the UT box with it, would make it fire resistant. As mentioned in Chapter 3.5.4.5 about high voltage cables, the magnitude of electric voltage powering the silicon sensors is up to 500V. Hence, it can create danger of fire in dry air environment.

Final choice for UT detector box flushing is the nitrogen.

Requirements for the dry air:

- it must be sufficiently dry,
- it must be oil free – no oil form dry gas installation can enter the detector box. It would damage the silicon sensors.
- there must be slight over pressure inside the UT box in order to avoid moisture from outside of the box going inside it.

3.6. C-Frame integration

It is very important to position UT detector box in correct place with respect to LHCb interaction point (IP). Therefore, proper UT box mounting system must be developed in order to fulfill this need.

Upstream tracker detector C-Frame is an interface between LHCb cavern and the UT detector box, Figure 3.2, number 2. From the cavern side, C-Frame is attached to the rails, which are the part of LHCb cavern infrastructure and they are precisely positioned with respect to interaction point (IP). On the other side, C-Frame is attached to the UT detector box made of carbon reinforced Airex foam. In this way, C-Frame provides positioning and support for the UT detector box.

In this chapter the requirements, purpose and geometry of the UT C-Frame will be described.

3.6.1. C-Frame requirements

Main requirements for the UT C-Frame are the following:

1. **UT C-Frame must allow for A and C side of the UT detector box to open**
   Due to maintenance needs, (of the UT detector itself, but also of the beryllium beam pipe crossing it), UT C-Frame design should fulfill the requirement of UT detector opening and accessibility (Chapter 3.5.1).

2. **UT C-Frame has to support UT detector box**
   The UT C-Frame shall provide support for UT detector box and precise positioning of the box with respect to the interaction point (IP).

3. **UT C-Frame should provide a support for a cable chain**
   One end of each (four) cable chains going into detector is attach to the C-Frame (on top and bottom of it) – Figure 3.2. Hence, each C-Frame has to withstand a load from two cable chains, as well as, provide required supporting structure for supporting them.

4. **UT C-Frame shall provide a support for PEPI**
   On the top and bottom of the UT detector box, there are PEPI volumes located – Figure 3.2. They are attached directly to the horizontal beams of the UT C-Frame. Therefore, construction of the C-Frame should provide enough freedom PEPI inside.
   For example, welds between the C-Frame plates cannot be too big and bulky. They must be machined afterwards in order to liberate the space for PEPI electronics.

5. **UT C-Frame needs to support patch panels**
   There is an interface needed between cables coming from a cable chain and before they go inside PEPI. This interfaces are called "patch panels". They must be attached to the C-Frame as well. Hence, C-Frame must allow for this.

6. **UT C-Frame should provide a support for local CO_2 cooling box**
   Before entering UT detector box, CO_2 cooling lines goes through local box, which further distributes coolant inside the UT detector box. Local CO_2 cooling box must be attached to the C-Frame. Therefore, C-Frame shell allow for attaching the box.

7. **UT C-Frame must be rigid**
   The UT C-Frame must be stiff enough to withstand forces applied to it and do not transmit them to the carbon box or to delicate staves inside it.

8. **UT C-Frame should be made of material, which have low activation level**
   In order to access the detector area during technical stops, C-Frame material should not irradiate too much. It is in particular important, due to the fact that, C-Frame is a large structure.

3.6.2. C-Frame geometry

Upstream tracker detector C-Frame is an interface between LHCb cavern rails and the UT detector box, Figure 3.2, number 2. It is attached to the cavern rails in the way allowing for A and C side opening.

On the bottom face of the C-Frame there are 4 sliders attached, Figure 3.40 c. They transfer the load of the frame and detector box to the bottom rail, and allow to slide along it. In addition, there is an interface between C-Frame and sliders made of precise thickness steel plates, allowing for shimming and accurate C-Frame positioning on rails.

Because of the 0.206° inclination of the beam pipe inside the LHCb cavern, bottom C-Frame shimming plates must be machined with respective angle, in order to provide correct detector position with respect to the beam line. The UT detector silicon sensors curtains must be perpendicular to the beam line.

Top part of the C-Frame is attached to the top rail using rolling guidance – Figure 3.40 b, which allows longitudinal movement and provides stability to the construction.

UT box is precisely attached to the C-Frame using inserts and dowel pins. C-Frame connects with each half of the UT detector box by top, bottom and side plates, Figure 3.40 a.

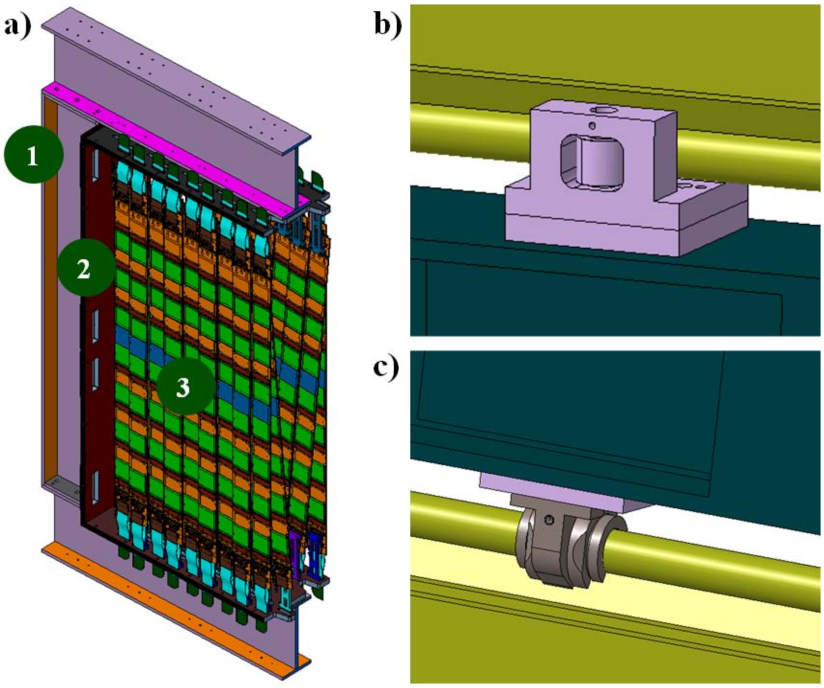

Figure 3.40 a) UT C-Frame and box with staves; b) Top C-Frame rolling guidance; c) Bottom C-Frame supporting slider [26]

Rysunek 3.40 a) Rama-C wspierająca detektor UT wraz ze skrzynką detektora zawierającą stavey; b) Górna rolkowa prowadnica ramy-C; c) Dolny suwak wspierający ramę-C [26]

In the Figure 3.40 a, following components can be distinguished:

1. UT C-Frame.
2. UT detector box made from carbon reinforced sandwich plates (chapter 3.3.3) – attached to C-Frame.
3. Staves with silicon sensors inside UT box – attached to top and bottom carbon box plates using staves supports (Chapter 3.5.4.2).

Outer dimensions of the UT C-Frame are dictated by the space allocated in between the rails inside LHCb cavern. Inner dimensions of the C-Frame must match the UT detector box size.

Dimensions of the C-Frame supporting one halve of the UT detector box are the following (Figure 3.41 a b):

- outer height (y-axis): 2650 mm,
- outer width (x-axis): 1340 mm,
- inner height (y-axis): 1970 mm,
- inner width (x-axis): 1025 mm,
- depth (z-axis): 170 mm.

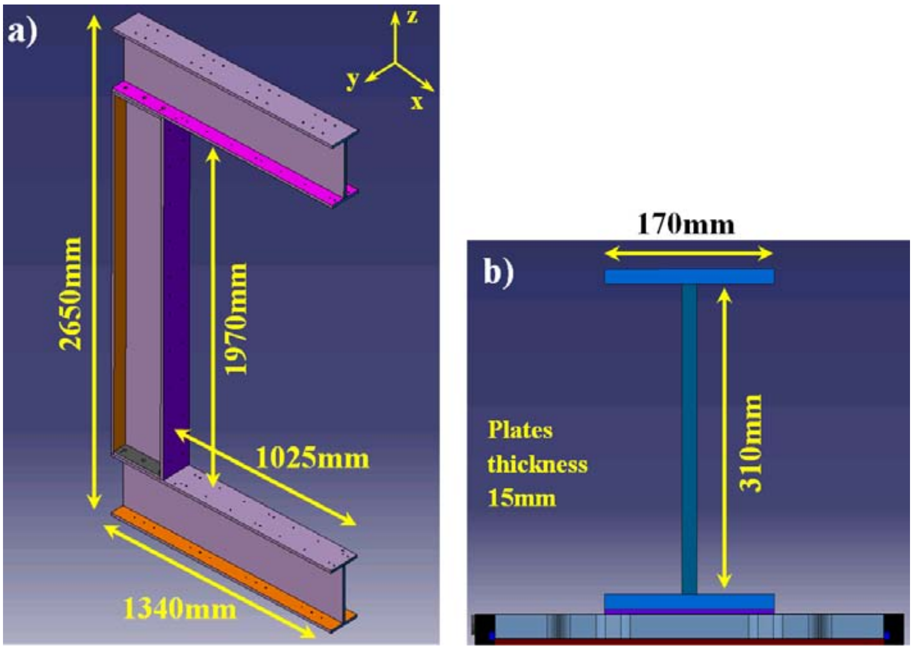

Figure 3.41 a) C-Frame external dimensions; b) C-Frame cross-section

Rysunek 3.41 a) Zewnętrzne wymiary ramy-C; b) Przekrój ramy-C

As it appears from Figure 3.41 b, upstream tracker detector C-Frame has a cross-section of an I-beam. This design fulfills the requirement of rigidity, and allows the C-Frame to withstand the load applied to it.

All plates of the UT C-Frame are 15mm thick. They contribute to C-Frame durability and in addition allow to mount on them all the necessary components. For example they can host blind threaded holes, or precise positioning holes for dowel pins, in order to accurately mount required equipment.

3.6.3. C-Frame material

Final material choice will be made after all forces applied to the C-Frame will be identified and final FEM analysis completed. However, not only mechanical rigidity is taken into account when it comes to choose C-Frame material. CO_2 cooling lines guided along C-Frame, as well as, heat dissipated by PEPI volumes attached to it, may affect thermal contraction/expansion of aluminum C-Frame. From this reason and also because mechanical stiffness is mandatory, the material used to build the UT C-Frame will be stainless steel 316L. It is worse in terms of activation, but precise positioning of sensors and long term reliability plays first role in this case.

3.7. PEPI integration and mechanics

PEPI – (Peripheral Electronics) – hosts electronic boards, which collects signals from the detector sensors and passes them out of the detector area. Those boards needs to be properly supported, maintain connected with both, staves inside the detector, as well as, with cables coming from the cable chain. In addition they need to be cooled down, in order to maintain their performance. There are four PEPI volumes per each detector half, two on the top and two on the bottom – Figure 3.42. They are attached to the C-Frame.

3.7.1. PEPI requirements

Main requirements for the UT PEPI are the following:

1. **UT PEPI must provide support for electronic boards**
   There are several different PCB's (Printed Circuit Boards) inside PEPI volume. All of them need mechanical support and precise positioning in order to connect with cables, as well as, with other electronic boards.

2. **UT PEPI has to provide cooling for DCB's (Data Concentration Boards)**
   Data concentration boards process signals from silicon sensors and send them out using fiber optic cables. The electronic chips on these boards needs to stay within certain temperature (below 40°C), in order to maintain boards performance. Hence, they must be cooled, using water cooling, which has to be included inside the PEPI volume.

3. **UT PEPI shell provide support for cables**
   There are various types of cables inside PEPI volume, which need support. The support provided must meet cable type requirements e.g. minimum bending radius for fiber optic cables is much higher than for other cables. PEPI volume design must take it under consideration.

4. **UT PEPI should be enclosed**
   Many electronic components is vulnerable to dust and other type of pollution. Even the LHCb cavern environment is rather clean, it is desirable to protect electronic boards inside the PEPI against the surroundings. Hence, PEPI volume design should include a protective cover around it.

5. **UT PEPI needs to be semi gas tight**
   Due to large temperature difference inside PEPI and inside detector box, there is a risk of moisture production in the pigtails area. This moisture could then penetrate inside the detector box along pigtails. Hence, PEPI volume will be flushed with dry air to avoid eliminate such possibility. Additionally, it will help with electronic cooling by forcing convection inside the PEPI volume. Therefore, PEPI volume must me reasonably gas tight in order to fulfill those requirements.

3.7.2. PEPI layout

This chapter describes integration studies inside the PEPI volume. In the Figure 3.42 3D assembly of PEPI volume is presented.

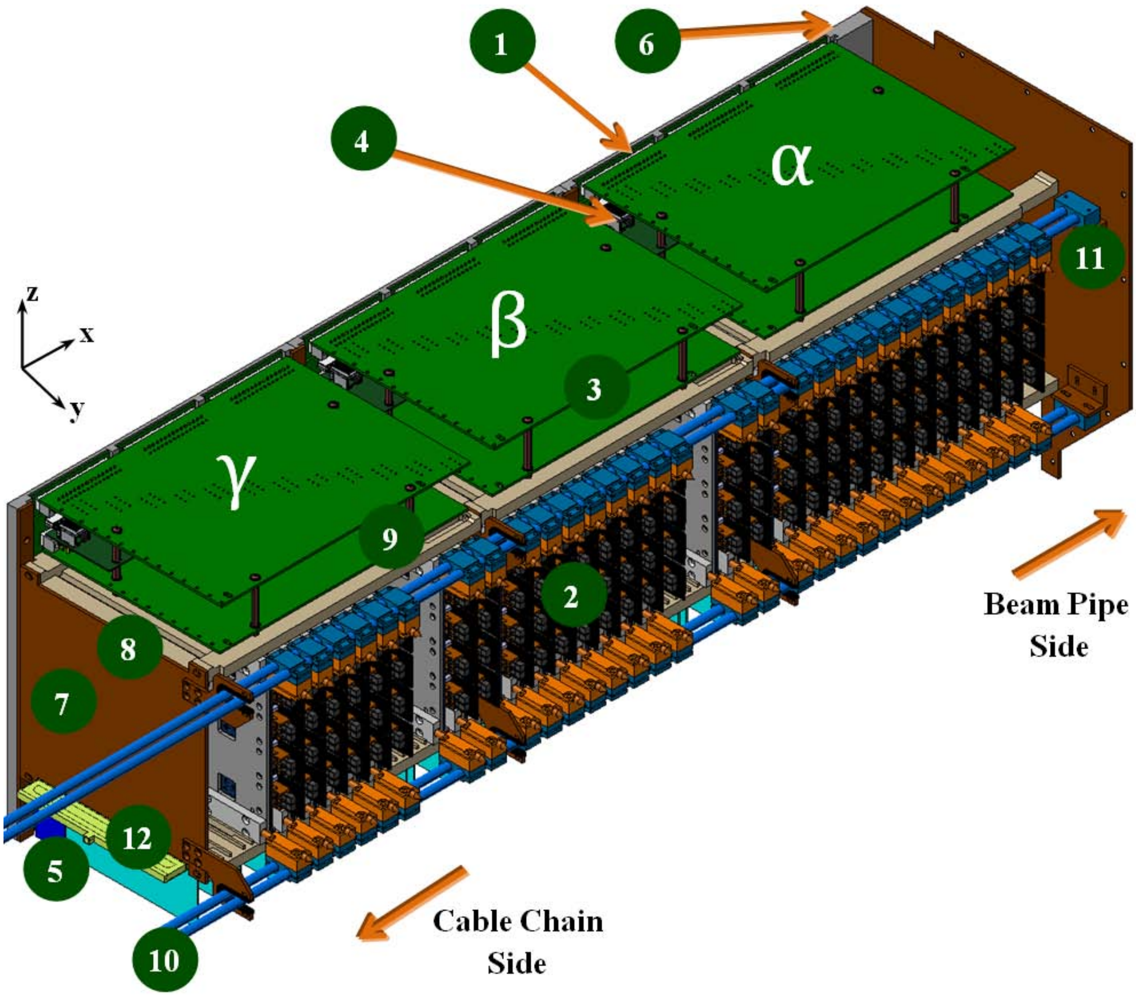

Figure 3.42 PEPI 3D assembly
Rysunek 3.42 Złożenie 3D PEPI

In the Figure 3.42, following components of the PEPI volume can be distinguished:

1. Backplane.
2. DCB (Data Concentration Board) cards equipped with cooling interface.
3. Low voltage power breakout boards – inner (bottom) and outer (top).
4. Telemetry breakout boards.
5. Data read-out cables (Pigtails).
6. Base plates – supporting backplanes.
7. Walls – supporting DCB card guides and water cooling pipes.
8. DCB card guides – provides rough guidance of DCB card to the backplane connector.
9. Stand-offs – supporting low voltage power breakout boards and telemetry breakout boards.
10. Water cooling pipes – supplies DCB's with coolant.
11. Water return clamp with its support.
12. Dry air duct – supplying bottom part of the PEPI volume with dry air.

Inside PEPI volume there are three different compartments – alpha, beta and gamma. Each one of them is about 300mm wide, which gives total length for 3 compartments of ~900mm (along x-axis). Height of the PEPI volume is defined by space between I-beam plates in the C-Frame (Figure 3.41 b) and equals 310mm (along z-axis). Width of the PEPI volume is defined by backplane thickness, DCB cards length together with their cooling interface and fiber optic cables minimum bending radius. Totally in y-axis PEPI is 282.5mm wide. Consecutive compartments differ by signal density, and therefore different amount of DCB cards is attached to the backplanes in each compartment (Figure 3.42). The further from the beam pipe the lower signal density and less DCB cards are connected in each compartment – 12 cards in alpha compartment, 10 cards in beta compartment and 8 cards in gamma compartment. It has an impact on the amount of cables going to each compartment. Alpha compartment is the most crowded in terms of cable connections. Moreover, all cables going to alpha compartment has to pass through gamma and beta compartments [4]. More about cables can be found in Chapter 3.7.4 describing PEPI cabling. Weight of completely assembled PEPI volume is estimated for around 80kg.

There are two different types of PEPI volume – True and Mirror [3]. They differ between detector halves and use different backplane design. The PEPI diagram shown in Figure 3.43 a, describes placement of True and Mirror PEPI volumes throughout the UT detector. In the Figure 3.43 b, there is one half of the detector C-Frame presented with 4 PEPI volumes attached.

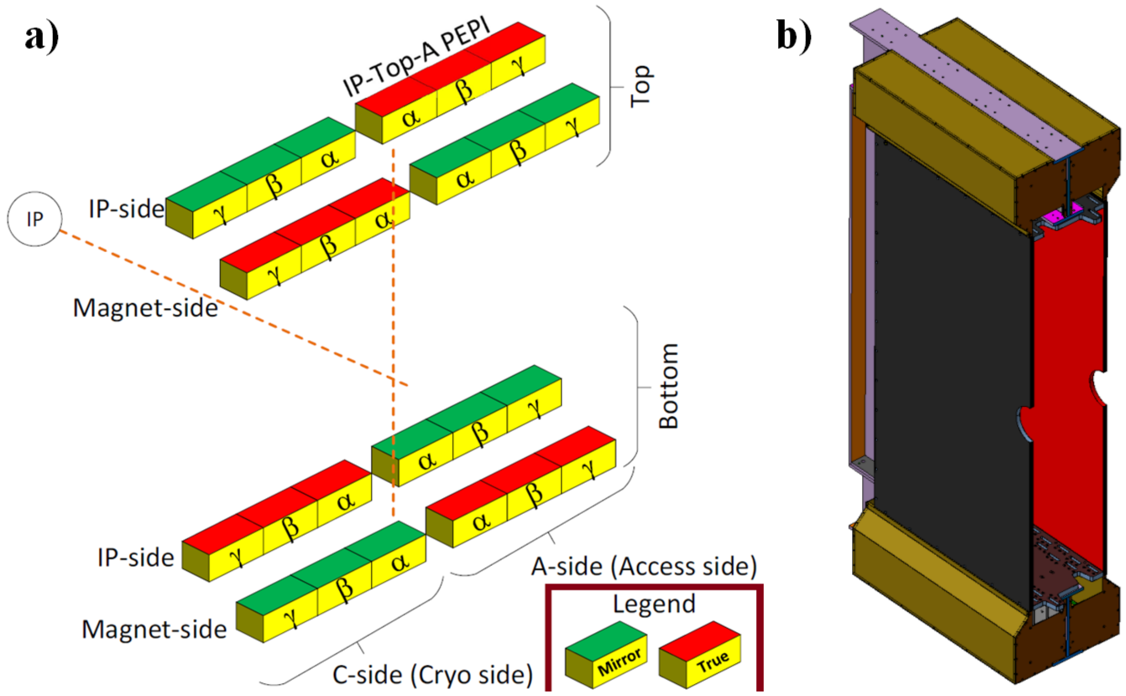

Figure 3.43 a) Layout of True and Mirror PEPI volumes; b) C-Frame with 4 PEPI volumes [26], [34]

Rysunek 3.43 a) Rozkład Prawdziwych i Odbitych objętości PEPI;
b) Rama-C i 4 objętości PEPI [26], [34]

3.7.3. PEPI electronics

There are several electronic boards, which needs to be integrated inside PEPI volume. They are marked with 1, 2, 3 and 4 numbers in Figure 3.42. This chapter shortly characterize them.

3.7.3.1. Backplane

Main electronic board inside PEPI volume is a backplane – Figure 3.44. It is also the most complex board. Is the biggest among others 300 x 276 mm. It hosts 12 DCB connectors, 12 data read-out cables (Pigtails) connectors, 6 low voltage power connectors and 3 telemetry connectors. In addition it consists of 28 layers and three additional boards behind for pigtails powering. All cables and other electronic boards are connected to the backplane. There are 3 backplanes per PEPI volume.

Due to its complexity and multiple layer construction, there is no possibility to make holes in it, in order to get mechanical fixation. Backplane is pressed against the base plate using walls and DCB card guides.

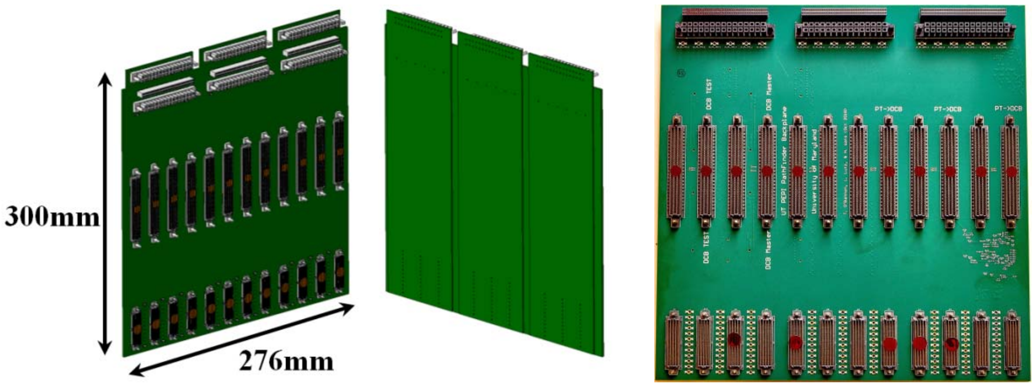

Figure 3.44 Backplane [2]
Rysunek 3.44 Backplane [2]

3.7.3.2. DCB cards

DCB – (Data Concentration Board) – Figure 3.45. Process signals from silicon sensors and send them further out using fiber optic cables. DCB's are connected to the backplane in the middle part of it. They require certain support to avoid stressing backplane connector and cooling in order to maintain their performance. Each DCB card has 4 mezzanine boards, shown in black in Figure 3.45, which hosts fiber optic connectors for data transfer. There are 30 to 36 data concentration boards per PEPI volume.

Each DCB card equipped with cooling interface weights about 1kg. Due to lack of space inside the PEPI volume and the fact that, all DCB's must be connected to cooling lines, the water cooling pipes act also as a support for the data concentration boards.

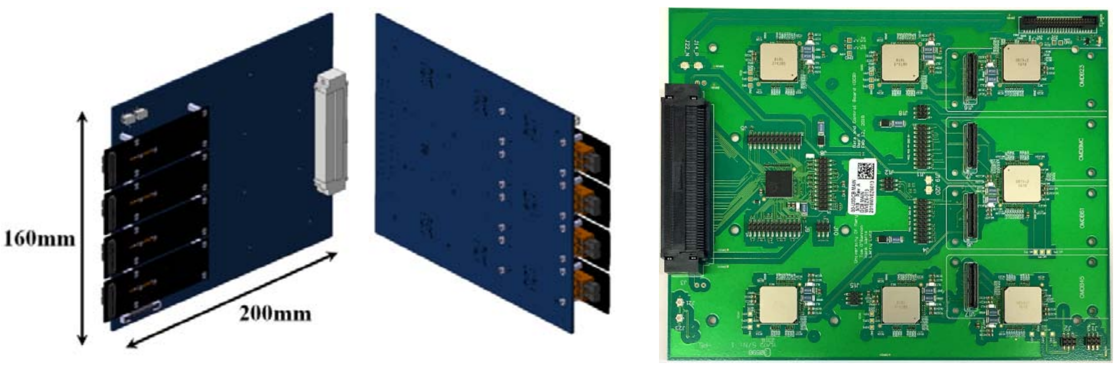

Figure 3.45 Data Concentration Board
Rysunek 3.45 Płyta Koncentracji Danych

3.7.3.3. Low Voltage Power Breakout Boards

LVPBB – (Low Voltage Power Breakout Board) – Figure 3.46. Provides intermediate connection between low voltage cables coming from cable chain and the backplane. LV litz wires are soldered to the LVPBB and the board is connected to the backplane, in the upper part of it. There are two LVPBB per backplane. Inner (located just above DCB's), serves for powering DCB cards and outer (located at the very top of the backplane), providing power for pigtails connectors. There are 6 low voltage power breakout boards per PEPI volume.

LVPBB's are supported by stand-offs, which comes from one of the DCB cards guides.

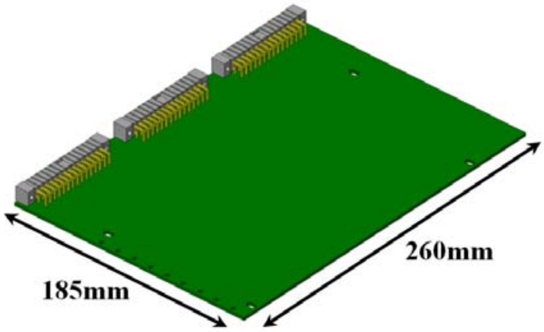

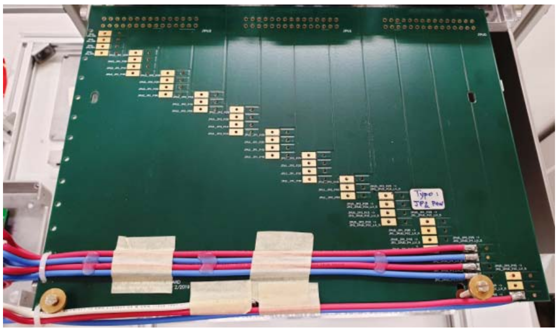

Figure 3.46 Low voltage power breakout board
Rysunek 3.46 Płytka rozgałęźna zasilania niskiego napięcia

3.7.3.4. Telemetry Breakout Boards

TelemetryBB – (Telemetry Breakout Board) – Figure 3.47. Provides intermediate connection between Ethernet cables coming from cable chain and the backplane. Ethernet cables connects to telemetry boards using RJ45 connectors. There are 18 connectors per board and 3 telemetry breakout boards per PEPI volume, which gives 54 Ethernet cables per PEPI.

Telemetry breakout board is located between low voltage power breakout boards and is supported by stand-offs as well.

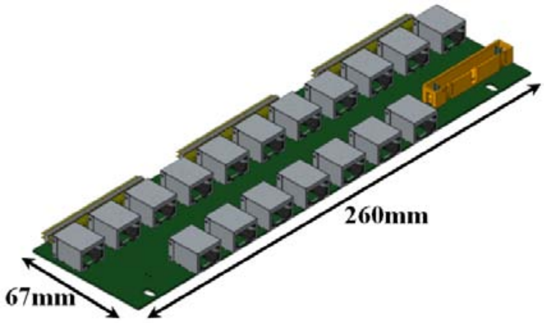

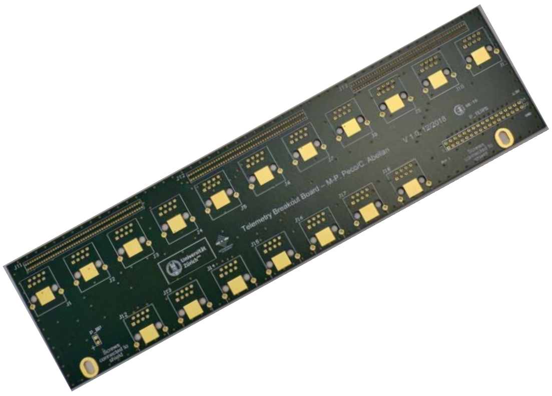

Figure 3.47 Telemetry breakout board
Rysunek 3.47 Płytka rozgałęźna sygnałów telemetrycznych

3.7.4. PEPI cabling

There are four different types of cables connected to PEPI. Each one of them serves different purpose, is made of different material and requires support in slight different way. Within PEPI volume, two main bunches of cables can be distinguished. First bunch, data read-out cables (Pigtails), which comes from inside the UT detector box and connects to PEPI backplane. Second bunch, low voltage cables, telemetry cables and fiber optic cables. They are attached respectively to low voltage boards, telemetry boards and data concentration boards, and guided outside PEPI volume, into the cable chain.

Inside PEPI volume there are three different compartments – alpha, beta and gamma. Alpha compartment (alpha backplane) serves for sensors located the closest to the beam pipe, therefore it has the heaviest load in terms of signal density and it is most crowded in terms of cable connections. Moreover, all cables going to alpha compartment has to pass through gamma and beta compartments – Figure 3.48 a. Furthermore, cables coming into, or going outside the PEPI volume, passes through only one wall of the PEPI volume, which is located on the cable chain side. Space available for routing low voltage and telemetry cables is shown in the Figure 3.48 b.

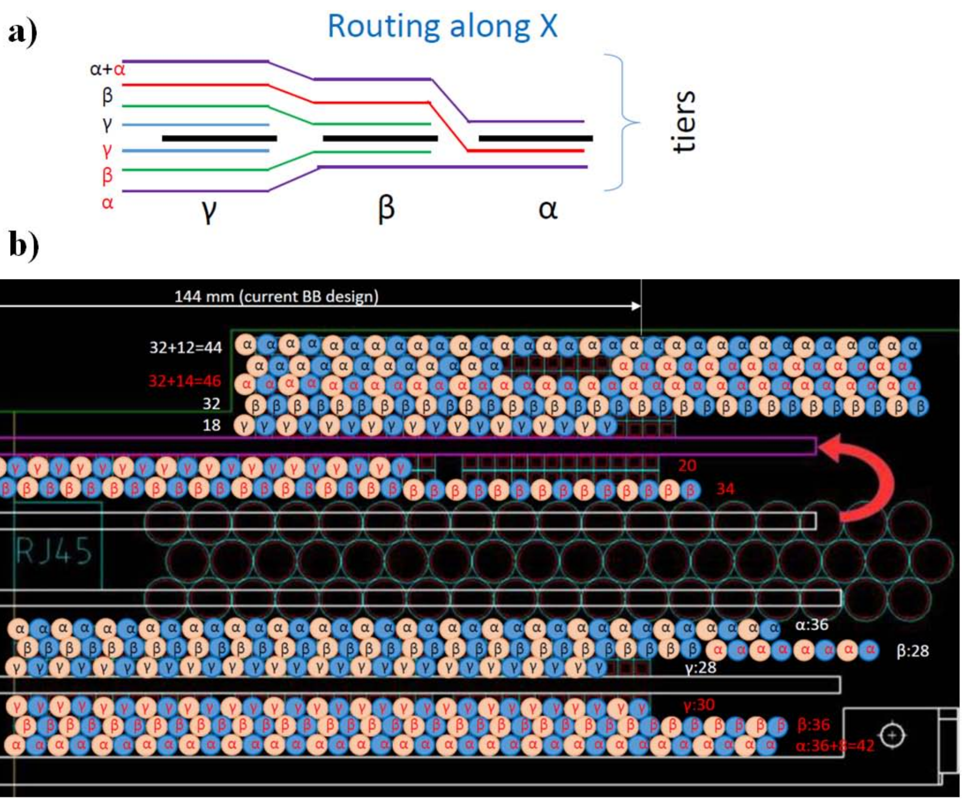

Figure 3.48 a) Low voltage cables routing from patch panel to respective compartments; b) Space available for low voltage and telemetry cables [37]

Rysunek 3.48 a) Prowadzenie kabli niskiego napięcia z panelu przejściowego do odpowiednich przedziałów; b) Przestrzeń dostępna dla kabli niskiego napięcia i kabli telemetrycznych [37]

3.7.4.1. Data read-out cables (Pigtails) inside PEPI volume

Data read-out cables (Pigtails) were described in details in Chapter 3.5.4.4. They connect UT staves, which hosts silicon sensors inside the detector box with backplane in the PEPI volume. They conduct signals from the silicon sensors and provide low voltage power for electronics embedded inside the staves. One PEPI volume hosts 32 to 36 pigtail cables. Figure 3.49 shows bottom part of the PEPI volume crowded with pigtail cables. They can also be seen in half-transparent green color in a Figure 3.50. Space available for pigtails inside PEPI volume is also presented in reference [3].

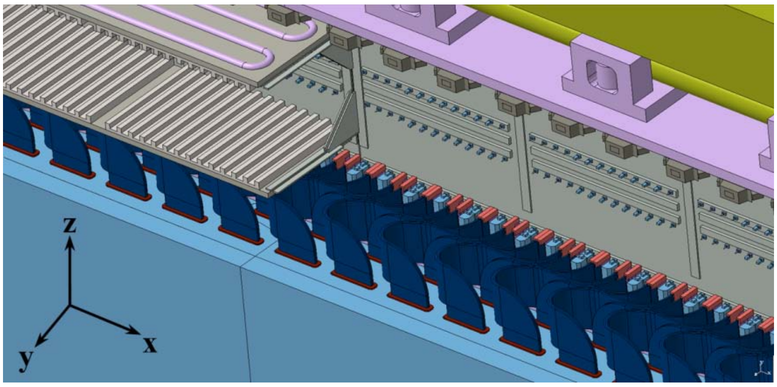

Figure 3.49 Pigtails inside PEPI volume [36], [3]

Rysunek 3.49 Kable typu "Pigtail" wewnątrz przestrzeni PEPI [36], [3]

3.7.4.2. Low voltage cables

Low voltage cables are used to power ASICs chips located on staves, as well as, DCB cards. There are 3 different LV power rails 1.2V, 1.5V and 2.5V. The cables coming from cable chain are 4mm^2 litz wires. They need to reach each backplane compartment inside the PEPI volume. Single backplane has 6 LV connectors with 30 pins each. There are 3 backplanes in one PEPI volume. Total amount of low voltage cables per PEPI volume is 540 pieces. The length of the cables varies dependably, which backplane inside the PEPI volume they need to reach. For an alpha backplane, (closest to the beam pipe), it is about 100cm, for beta backplane about 70cm, for gamma backplane around 40cm. Low voltage cables are routed between low voltage power breakout boards and telemetry breakout boards. An external diameter of LV cable is 3.4mm. Weight of a bunch of LV cables is estimated for about 12kg.

3.7.4.3. Telemetry cables (sense wires)

Telemetry cables serves for conducting signals sent by sensors embedded within hybrids chips on staves, which are used for monitoring detector performance. There are two main types of sensors read by telemetry cables. Platinum PT100 temperature sensor and voltage sensors, which measures the voltage supplied by regulators.

Telemetry cables are standard Ethernet cables and connects to telemetry boards using RJ45 connectors. It was necessary to flip by 180 degrees outer low voltage power breakout board, (marked in pink color in the Figure 3.48, and described as BB1), in order to fit 54 pieces, 8mm in diameter, shielded Ethernet cables, between inner and outer low voltage power breakout boards.

3.7.4.4. Fiber optic cables

The main issue in routing fiber optic cables is the fact that, they must be provided with proper minimum bending radius. Bending radius for fiber optics cannot be too tight, because it could cause the cable to crack and precious information conducted by cable would be lost or interfered. Because fiber optics conduct light instead of current, their bending radius needs to be much bigger than standard cable to allow for light reflection inside the fiber. Therefore, they consume more space and need bigger loops in the points, where they turn. For example, bending radius of single fiber (~1mm in diameter) coming from single DCB fiber optic connector, cannot be smaller than 40mm.

There are 30 to 36 DCB's inside one PEPI volume. Each one has 8 fiber optic connectors, which gives 288 fiber optic cables in the most crowded PEPI volume. Fiber optic cables are build as bunches, 12 fibers serving for one halve of 3 consecutive DCB cards, join together into one thicker cable, which is routed towards patch panel – Figure 3.50.

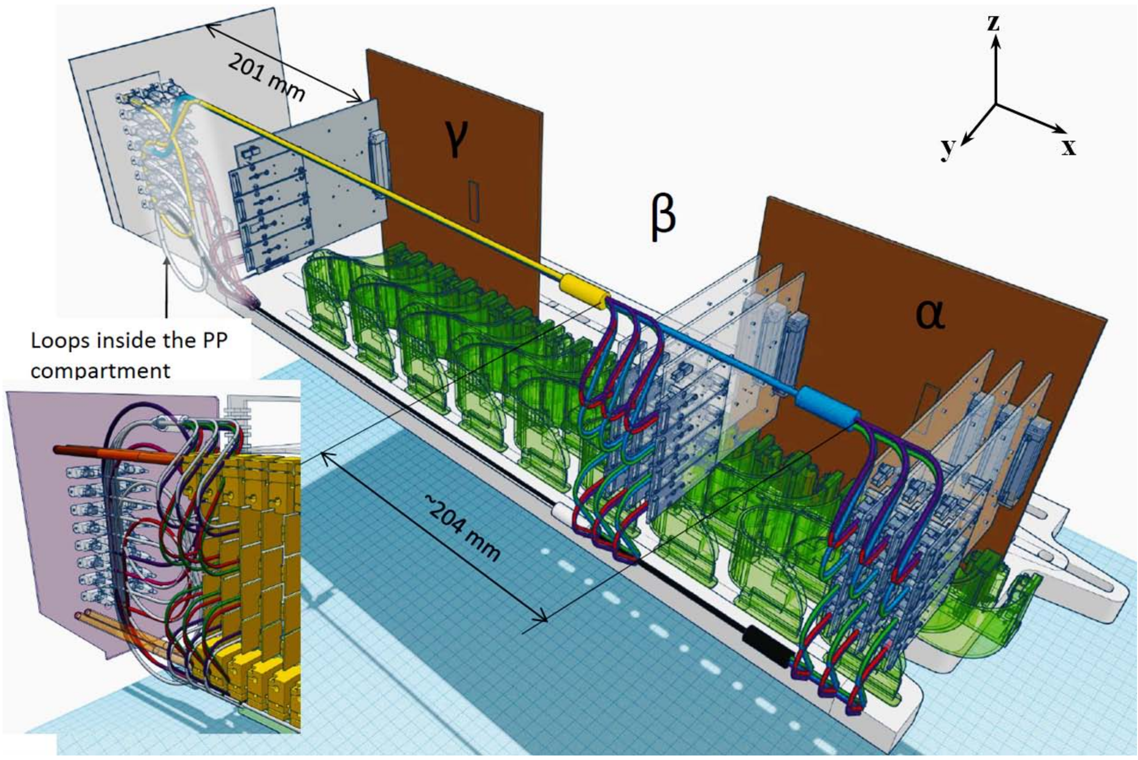

Figure 3.50 Fiber optic cables routing inside PEPI volume [37]
Rysunek 3.50 Prowadzenie światłowodów wewnątrz przestrzeni PEPI [37]

3.7.5. PEPI cabling patch panel

Patch panel is an intermediate element between cable chain and PEPI. It allows for connections between cables coming from cable chain and cables going inside PEPI volume. There are 3 patch panels serving PEPI volume cabling, (for low voltage cables, telemetry cables and fiber optic cables), and one additional patch panel which serves for high voltage cables going inside UT detector box. Figure 3.51 shows early stage of patch panels design and integration studies.

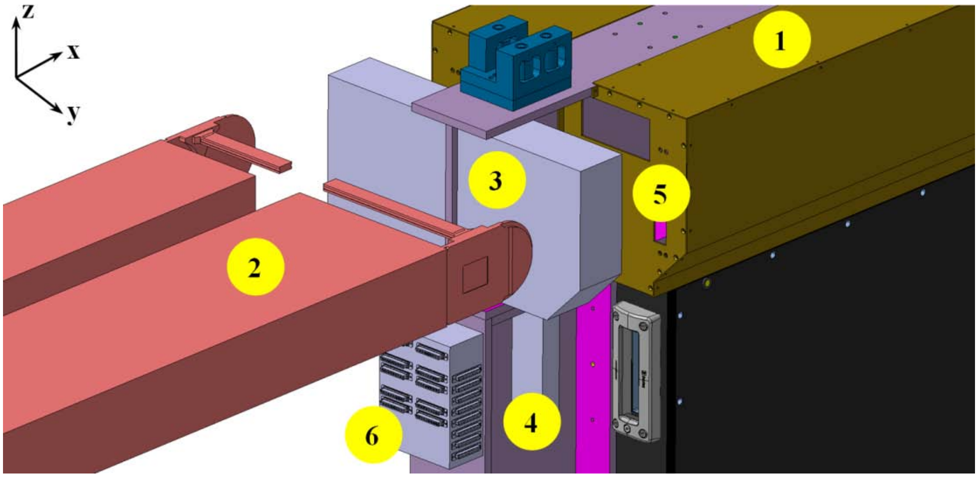

Figure 3.51 UT patch panels
Rysunek 3.51 Panele przejściowe UT

In the Figure 3.51, following components of the PEPI cabling patch panel system can be distinguished:

1. PEPI volume.
2. Cable chain.
3. Low voltage cables patch panel.
4. Telemetry cables patch panel.
5. Fiber optic cables patch panel.
6. High voltage cables patch panel.

An element marked in Figure 3.51 with number 5 is only one PEPI enclosure wall, through which, all bunches of cables have to pass inside PEPI volume. In addition to that, water cooling pipes and dry air supply lines has to be delivered through the same side as well.

The low voltage cables patch panel, (Figure 3.51, number 3), has to play one additional role than only intermediate connection between cable chain cables and PEPI volume cables. Because outputs from low voltage regulator boards located inside service bays crates are not fully compliant with inputs on the backplane inside PEPI, LV cables patch panel must allow for regrouping cables inside it, and only after that, pass properly grouped cables inside PEPI volume.

One of the solutions for building low voltage patch panel is to make it as an array of single, gold plated pins placed in 3D printed connectors, which can be print in ABS at CERN, Figure 3.52.

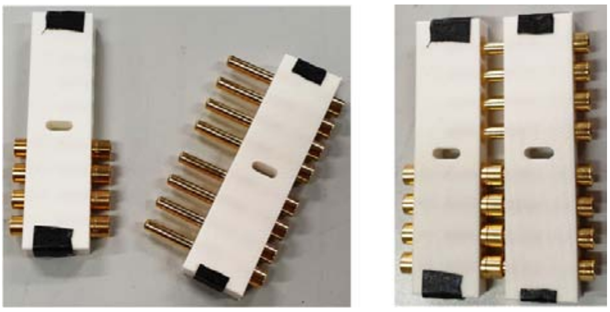

Figure 3.52 Low voltage patch panel prototype
Rysunek 3.52 Prototyp panelu przejściowego niskiego napięcia

The biggest advantage of this solution is flexibility and adaptability. Connectors can be adjusted in size, dependably from needs, which is important due to tight envelope available for patch panels.

3.7.6. PEPI Mechanics

There are several mechanical elements, which needs to be integrated inside PEPI volume, in order to support electronic boards, cables and provide cooling to electronics. They are marked with 6 to 9 numbers in Figure 3.42. Due to very limited space, each element has to play multiple roles, to satisfy all the requirements. Mechanical skeleton of the True PEPI volume can be seen in Figure 3.53.

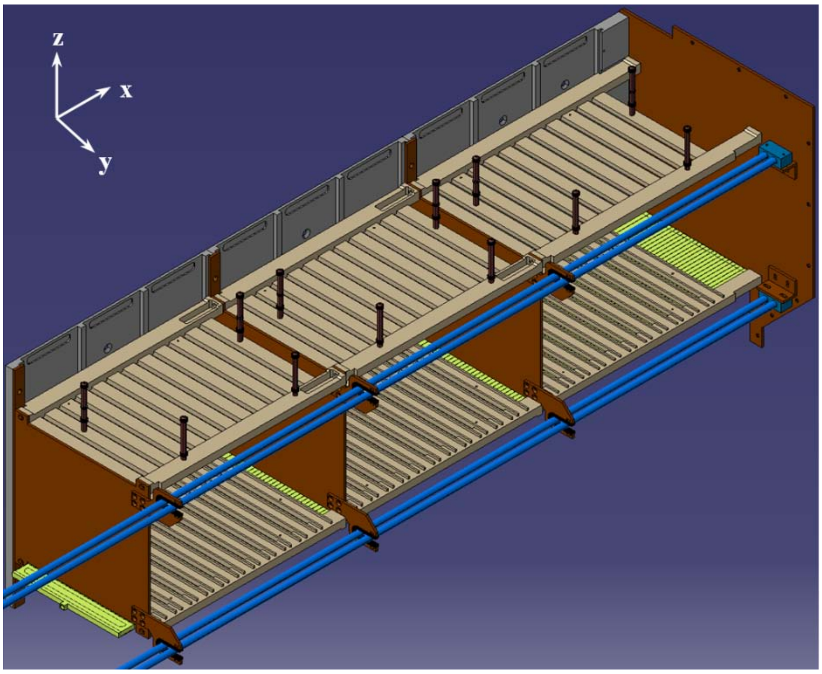

Figure 3.53 PEPI mechanics
Rysunek 3.53 Mechanika PEPI

3.7.6.1. Base plate

Base plates serves to support backplanes [2]. They act as an interface between C-Frame I-beam and backplanes, as well as, another PEPI mechanics. As there are three compartments in single PEPI, the same are three base plates respectively for alpha, beta and gamma compartment. They differ by the way how they support backplane. Beta and gamma base plates use walls to press backplane on the edges, while alpha base plate uses a groove channel and M3 nylon screws in order to fix the backplane in place. Due to the fact that, alpha compartment may need to overhang beyond C-Frame towards another half of the detector, it was necessary to have different inner wall fixation and different backplane fixation.

Vertical ribs located on base plates seen in Figure 3.53 and Figure 3.54 a, b, prevents the backplane from bending during inserting DCB cards. Base plates play also a heat sink role for the backplane, because they are made of aluminum alloy 6082 – T6. Figure 3.54 b, shows special type of base plate for Pathfinder test. It contains openings for additional electronic boards.

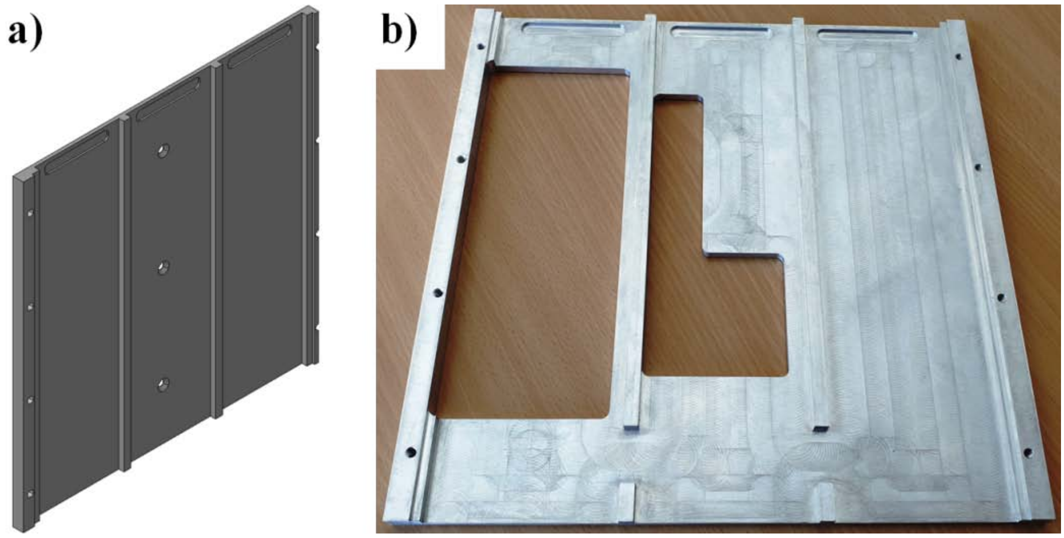

Figure 3.54 a) Base plate "gamma" 3D model; b) Base plate for "Pathfinder" test
Rysunek 3.54 a) Model 3D płyty bazowej "gamma"; b) Płyta bazowa do testu "Pathfinder"

3.7.6.2. Walls

Walls support DCB card guides and water cooling pipes. In addition to that, inner wall supports PEPI enclosure and act as a part of enclosure itself. Furthermore, it supports water return clamp as well. An opening in bottom part of the inner wall allows for pigtails accommodation. There are three regular walls for beta and gamma compartments – Figure 3.55, a, b and one special, inner wall – Figure 3.55, c, for alpha compartment, closing PEPI volume from the beam pipe side. Because walls are main structural element supporting PEPI mechanics, they are made of stainless steel 304 L.

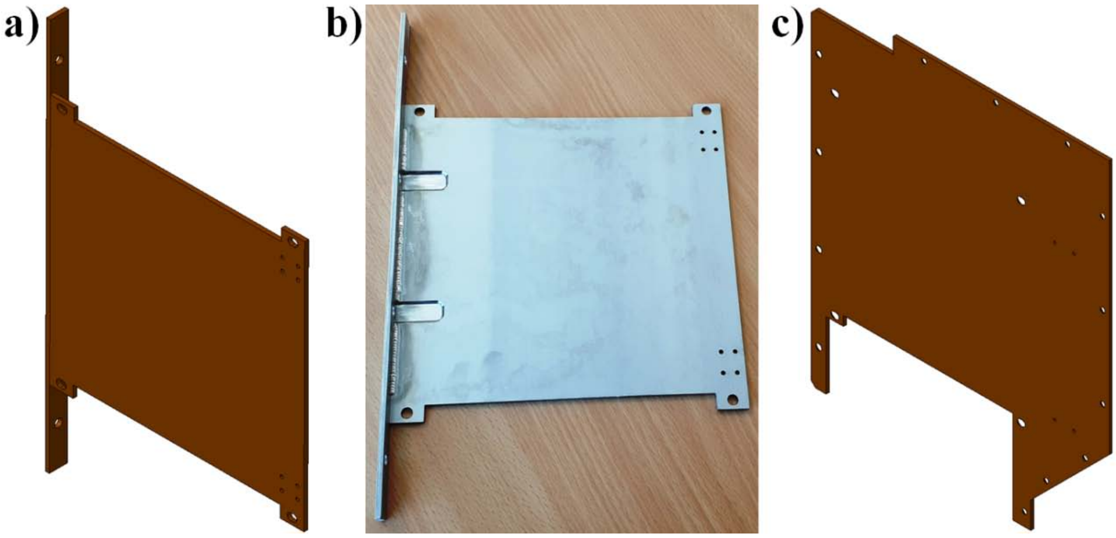

Figure 3.55 a) Regular wall 3D model; b) Regular wall – manufactured;
c) Wall for alpha compartment 3D model
Rysunek 3.55 a) Regularny mur – model 3D; Regularny mur – wyprodukowany;
c) Mur dla przedziału alfa – model 3D

3.7.6.3. Water cooling pipes support

As mentioned in Chapter 3.7.3.2, about DCB cards, each DCB card equipped with cooling interface weights about 1kg. Due to lack of space inside the PEPI volume and the fact that, all DCB's must be connected to cooling lines, the water cooling pipes act also as a support for the data concentration boards. The water cooling pipes must be therefore supported, in order to provide precise positioning of the DCB cards. Support for pipes is attached to PEPI walls, Figure 3.56. Therefore, water pipes can be supported in several points on their entire length inside PEPI volume. However, they cannot be over-constraint, hence, slight freedom in vertical direction is given in the pipe supports using EPDM rubber grommets, Figure 3.56. Due to DCB cooling interface construction (copper heat pipe pressed in rectangular channel) deformation of the heat pipe in the area close to water cooling pipes have been observed during tests – Figure 3.73 b. Hence, more slack is needed in plane perpendicular to the water pipes to allow for compensation of this phenomenon. Water cooling pipes supports, the same as walls, are made of stainless steel 304 L.

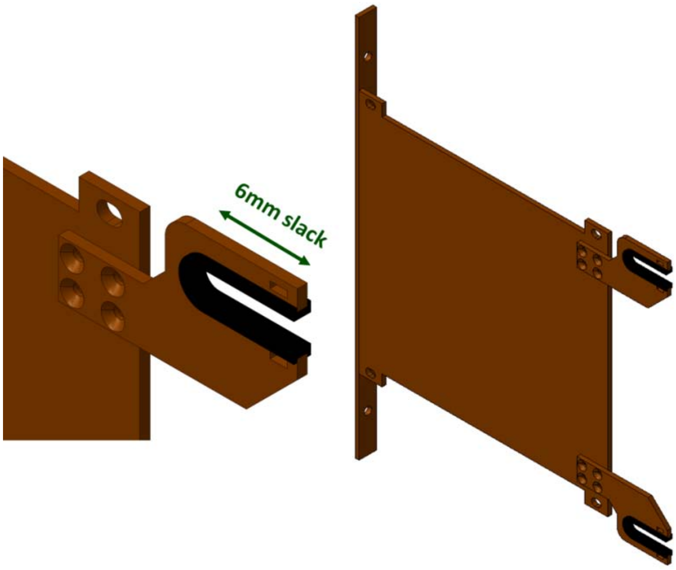

Figure 3.56 Water cooling pipes support
Rysunek 3.56 Podpora dla rur chłodzenia wodnego

3.7.6.4. DCB card guide

DCB card guides serves to guide data concentration boards towards backplane connectors. There is one channel per each DCB card (12 cards per backplane). They are also used for pressing backplane against base plates. In addition to that, and because they come in contact with the front part of backplane, they prevent backplane from bending during disconnecting the DCB cards. They also stiffen the PEPI mechanics construction and provide support for stand-offs, as well as, for dry air duct. There are two different types of guides. Regular for beta and gamma compartments and special for alpha compartment. They differ with length between the walls in the compartments. DCB card guides are machined from aluminum alloy 6082 – T6.

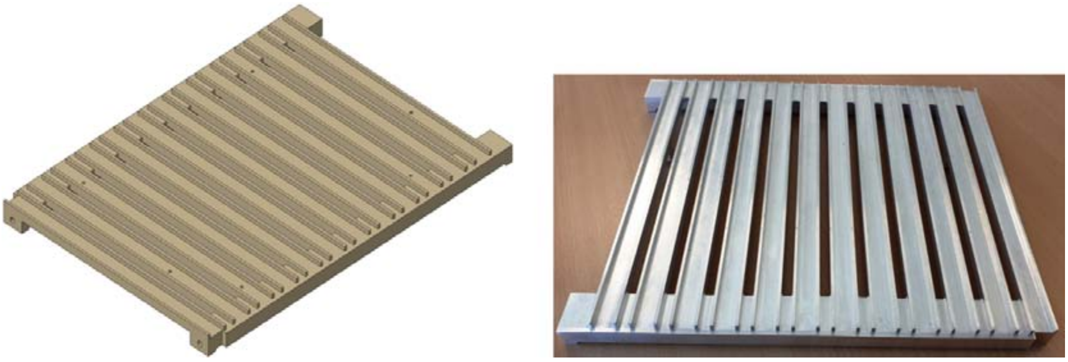

Figure 3.57 DCB card guide
Rysunek 3.57 Element prowadzący karty DCB

3.7.6.5. Stand-offs

Stand-offs provide support for low voltage power breakout boards (inner and outer), as well as for telemetry boards placed between them – Figure 3.58. Stand-offs material is stainless steel or brass. Stand-offs need to be made of conductive material, because telemetry boards design requires connecting them with grounding through stand-offs and DCB card guides. In contrary, low voltage power breakout boards, shall be electrically decoupled from stand-offs. For this reason EPDM rubber washers are used as an interface between stand-offs and LV boards.

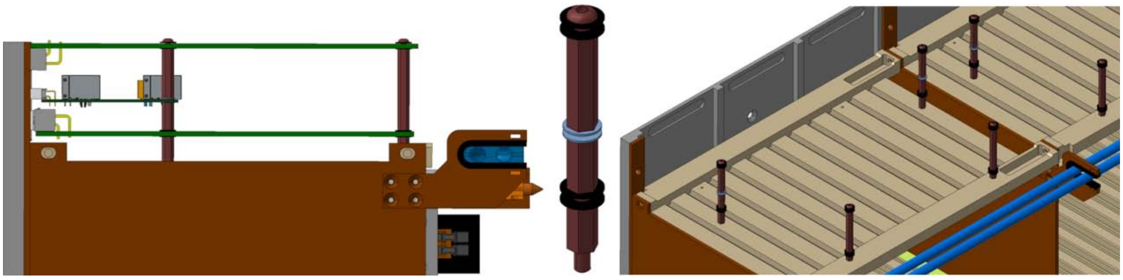

Figure 3.58 Stand-offs
Rysunek 3.58 Stand-offy

3.7.6.6. Enclosure

In order to satisfy both PEPI volume requirements in terms of being enclosed and semi gas tight, a PEPI enclosure has been designed – Figure 3.59. It is made of thin 1mm aluminum plates and supported by inner wall, as well as, by the C-Frame.

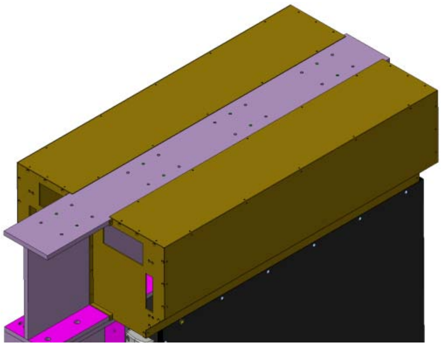

Figure 3.59 PEPI enclosure
Rysunek 3.59 Osłona PEPI

3.7.6.7. PEPI cooling

In order to fulfill requirement of keeping PEPI electronics below 40°C, water cooling has been applied inside PEPI volume.

- Water cooling pipes

PEPI volume uses demineralized water for electronics cooling. Demineralized water has been chosen, because it is non-conductive. It is important to protect the front-end electronics in case of a leak. Especially in PPEI, where access is extremely difficult after full assembly. However, using demineralized water is challenging from material engineering point of view. Demineralized water cannot be used with copper or aluminum, because it can cause corrosion of those materials. Although it is not perfect in terms of heat transfer, stainless steel must be use, for demineralized water cooling pipes.

Water cooling pipes used inside PEPI must be very precise in terms of diameter, straightness and surface finishing, in order to provide good thermal conduction and maintain good contact with cooling clamps. Precise seamless pipes provided by SANDWIK, made according to DIN 2391/EN 10305-1 norm were chosen. For example, given norm ensures outside diameter variations +/- 0.08mm, for 8mm pipe diameter with 1mm wall thickness. Pipes received at CERN and measured, were even better than that, within 0.02mm.

Tubes used for PEPI cooling are 8mm outside diameter and wall thickness of 0.5mm, in order to improve heat exchange between coolant and cooling interface. They can be seen in Figure 3.60.

Figure 3.60 Stainless steel pipes used for PEPI water cooling
Rysunek 3.60 Rurki ze stali nierdzewnej używane do chłodzenia wodą PEPI

3.7.6.8. DCB cooling interface

DCB cards are the hottest elements inside PEPI volume. Hence, they require cooling, in order to ensure their performance. DCB cooling interface consists of several elements indicated in Figure 3.61. DCB card with mezzanine boards, containing fiber optic connectors, and fully equipped with cooling interface, can be seen in Figure 3.71.

Production drawings of the DCB cooling interface elements, as well as, assembly drawing is attached in the thesis Appendix.

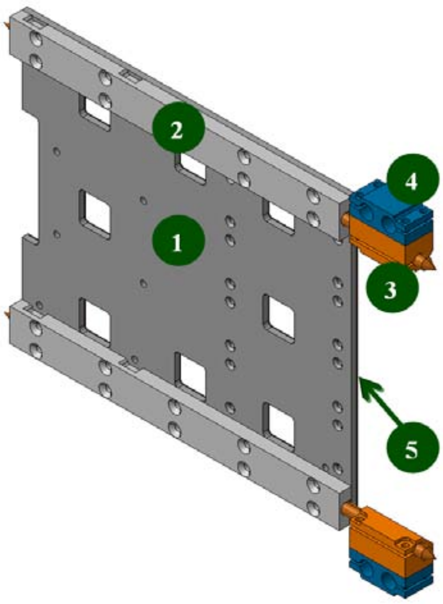

Figure 3.61 DCB cooling interface
Rysunek 3.61 Interfejs chłodzący kartę DCB

In the Figure 3.61, following components of the DCB cooling interface can be distinguished:

1. Heat spreader – Figure 3.62.
2. Heat spreader clamp with water-filled copper heat pipe pressed inside – Figure 3.63.
3. Heat pipe clamp – Figure 3.64.
4. Water pipe clamp – Figure 3.67.
5. Gap filler – Figure 3.70.

- DCB heat spreader

DCB heat spreader (Figure 3.62) removes heat from DCB card and passes it through to two water-filled copper heat pipes located on both of its edges. It is made of 3mm thick aluminum plate and bolted to electronic board using several screws located throughout all its surface in order to ensure equal pressing force. There are several square cut-outs in the heat spreader in order to liberate space for DCB electronics. Rectangular cut-out on one of its edges is to accommodate DCB connector. Heat spreader is machined from aluminum alloy 6082 – T6.

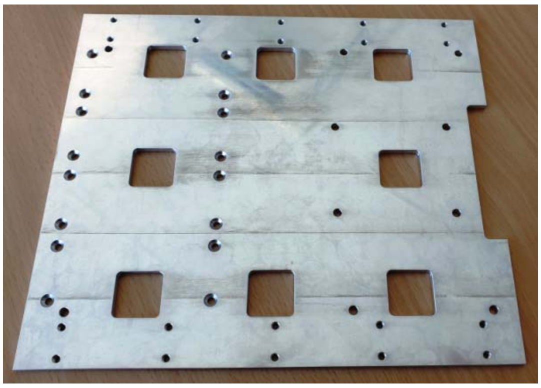

Figure 3.62 DCB heat spreader
Rysunek 3.62 Radiator karty DCB

Heat spreader overhangs DCB card by 3mm on top and bottom in order to prevent edge of electronic board from contact with the card guide channel – Figure 3.71 and Figure 4.18.

- Heat spreader clamp

Heat spreader clamp with water-filled copper heat pipe pressed inside it (Figure 3.63), act like a heat duct removing heat from DCB heat spreader and transmitting it towards water cooling pipes for dissipation. It is attached to the heat spreader using 10 M3 screws (Figure 3.72), which are positioned symmetrically on both sides of the heat pipe channel, in order to exert equal pressing force on both sides of the heat pipe through entire length of the clamp. The diameter of the copper heat pipe is 6mm and it goes through an entire length of the heat spreader clamp, directly touching heat spreader plate. Heat spreader clamp is made from aluminum alloy 6082 – T6.

Figure 3.63 Heat spreader clamp with water-filled copper heat pipe pressed inside
Rysunek 3.63 Zacisk radiatora DCB z wypełnioną wodą miedzianą rurką cieplną wewnątrz

- Heat pipe clamp

Heat pipe clamp (Figure 3.64) is a first element of an intermediate interface between heat pipe and water pipe – Figure 3.73 a, Figure 3.74. It is clamped over copper heat pipe on one side and screwed with water pipe clamp on the other side, transmitting heat from copper heat pipe towards water pipe. It is machined from aluminum alloy 6082 – T6.

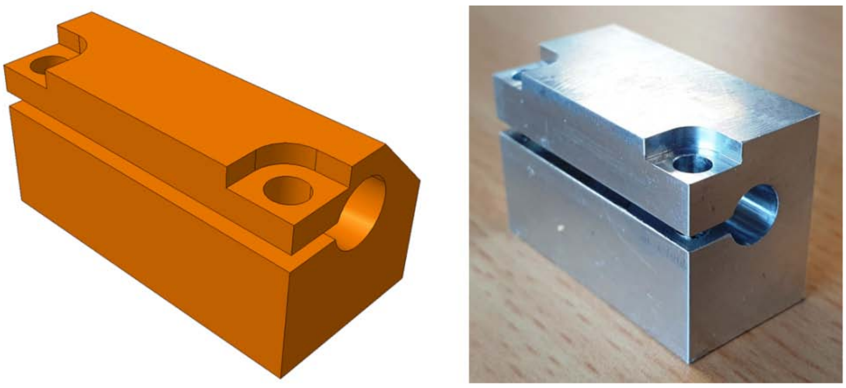

Figure 3.64 Heat pipe clamp
Rysunek 3.64 Zacisk rurki cieplnej

- Heat pipe clamp assessment

In order to learn if heat pipe clamp can be tighten around copper heat pipe the ANSYS finite element analysis (FEM) has been performed.

In order to learn how much force can be applied to each clamp screw, the analytical calculation was made, and then used in ANSYS analysis.

Each of two bolts tightening heat pipe clamp can be screwed for 4mm into threaded part of the clamp. Screws themselves are made from stainless steel, while clamps from aluminum alloy 6082 – T6. Therefore, weaker material, which is aluminum, has been taken into consideration.

Calculation of maximum force, which can be applied to the screw, before thread in aluminum will be damaged.

<u>Boundary conditions:</u>

- material, in which bolt is screwed – aluminum alloy 6082 – T6;
  - ultimate tensile strength (Rm): 300 MPa,
  - yield strength (Re): 255 MPa,
- depth of the thread: 4mm;
- screw – M3;
  - pitch: 0.5mm,
  - d: 3mm (thread diameter),
  - D_1: 2.46mm (screw core diameter).

An equation for calculation height of the nut/depth of the thread according to surface pressure condition is presented in Formula 3.2.

$$H \geq \frac{4F * p}{\pi * (d^2 - D_1^2) * k_d}$$ Formula 3.2

where:
F – force [N];
H – active height of the nut [mm];
p – thread pitch [mm];
k_d – allowable thread stress (surface pressures) [Pa].

Transformed equation to calculate the force, when height of the nut/depth of the thread is given – Formula 3.3.

$$F \leq \frac{H * [\pi * (d^2 - D_1^2) * k_d]}{4 * p}$$ Formula 3.3

$k_d = 0.2*kc$
k_c – allowable compression stress
$k_c = 0.6*Re$

$k_c = 0.6*255 = 153$ [MPa]

$k_d = 0.2*153 = 30.6$ [MPa]

$$F \leq \frac{4 * [3.14 * (3^2 - 2.46^2) * 30.6]}{4 * 0.5}$$

$F \leq 566.87 \cong 567\ [N]$ – it is the point where thread plasticisation begins.

Safety coefficient: 30%

$$567 * 0.7 = 396.9 \cong \mathbf{400\ N}$$

There are two screws for heat pipe clamp tightening, therefore 800N force can be exerted – Figure 3.65.

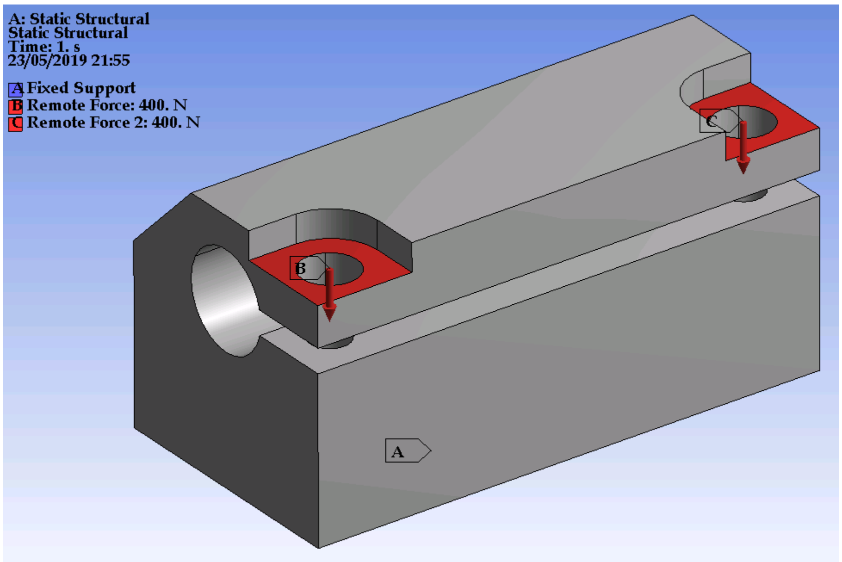

Figure 3.65 Distribution of forces for FEM analysis of heat pipe clamp
Rysunek 3.65 Rozkład sił dla analizy MES zacisku rurki cieplnej

In order to check if the heat pipe clamp can be tighten around heat pipe the deformation of the clamp has been investigated – Figure 3.66.

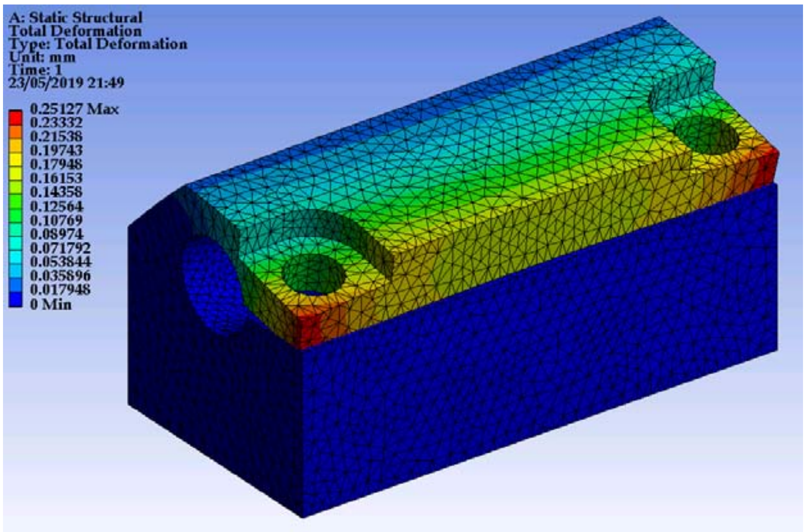

Figure 3.66 Total deformation of heat pipe clamp
Rysunek 3.66 Całkowita deformacja zacisku rurki cieplnej

The heat pipe has the nominal diameter of 6mm, the hole in the heat pipe clamp to accommodate the pipe has the diameter of 6.05mm.

The FEM analysis shows deformation of the heat pipe clamp on the level of 0.1mm to 0.25mm. This is enough in order to tighten the clamp over heat pipe.

In order to ensure good heat transfer between elements thermal grease or graphite foil will be used as an interface.

- Water pipe clamp

Water pipe clamp (Figure 3.67) is a second element of an intermediate interface between heat pipe and water pipe – Figure 3.73 a, Figure 3.74. From one side it clamps over both water pipes, supply and return, from the other side it is screwed into the heat pipe clamp, transmitting heat from copper heat pipe towards water pipe. It is made from aluminum alloy 6082 – T6.

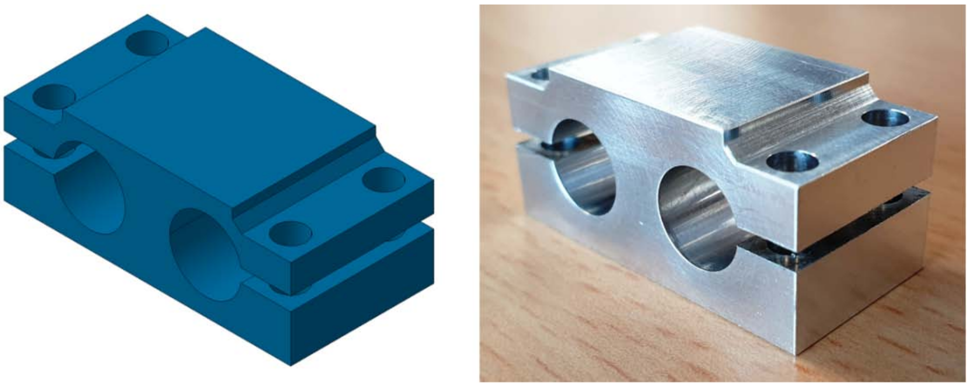

Figure 3.67 Water pipe clamp
Rysunek 3.67 Zacisk rury wodnej

- Water pipe clamp assessment

For the water pipe clamp there are two tightening screws per side (per pipe) – Figure 3.68. Therefore similar to heat pipe clamp 800N of force per clamp side can be exerted.

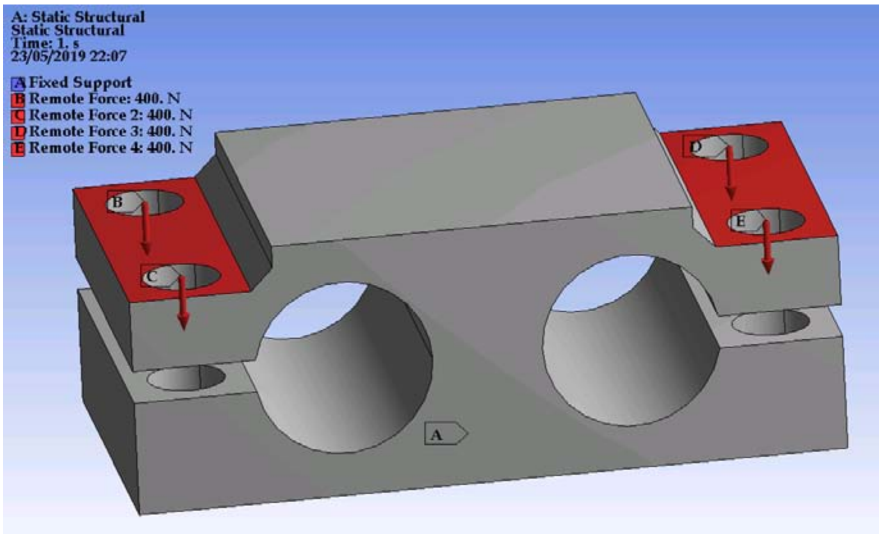

Figure 3.68 Distribution of forces for FEM analysis of water pipe clamp
Rysunek 3.68 Rozkład sił dla analizy MES zacisku rurki wodnej

In order to check if the water pipe clamp can be tighten around water pipes the deformation of the clamp has been investigated – Figure 3.69.

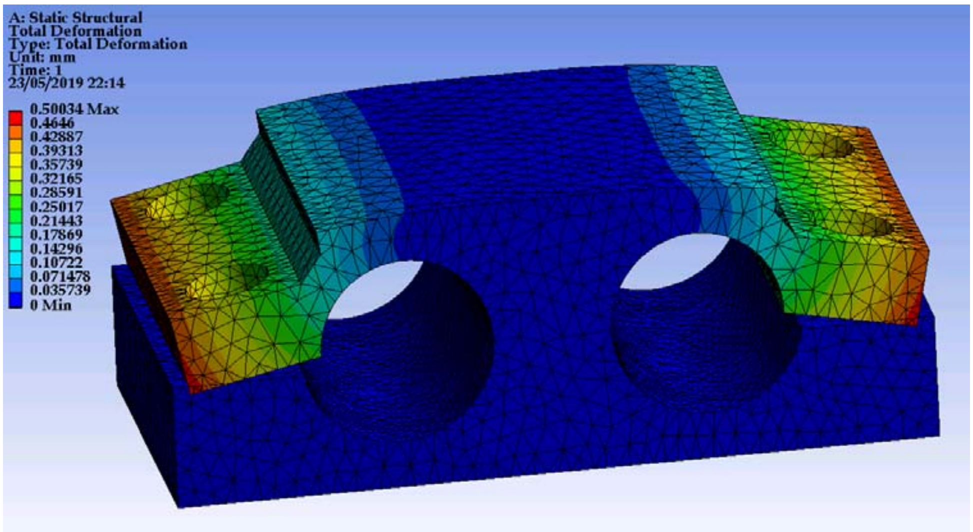

Figure 3.69 Total deformation of water pipe clamp
Rysunek 3.69 Całkowita deformacja zacisku rurki wodnej

The water pipe has the nominal diameter of 8mm, the hole in the water pipe clamp to accommodate the pipe has the diameter of 8.1mm.

The FEM analysis shows deformation of the water pipe clamp on the level of 0.2mm to 0.5mm. This is enough in order to tighten the clamp over water pipes.

In order to ensure good heat transfer between elements thermal grease or graphite foil will be used as an interface.

- Gap filler

Gap filler (Figure 3.70) is used between DCB card and the heat spreader. It plays two roles. Firstly, it fills all the imperfections in terms of heat spreader machining like planarity, straightness, roughness. It prevents from the situation, when badly machined heat spreader would touch DCB card only in one or two points. Hence, it enlarge heat exchange area. Secondly, gap filler is made of thermal conductive material. Therefore it improves cooling performance. Same as in heat spreader, also in gap filler there are respective cut-outs for DCB electronics. Gap filler has a thickness of 0.5mm, and is made from Farnell 189-3443 material.

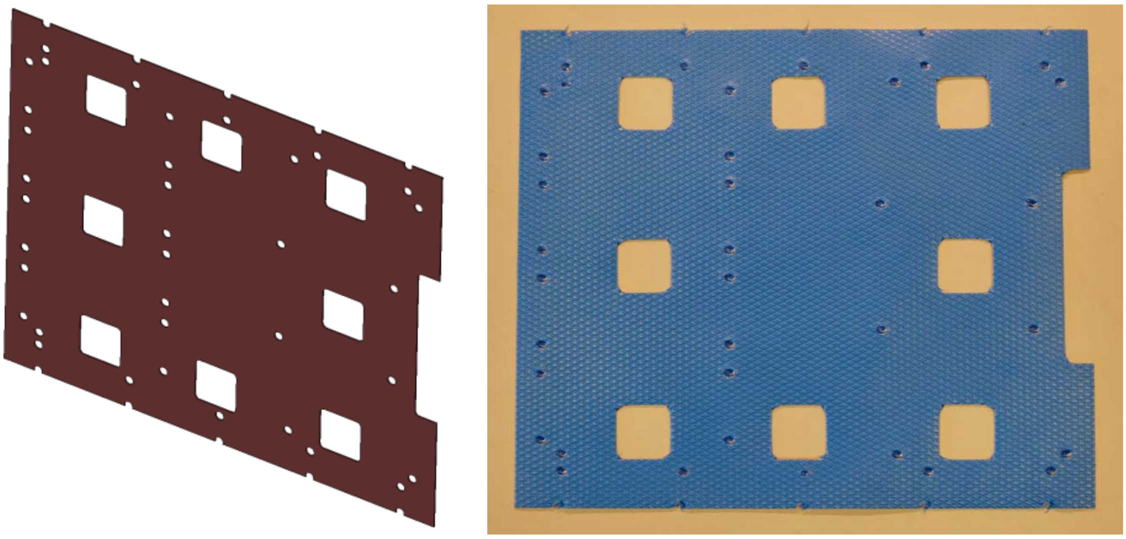

Figure 3.70 Gap filler
Rysunek 3.70 Wypełniacz

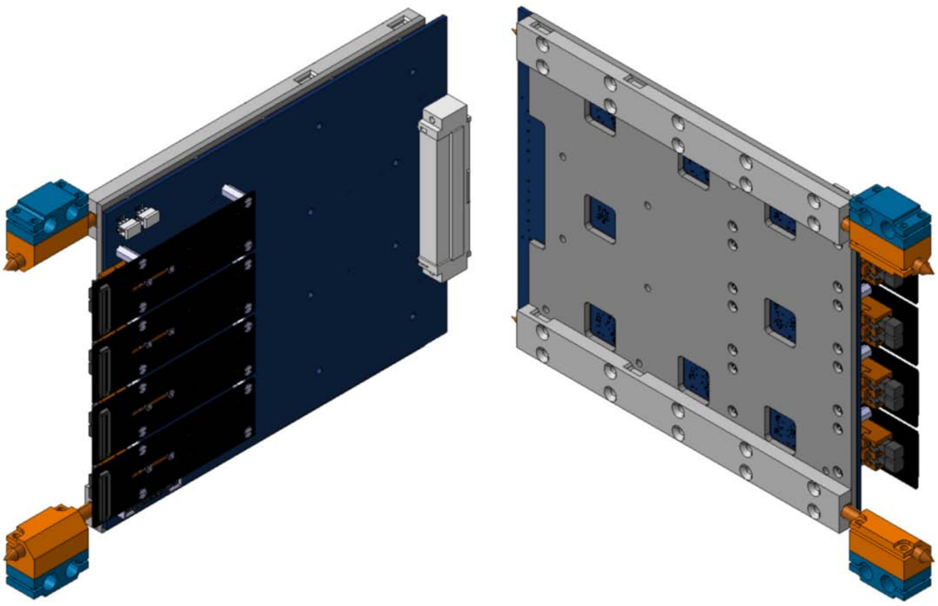

Figure 3.71 DCB with cooling interface
Rysunek 3.71 Karta DCB z interfejsem chłodzącym

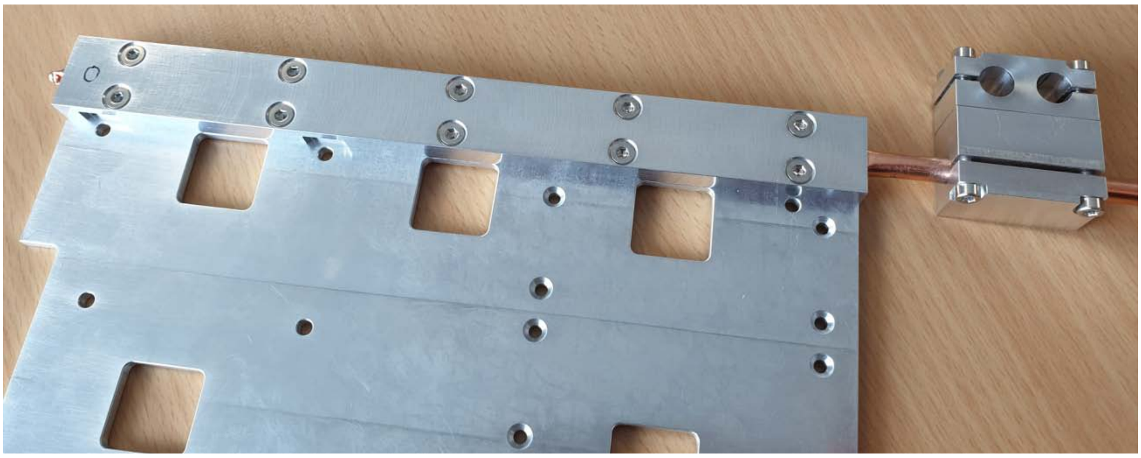

Figure 3.72 DCB heat spreader with heat spreader clamp, heat pipe and heat pipe clamp
Rysunek 3.72 Radiator DCB wraz z zaciskiem, rurką cieplną i zaciskiem rurki cieplnej

Figure 3.73 a) Heat pipe to water pipe interface 3D model and manufactured elements;
b) Pressing area – heat pipe deformation (flattening)
Rysunek 3.73 a) Interfejs rurki cieplnej do rury wodnej model 3D i wyprodukowane elementy;
b) Obszar wtłaczania rurki – deformacja rurki cieplnej (spłaszczenie)

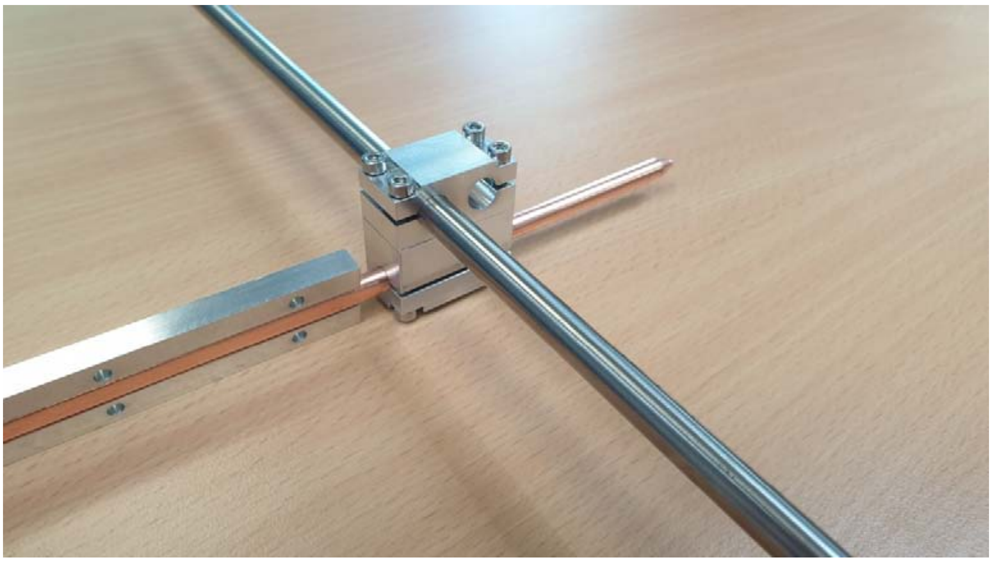

Figure 3.74 Copper heat pipe and stainless steel water pipe connected by heat exchange interface
Rysunek 3.74 Miedziana rurka cieplna i rurka z wodą chłodzącą ze stali nierdzewnej połączone interfejsem wymiany ciepła

- Water cooling pipes return clamp

It is another challenging element for integration inside PEPI volume. Due to lack of space, there is no possibility to make a U-turn of the stainless steel water pipe. In order to provide return for water cooling in the most crowded PEPI alpha compartment, a special return clamp had to be developed. – Figure 3.75 a. Two water pipes will be welded to the clamp and inside it, there will be a U-channel connecting their ends (Figure 3.75 b), and providing a return. It is planned to print return clamp in stainless steel (of the same grade as pipes), using SLS (Selective Laser Sintering) 3D printing technology.

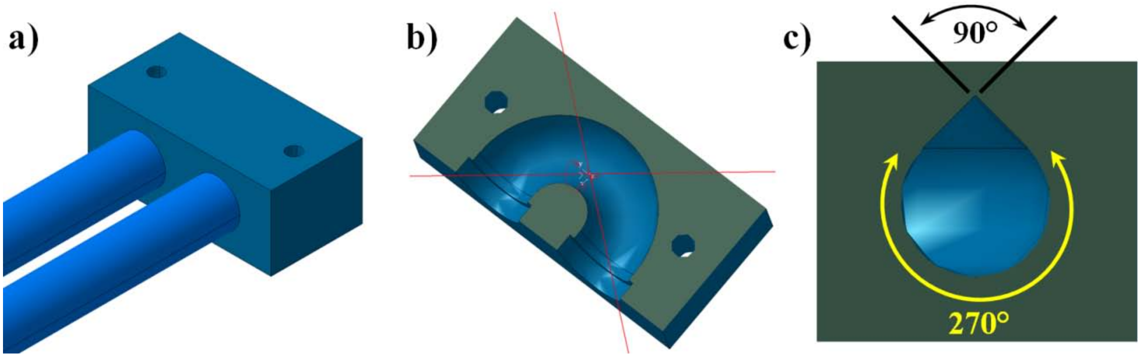

Figure 3.75 a) Return clamp with cooling pipes; b) Return clamp channel; c) Return clamp channel cross-section

Rysunek 3.75 Zacisk powrotny z rurkami chłodzącymi; b) Kanał powrotny; c) Przekrój kanału powrotnego

The channel inside return clamp has a special cross-section similar to a water drop shape (Figure 3.75 c). It is like that in order to allow SLS 3D printing without necessary of putting supporting material inside the channel. This shape has negligible influence for a water flow inside the clamp.

SLS 3D printed water return clamps, with further adjustment of cut corners for material savings, can be seen in Figure 3.76.

Figure 3.76 SLS 3D printed water returned clamps

Rysunek 3.76 Zaciski zwrotne wydrukowane w 3D przy użyciu technologii SLS

- Dry air duct

Dry air duct inside PEPI volume serves two different purposes. Firstly, it provides with sufficiently dry air in the area, where pigtails coming from inside the UT detector box. Due to around 50°C temperature difference between ambient LHCb cavern temperature and temperature inside the UT box, it is necessary to avoid condensation on pigtails inside PEPI volume. Secondly, dry air will also be directed to mezzanine boards of the DCB cards, which are the most hot elements inside PEPI volume. They host fiber optic output connectors for data transfer. Therefore their temperature need to be regulated. Dry air is not intended for cooling DCB cards. However, it is beneficial to flush it into mezzanine boards, because flow of the air will force convection inside the PEPI volume (between DCB cards), which improves heat dissipation. Natural convection inside PEPI volume is very low, due to very compact design.

Dry air duct is meant to be built from chamber polycarbonate plate with 3D printed inlet manifold and end cap in ABS material. Multi pipes construction of the duct allows to deliver dry air into multiple pigtails, while still having good control on the pressure drop inside the duct.

Dry air duct can be seen in the Figure 3.77 in yellow color, behind pigtails marked in aqua color.

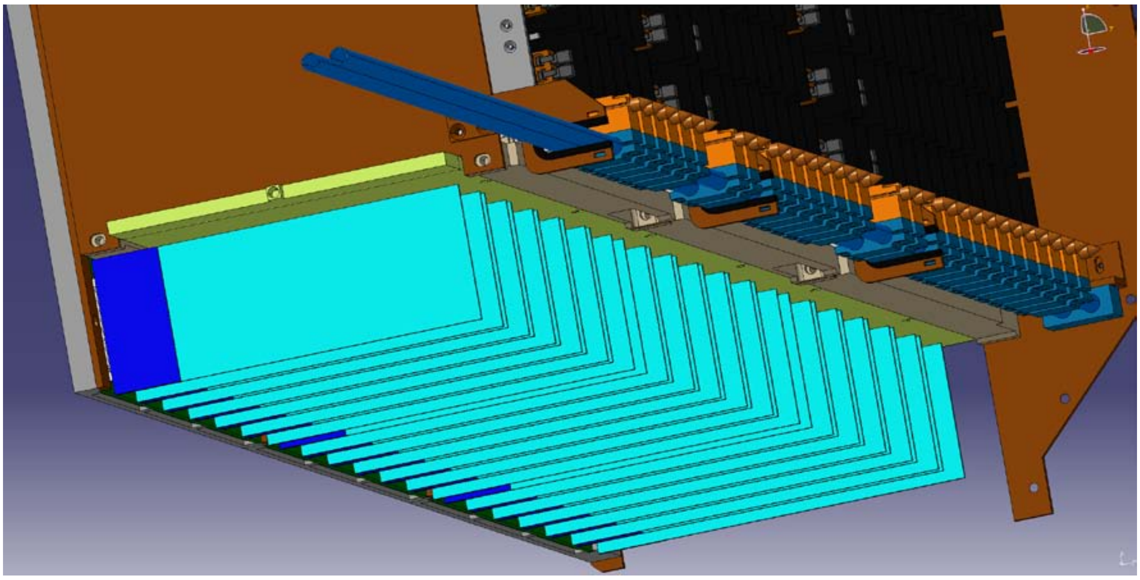

Figure 3.77 Lower part of PEPI volume with dry air duct
Rysunek 3.77 Dolna część objętości PEPI z kanałem suchego powietrza

3.8. Cable chain integration

Cable chain is an important element of Upstream Tracker detector layout. It hosts cables coming from service bays area towards PEPI volume above and below the UT detector box, and allows for detector opening and closing along the LHCb cavern mounting rails – Figure 3.81 number 8.

There are 4 cable chains, two per detector half – Figure 3.78. Each one serves for two PEPI volumes.

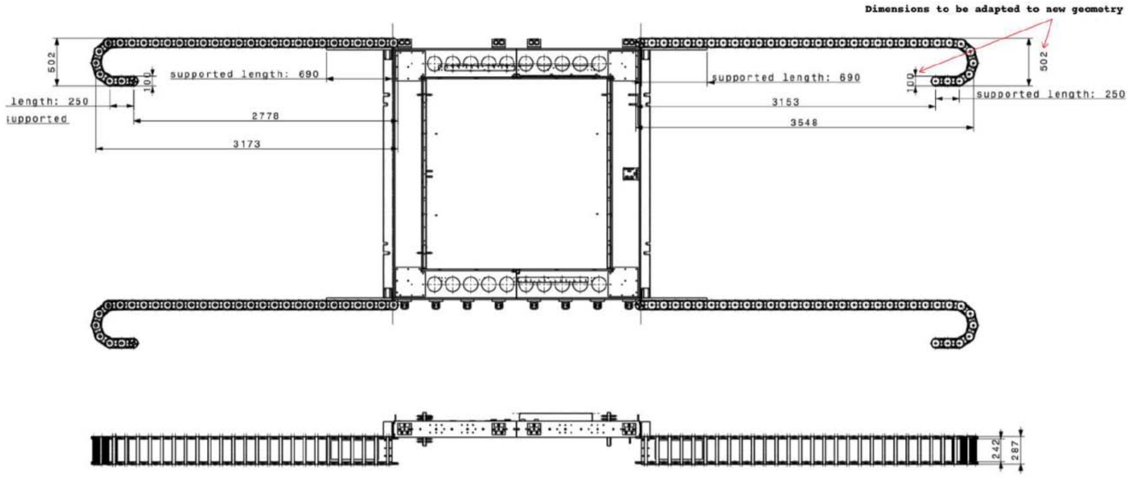

Figure 3.78 Cable chain geometry [40]
Rysunek 3.78 Geometria łańcucha kablowym [40]

The existing Trigger Tracker cable chain has a cross-section of 290x100mm. Because new Upstream Tracker detector needs significantly higher amount of cable connections, its cable chain will be larger, with cross-section about 345x285mm – Figure 3.79.

Weight of all cables inside single cable chain has been estimated for about 600kg. Hence, the cable chain must be a robust, well supported structure, or be of a heavy self supporting type.

Length of cables going through cable chains is about 6m.

Because of its size, integration of new UT cable chain inside the LHCb cavern is a very challenging task. It must remain in the same position as the previous one. Therefore, and because of its larger envelope, there are several collisions occur during integration. New Upstream Tracker cable chain collides with access, walking platforms, especially on C-Side. moreover, in opened position, PEPI volumes themselves seem to collide with platform supporting pillars on C-Side. platforms must be reconstructed in order to allow for UT detector opening.

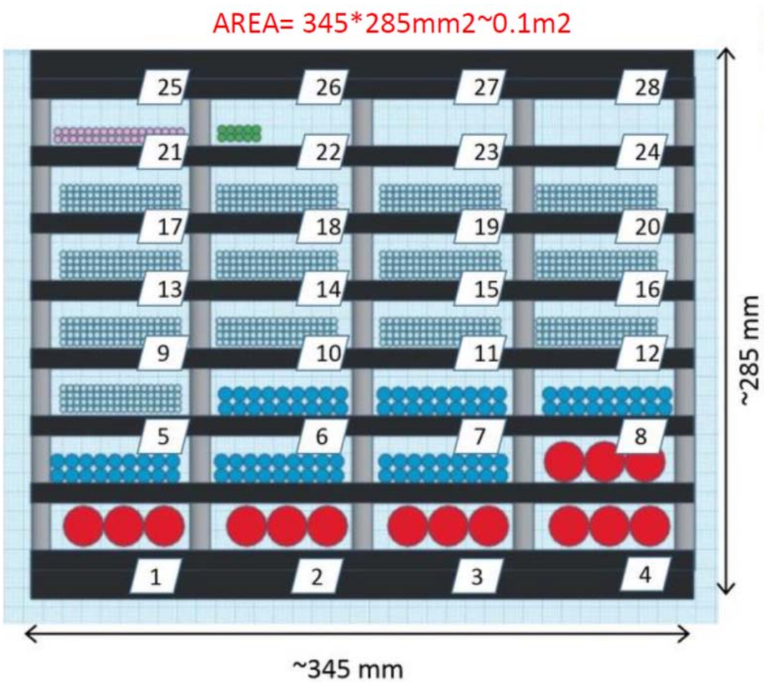

Figure 3.79 Cables compartments cross-section in cable chain [40]
Rysunek 3.79 Przekrój przedziałów kablowych w łańcuchu kablowym [40]

In the Figure 3.79, following cable compartments inside the cable chain can be distinguished:

1-4, 8	High voltage cables: 15pcs., (36 core cables), OD = 20mm.
5-7, 10-12	Low voltage sense wires: 108pcs., (4 pair each, 864 wires, 0.26mm^2), OD = 7mm.
9, 13-24	Low voltage cables (round litz wires): 936pcs., OD = 3.1mm, 3.83mm^2.
25	Data fiber optic cables: 34pcs., (12-fibre bundles), OD = 3.5mm.
26	Environment monitoring cables: 10pcs., OD = 4mm fibers.

A sample of plastic cable chain from igus company can be seen in Figure 3.80.

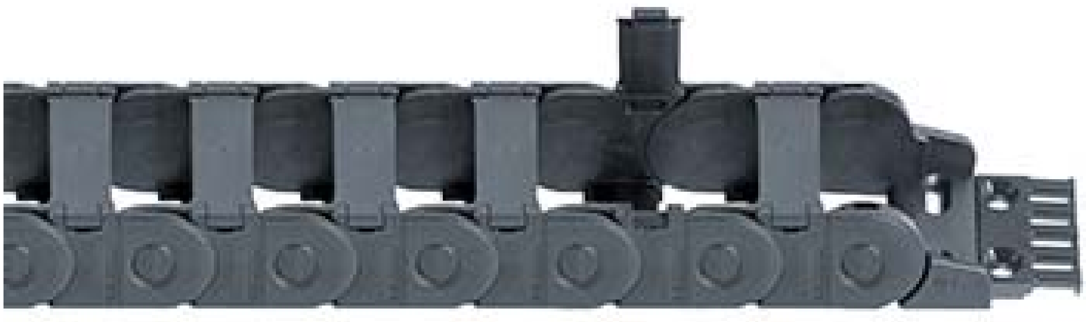

Figure 3.80 Sample of a cable chain [41]
Rysunek 3.80 Próbka łańcucha kablowego [41]

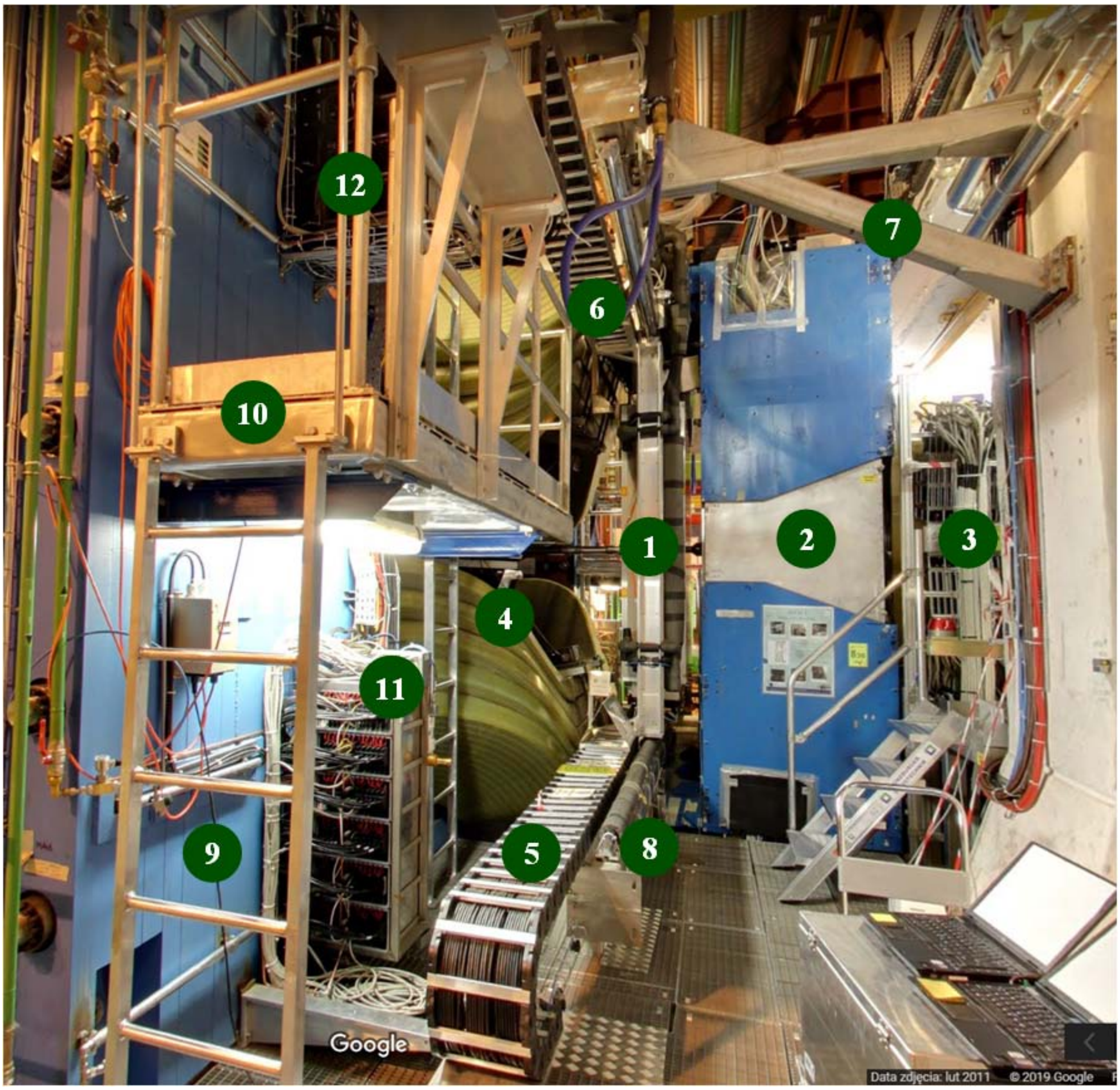

Figure 3.81 LHCb cavern, UT detector area, A-Side
Rysunek 3.81 Caverna LHCb, obszar detektora UT, Strona-A

In the Figure 3.81, following elements of Upstream Tracker detector area inside LHCb cavern can be distinguished:

1. TT (Trigger Tracker) detector – will be replaced by UT (Upstream Tracker) detector.
2. RICH detector.
3. VELO detector – closest to LHCb Interaction Point (IP).
4. LHCb magnet.
5. Bottom cable chain.
6. Top cable chain.
7. Top rail support.
8. Bottom rail.
9. Magnet wall.
10. Platform for access to top service bays rack, top rail and top cable chain.
11. Bottom service bays rack attached to magnet wall.
12. Top service bays rack attached to magnet wall. Seen in details in Figure 3.93.

3.9. Service bays integration and mechanics

Inside LHCb cavern service bays provide intermediate connection between cables going into cable chain, (to UT detector), and cables coming from the surface facilities. For example, low voltage power supply cables, so called "Marathons", connects inside the SBC crate with low voltage regulator boards, which supplies power to PEPI electronics, and further to staves inside the UT detector box.

As well as LV cables, also telemetry cables and fiber optic cables have their intermediate connection in service bays area. There are 4 SBC racks, which serve the UT detector, two racks per detector half. They are located at the end of cable chains and attached to the LHCb magnet wall – Figure 3.2 number 6. The most challenging and difficult task in terms of service bays integration is cables management and routing.

3.9.1. Service bays crate

Service Bays Crate – SBC, hosts low voltage regulator boards – LVRs, (each one, up to 18 of them), which provides power for PEPI electronics. Those boards needs to be properly supported, maintain connected with both, output cables going to the cable chain, as well as, with input cables coming from surface facilities. In addition, due to high current supply, LVRs require cooling, in order to maintain their performance. Single crate equipped with 18 low voltage regulator boards and a patch panel, which hosts cable connectors and cable trays for cable management, weights about 50kg.

3.9.1.1. Service bays crate requirements

Main requirements for the UT service bays crate are the following:

1. **UT service bays crate must provide support for electronic boards**
   Low Voltage Regulator Boards – LVRs, are the critical components for the detector power supply. They require proper mechanical attachment inside service bays crate.

2. **UT service bays crate has to provide cooling for LVRs**
   Due to high current supply, low voltage regulator boards require cooling, for proper operation. SBC must be designed in the way allowing for cooling LVR boards.

3. **UT service bays crate shall provide proper cable management**
   LVR boards inside service bays crates need to be connected with output cables going to the cable chain, as well as, with input cables coming from surface facilities. The amount of cables is enormous. Their total mass is huge. They must be properly guided through SBC patch panels in a correct way to reach their destinations. Moreover, some cables must be firmly attached to the patch panel, in order to avoid hanging on, and stressing the electronic boards. This particularly applies to thick, stiff and very heavy Marathon cables, which comes from the surface.

4. **UT service bays crate should be accessible**
   A design of the SBC shall allow for easy installation and removal of low voltage regulator boards. As LVRs are UT detector power supplies, they may wear out with time. Therefore, service bays crate must allow for quick exchange of damaged units.

3.9.1.2. Service bays crate layout

This chapter describes integration studies of the SBC – (Service Bays Crate). In the Figure 3.82 3D assembly of SBC is presented.

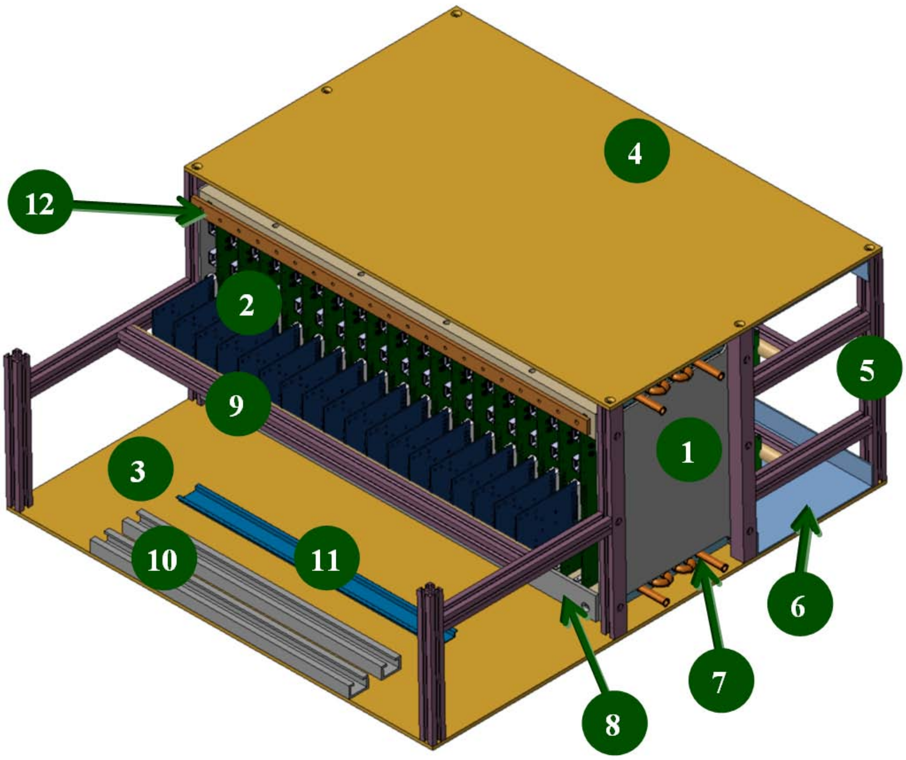

Figure 3.82 Service bays crate 3D assembly
Rysunek 3.82 Złożenie 3D kraty serwisowej

In the Figure 3.82, following components of the SBC can be distinguished:

1. Service bays crate.
2. LVRs – low voltage regulator boards inside SBC.
3. Patch panel plate – marathons direction.
4. Patch panel plate – cable chain direction (on both sides of the crate).
5. Bosch profiles frame for stiffness, flexibility and adjustability.
6. Cable tray for cable management (on both sides of the crate).
7. Cold plates with water cooling pipes, connected to LVR board guides.
8. Stopper for LVR boards.
9. Pressing bar, preventing auxiliary power breakout boards from disconnecting from LVRs.
10. Marathon cables fixation rails.
11. Marathon cables connectors mounting rail.
12. Grounding bar, made of copper.

3.9.1.3. Service bays crate electronics

Low voltage regulator board – LVR, supplies power to PEPI electronics. It consists of main electronic PCB (Figure 3.83, number 1) and several auxiliary cards connected to it. Card marked with number 3 in Figure 3.83 is an input power breakout board from Marathon cables, which provide low voltage power to the service bays. Two cards marked with number 2 in Figure 3.83 are output power breakout boards supplying power to the PEPI. Two expandable wedge-locks are attached to the LVR board (Figure 3.83, number 4) in order to provide fixation of the PCB inside the service bays crate channel.

LVR board placed inside the crate's channels can be seen in Figure 3.84.

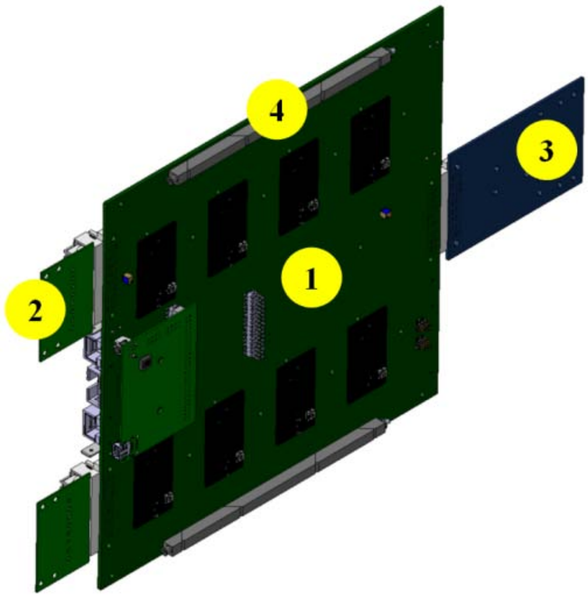

Figure 3.83 Low voltage regulator board
Rysunek 3.83 Płytka regulatora niskiego napięcia

3.9.1.4. Service bays crate cabling

The most challenging task in SBC area is cable management. Service bays crate is a power supply for the UT detector. Therefore, not only the amount, but also a cross-section and weight of cables in significant. In addition, and because of its role, SBC is an intermediate point between cables coming from the power plant and cables going into cable chain, for powering PEPI. Hence, the amount of cables is huge.

- Incoming cables

Incoming low voltage power cables, called Marathons, are thick 2x25mm^2 cross-section wires, with outside diameter of 23mm. Five of them connects to each service bays crate. They must be properly guided and firmly supported, as copper cables of this cross-section are very heavy and bulky objects.

▪ Outgoing cables

Outgoing low voltage power cables, (cables leaving from two power breakout boards marked with number 2 in Figure 3.83), are 3.3mm^2 cross-section wires with outside diameter of 3.6mm. There are 8 cables leaving from each breakout board and two breakout board per LVR, which gives 16 cables per LVR board. There are 18 LVR boards in single service bays crate, so there is 288 thick LV wires per crate. There are 4 crates inside the rack, hence, total amount of LV cables is around 1152 pieces.
In order to deal with such amount of cables, and also to make cables inside cable chain simpler, an intermediate step was developed. Cables outgoing from SBC are shorter and easier to route, just outside SBC area. After that they are crimped with 4mm^2 litz wires (cables going through cable chain to PEPI). This solution, allows for easier cable routing in SBC. In addition, it allows for all litz wires inside cable chain to be of the same length.

3.9.1.5. Service bays crate mechanics

Service bays crate main compartment marked with number 1 in Figure 3.82, can be seen in details in Figure 3.84.

Production drawings of the service bays crate elements, as well as, assembly drawing is attached in the thesis Appendix.

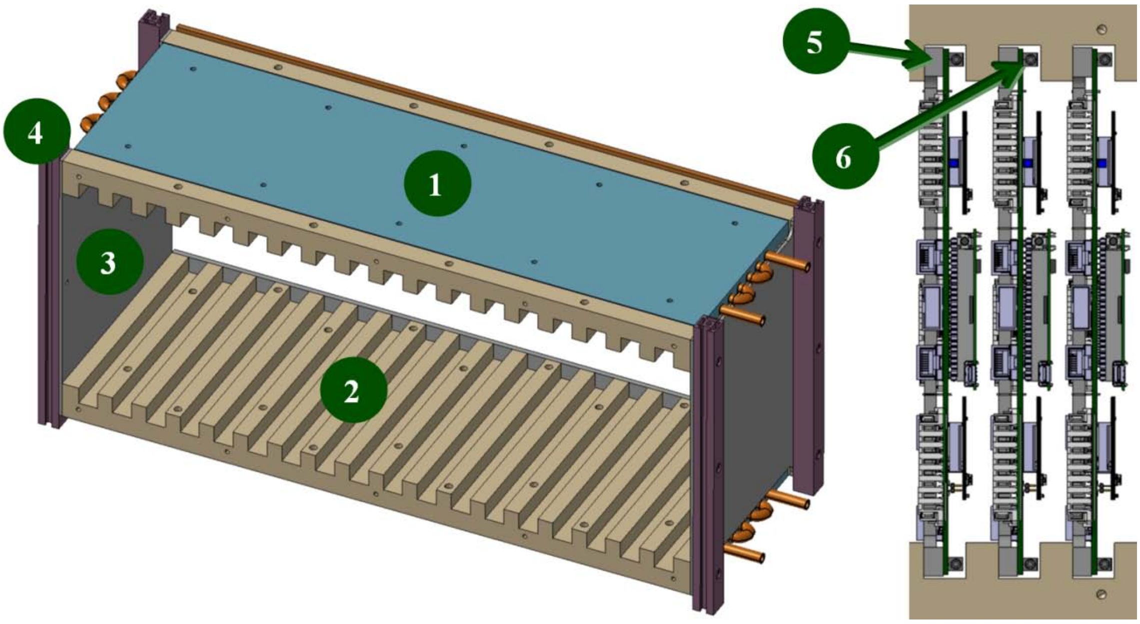

Figure 3.84 SBC mechanics
Rysunek 3.84 Mechanika SBC

In the Figure 3.84, following components of the SBC mechanics can be distinguished:

1. Cold plate with copper cooling pipes embedded inside it, attached to the LVR board guide.
2. LVR board guide with channels for LVRs.
3. Side wall.
4. Corner profile.
5. LVR heat sink.
6. Wedge-lock (expandable) for LVR board tightening inside the channel.

- Side walls

Made of 3mm aluminum plate side walls (Figure 3.85, number 1), provide support and given positioning for top and bottom LVR board guide plates, with respect to each other. They are made from aluminum alloy 6082 – T6.

- Corner profiles

Corner profiles (Figure 3.85, number 2), are used in order to stiffen the crate's construction. They connect to the top and bottom LVR board guide plates through the side wall plates, as well as, with the side wall plates themselves in the middle of their length. They are 20x20mm aluminum Bosch profiles, which makes them flexible, for easy connection with patch panel plates and profiles. They also act as a sliders, when crate is placed inside the rack structure.

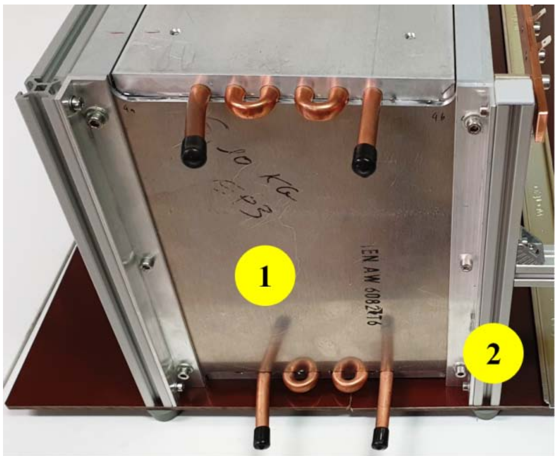

Figure 3.85 Side wall with Bosch profile
Rysunek 3.85 Boczna ściana z profilami Bosch-a

- LVR board guide

LVR board guide hosts channels for low voltage regulator boards. Each crate has two board guides top and bottom. They act as an intermediate interface between LVRs equipped with heat sink and the cold plate, conducting heat from SBC electronics towards cold plates.

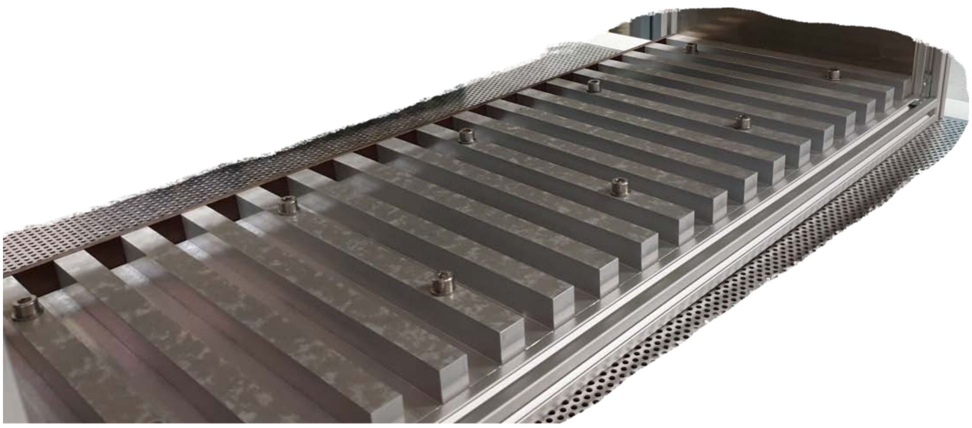

Figure 3.86 LVR board guide
Rysunek 3.86 Element prowadzący karty LVR

LVR board guide element is equipped with large pocket (Figure 3.88 b) in order to fit cold plate inside. It is machined from aluminum alloy 6082 – T6.

3.9.1.6. Service bays crate cooling

Because LVR board is a power supply, it requires cooling in order to maintain stable performance. Mixed water have been chosen for coolant inside service bays crate. Temperature of the water inside the cooling system is 13°C.

First element in SBC cooling interface is LVR heat sink, which is attached to low voltage regulator board. It touches power regulator chips on LVR board through a gap filler and removes heat from them. Afterwards, it passes the heat through channel walls to the cold plate, in which water cooling pipes are embedded, for heat dissipation.

- LVR heat sink

Heat sink (Figure 3.87 a and Figure 4.28) is an aluminum plate directly attached to the LVR board. It is custom machined with special threaded stand-offs (Figure 3.87 a) and pockets (Figure 3.87 b), in order to fit electronic layout of the low voltage regulator board. The planarity of the heat sink plate must be very fine, because of the ceramic capacitors used on LVR PCB. The electronic board cannot be stressed too much during tightening the heat sink, otherwise they brake, causing failure to electronics. The material of the heat sink is aluminum alloy 6082 – T6.

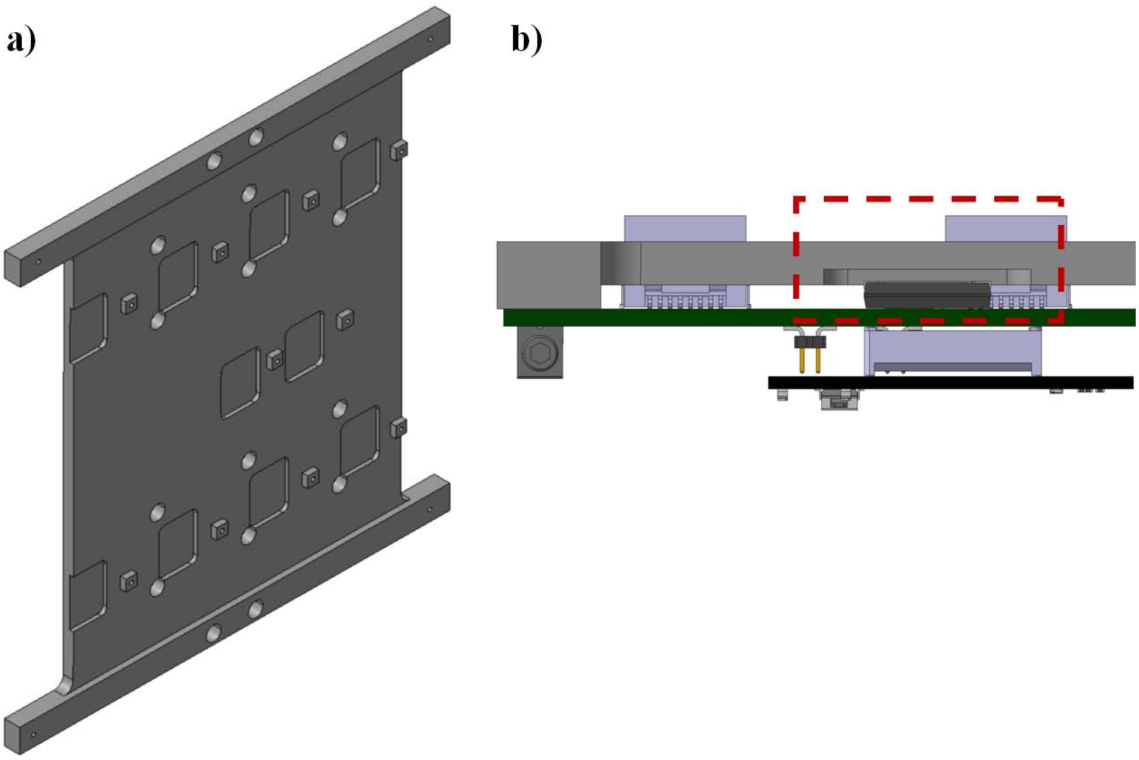

Figure 3.87 a) LVR heat sink; b) Pocket for an electronic chip inside the heat sink [7]
Rysunek 3.87 a) Radiator karty LVR; b) Kieszeń na układ scalony w radiatorze [7]

- Cold plate

The cold plate (Figure 3.88 a) is attached to the LVR board guide in such a way that copper cooling pipes directly touch LVR board guide (Figure 3.88 b), in order to dissipate as much heat as possible. There is thin thermal paste interface between the parts, which improves heat transfer. As there are two LVR board guides in single SBC, there are also two cold plates attached to them. This provides sufficient cooling power for heat dissipation.

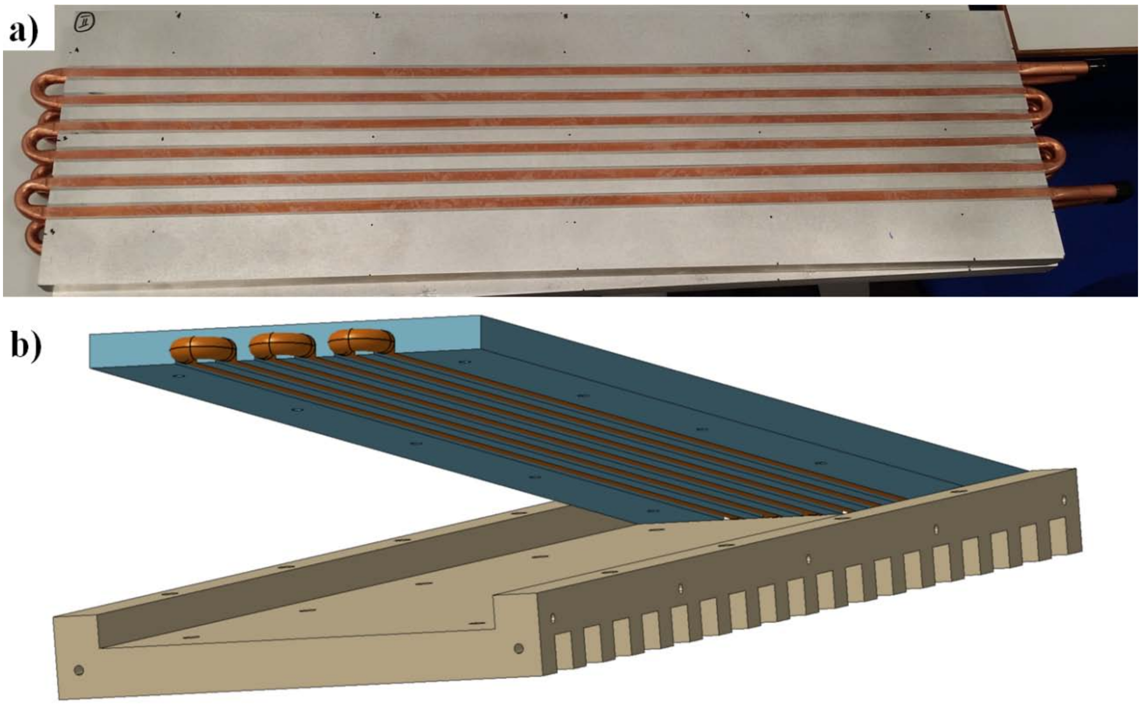

Figure 3.88 a) Cold plate; b) Exploded view of cold plate and LVR board guide connection
Rysunek 3.88 a) Płyta chłodząca; b) Rozstrzelony widok połączenia płyty chłodzącej i elementu prowadzącego karty LVR

An assembled pilot carte can be seen in Figure 3.89.

Figure 3.89 Prototype (pilot) SBC crate
Rysunek 3.89 Prototypowa (pilotowa) krata SBC

3.9.2. Service bays rack

Service bays rack – SBR, hosts 4 service bays crates inside and in addition a control box containing sense wires on top of it. There are 4 service bays racks inside LHCb cavern providing services for UT detector. Two racks per detector half. Rack must be a robust structure, because weight of 4 fully equipped crates, (with electronics, cooling and cabling), have been estimated for about 1000kg. One rack serves two PEPI volumes. Hence, there are about 1100 low voltage cables (4mm^2 litz wires), 108 telemetry (Ethernet) cables, 48 fibers and 5 (56 wires) high voltage cables going from rack output side to the cable chain. Respectively, from the rack input side, there is similar amount of cables coming from the surface facilities.

3.9.2.1. Service bays rack requirements

Main requirements for the UT service bays rack are the following:

1. **UT service bays rack must provide support for several SBCs**
   SBR design has to allow for proper installation of 4 service bays crates inside it. In rack, there must be space foreseen for cabling, as well as, for water cooling manifolds for crates cooling system.

2. **UT service bays rack has to be robust**
   Due to its role, which is supporting 4 fully equipped service bays crates, with all cables attached to them, service bays rack must withstand significant load. The only place, where the rack can be installed in LHCb cavern is the magnet wall. Therefore, rack design has to take into account several different conditions.

3. **Service bays rack must fit in given space in LHCb cavern**
   Because service bays rack for new Upstream Tracker detector replaces rack for old Trigger Tracker detector, it must be located in the same place in LHCb cavern. UT rack is much bigger and populated with more cables. Hence, the space available is very tight and the rack has to be as compact as possible, in order to avoid collision with other elements in LHCb cavern, for example cable chain.

3.9.2.2. Service bays rack layout

There are 4 service bays crates placed inside one service bays rack. In order to save space between magnet wall and cable chain, crates inside the rack are oriented vertically, with cooling pipes from cold plates directed upwards – Figure 3.90.

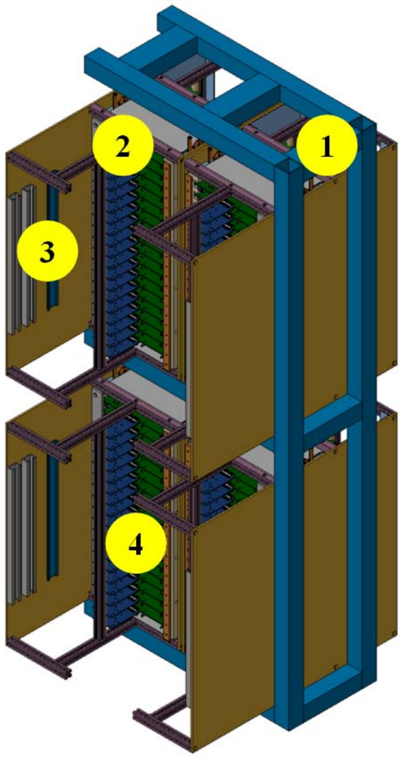

Figure 3.90 Service bays rack 3D assembly
Rysunek 3.90 Złożenie 3D szafy serwisowej

In the Figure 3.90, following components of the service bays rack can be distinguished:

1. Service bays rack structure.
2. Service bays crates placed inside the rack.
3. Patch panels with connector rails and cable trays for cable management.
4. Low voltage regulator boards inside service bays crates.

3.9.2.3. Service bays rack mechanics

In order to fulfill its requirement of robustness service bays rack is constructed from square and rectangular steel profiles. Profiles are welded together to provide strong and rigid frame – Figure 3.91.

Several different profiles can be distinguished in rack structure:

- Vertical profiles have a square cross-section of 50x50x3mm. There are two of them in rack construction and they define total rack height – Figure 3.91, number 1.
- Long horizontal profiles have a square cross-section of 50x50x3mm. There are six of them in rack construction and they define total rack width. On one end they are attached to the magnet, on another end welded to the vertical profiles – Figure 3.91, number 2.
- Short horizontal profiles have a rectangular cross-section of 50x70x3mm. There are nine of them in rack construction and they define total rack depth. They are welded on both ends to the rack long horizontal profiles and they provide support for service bays crates – Figure 3.91, number 3.

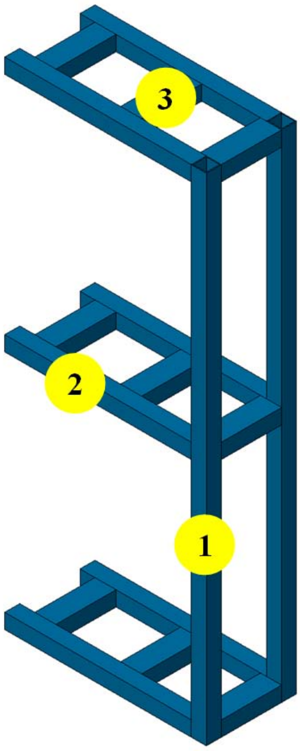

Figure 3.91 Service bays rack structure
Rysunek 3.91 Struktura szafy serwisowej

3.9.2.4. Service bays rack material

Due to close proximity of the magnet and strong magnet field, material used for building service bays rack structure, must be stainless steel. This is because of two reasons. First, strong magnet field could exert additional forces on the rack structure causing undesirable problems. Second, large rack structure made of black steel could interfere with magnetic field in unforeseen way and distort it.

Because profiles making rack structure will be welded together, another restriction/requirement must be taken into account. Stainless steel in grade 304 is tricky to weld. Due to heat influence in the welding area it changes its crystal structure and weld regions may became magnetic. Due to this fact, stainless steel 316L has been chosen for the service bays rack material.

3.9.2.5. Service bays rack assessment

In order to check if proposed approach to construct service bays rack is robust enough to withstand foreseen load, FEM analysis in ANSYS has been performed.

Analysis conditions:

- Material: structural steel
  - Tensile ultimate strength: 460MPa,
  - Tensile yield strength: 250MPa),

- Assumed load: 1000kg (one sixth of the total load placed on the end of each long horizontal rack profile – Figure 3.92 a),
- Self-weight of the structure,
- Mesh element size 10mm.

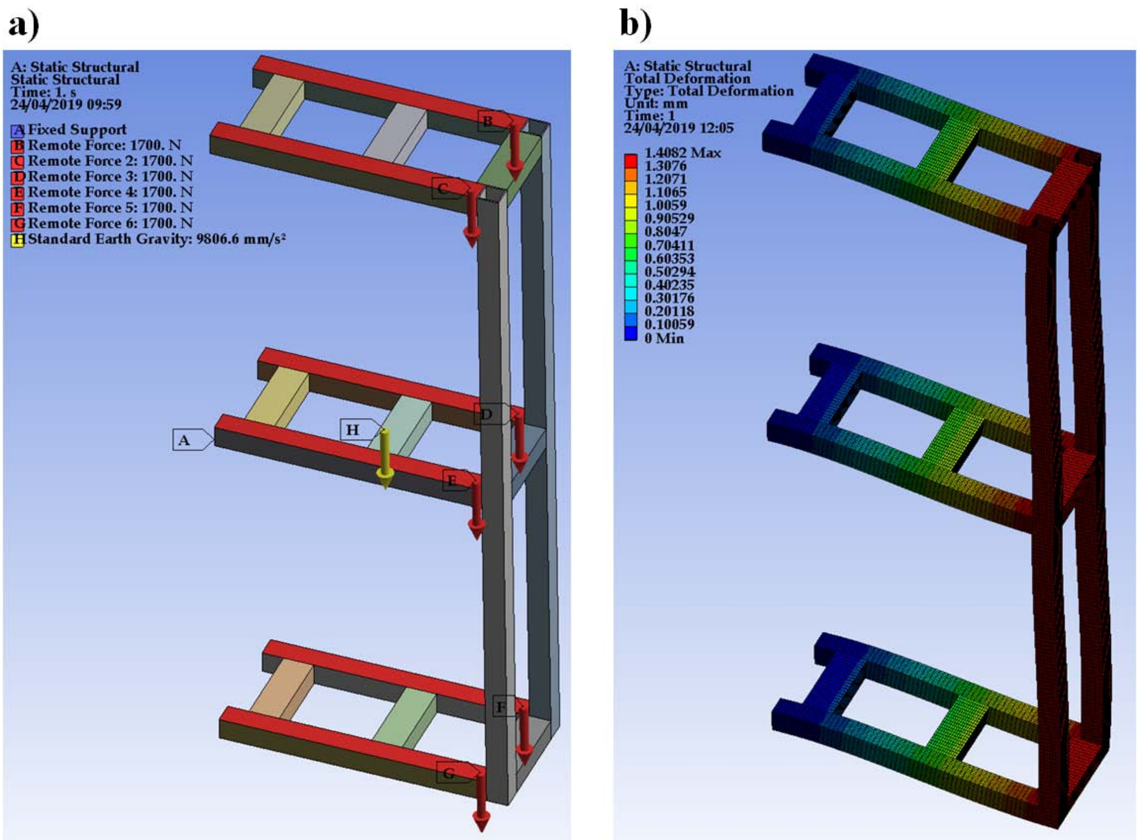

Figure 3.92 a) Forces layout for FEM analysis; b) Total deformation

Rysunek 3.92 a) Rozkład sił do analizy MES; b) Całkowita deformacja

An outcome from the analysis is as follows:

- Maximum deformation: 1.4mm – Figure 3.92 b,
- Maximum stress: 235MPa.

The rack assessment in ANSYS indicated that proposed structure is capable to withstand forces applied.

3.9.2.6. Service bays rack integration inside LHCb cavern

In one direction, service bays rack must fit between magnet wall and cable chain, where is about 700mm of space available. In another direction, it must be placed between two long distance power cable trays (so called "marathons"), where is about 1000mm of space available. Figure 3.93 shows old Trigger Tracker rack placement on the magnet wall with respect to the cable chain. It was relatively small in comparison to new Upstream Tracker rack, which replaces TT one.

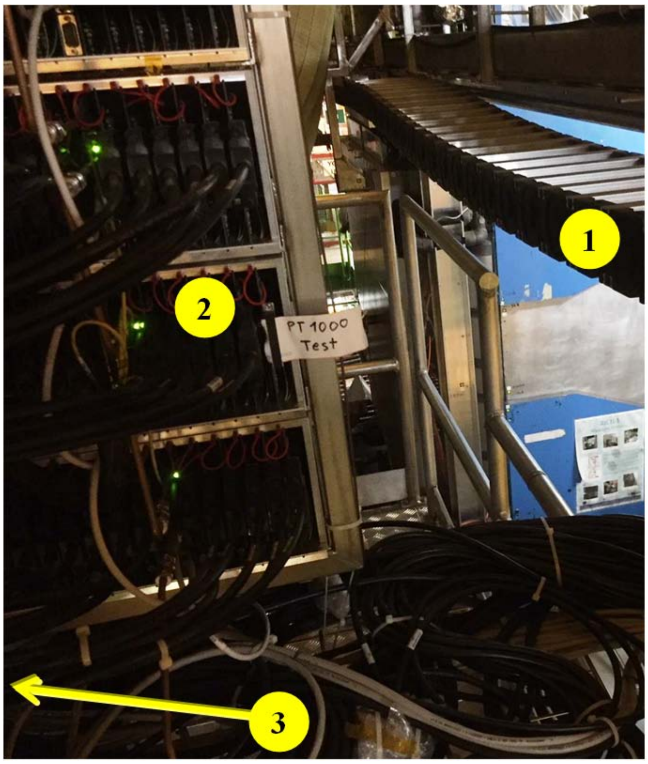

Figure 3.93 Rack in the LHCb cavern [5]
Rysunek 3.93 Szafa serwisowa w cavernie LHCb [5]

In the Figure 3.93, there is space for rack placement in the LHCb cavern presented:

1. Cable chain.
2. Old TT rack attached to the magnet wall.
3. Magnet wall side.

4. **Prototype of critical UT detector areas**

3D models and assemblies in Catia are very helpful in designing detectors at CERN. However they cannot answer all the questions, which engineers might have. For example it is difficult to assess actual size of an element, as well as, accessibility in tight areas and possibility to operate tools using only 3D modeling. There is no way to model in Catia the stiffness of a rubber seal. It must be tested in mock-up on the physical object.

That is why mock-ups and prototypes are built, in order to cross-check 3D models and introduce further improvements into designed structure or element.

4.1. Mock-up

Mock-up is a fake part made for example using 3D printing technology. Building a mock-up of the parts and assemblies it makes easier to understand an actual size of an object or a structure. Hence, it is easier to assess, if the part fits in given envelope (given space/volume) or not. Using mock-ups the sequence of installing the parts in assembly can be investigated in further details too. It is also helpful in order to understand, if any kind of special tooling might be needed during final installation. Properly built and studied mock-up can save a lot of time during assembling of the final device and prevent from damaging delicate parts, like staves with silicon sensors in UT.

4.1.1. UT mock-up of one detector half

In order to investigate staves mounting system (staves supports), PEPI electronics, and especially pigtails cables connecting staves and PEPI, a mock-up of one UT detector half has been constructed – Figure 4.1. It was important to check pigtails length, connectivity, stiffness and sealing system to understand the issues and introduce necessary corrections in the design.

C-Frame was built from aluminum, in full size, and check in terms of self-weight sag – Figure 4.9.

Staves supports were machined from stainless steel in their original form – Figure 4.4.

Dummy staves were made from aluminum to test their mounting system, assembly sequence and how they overlap.

Top and bottom UT detector box plates were machined from aluminum to make them cheaper and quicker to build, than carbon fiber reinforced sandwich structure. Stave supports positioning dowel pins and holes were machined in the plates – Figure 4.5.

Connectors on staves, pigtails and backplane were 3D printed in PLA or ABS material (Figure 4.8 c) and glued in correct position.

Fake pigtails were made from composite material combined with thin 0.2mm aluminum sheet and 0.05mm kapton layers on both sides of it – Figure 4.2, Figure 4.3 and Figure 4.8 a, b.

Backplane in PEPI volume was made from aluminum plate with 3D printed connectors glued on it. In further iteration, full backplane together with connectors was 3D printed as one piece – Figure 4.6.

DCB cooling interface (heat spreader and clamps) were 3D printed – Figure 4.7.

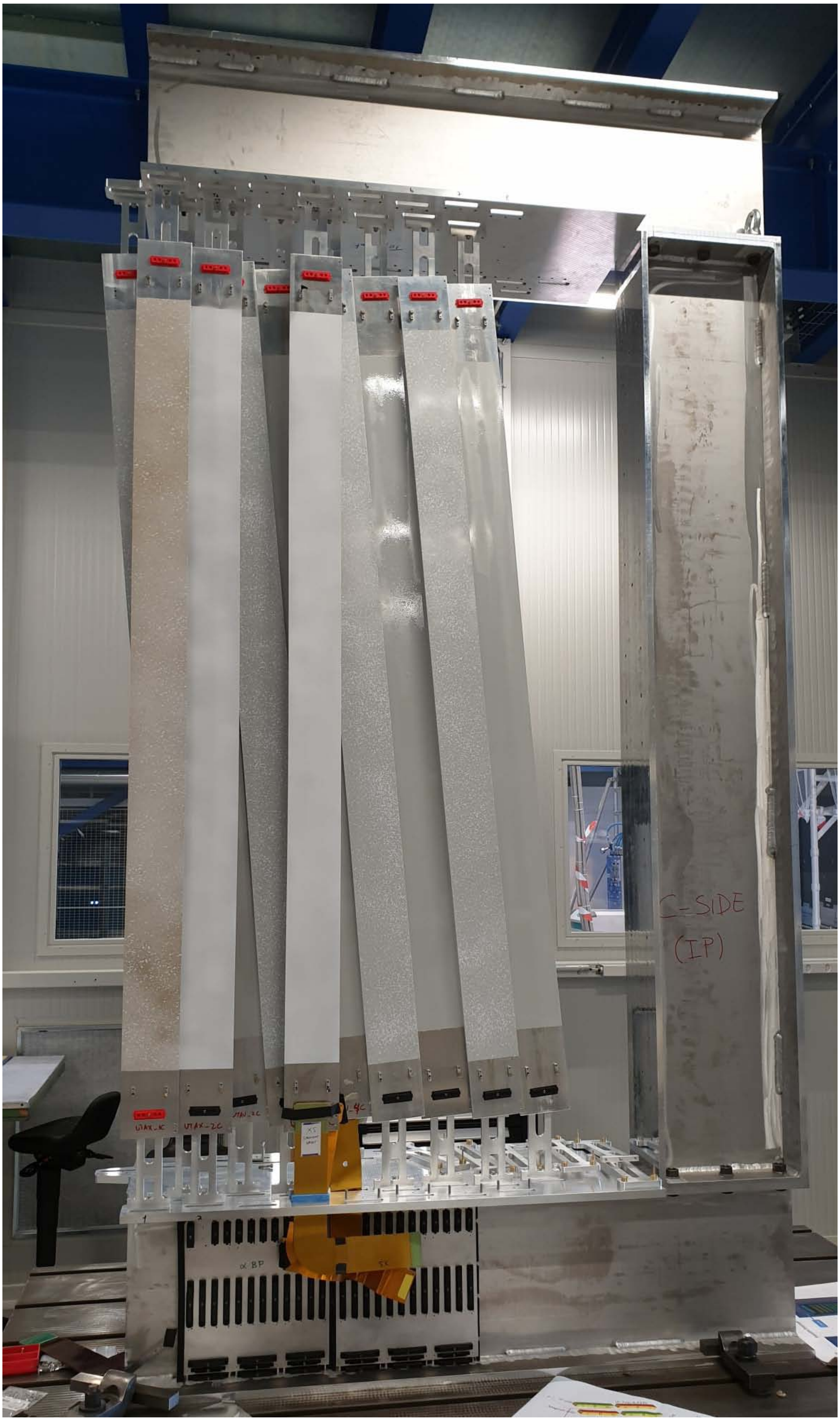

Figure 4.1 UT C-Side mock-up
Rysunek 4.1 Makieta UT strona-C

Figure 4.2 PEPI and data read-out cables (pigtails)
Rysunek 4.2 PEPI i kable odczytu danych

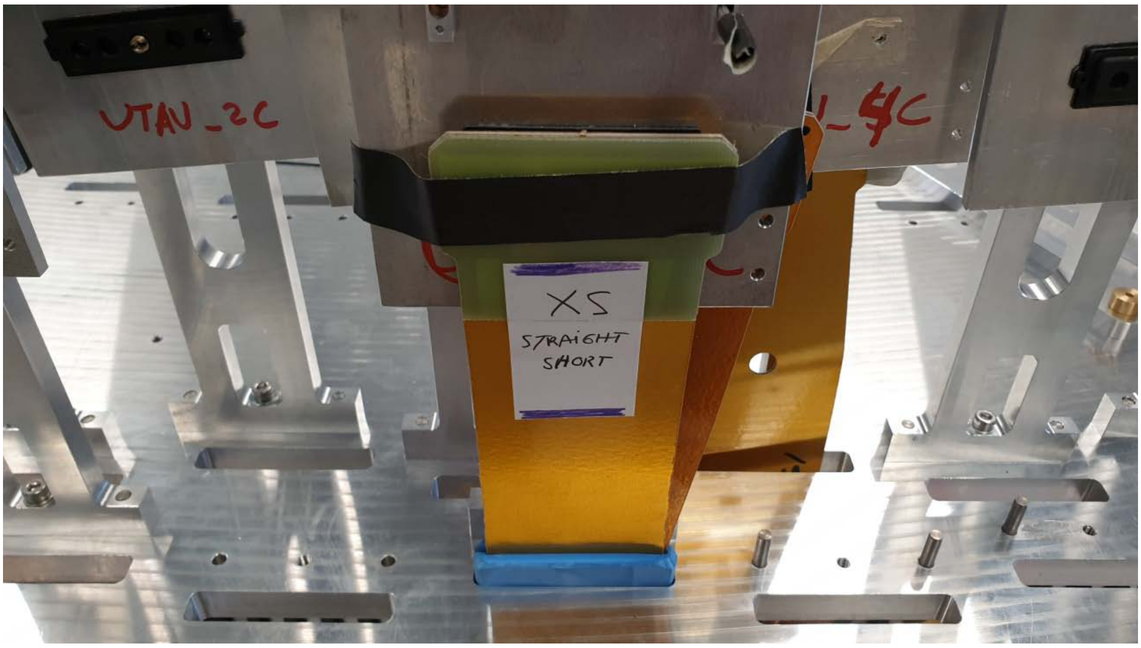

Figure 4.3 Data read out cable (pigtail) attached to stave connector
Rysunek 4.3 Kabel odczytu danych podłączony do stave'a

Figure 4.4 Staves supports
Rysunek 4.4 Podpory stave-ów

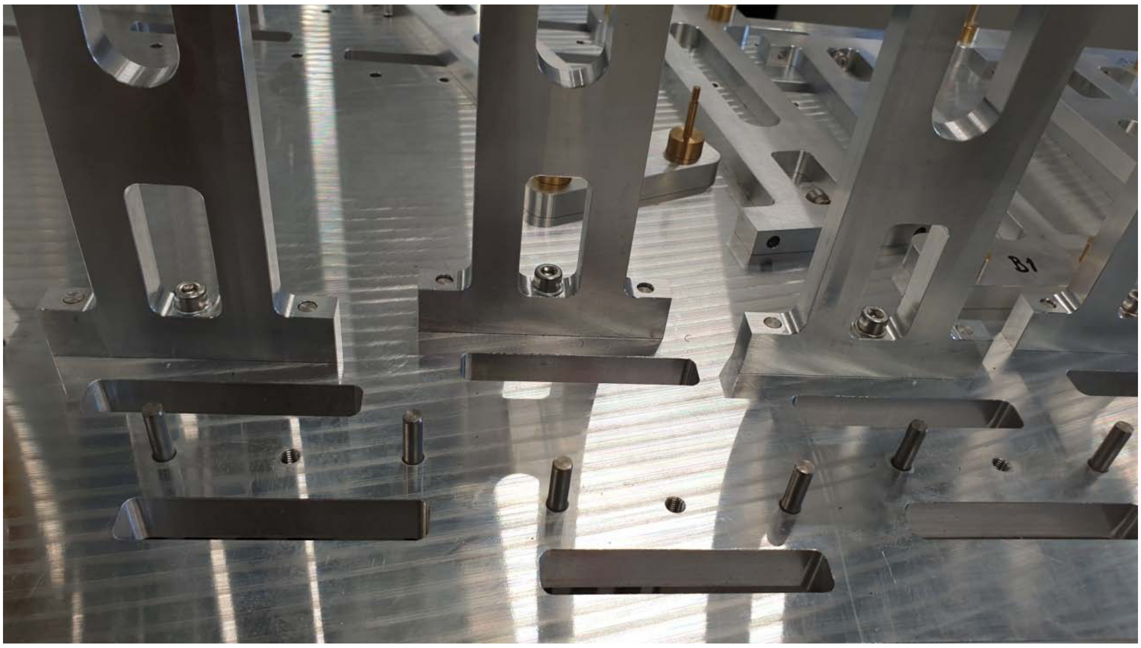

Figure 4.5 Staves supports interface to the detector box plate
Rysunek 4.5 Interfejs podpór stave-ów i płyty skrzyni detektora

Figure 4.6 3D printed backplane
Rysunek 4.6 Backplane wydruk 3D

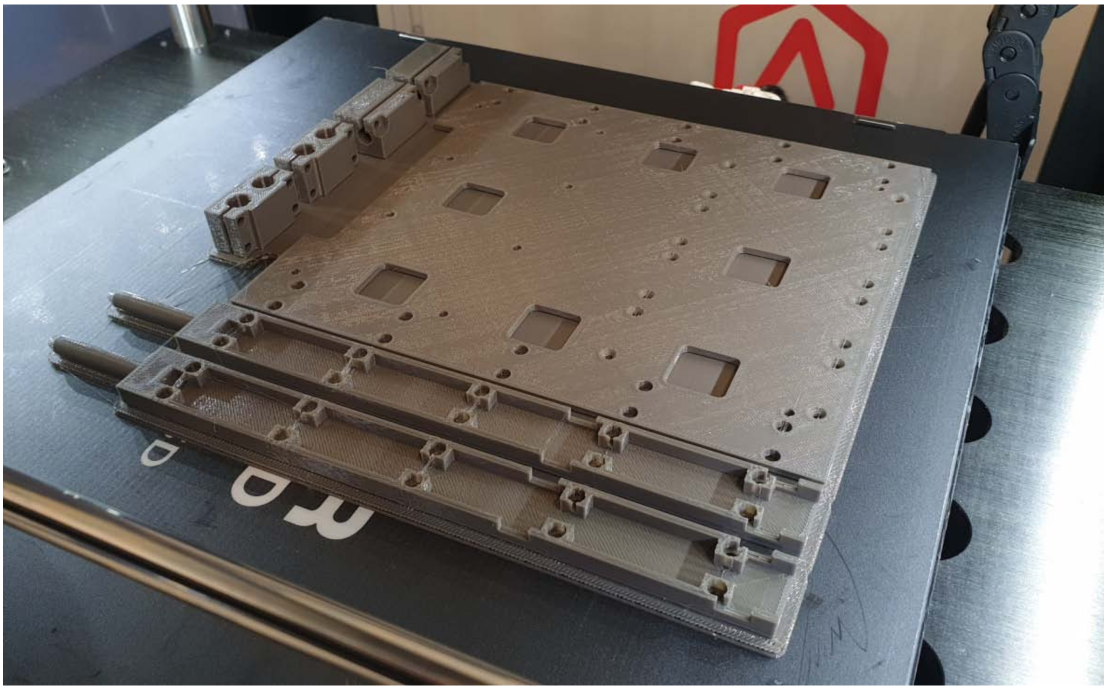

Figure 4.7 3D printed DCB cooling interface
Rysunek 4.7 Interfejs chłodzący kartę DCD wydrukowany w 3D

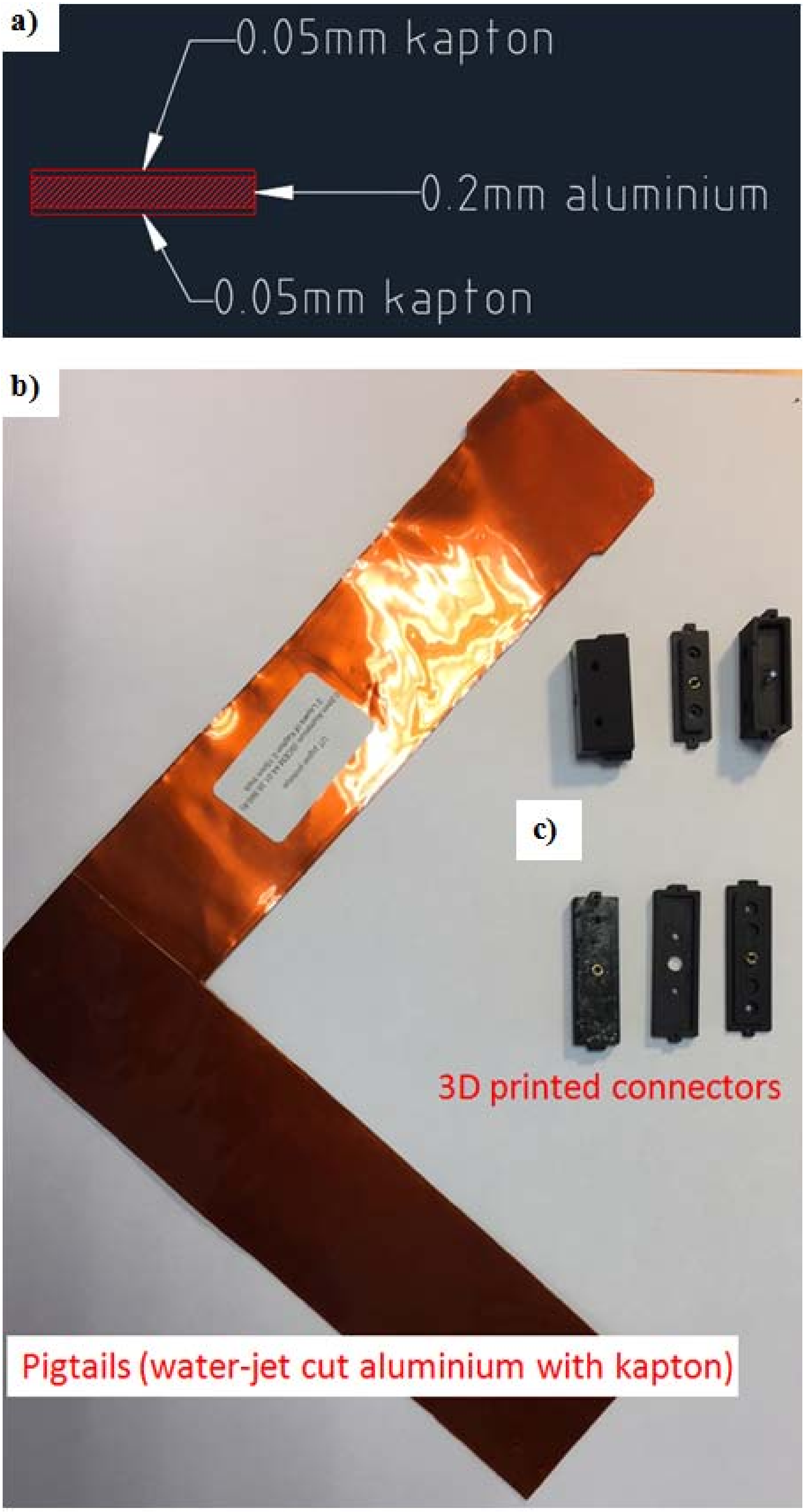

Figure 4.8 a) Fake data read-out cable cross-section; b) Fake data read-out cable; c) Fake connectors [38]

Rysunek 4.8 a) Przekrój makiety kabli odczytu danych; b) Makieta kabla odczytu danych; c) Makieta konektorów [38]

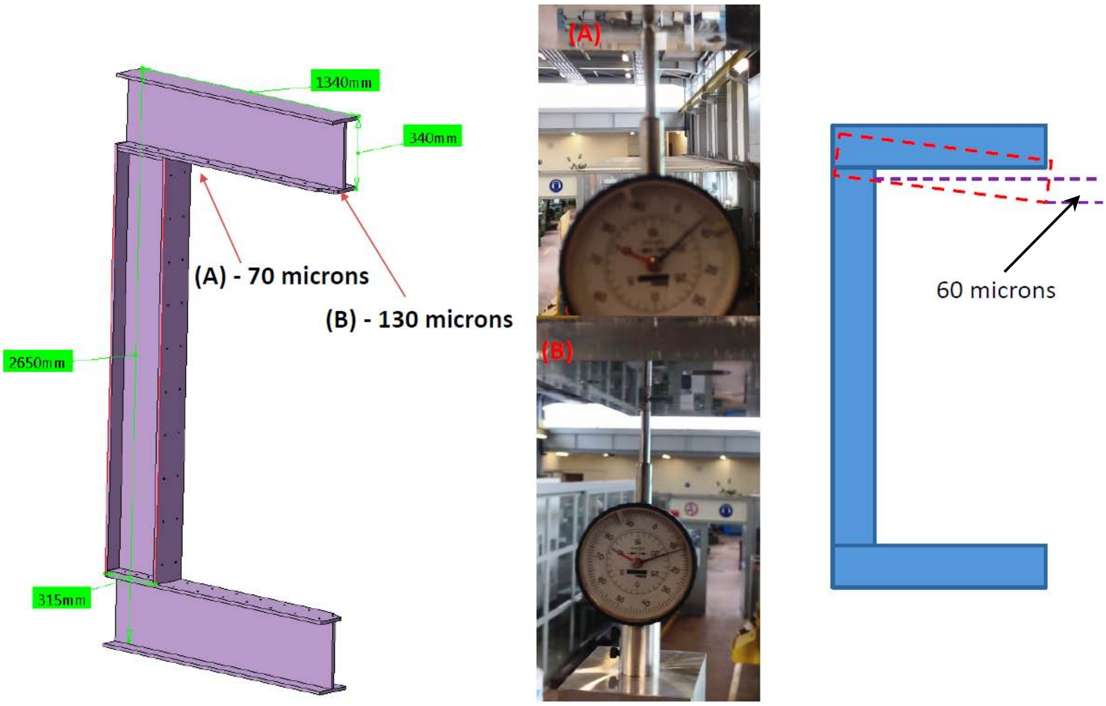

Figure 4.9 C-Frame checks [38]
Rysunek 4.9 Testy ramy-C [38]

4.1.2. Lessons learned from building a mock-up

One pigtail cable is not a solitary object presented in Figure 4.8 b. In order to provide 400 paths, single pigtail consist of up to 9 cables like this. They are placed parallel to each other with connectors on both ends – Figure 4.26. During building a mock-up it was observed that, pigtails are very stiff and exert significant force on stave connectors. It was clear that, connectors will be damaged or disconnected. On the basis of those observations, additional special clamps were developed in order to prevent it from happening – Figure 3.35. Because pigtails connectors consists of 400 delicate pins, a system precisely guiding them during connection phase is under development.

During mock-up investigation on pigtails, it was observed that, some of the pigtails types are too long and can be shortened. On the other hand, some of the pigtails types were too short and they could not reach backplane connectors. If not building a mock-up, that would be a catastrophic discovery during final installation.

Another useful observation was made on rubber seal tightening the pigtails in place and sealing the box. They seem to be too wide with respect to the holes in the box. Moreover, a rubber with softer grade would adapt better and require less force to fit in.

C-Frame checks revealed self-weight sag of the top part of the C-Frame by about 130um – Figure 4.9. This value has influence on all staves installed inside the UT detector box, and helps to assess how much slack staves supports should have, in terms of mechanical deformations.

During building C-Frame prototype, it was learned that, overall precision below 250um can be achieved on C-Frame machining and assembling.

Prototype C-Frame plates were welded. During installing base plates and backplanes in PEPI area, it was quickly seen that, welds must be machined afterwards, in order to fit PEPI electronics in place.

Observation of staves in mock-up revealed a need for the staves to be parallel during insertion into staves supports.

The overall manufacturing techniques and concept have been validated for C-Frame, UT detector box, stave supports, and other elements.

Final lesson was that access to staves and their connectors is very hard after installation. Moreover, dismantling of staves in case of failure is very complicated.

4.2. Prototype

In contrast to mock-p, prototype is a functional device, which can be tested in terms of its principal purpose. It is common practice to build a prototype of main detector components, like data dead-out electronics, in order to test for example connectivity and signal integrity. At LHCb Upstream Tracker detector collaboration two prototypes of critical UT detector areas were built.

4.2.1. Pathfinder test

Pathfinder test is a stand-alone test of pathfinder backplane to check its connectivity with all the boards attached to it: 2 DCBs, telemetry board, 2 low voltage power breakout boards. It uses prototype parts in order to check their performance. To emulate signals coming from pigtails, special cards called "COMET boards" were design, and plugged from the back of the pathfinder backplane. They send 320 MHz data like that coming from the staves through the pigtails. These data go through test lines to a given DCB slot, and allows for testing the full data path inside the DCBs.

In order to support all the boards, mechanical structure had to be designed. Because it was a good opportunity to test PEPI mechanics concept, pathfinder mechanics was design to closely mimic one of the PEPI compartments – Figure 4.10, Figure 4.11, Figure 4.12.

Production drawings of the Pathfinder support elements, as well as, assembly drawing is attached in the thesis Appendix.

In the Figure 4.10, following components of the pathfinder support (also called pathfinder crate) can be distinguished:

1. Pathfinder base plate – Figure 4.13.
2. Pathfinder DCB card guides.
3. Pathfinder walls with water pipes support.
4. Pathfinder Bosch profiles construction for stability and support.

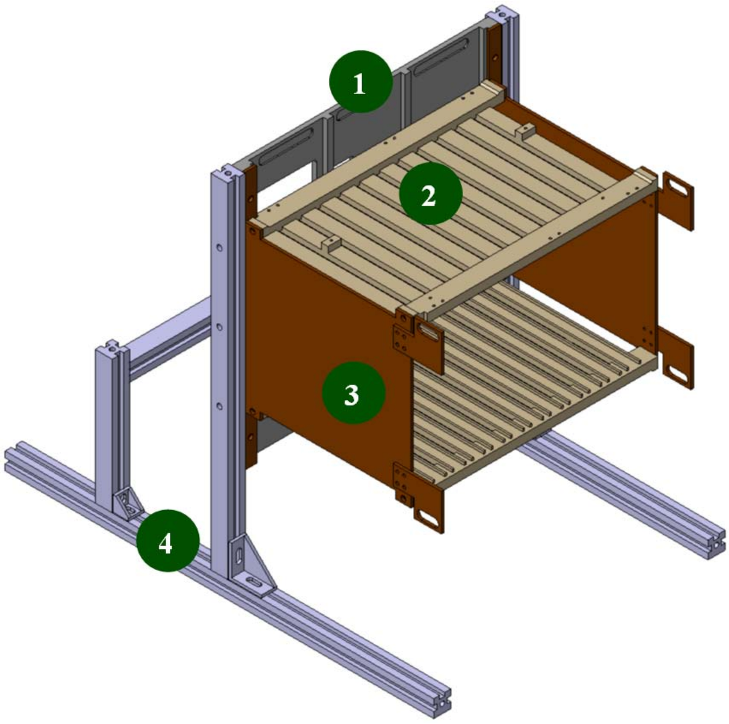

Figure 4.10 Pathfinder support 3D assembly [6]
Rysunek 4.10 Złożenie 3D podpory dla testu pathfinder [6]

Constructing pathfinder support as a single PEPI compartment, allowed for detail investigation about overall PEPI mechanics concept, required machining precision and usability of this solution.

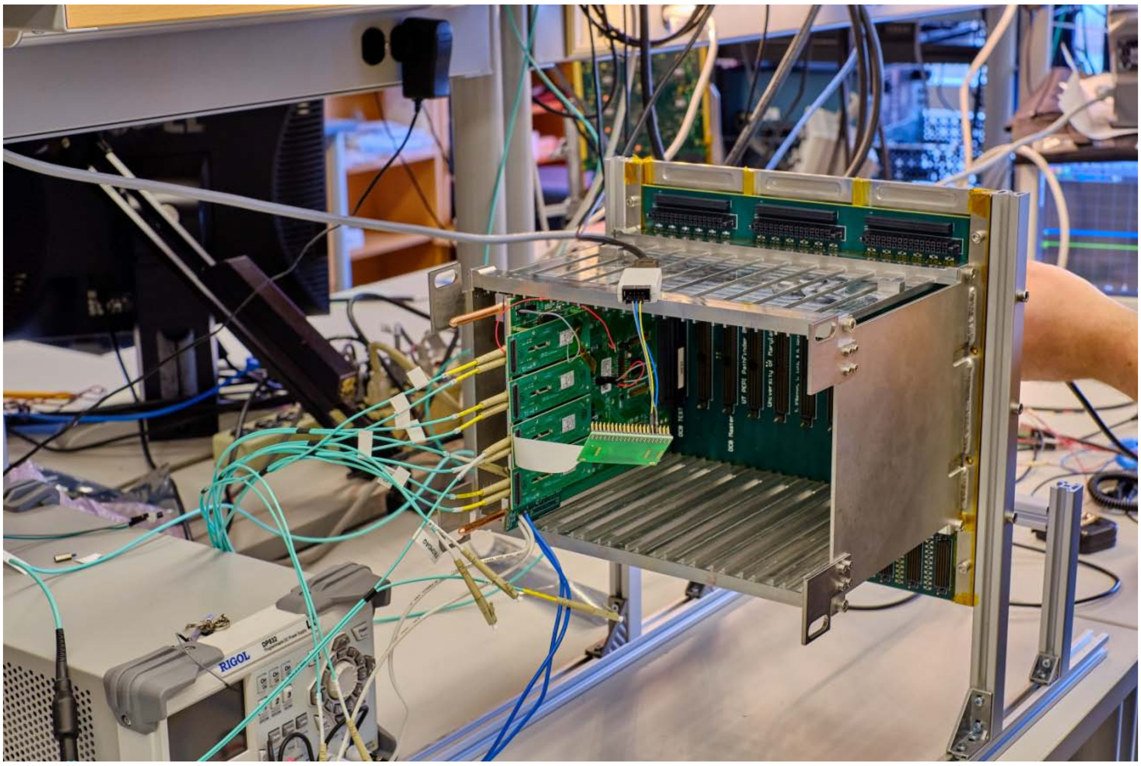

Figure 4.11 Pathfinder test, DCB card inside card guides [39]
Rysunek 4.11 Test pathfinder, karta DCB wewnątrz prowadnic [39]

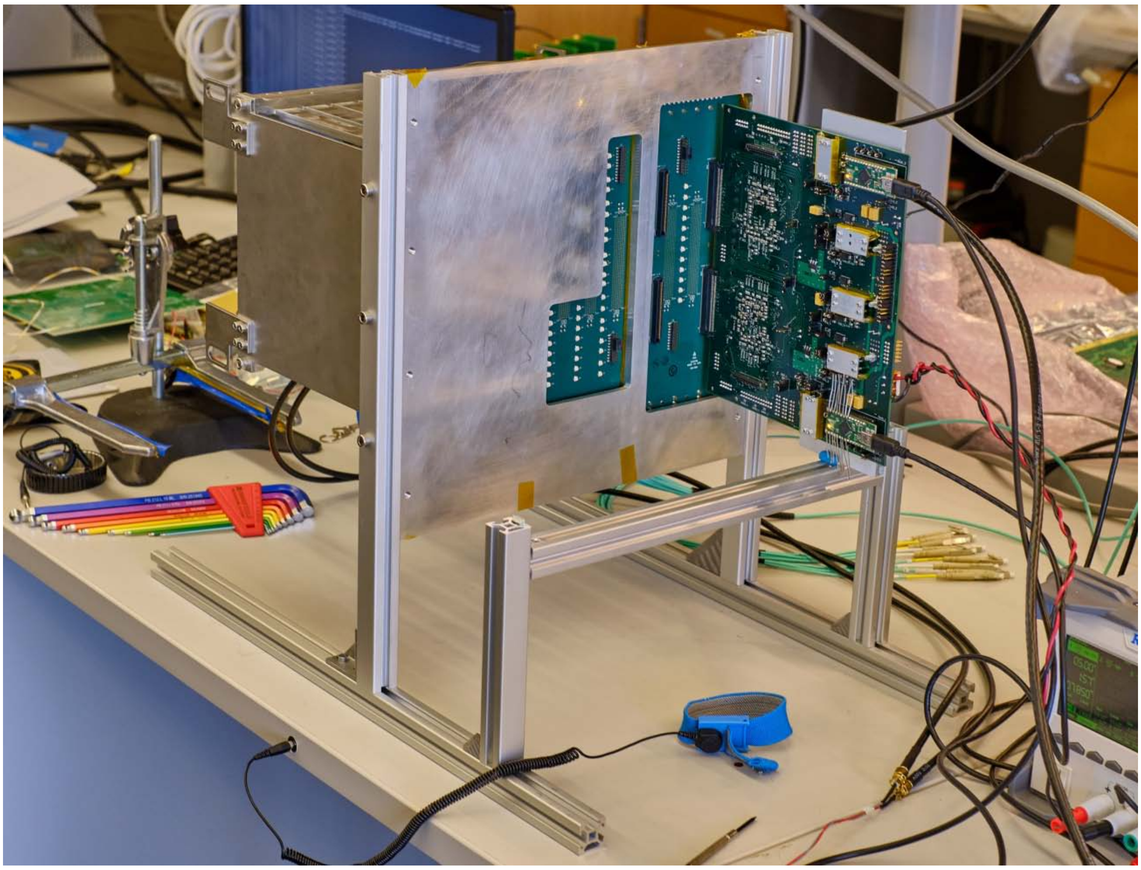

Figure 4.12 Pathfinder test, COMET board attached from the back of the backplane [39]
Rysunek 4.12 Test pathfinder, płyta COMET podłączona z tyłu backplane [39]

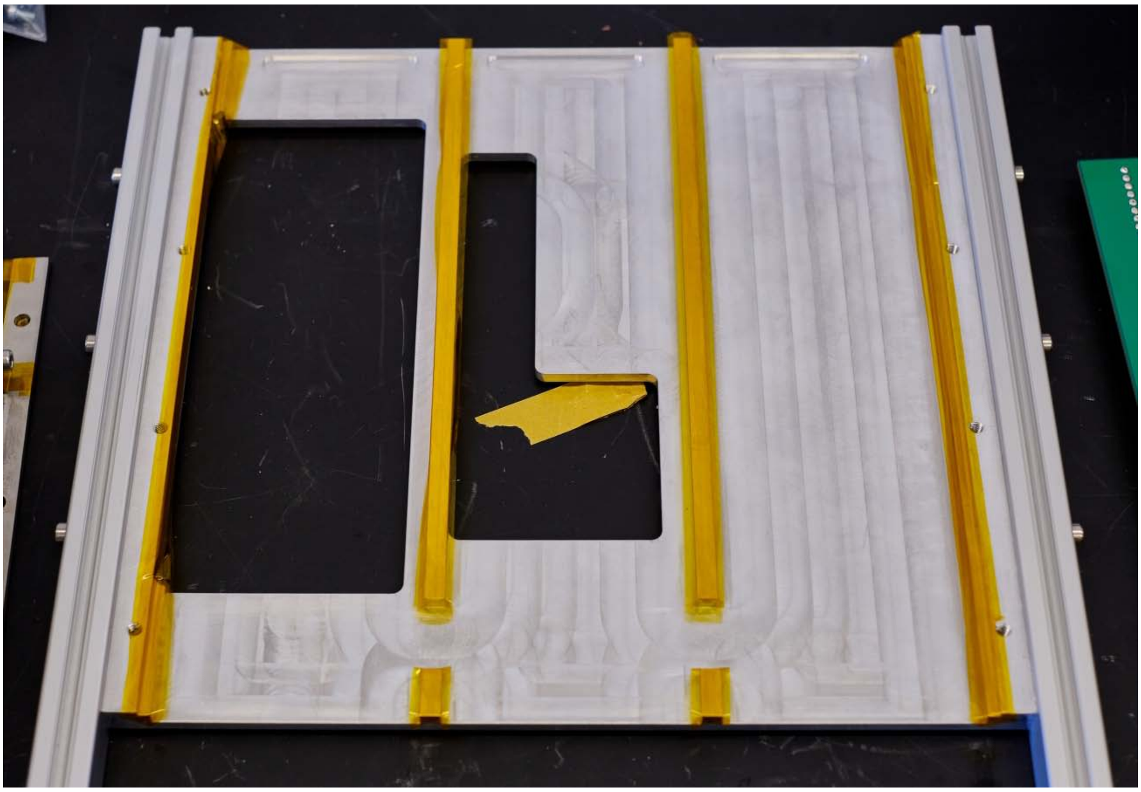

Figure 4.13 Pathfinder base plate with kapton [39]
Rysunek 4.13 Płyta bazowa dla testu pathfinder pokryta warstwą kapton-u *[39]*

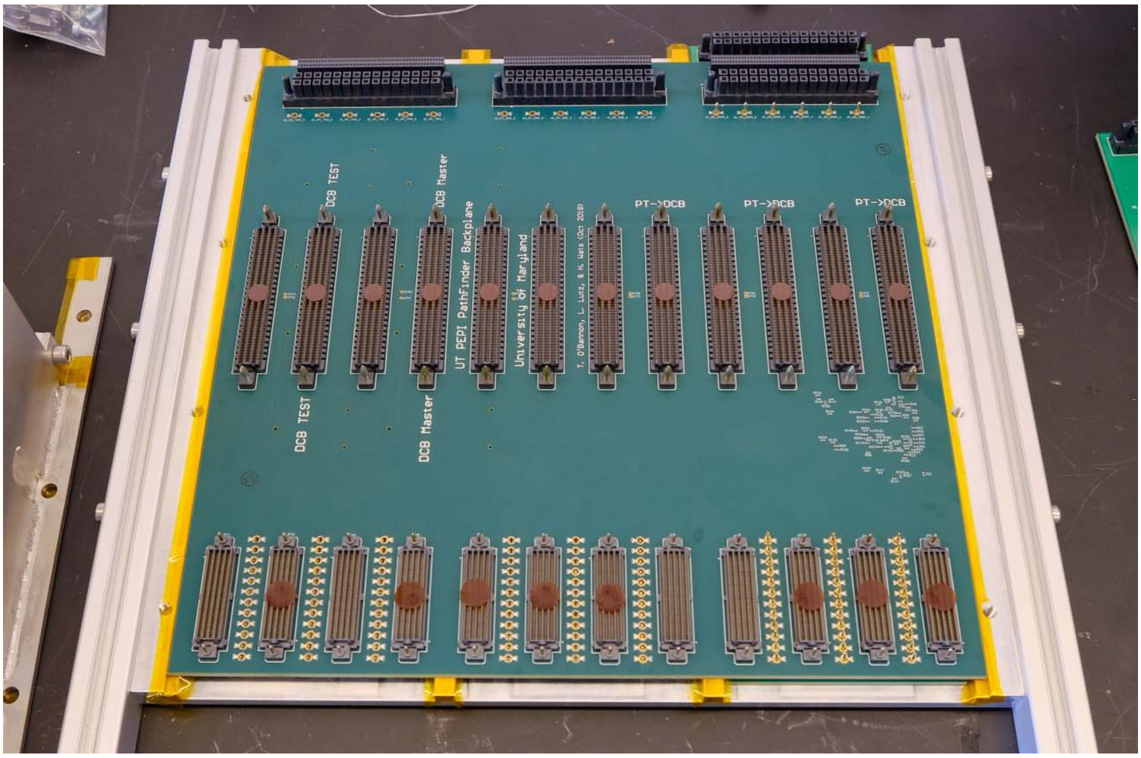

Figure 4.14 Pathfinder backplane placed on base plate [39]
Rysunek 4.14 Pathfinder backplane umieszczona na płycie bazowej [39]

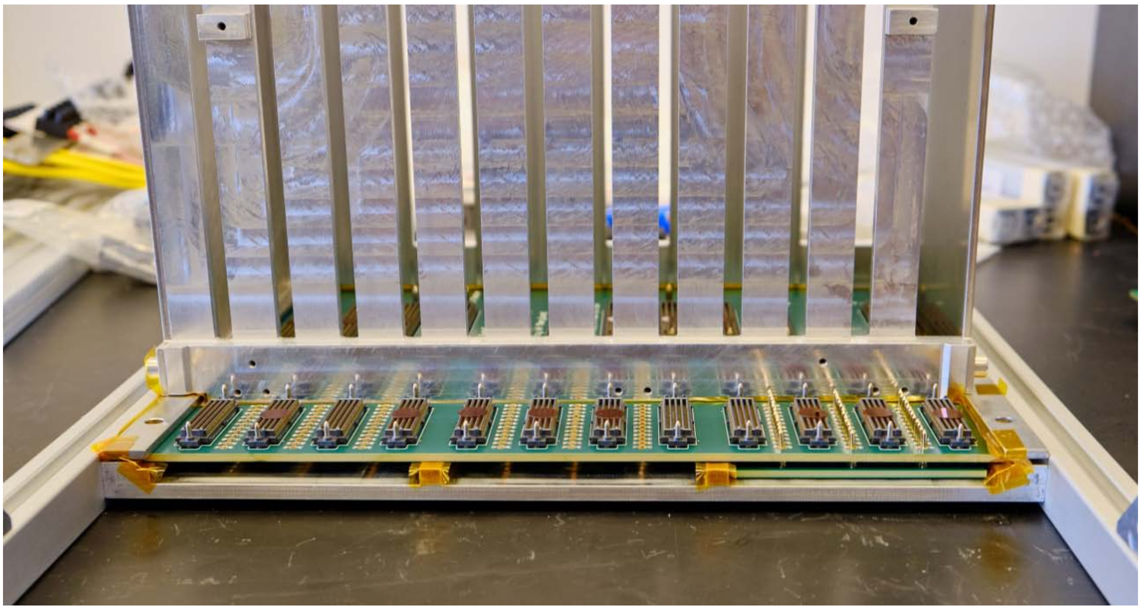

Figure 4.15 DCB card guide pressing backplane against base plate [39]
Rysunek 4.15 Prowadnica kart DCB przyciskająca backplane do płyty bazowej [39]

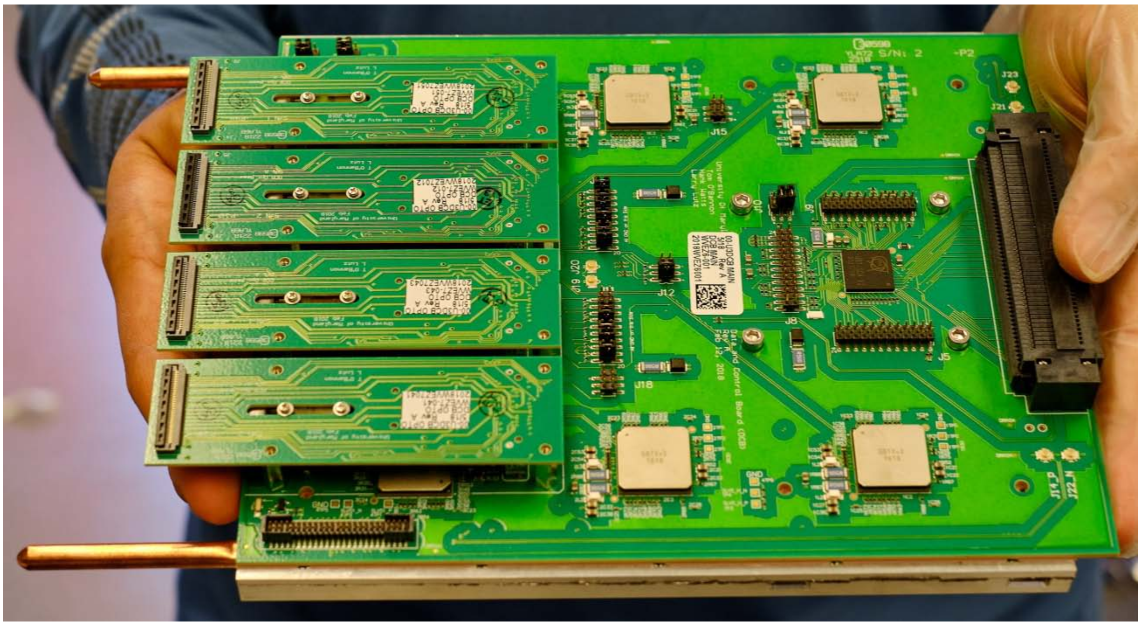

Figure 4.16 DCB card, connector side [39]
Rysunek 4.16 Karta DCB od strony konektora [39]

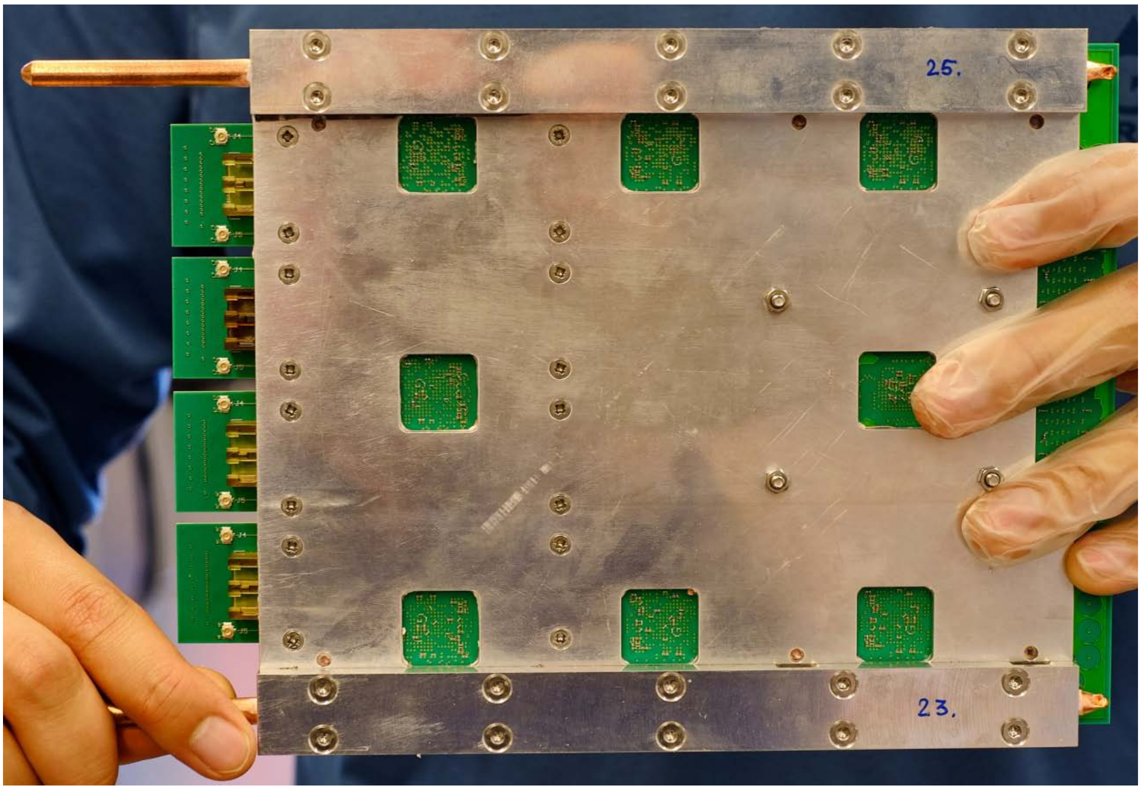

Figure 4.17 DCB card, cooling interface side [39]
Rysunek 4.17 Karta DCB od strony interfejsu chłodzącego [39]

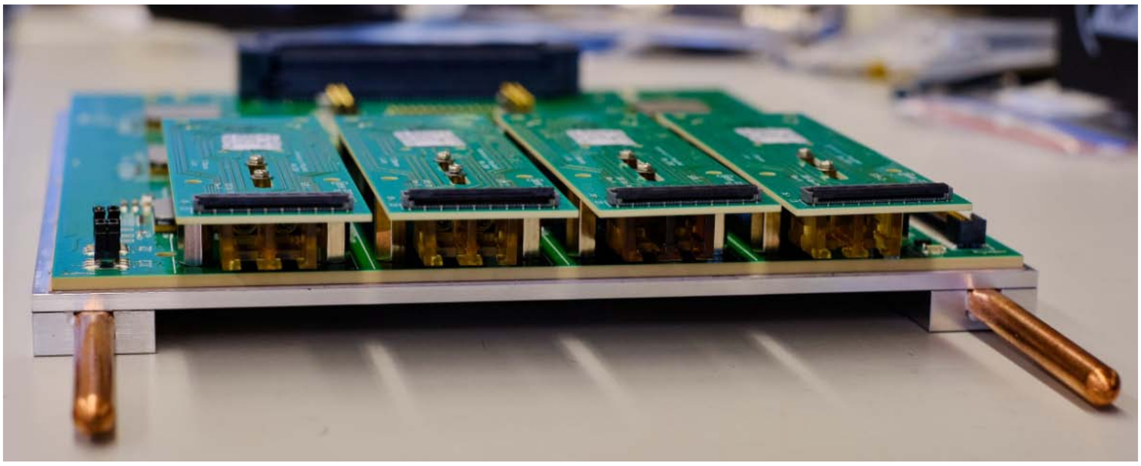

Figure 4.18 DCB card, gap filler, mezzanine boards with stand-offs and heat spreader [39]
Rysunek 4.18 Karta DCB, wypełniacz, płytki mezzanine z odstępnikami i radiator [39]

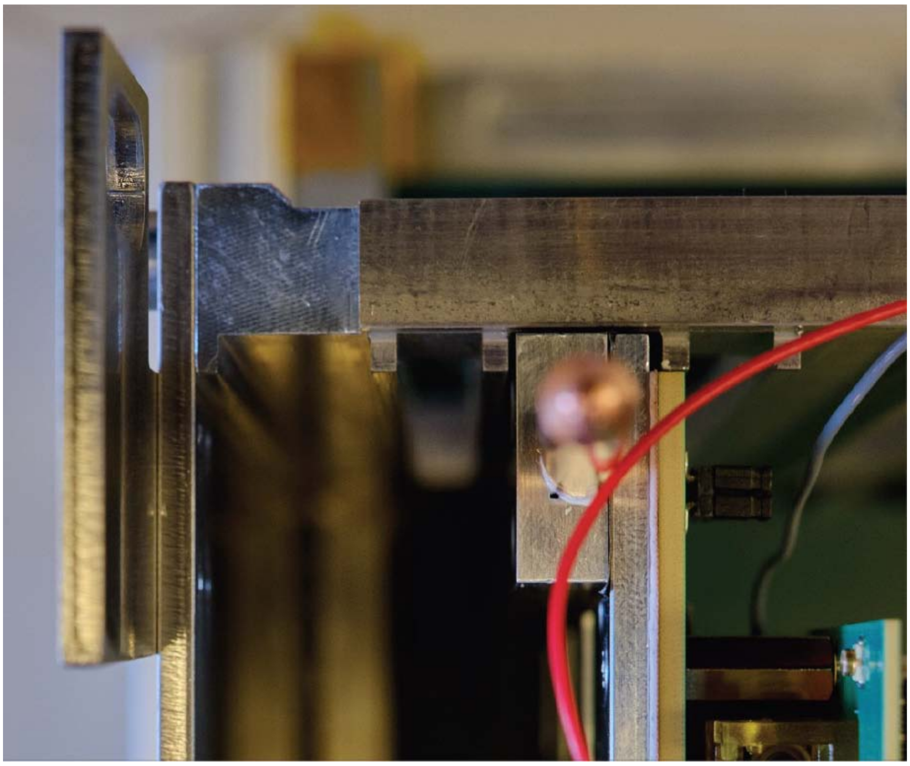

Figure 4.19 DCB card inserted in channel [39]
Rysunek 4.19 Karta DCB w kanale prowadzącym [39]

4.2.1.1. Observations from pathfinder test

Heat spreader clamp and heat spreader, as well as, heat pipe clamp and water pipe clamp will be mounted together using thermal interface of thin ~0.05mm graphite foil (seen in Figure 4.16), in order to avoid any air gaps between elements and improve heat transfer.

However, first tests in Pathfinder crate reviled a significant problem with this solution. Graphite foil, which is fractured on the edges during cutting procedure, can dethatch and become conductive flakes floating in the PEPI volume and possibly making short-cuts in electronics. Because graphite foil is very conductive material, this situation must be avoided for all costs, to prevent from damaging electronics, and in worst case scenario, to prevent form causing a fire.

There are two proposed solutions for this problem. First, graphite foil sheets can be cut 1 or 2mm smaller than the clamp size, in order to be completely covered by the element. It also must be cut using sharp tool, for the edges to be straight and clean, without fractures. Second solution is to use thermal paste as an interface instead of sing graphite foil.

One of the requirements was to cover with insulating kapton film all mechanical elements, which come in contact with electronics. It is necessary in order to eliminate short-cuts. The base plate (Figure 4.13) is in particular interest as it supports backplane – Figure 4.14.

Pathfinder test allowed for testing the mechanism of pressing backplane against base plate using DCB card guides, seen in Figure 4.15. The elements fits well and mechanical tolerances are fine. However, after closer studying of this solution, an improvement has been made. It is beneficial to change the holes in walls, which hold DCB card guides, for elongated holes, instead of simple round holes. Doing so, the pressure exerted on the backplane can be regulated independently from backplane thickness and allow to avoid over-constraining the system.

Using real piece heat spreader for DCB card allow for testing if all the holes for mounting these pieces together are in correct position and all the square openings for electronic components are large enough to accommodate all the elements – Figure 4.17.

It also allowed for testing the gap filler between cooling interface and DBC card (seen in Figure 4.18), as well as, overhang value of the heat spreader over DCB card.

Constructing full DCB cooling interface allow for testing cooling properties when DCB cards are under full load. One of the tests called "burn-out test" will check it out.

Observations during inserting DCB cards into the backplane showed that, DCB card guide channels might be too wide – Figure 4.19. Although they were designed to only roughly guide DCB cards towards backplane connectors, it is worth to study alternative approach in more details.

Backplane placed on base plate is free in vertical position. Before backplane is tighten on both edges, it can slide down, when in vertical position. A solution seem to be adding a shelf supporting backplane on base plate, when placed in vertical position.

Backplane is not precisely positioned on the base plate. Due to extremely dense copper paths on the backplane (28 layers) there is no possibility to make positioning holes in backplane. It would be beneficial to position backplane on base plate using dowel pins. This would give exact positions of the backplane connectors with respect to PEPI mechanics and then allow for tightening DCB board guides channels for precise guiding DCB cards towards backplane.

4.2.2. Slice test

In comparison to mock-up, slice test is a prototype. It uses real parts like staves and pigtails in order to check their performance. It was designed to test one stave in real environment. Special slice test box was made and equipped with dedicated CO_2 cooling distribution system, in order to test stave performance under nominal working conditions.

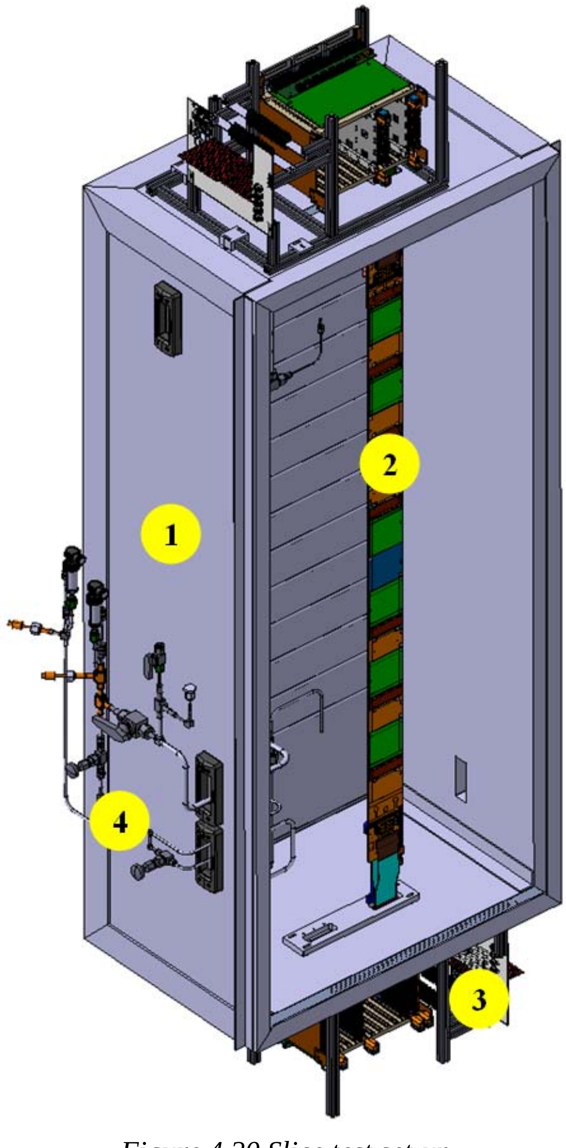

Figure 4.20 Slice test set-up
Rysunek 4.20 Konfiguracja slice testu

In the Figure 4.20, following components of the slice test set-up can be distinguished:

1. Slice test box – Figure 4.22.
2. Tested stave – Figure 4.27.
3. Pathfinder crate with prototype patch panels – Figure 4.21.
4. CO_2 cooling distribution system for slice test box.

During slice test, stave inside the box is mounted on original stave supports (Figure 4.24 a) with brass pins (Figure 4.24 b), in order to test their design and assembly procedure. Moreover, samples of pigtails (Figure 4.25 and Figure 4.26) are used to connect stave with pathfinder crates, which closely mimic original PEPI compartments. It allows to check the connectivity between sensors inside the box and PEPI electronics. It allows as well for testing how multiple pins connectors meet each other in close to real conditions.

Because slice test needs full cabling connectivity for one stave, it was a god opportunity to test various ideas of patch panels – Figure 4.21.

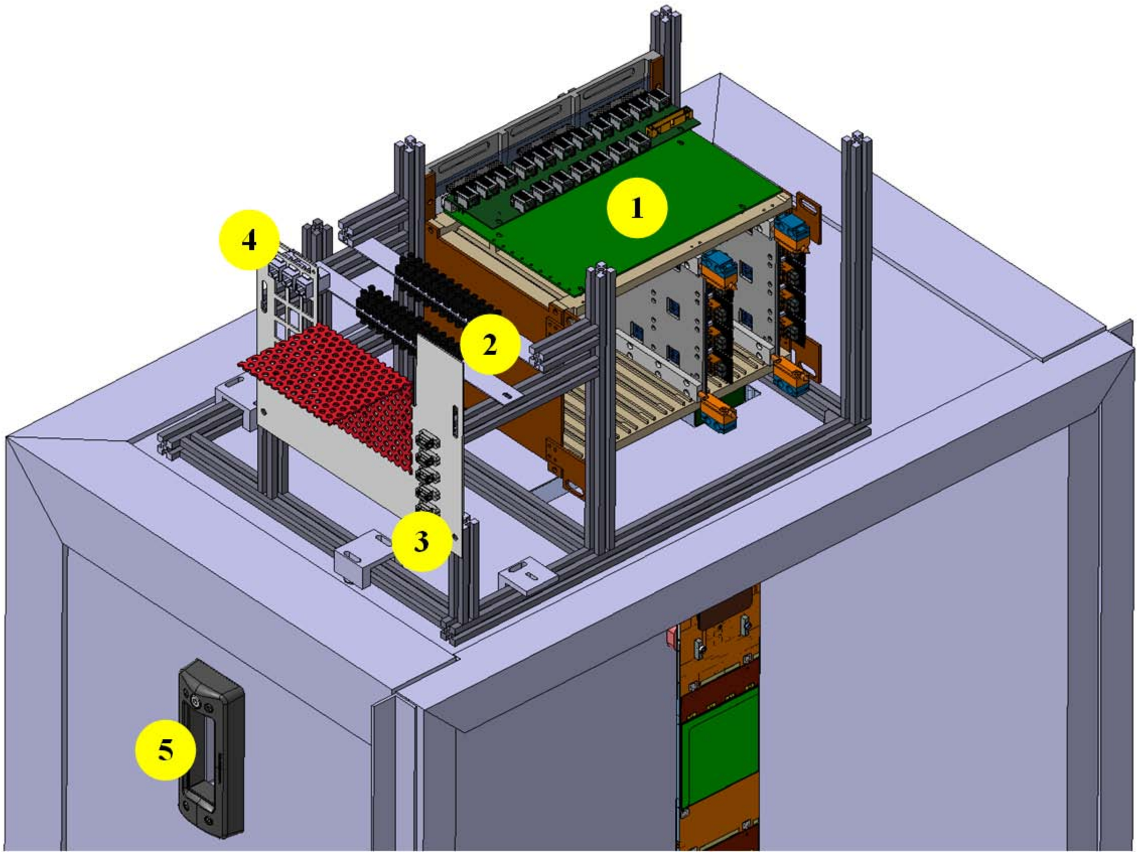

Figure 4.21 Pathfinder support adapted for slice test, with prototype patch panels
Rysunek 4.21 Podpora testu pathfinder dostosowana do slice testu, wraz z prototypowymi panelami przejściowymi

In the Figure 4.21, following components of the slice test patch panels can be distinguished:

1. Pathfinder support – Figure 4.23.
2. Low voltage cables patch panel.
3. Fiber optic cables patch panel.
4. Telemetry cables patch panel.
5. Opening in slice test box for high voltage cables.

In order to test Roxtec sealing solution, which is planned to be installed in final UT detector box, a sample of this device will be installed in slice test box for cables and CO_2 pipes sealing – Figure 4.21 number 5, seen also in Figure 4.22.

Figure 4.22 Slice test box with dummy stave installed
Rysunek 4.22 Skrzynka slice testu z zainstalowaną makietą stave'a

Figure 4.23 Pathfinder crate with patch panels for slice test
Rysunek 4.23 Krata pathfinder z panelami przejściowymi dla slice testu

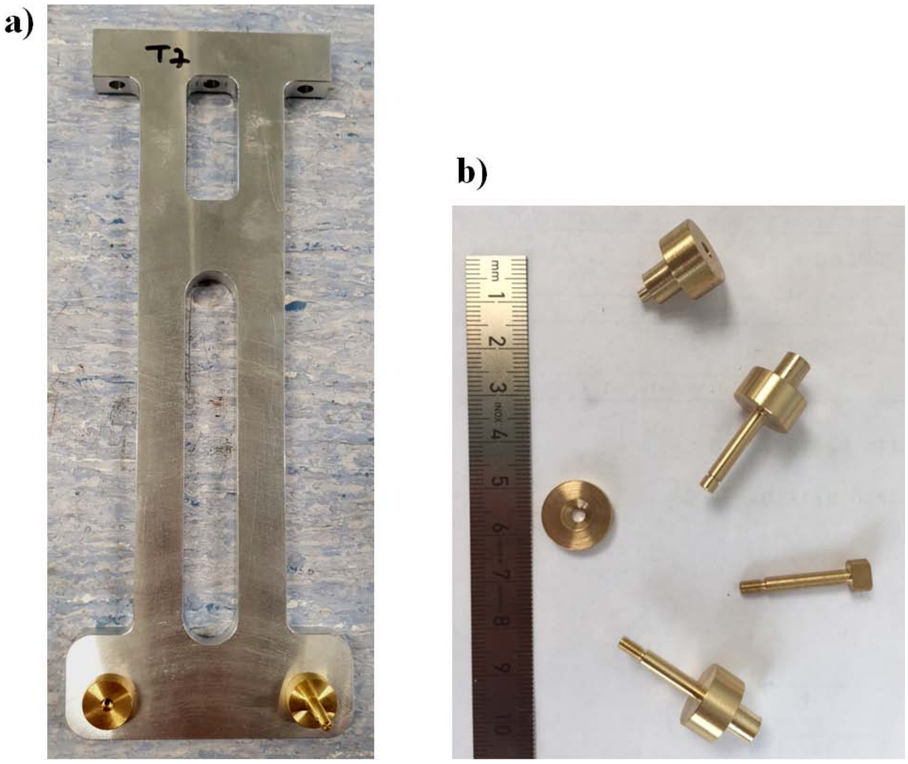

Figure 4.24 a) Stave support; b) Brass pins for stave mounting
Rysunek 4.24 a) Podpora stave'a; b) Mosiężne piny do mocowania stave'a

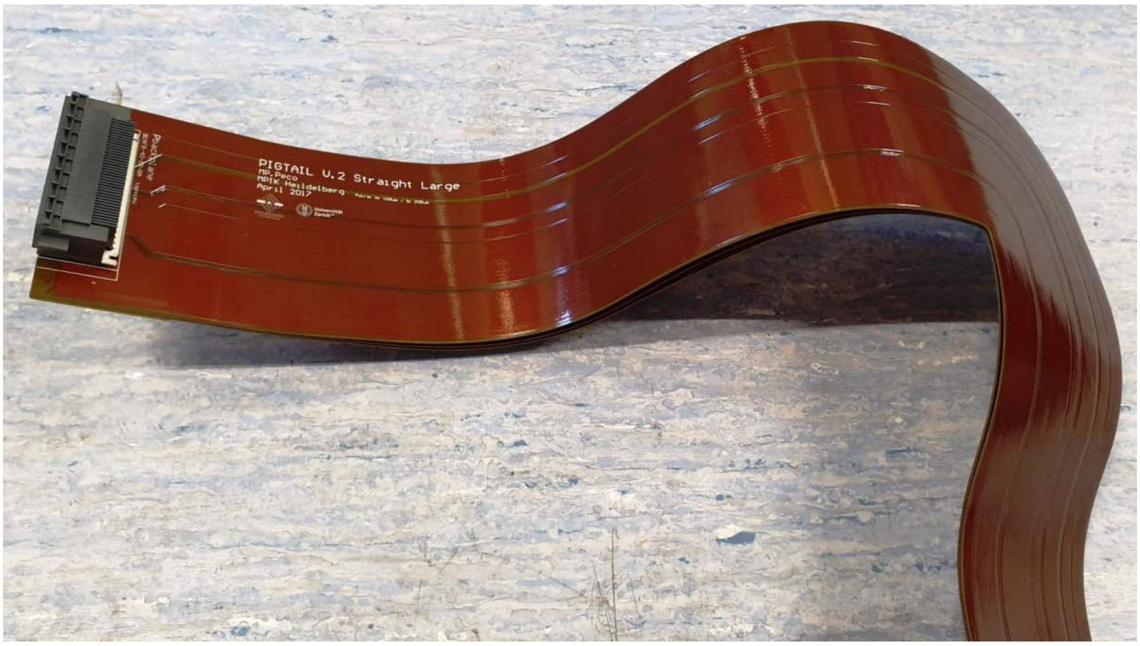

Figure 4.25 Data read-out cable (pigtail) PEPI volume part
Rysunek 4.25 Kabel odczytu danych część znajdująca się wewnątrz PEPI

Figure 4.26 Full size data read-out cable (pigtail) with connectors on both ands
Rysunek 4.26 Kabel odczytu danych w pełnym rozmiarze z konektorami na końcach

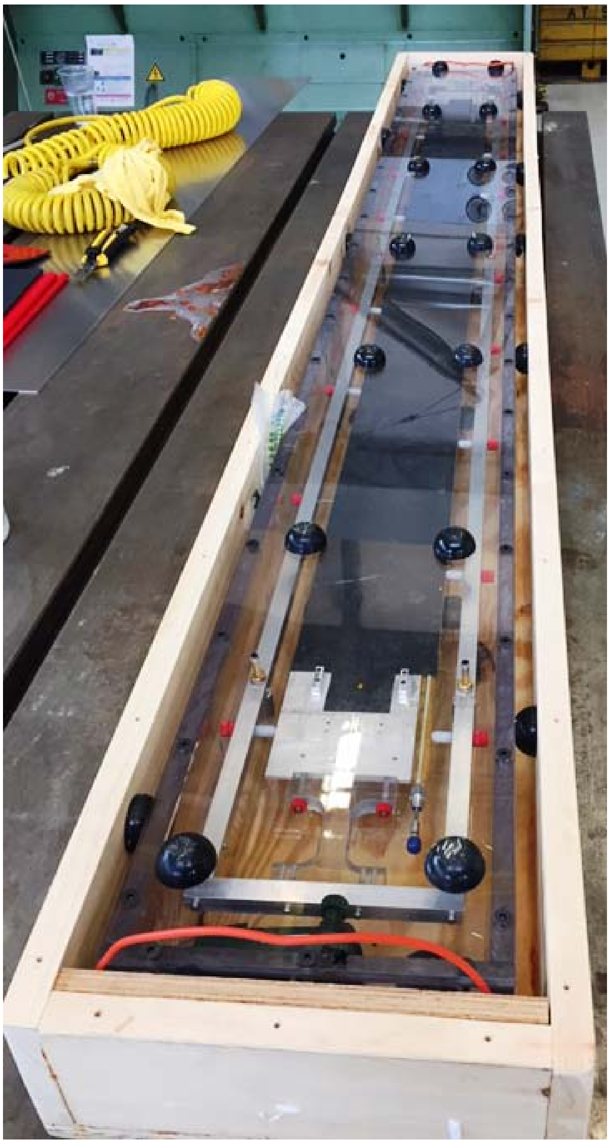

Figure 4.27 Real stave in transport box
Rysunek 4.27 Autentyczny model stev'a w pudełku transportowym

During slice test also prototype (pilot) service bays crate (SBC) will be used together with prototype low voltage regulator boards (LVR) and LVR heat sink.

Prototype LVR heat sink with pockets and machined stand-offs in order to accommodate electronic chips can be seen in Figure 4.28. Special heat sink shape, which allows to accommodate the connectors attached to LVR board is shown in Figure 4.29. The pocket with gap pad is presented in Figure 4.32.

LVR boards are held in their channels using expandable wedge-loks attached to them – Figure 4.30 and Figure 4.31.

Pilot service bays crate together with prototype marathon cables patch panel can be seen in Figure 4.33. Service bays crate placed inside slice test rack is presented in Figure 4.34.

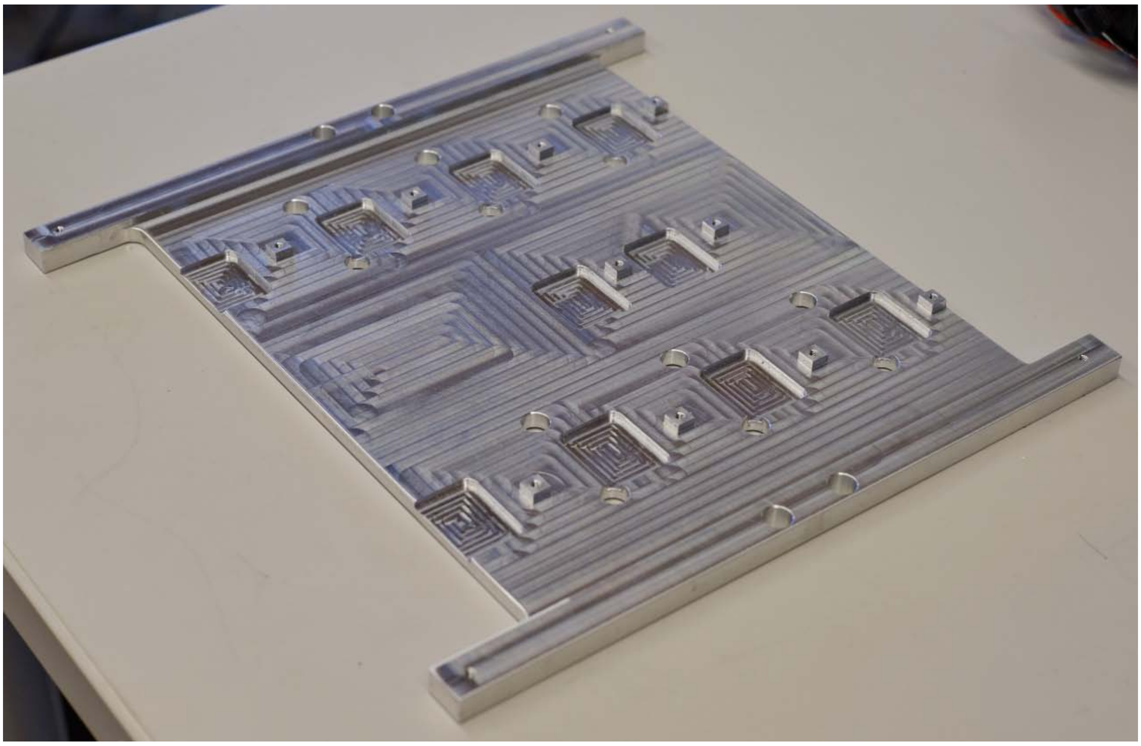

Figure 4.28 LVR heat sink [39]
Rysunek 4.28 Radiator LVR [39]

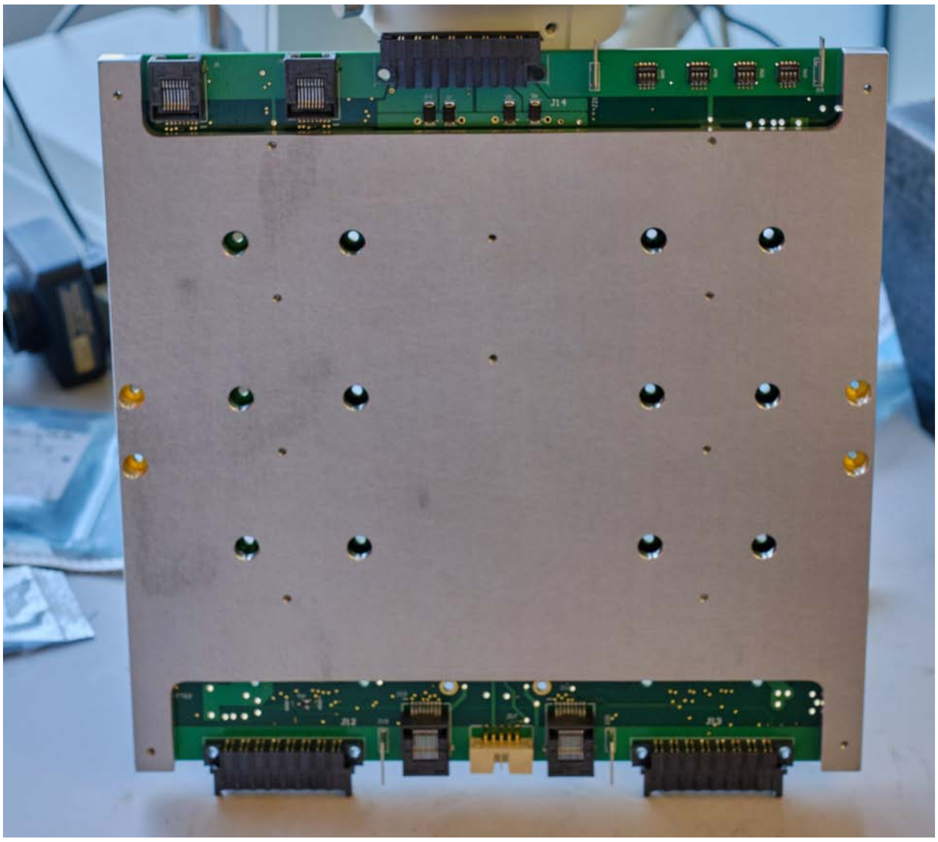

Figure 4.29 LVR board with heat sink [39]
Rysunek 4.29 Karta LVR z radiatorem [39]

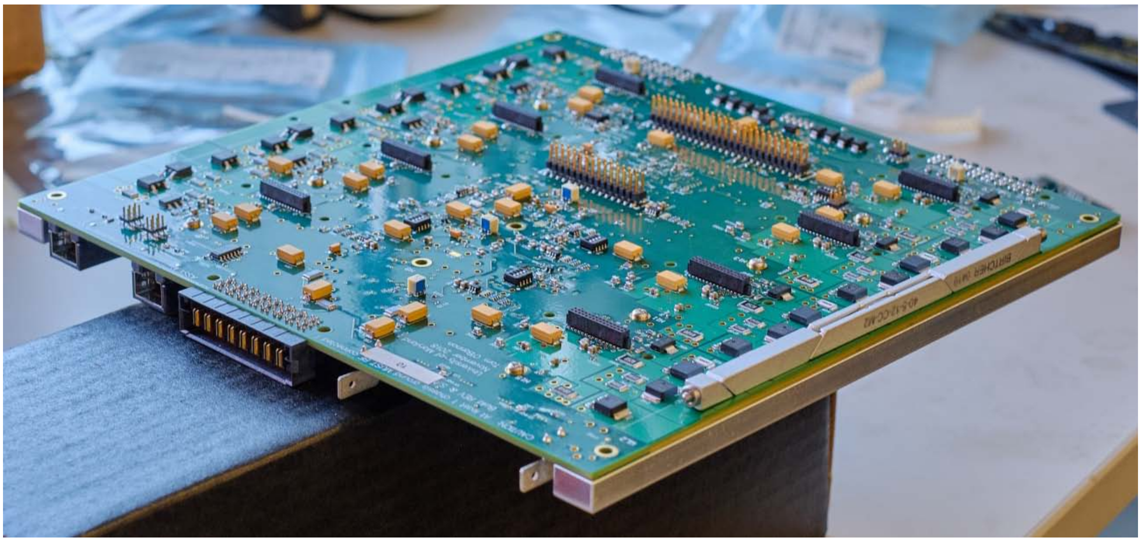

Figure 4.30 LVR board with wedge-lok [39]
Rysunek 4.30 Karta LVR z wedge-lok [39]

Figure 4.31 Wedge-lok [39]
Rysunek 4.31 Wedge-lok [39]

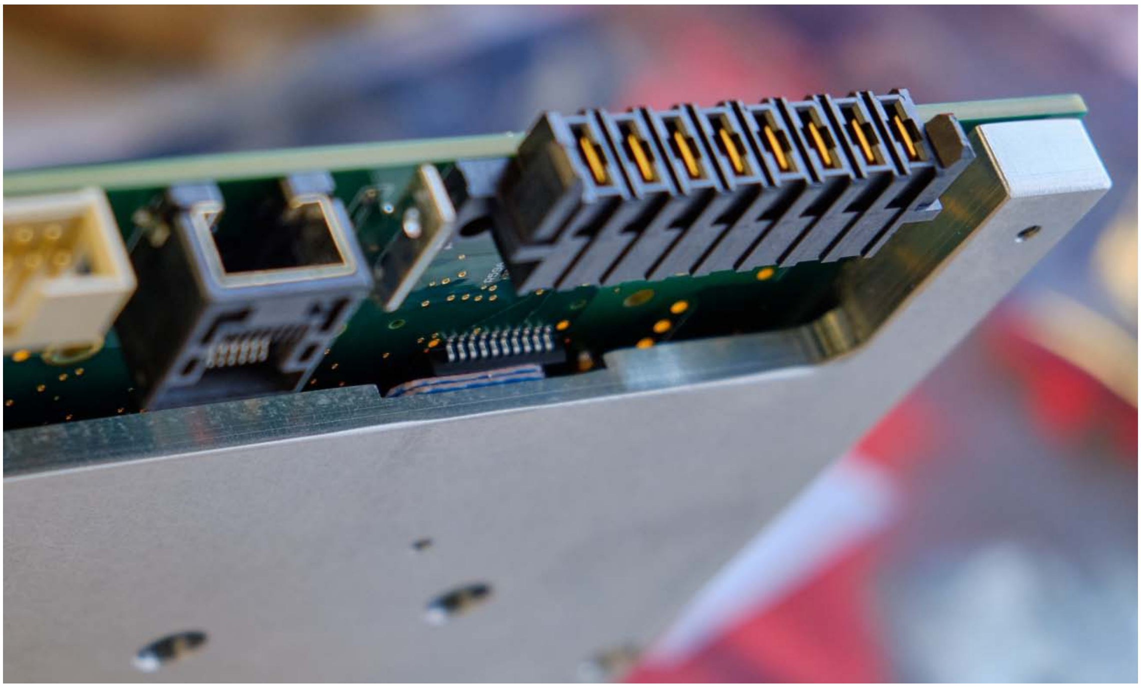

Figure 4.32 Pocket with gap pad in LVR heat sink to accommodate electronics [39]
Rysunek 4.32 Kieszeń z wypełniaczem w radiatorze LVR aby pomieścić elektronikę [39]

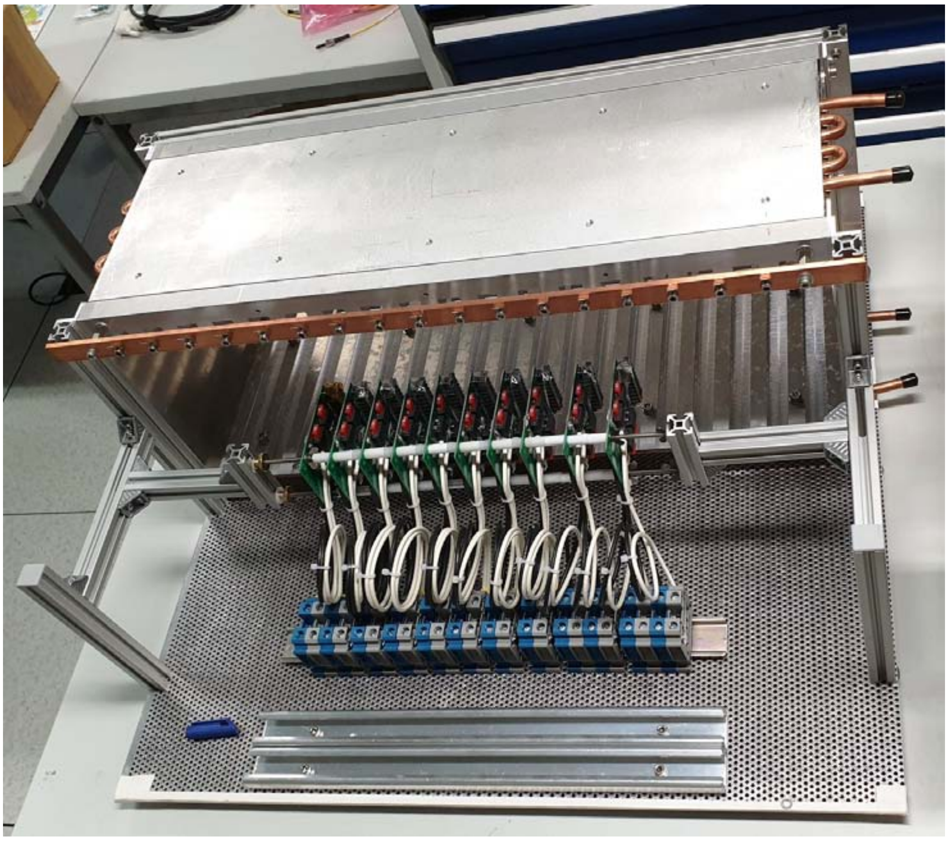

Figure 4.33 Prototype (pilot) SBC crate with prototype marathons LV cables patch panel
Rysunek 4.33 Prototypowa (pilotażowa) krata SBC z prototypowym panelem przejściowym dla długodystansowych kabli zasilających niskiego napięcia (marathons)

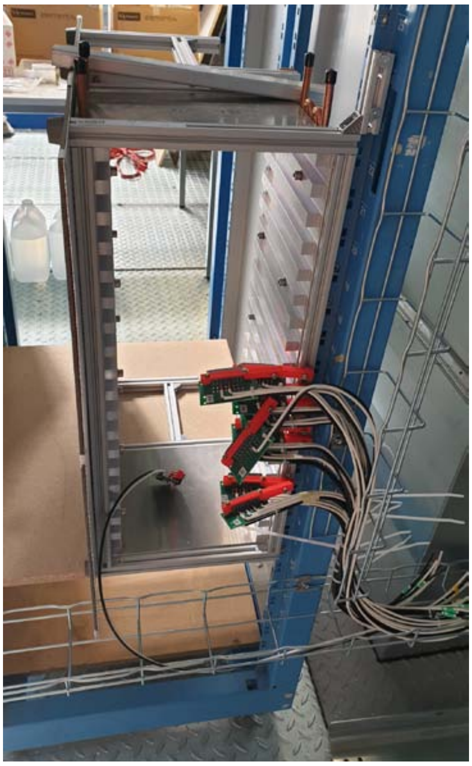

Figure 4.34 Service bays crate placed inside slice test rack
Rysunek 4.34 Krata serwisowa umieszczona w szafie slice testu

5. **Conclusions**

Designing infrastructure at CERN is a challenging task. Each part of equipment has to meet several uncompromising requirements.

The design phase of each detector element is an iterative process. From the conceptual design which gradually becomes a final geometry over many discussions. Each new iteration has to be consulted within interdisciplinary collaboration, in order to ensure that it meets the requirements and provide good cooperation of new part with neighboring elements.

Fulfilling contradicted requirements of the components for example, lightweight and durability leads to building parts from composite materials. Good example, is the sandwich box for UT detector.

In order to test assembly process and to avoid integration mistakes, as well as, to assess accessibility and investigate if special tools are needed, digital models need to be validated by mock-up.

Building Upstream Tracker detector box mock-up reviled following areas for improvement:

- some of data read-out cables (pigtails) are too long, some of them are too short;
- stiff pigtails exerting significant force on stave connectors, clamps mandatory;
- special pigtails mounting tool necessary for installation;
- rubber gaskets for sealing elongated holes in detector box plate are too wide and they are very hard to place inside the hole;
- above mentioned gaskets could also be made from softer grade rubber;
- C-Frame needs to be more robust, stainless steel will be used instead of aluminum;
- welds between C-Frame plates must be machined afterwards, in order to fit PEPI electronics in place;
- after installation access to staves is restricted;
- dismantling of staves in case of failure is very challenging.

Different material properties in harsh experiment environment must be taken into account. Radiation exposure, forces careful choice of material which can be used in LHCb cavern. Depends from the distance from LHCb interaction point (IP) and the beam pipe different materials has to withstand different radiation doses and maintain their performance with time.

Some materials are excluded completely from being used in the LHCb cavern. For example, cables containing halogen. They must be halogen free. They must also be fire resistant or at least fire retardant.

All materials used in LHCb cavern must be RoHS compliant – RoHS (Restriction of Hazardous Substances), and properly utilized, after their lifetime is over.

Strong magnet field in close proximity of the detector exclude using parts made from standard construction (black) steel.

3D printed elements are allowed in the LHCb cavern. However, they cannot be made from PLA (polylactic acid), which is sourced from corn. It is fully biodegradable, but is not suitable for using in the cavern due to its vulnerability for humid and radiation environment. It is easy for printing, but degrades very fast in rough conditions.

ABS (Acrylonitrile butadiene styrene) – it is mechanically robust polymer with good radiation hardness, and is allowed for use in the cavern.

PVC (polyvinyl chloride) – use is restricted, because it gives a lot of dense smoke in case of fire.

Nylon – becomes brittle with time in radioactive environment and loses its durability. As a consequence nylon screws or other construction elements may fail.

Because LHCb experiment and Upstream Tracker detector is designed by international collaboration, proper communication is vital for achieving the success. For example, exchanging CAD models with proper integration axis system and respecting envelopes of the surrounding equipment.

Within tight PEPI volume, each mechanical element has to play multiple roles, in order to meet all the requirements. For example, walls support DCB card guides and water pipes support; DCB card guides lead data concentration boards towards backplane and pressing backplane against the base plate.

Similar situation is inside UT detector box, where stave supports are also used for high voltage cables support.

Integration studies performed in computer aid design software (CAD) is very important in order to fit all required detector components in very tight space. Many sub-systems of the detector crosses each other. However, they cannot interfere between. 3D assembly investigation followed by mock-up must prevent it from happening.

Building the detector at CERN is similar to building a space probe. In terms of quality assurance, prototyping and testing UT detector must be constructed in similar way. After placing it in LHCb cavern, there is almost no possibility for corrections. After commissioning the detector has to work for 10 years with only minimum maintenance.

That is why, prototypes are built and each part of the detector is carefully tested.

Constructing Pathfinder prototype reviled following areas for improvement:

- conductive flakes from graphite foil must be prevented from happening;
- replacing graphite foil with thermal grease could be a solution;
- elongated holes in walls (in PEPI volume) for adjusting DCB card guide pressing force on the backplane;
- DCB card guides channel width may need adjustment;
- adding backplane vertical fixation can be beneficial;

- dowel pins for precise positioning of the backplane on the base plate would be beneficial, however, it requires making holes in backplane, which is a challenging task due to 28-layers construction.

6. **References**

Some of the references included in thesis are CERN protected documents. In case of necessity of use please contact thesis author, Michal Galka: michal.galka8@gmail.com or his CERN supervisor, Joao Carlos Batista Lopes: Joao.Carlos.Batista.Lopes@cern.ch.

[1] Michal Galka, *UT detector box integration*, CERN, June 2017
Available at:
https://indico.cern.ch/event/646589/contributions/2625957/attachments/1475446/2285248/UT_Intergration_meeting_13.06.2017.pdf
Access day: 08.04.2019

[2] Michal Galka, *PEPI Chassis Integration*, LHCb Week - UT parallel session at CERN, June 2018
Available at:
https://indico.cern.ch/event/735726/contributions/3034320/attachments/1665854/2670534/LHCb_Week_PEPI_Integration_12.06.2018_-_Final.pdf
Access day: 08.04.2019

[3] Michal Galka, *PEPI Chassis Integration*, CERN, July 2018
Available at:
https://indico.cern.ch/event/741044/contributions/3059510/attachments/1682821/2704181/PEPI_Integration_06.07.2018.pdf
Access day: 08.04.2019

[4] Michal Galka, *PEPI Chassis Integration (2nd iteration of power boards support inside PEPI)*, CERN, July 2018
Available at:
https://indico.cern.ch/event/745928/contributions/3090075/attachments/1694496/2729503/PEPI_Integration_31.07.2018.pdf
Access day: 08.04.2019

[5] Michal Galka, *PEPI & SBC Mechanics Integration*, UT integration - assembly and commissioning workshop at CERN, October 2018
Available at:
https://indico.cern.ch/event/759996/contributions/3152322/attachments/1733594/2803014/LHCb_Workshop_PEPI__SBC_15.10.2018.pdf
Access day: 08.04.2019

[6] Michal Galka, *Pathfinder Support*, CERN, November 2018
Available at:
https://indico.cern.ch/event/768810/contributions/3194546/attachments/1746172/2992672/Pathfinder_Support_02.11.2018.pdf
Access day: 08.04.2019

[7] Michal Galka, *LVR_Mechanics*, CERN, February 2019
Available at:
https://indico.cern.ch/event/793703/contributions/3297540/attachments/1788864/2914586/LVR_Mechanics_-_01.02.2019.pdf
Access day: 08.04.2019

[8] Oskar Mårtensson, *LHCb Upstream Tracker box Thermal studies and conceptual design*, January 2016.
Available at:
http://www.diva-portal.se/smash/get/diva2:901679/FULLTEXT01.pdf
Access day: 03.12.2018

[9] Olivier Jamet, *Exchange Of Cad Models Within The LHCb Collaboration*, September 2014
Available at:
https://edms.cern.ch/ui/file/1417892/1/Exchange_of_CAD_models_within_LHCb_collaboration.pdf
Access day: 03.12.2018

[10] Werner Herr and Bruno Muratori, *Concept of luminosity*
Availiable at:
https://cds.cern.ch/record/941318/files/p361.pdf
Access day: 03.12.2018

[11] Olivier Brunning, Lucio Rossi, *The High Luminosity Large Hadron Collider. The New Machine for Illuminating the Mysteries of Universe*, World Scientific Publishing Co. Pte. Ltd. / CERN 2015
Available at:
https://www.worldscientific.com/doi/pdf/10.1142/9581
Access day: 03.12.2018

[12] https://home.cern/about/who-we-are/our-history
Access day: 03.12.2018

[13] https://dzienniknaukowy.pl/assets/media/lhc.jpg
Access day: 03.12.2018

[14] http://rsta.royalsocietypublishing.org/content/roypta/373/2032/20140044/F1.large.jpg
Access day: 03.12.2018

[15] https://home.cern/science/accelerators/large-hadron-collider
Access day: 03.12.2018

[16] https://upload.wikimedia.org/wikipedia/commons/b/ba/Cern-accelerator-complex.svg
Access day: 03.12.2018

[17] https://home.cern/science/experiments/alice
Access day: 03.12.2018

[18] https://home.cern/science/experiments/atlas
Access day: 03.12.2018

[19] https://home.cern/science/experiments/cms
Access day: 03.12.2018

[20] https://home.cern/science/experiments/lhcb
Access day: 03.12.2018

[21] The LHCb Collaboration, *LHCb Tracker Upgrade Technical Design Report*, CERN, February 2014
Available at:
https://cds.cern.ch/record/1647400/files/LHCB-TDR-015.pdf
Access day: 03.12.2018

[22] The LHCb Collaboration, *Letter of Intent for LHCb Upgrade*, CERN, March 2011
Available at:
https://cds.cern.ch/record/1333091/files/LHCC-I-018.pdf
Access day: 03.12.2018

[23] https://home.cern/science/experiments/how-detector-works
Access day: 03.12.2018

[24] http://lhcb-public.web.cern.ch/lhcb-public/en/LHCb-outreach/multimedia/LHCbDetectorpnglight1.png
Access day: 10.12.2018

[25] https://3c1703fe8d.site.internapcdn.net/newman/csz/news/800/2017/lhcbobserves.png
Access day: 10.12.2018

[26] Jacky Rochet, *3D digital mock-up*, October 2018
Available at:
https://indico.cern.ch/event/759996/contributions/3152321/attachments/1733353/2803022/UT_WORKSHOP_15-10-2018.pdf
Access day: 10.12.2018

[27] Olivier Jamet, Joao Carlos Batista Lopes, *Conceptual design report UT BOX*, June 2016
Available at:
https://edms.cern.ch/document/1446971
Access day: 10.12.2018

[28] François Boyer, *Procedure for the fabrication of the UT box prototype*, CERN, May 2016
Available at:
https://edms.cern.ch/ui/file/1698508/3/Procedure_for_the_fabrication_of_UT_box_prototype.pdf
Access day: 17.12.2018

[29] François Boyer, *Tensile test on G10 insert trapped in composite sandwich plate Final*, CERN, April 2018
Available at:
https://edms.cern.ch/ui/file/1698508/3/Tensile_test_on_G10_insert_trapped_in_composite_sandwich_plate_Final.pdf
Access day: 17.12.2018

[30] Joao Batista, Olivier Jamet, Oskar Martensson, Burkhard Schmidt, *Integration in the experiment: Frame – Box – CO2 cooling plant*, CERN, June 2015
Available at:
https://indico.cern.ch/event/394628/contributions/1832289/attachments/790110/1082987/UT_Review_Box-Frame-Cooling_19June2015.pdf
Access day: 04.02.2019

[31] Ray Mountain, *UT BARE STAVE – Design, Components, Construction*, Syracuse University, for the LHCb UT Group at CERN, June 2015
Available at:
https://indico.cern.ch/event/394628/timetable/#20150619
Access day: 04.02.2019

[32] Joao Carlos Batista Lopes, *UT stave position*, CERN, June 2018
Available at:
https://edms.cern.ch/document/1908308
Access day: 04.02.2019

[33] Simone Coelli, *UT mechanics and cooling system open issues*, LHCb UT workshop, Syracuse University, September 2017
Available at:
https://indico.cern.ch/event/655588/contributions/2724278/attachments/1524357/2382932/2017-09-15_LHCb_UT_workshop_SIMONE_COELLI.pdf
Access day: 11.02.2019

[34] Joao Carlos Batista Lopes, *PEPI_diagram_v2*, CERN, July 2018
Available at:
https://edms.cern.ch/document/1979148
Access day: 11.02.2019

[35] Joao Carlos Batista Lopes, *UT pigtails integration and length check*, CERN, February 2019
Available at:
https://indico.cern.ch/event/801859/contributions/3333052/attachments/1801696/2939252/Pigtails_recommended_dimensions_25_feb_2019.pdf
Access day: 04.03.2019

[36] Jason Andrews, *The end-of-stave region and transition outside the box*, University of Maryland, June 2016
Available at:
https://indico.cern.ch/event/522418/contributions/2220187/attachments/1301625/1943393/AndrewsJ_2016.06.30.pdf
Access day: 11.03.2019

[37] Petr Gorbounov, Michal Galka, Joao Carlos Batista Lopes, Carlos Abellan Beteta, Maria Del Pilar Peco Regales, *PEPI patch panels and cabling*, CERN, October 2018
Available at:
https://indico.cern.ch/event/759996/contributions/3152323/attachments/1733570/2803836/PG_Patch_panels.pdf
Access day: 08.04.2019

[38] Joao Carlos Batista Lopes, *Lessons learnt from UT mock-up*, CERN, October 2018
Available at:
https://indico.cern.ch/event/759996/contributions/3152324/attachments/1733449/2823150/Lessons_learnt_from_UT_mockup.pdf
Access day: 13.05.2019

[39] Manuel Franco Sevilla, *PEPI and LVR report*, University of Maryland, April 2019
Available at:
https://indico.cern.ch/event/788485/contributions/3377243/attachments/1821431/2979335/19-04-01_umd_pepi_lvr_report.pdf
Access day: 13.05.2019

[40] Joao Carlos Batista Lopes, *cable chain*, CERN, November 2018
Available at:
https://indico.cern.ch/event/770853/contributions/3202200/attachments/1756251/2847502/cable_chain.pdf
Access day: 20.05.2019

[41] https://www.igus.ch/contentData/wpck/images/global/1_3/echain-e21.jpg
Access day: 20.05.2019

[42] Rolf Lindner, *Envelope and clearance definition*, CERN, May 2003
Available at:
https://edms.cern.ch/ui/file/386061/1/LHCb-envelope.pdf
Access day: 20.05.2019

[43] *LHCb Collaboration as of 15-Jun-2018*, CERN, June 2018
Available at:
http://lhcb.web.cern.ch/lhcb/lhcb_page/collaboration/organization/list_of_members/old_lists/members_default.pdf
Access day: 20.05.2019

7. Summary

Building detectors of this scale is very challenging task. It is also quite overwhelming and hard to imagine that, LHCb experiment weight 5600 tones, in order to detect tiny little sub-atomic particles, which are almost weightless.

This thesis treats about integration and engineering studies performed at CERN in LHCb collaboration during design phase of Upstream Tracker detector.

At the beginning of this thesis, CERN laboratory is described. Its mission, accelerator complex and main experiments performed around LHC ring.

Next, LHCb experiment is presented with short description of its sub-detectors, designed by international collaboration.

Main chapter and its consecutive sub-chapters describe Upstream Tracker detector mechanics and integration with details. Starting from tools using for integration within international collaboration like proper axis systems and definition of envelope.

To show complexity of the project, UT detector layout is described. Then detail attention is paid to integration inside detector box. The requirements of the box environment are presented together with explanation how to meet them all. The UT sandwich box material is described with details.

Then, C-Frame integration and geometry is presented. To show how UT detector box is supported inside LHCb cavern.

Next chapter, treats with details about PEPI volume integration studies. There are subchapters about PEPI mechanics, cabling, electronics and cooling. DCB cooling interface is described and clamps assessment presented.

Another chapter, shows cable chain integration. It gives detailed explanation of how many different cable types are hosted inside cable chain. Estimated weight and size of the cable chain is presented.

Then, service bays crate (SBC) is described. It hosts low voltage regulator boards (LVR), which are power supply for the detector electronics.

Next chapter, describes service bays rack (SBR), which supports 4 service bays crates inside. It must be a robust structure, hence the FEM analysis of rack structure has been performed.

Last chapter is divided by two main sub-chapters one of them describes the mock-up and some techniques used for building fake parts. Another one, treats about prototyping tests performed for Upstream Tracker detector crucial parts, like PEPI electronics or staves.

There is also information provided what is the difference between mock-up and prototype.

In the Appendix to this thesis, there are several production drawings attached, of key elements of the Upstream Tracker detector.

All observations made during mock-up and prototypes construction are described in details, in thesis conclusions.

8. Podsumowanie

Projektowanie infrastruktury w CERN jest trudnym zadaniem. Każda część wyposażenia musi spełniać szereg bezkompromisowych wymagań.

Faza projektowania każdego elementu detektora jest procesem iteracyjnym. Od projektu koncepcyjnego, który stopniowo staje się ostateczną geometrią. Każda nowa iteracja musi być konsultowana w ramach interdyscyplinarnej współpracy, aby zapewnić, że spełnia ona wymagania i zapewnia dobrą współpracę nowej części z sąsiednimi elementami.

Spełnianie sprzecznych wymagań komponentów, na przykład: lekkość i trwałość prowadzi do budowy elementów z materiałów kompozytowych. Dobrym przykładem jest skrzynka detektora UT wykonana z kilku połączonych materiałów.

Budowa detektorów tej skali jest trudnym przedsięwzięciem. Jest również dość przytłaczające i trudno sobie wyobrazić, że należy wybudować eksperyment LHCb o masie 5600 ton, aby wykryć małe cząsteczki subatomowe, które są prawie nieważkie.

Niniejsza praca dyplomowa dotyczy badań integracyjnych i inżynierskich przeprowadzonych w CERN, w międzynarodowej współpracy LHCb podczas fazy projektowania detektora Upstream Tracker.

Na początku tej pracy opisano laboratorium CERN. Jego misję, kompleks akceleratorów i główne eksperymenty znajdujące się wokół pierścienia LHC.

Następnie przedstawiono eksperyment LHCb z krótkim opisem jego pod-detektorów, zaprojektowanym przez międzynarodową współpracę wielu instytutów.

Rozdział główny i kolejne jego podrozdziały opisują mechanikę detektora Upstream Tracker i jego integrację ze szczegółami. Począwszy od narzędzi wykorzystywanych do integracji w ramach współpracy międzynarodowej, takich jak odpowiednie systemy osi i definicja obwiedni/koperty (ang. envelope).

Aby pokazać złożoność projektu, opisano rozkład detektora UT. Następnie zwraca się szczególną uwagę na integrację wewnątrz detektora. Wymagania środowiska skrzynki UT są przedstawione wraz z wyjaśnieniem, jak je wszystkie spełnić. Materiał skrzynki UT o budowie kompozytowej jest opisany ze szczegółami.

Następnie prezentowana jest integracja C-Frame i geometria. Aby pokazać, w jaki sposób skrzynka detektora UT jest zamocowana w cavernie LHCb.

W następnym rozdziale omówiono szczegóły dotyczące badań integracji wewnątrz objętości PEPI. Kolejne podrozdziały dotyczące mechaniki PEPI, okablowania, elektroniki i chłodzenia. Opisano interfejs chłodzenia DCB i przedstawiono obliczenia i analizę MES zacisków interfejsu.

Kolejny rozdział przedstawia integrację łańcucha kabli. Podaje szczegółowe wyjaśnienie, ile różnych typów kabli jest umieszczonych w łańcuchu kablowym. Przedstawiono szacunkową masę i rozmiar łańcucha kablowego.

Następnie opisana jest skrzynka serwisowa (SBC). Znajdują się w niej płytki regulatora niskiego napięcia (LVR), które są zasilaniem elektroniki detektora.

W następnym rozdziale opisano szafę serwisową (SBR), która mieści 4 skrzynie serwisowe. Musi to być solidna konstrukcja, dlatego przeprowadzono analizę MES konstrukcji szafy.

Ostatni rozdział jest podzielony na dwa główne podrozdziały, z których jeden opisuje makietę i niektóre techniki wykorzystywane do budowy uproszczonych części. Kolejny, poświęcony testom prototypów wykonanym dla kluczowych części detektora Upstream Tracker, takich jak elektronika PEPI lub klepki (ang. stave).

Znajduje się tutaj również opis różnic pomiędzy makietą a prototypem.

W załączniku do niniejszej pracy znajduje się szereg rysunków technicznych kluczowych elementów detektora Upstream Tracker.

Wszystkie obserwacje poczynione podczas budowy makiety i prototypów są szczegółowo opisane we wnioskach pracy.

W celu przetestowania procesu montażu i uniknięcia błędów integracji, a także w celu oceny dostępności i zbadania, czy potrzebne są specjalne narzędzia, modele cyfrowe muszą zostać zweryfikowane przez makietę.

Zbudowanie makiety detektora Upstream Tracker (Rozdział 4.1.1) umożliwiło skorygowanie projektu w następujących obszarach:

- niektóre kable odczytu danych (ang. data read-out cables, nazywane w projekcie "Pigtails") są za długie, niektóre z nich są za krótkie;
- sztywne kable odczytu danych wywierają znaczną siłę na konektory klepek (ang. stave), potrzebne dodatkowe zaciski;
- specjalne narzędzie do montażu kabli odczytu danych niezbędne do ich instalacji;
- gumowe uszczelki do uszczelniania wydłużonych otworów w płycie skrzynki detektora są zbyt szerokie i bardzo trudno jest je umieścić w otworze;
- wyżej wymienione uszczelki powinny być również wykonane z miękkiej gumy;
- Rama-C musi być bardziej wytrzymała, jako materiał, zamiast aluminium zostanie użyta stal nierdzewna;
- spoiny spawalnicze pomiędzy płytami ramy-C muszą być później obrobione, aby wpasować elektronikę PEPI;
- po instalacji dostęp do klepek (ang. stave) jest ograniczony;
- demontaż klepek (ang. stave) w przypadku awarii jest bardzo trudny.

Należy wziąć pod uwagę różne właściwości materiału w trudnym środowisku eksperymentu. Narażenie na promieniowanie wymusza ostrożny wybór materiału, który może być użyty w cavernie LHCb. W zależności od odległości, od punktu interakcji LHCb (IP), jak również rury wiązki cząstek, różne materiały muszą wytrzymać różne dawki promieniowania i utrzymać swoje właściwości wraz z upływem czasu.

Niektóre materiały są całkowicie wyłączone z użytkowania w cavernie LHCb. Na przykład kable zawierające halogen. Nie mogą być zawierać halogenu. Muszą być również ognioodporne lub przynajmniej trudno palne.

Wszystkie materiały użyte w cavernie LHCb muszą być zgodne z normą RoHS – RoHS (ang. Restriction of Hazardous Substances) i właściwie zutylizowane po zakończeniu ich użytkowania.

Silne pole magnetyczne w pobliżu detektora wyklucza stosowanie części wykonanych ze standardowej stali konstrukcyjnej.

Elementy drukowane w 3D są dozwolone w cavernie LHCb. Nie można ich jednak wytwarzać z PLA (ang. polylactic acid), który pochodzi z kukurydzy. Jest w pełni biodegradowalny, ale nie nadaje się do stosowania w cavernie ze względu na jego wrażliwość na środowisko wilgotne i radiacyjne. Jest łatwy do drukowania, ale bardzo szybko ulega degradacji w trudnych warunkach.

ABS (akrylonitryl-butadien-styren) - jest to wytrzymały mechanicznie polimer o dobrej odporności na promieniowanie i jest dopuszczony do stosowania w cavernie.

PVC (ang. polyvinyl chloride) - zastosowanie jest ograniczone, ponieważ daje dużo gęstego dymu w przypadku pożaru.

Nylon - z czasem staje się kruchy w środowisku radioaktywnym i traci swoją trwałość. W konsekwencji śruby nylonowe lub inne elementy konstrukcyjne mogą zawieść.

Ponieważ eksperyment LHCb i detektor Upstream Tracker został zaprojektowany przez międzynarodową współpracę, odpowiednia komunikacja jest niezbędna do osiągnięcia sukcesu. Na przykład wymiana modeli CAD z odpowiednim systemem osi integracyjnych i przestrzeganie ustanowionych obwiedni/kopert (ang. envelope) otaczającego sprzętu.

Ze względu za bardzo zatłoczoną przestrzeń PEPI każdy element mechaniczny musi spełniać kilka zadań, aby spełnić wszystkie wymagania. Na przykład ściany zapewniają podporę dla prowadnic kart DCB i podpór rur chłodzenia wodnego. Prowadnice kart DCB (ang. DCB card guide) prowadzą płyty koncentracji danych w kierunku głównej płyty elektronicznej nazywanej w projekcie (ang. backplane) i dociskają główną płytę elektroniczną do płyty podstawy (ang. base plate).

Podobna sytuacja ma miejsce w skrzynce detektora UT, gdzie podpory klepek (ang. stave) są również używane do podparcia kabli wysokiego napięcia.

Badania integracyjne przeprowadzone przy pomocy oprogramowania CAD (ang. computer aid design) są bardzo ważne, aby dopasować wszystkie wymagane elementy detektora w bardzo ciasnej przestrzeni. Wiele podsystemów detektora krzyżuje się ze sobą. Nie mogą jednak kolidować ze sobą nawzajem. Budowa złożenia 3D, a następnie makiety, musi temu zapobiec.

Budowanie detektora w CERN jest podobne do budowania sondy kosmicznej. Pod względem zapewnienia jakości budowy, prototypów i testowania, detektor UT musi być skonstruowany w podobny sposób, gdyż po umieszczeniu go w cavernie LHCb praktycznie nie ma możliwości na poprawki. Po uruchomieniu detektora musi on pracować przez 10 lat przy minimalnej konserwacji.

Dlatego budowane są prototypy, a każda część detektora jest dokładnie testowana.

Prototyp Pathfinder (Rozdział 4.2.1) zrewidował następujące obszary detektora:

- należy zapobiegać powstawaniu płatków przewodzących z folii grafitowej;
- zastąpienie folii grafitowej smarem termicznym może być rozwiązaniem;
- wydłużone otwory w ścianach (w objętości PEPI) do regulacji siły nacisku prowadnicy karty DCB (ang. DCB card guide) na główną płytę elektroniczną (ang. backplane);
- szerokość kanału prowadnic kart DCB może wymagać zmiany;
- dodanie pionowego mocowania płyty montażowej może być korzystne;
- kołki ustalające do precyzyjnego pozycjonowania płyty montażowej na płycie podstawy byłyby korzystne, jednak wymaga to wykonania otworów w płycie montażowej, co jest trudnym zadaniem ze względu na 28-warstwową konstrukcję.

9. Appendix A : Technical drawings of UT components

List of production drawings attached to thesis:

1. Water Pipe Clamp
2. Heat Pipe Clamp
3. PEPI - Water Pipe Return Clamp_v.4
4. Water Pipe To Heat Pipe Interface
5. Heat Spreader Clamp
6. Heat Copper Pipe
7. Heat Pipe and Heat Spreader Clamp
8. DCB Heat Spreader
9. Gap Filler HS-DCB
10. DCB Cooling Interface
11. Wall Part_1 – Pathfinder
12. Wall Part_2 – Pathfinder
13. Wall – Pathfinder
14. Base Plate – Pathfinder
15. DCB Card Guide – Pathfinder
16. Water Pipe Support Wall
17. Bottom Stand Profile
18. Vertical Base Plate Profile
19. Vertical COMET Profile
20. Horizontal COMET Profile
21. Pathfinder Support
22. SBC - Service Bays Crate
23. SBC - LVR Board Guide
24. SBC - Cold Plate
25. SBC - LVR Heat Sink

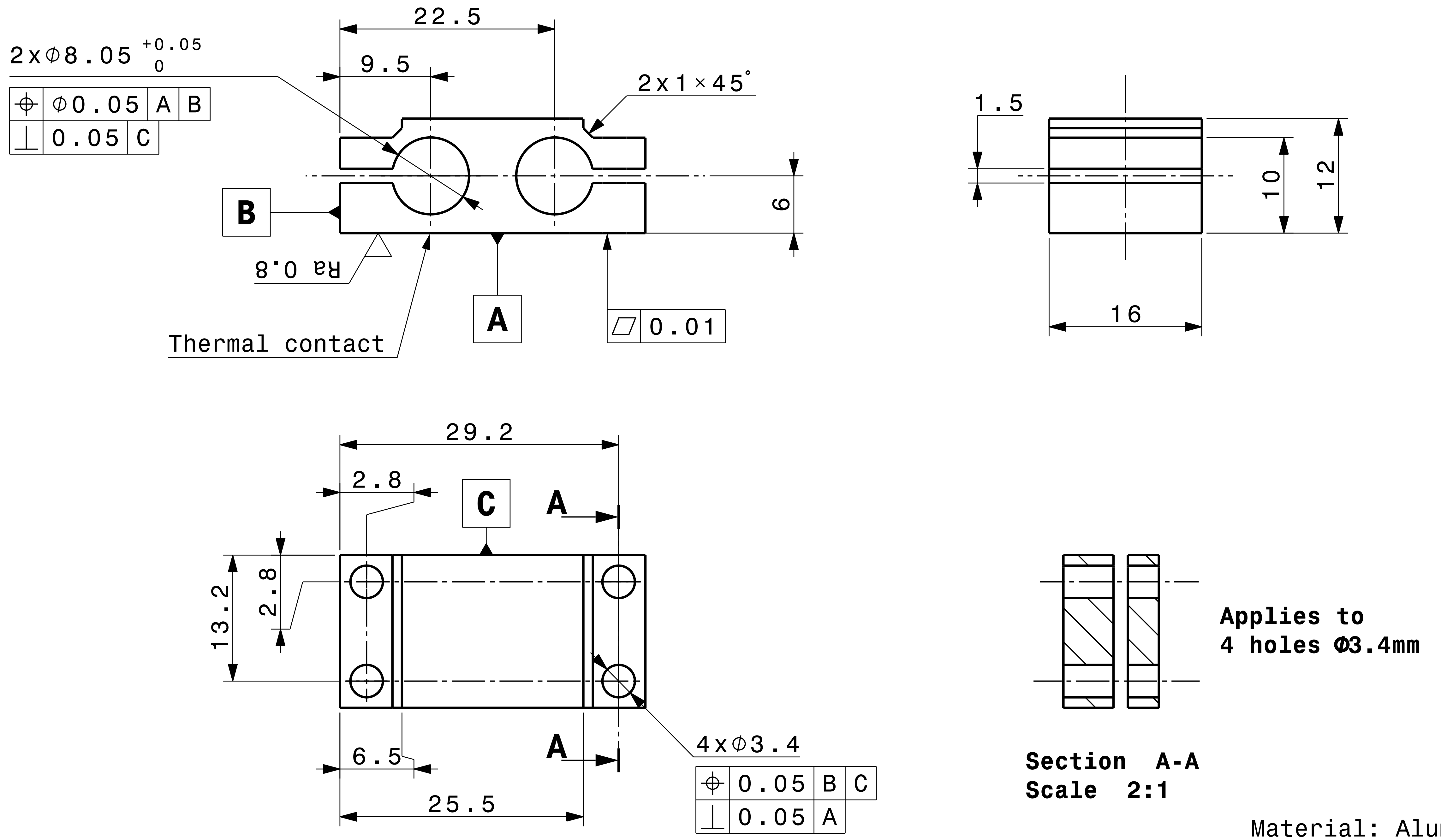

Section A-A
Scale 2:1

Material: Aluminium alloy 6082 - T6

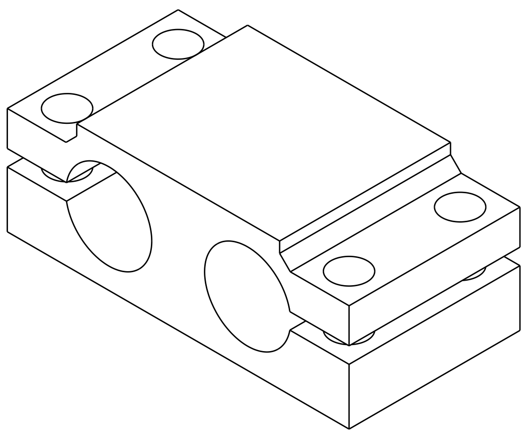

Isometric view
Scale: 2:1

MATERIAL	INITIAL STATE	FINAL STATE
Aluminum		

ISO GPS STANDARDS

ISO 2768-fH | Ra 3.2 | ISO 13715 +0.05 -0.05 | +0.05 -0.05

Unless otherwise mentioned, applicable ISO GPS standards are those prior to 2010-08-01 regardless of the drawing date

MASS 9.57 g

DESIGNATION
Water Pipe Clamp

DESIGNED	M.GALKA	FORMAT A3
CHECKED		
RELEASED		SCALE 2:1
APPROVED		

DESIGNED 2019-03-28

EQUIPMENT CODE LHBTUEL_ LHCb_TRACKING_SYSTEM_UT_Electronics

REFERENCES Doc No: ST0995960_02
LHBTUEL_0001

INDEX

LABEL NOT VALID FOR EXECUTION

QAC -

SHEET 1/1

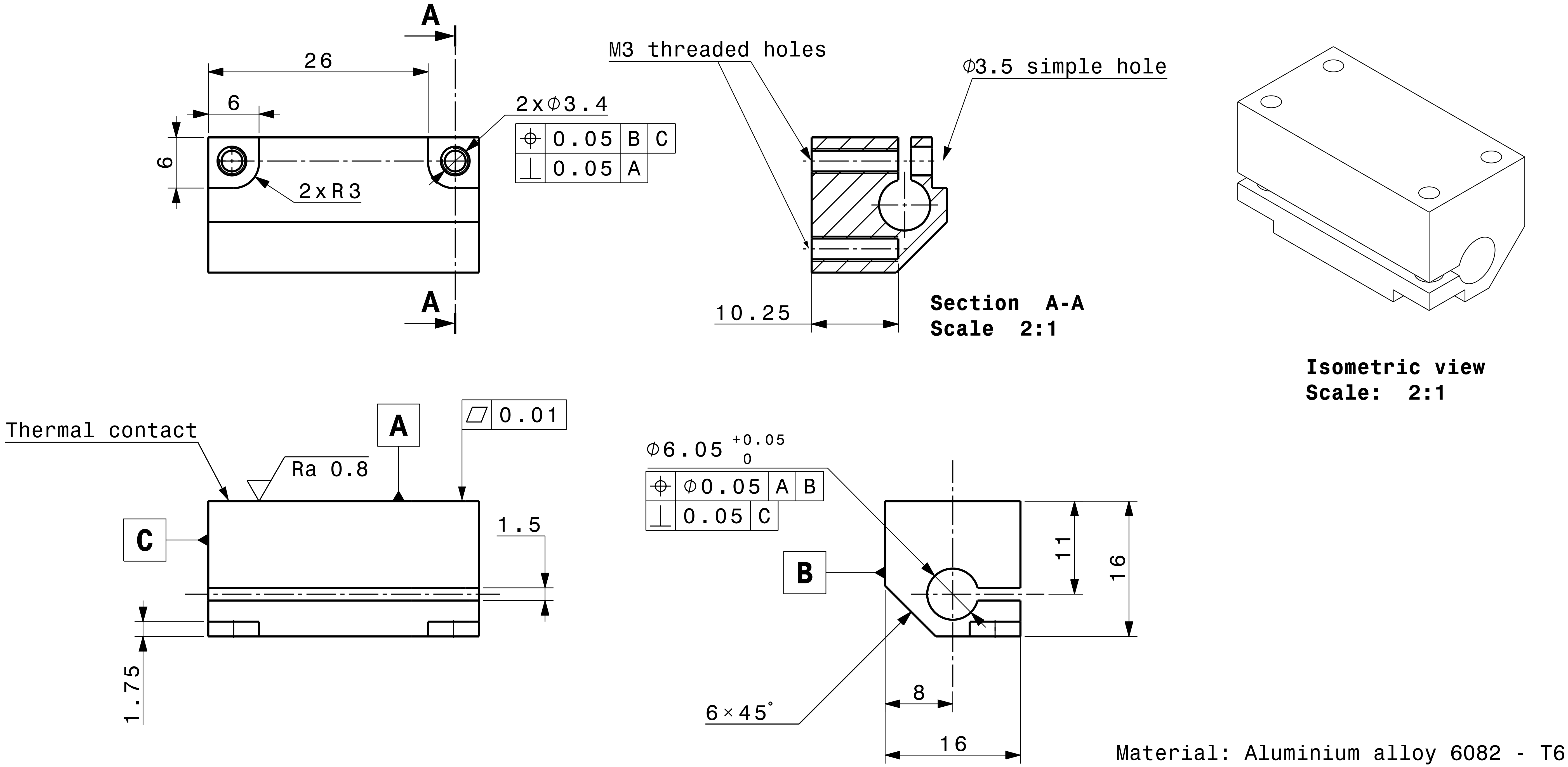

Material: Aluminium alloy 6082 - T6

MATERIAL	INITIAL STATE	FINAL STATE
Aluminum		

ISO GPS STANDARDS

ISO 2768-fH | Ra 3.2 | ISO 13715 +0.05 -0.05 | +0.05 -0.05

Unless otherwise mentioned, applicable ISO GPS standards are those prior to 2010-08-01 regardless of the drawing date

MASS 16.5 g

DESIGNATION			
Heat Pipe Clamp	DESIGNED	M.GALKA	FORMAT A3
	CHECKED		
	RELEASED		SCALE 2:1
	APPROVED		
	DESIGNED 2019-03-28		

EQUIPMENT CODE LHBTUEL_ LHCb_TRACKING_SYSTEM_UT_Electronics

CERN	REFERENCES	Doc No: ST0995935_02	INDEX	LABEL	QAC	SHEET
	LHBTUEL_0002			NOT VALID FOR EXECUTION	-	1/1

ORGANISATION EUROPEENNE POUR LA RECHERCHE NUCLEAIRE
EUROPEAN ORGANIZATION FOR NUCLEAR RESEARCH
GENEVE

TB v2.0 A3:Landscape

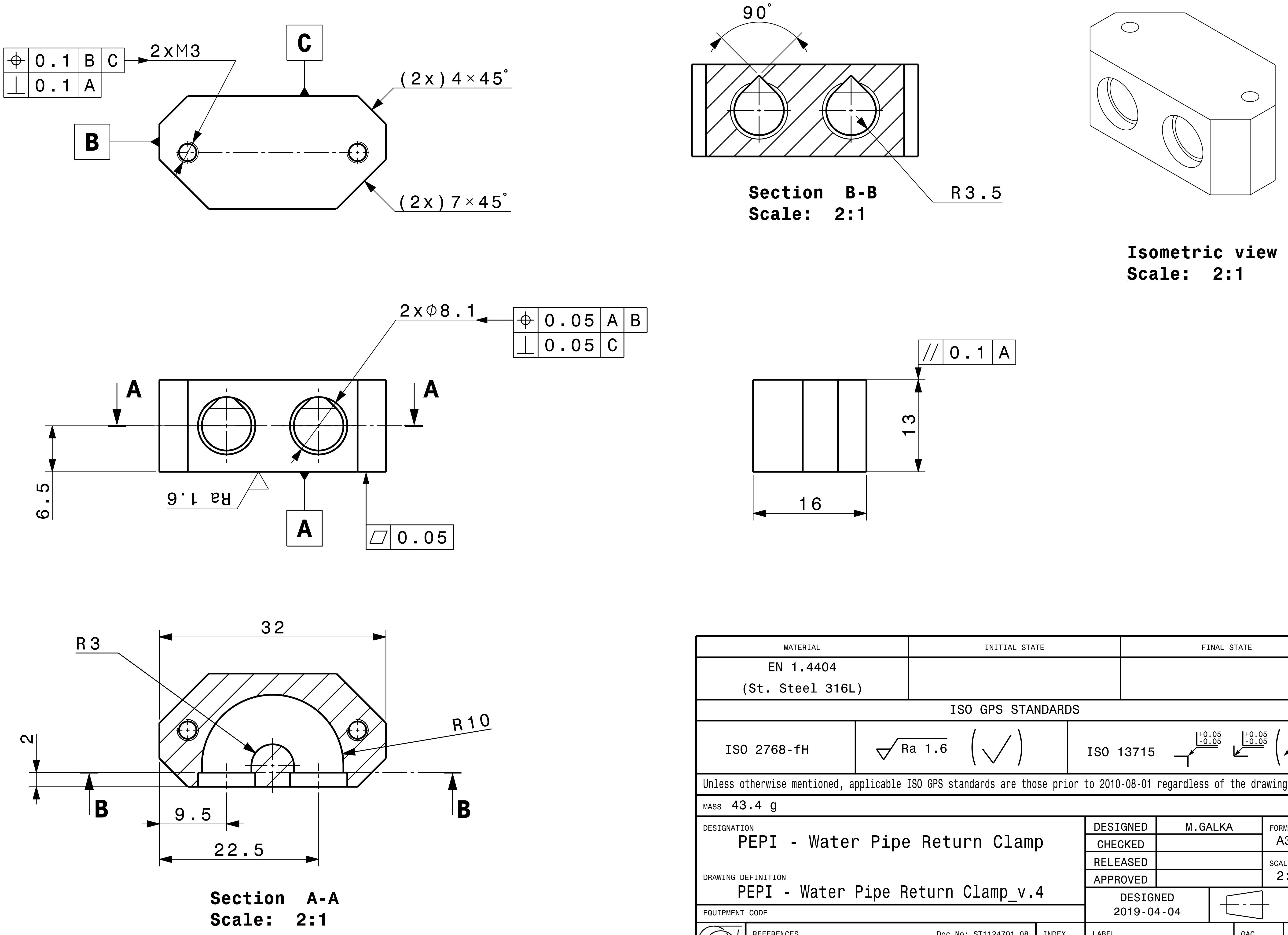

MATERIAL	INITIAL STATE	FINAL STATE
EN 1.4404 (St. Steel 316L)		

ISO GPS STANDARDS

ISO 2768-fH | Ra 1.6 | ISO 13715 +0.05 -0.05 +0.05 -0.05

Unless otherwise mentioned, applicable ISO GPS standards are those prior to 2010-08-01 regardless of the drawing date

MASS 43.4 g

DESIGNATION
PEPI - Water Pipe Return Clamp

DRAWING DEFINITION
PEPI - Water Pipe Return Clamp_v.4

EQUIPMENT CODE

DESIGNED	M.GALKA	FORMAT	A3
CHECKED			
RELEASED		SCALE	2:1
APPROVED			

DESIGNED 2019-04-04

CERN | REFERENCES | Doc No: ST1124701_08 | INDEX | LABEL NOT VALID FOR EXECUTION | QAC | SHEET 1/1

ORGANISATION EUROPEENNE POUR LA RECHERCHE NUCLEAIRE
EUROPEAN ORGANIZATION FOR NUCLEAR RESEARCH
GENEVE

TB v2.0 A3:Landscape

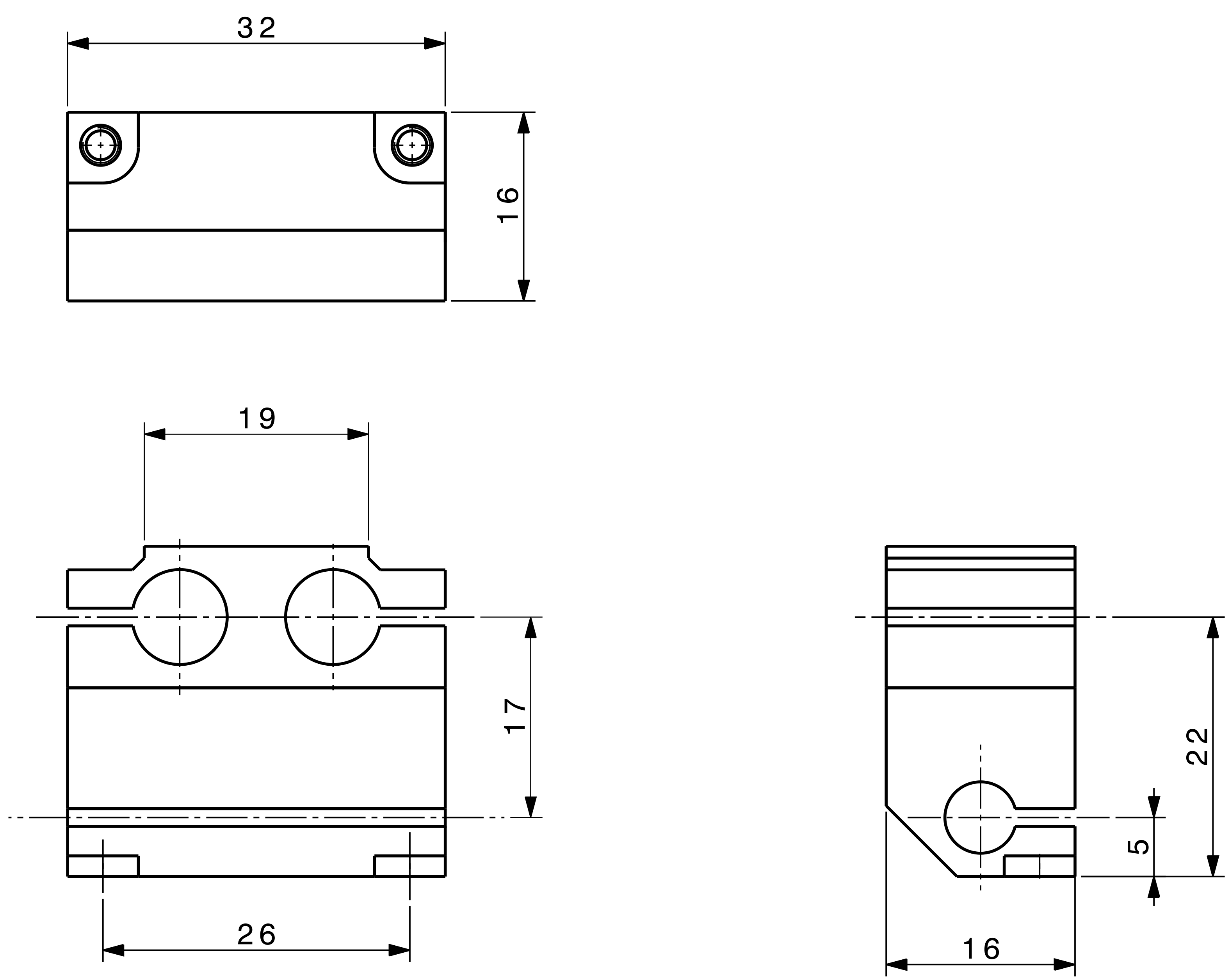

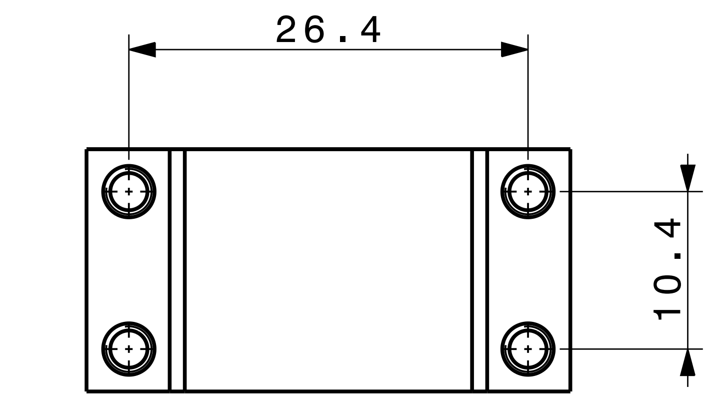

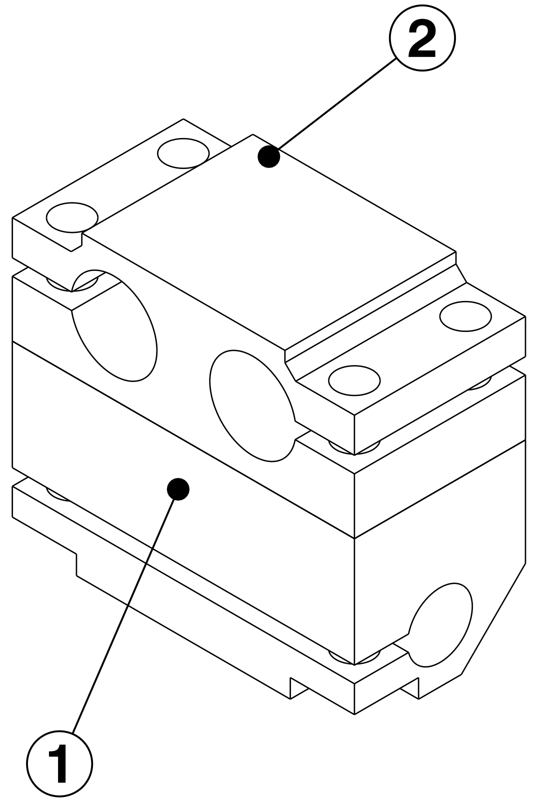

Isometric view
Scale: 2:1

BILL OF MATERIALS					
POS	QUANT	DESIGNATION	REFERENCE	MATERIAL	EDH SCEM
01	1	Heat Pipe Clamp	LHBTUEL_0002 ST0995935	Aluminum	
02	1	Water Pipe Clamp	LHBTUEL_0001 ST0995960	Aluminum	

DESIGNATION
Water Pipe to Heat Pipe Interface

DESIGNED	M.GALKA	FORMAT	A3
CHECKED			
RELEASED		SCALE	2:1
APPROVED			

DESIGNED 2018-11-30

EQUIPMENT CODE LHBTUEL_ LHCb_TRACKING_SYSTEM_UT_Electronics

REFERENCES Doc No: ST1000445_02
LHBTUEL_0003
INDEX
LABEL NOT VALID FOR EXECUTION
QAC -
SHEET 1/1

ORGANISATION EUROPEENNE POUR LA RECHERCHE NUCLEAIRE
EUROPEAN ORGANIZATION FOR NUCLEAR RESEARCH
GENEVE

TB v2.0 A3:Landscape

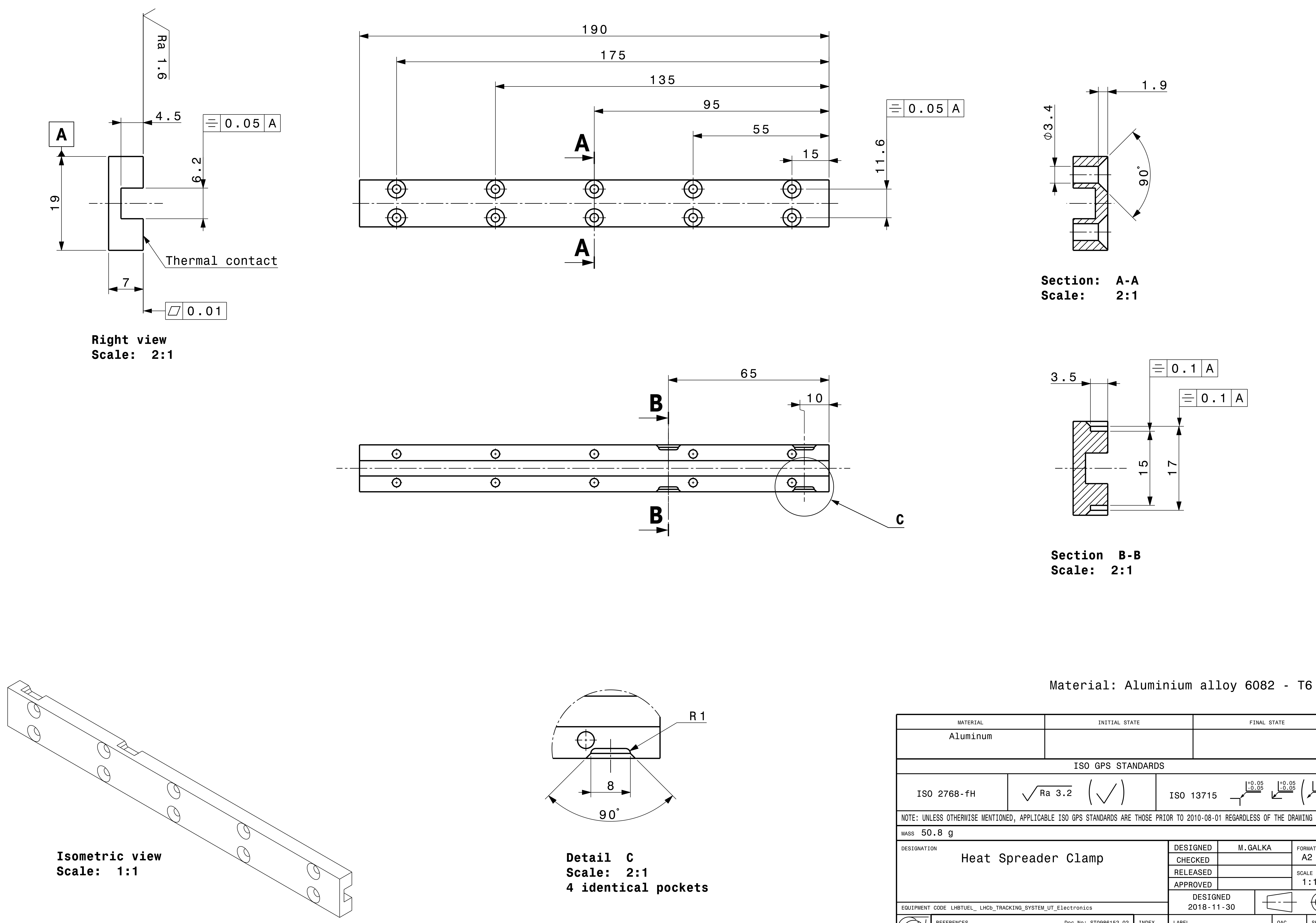

Material: Aluminium alloy 6082 - T6

MATERIAL	INITIAL STATE	FINAL STATE
Aluminum		

ISO GPS STANDARDS

ISO 2768-fH | Ra 3.2 | ISO 13715 +0.05 -0.05

NOTE: UNLESS OTHERWISE MENTIONED, APPLICABLE ISO GPS STANDARDS ARE THOSE PRIOR TO 2010-08-01 REGARDLESS OF THE DRAWING DATE

MASS 50.8 g

DESIGNATION
Heat Spreader Clamp

DESIGNED	M.GALKA	FORMAT A2
CHECKED		
RELEASED		SCALE 1:1
APPROVED		

DESIGNED 2018-11-30

EQUIPMENT CODE LHBTUEL_ LHCb_TRACKING_SYSTEM_UT_Electronics

REFERENCES Doc No: ST0986152_02
LHBTUEL_0004

INDEX

LABEL NOT VALID FOR EXECUTION | QAC - | SHEET 1/1

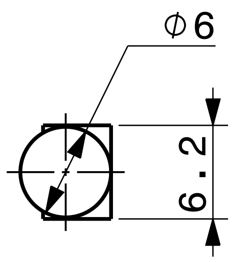

Right view
Scale: 2:1

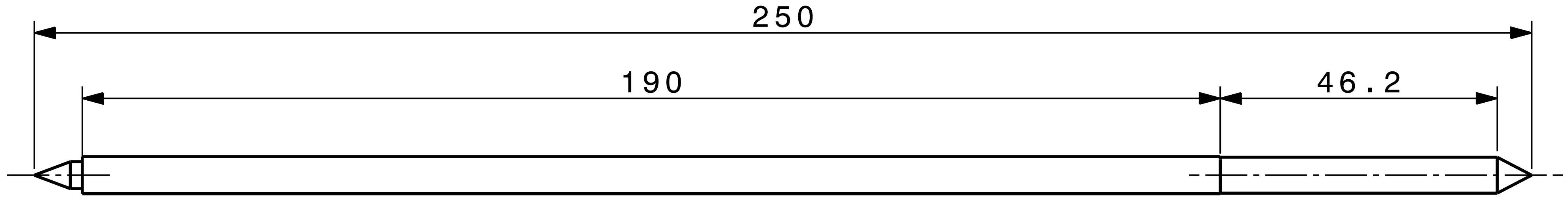

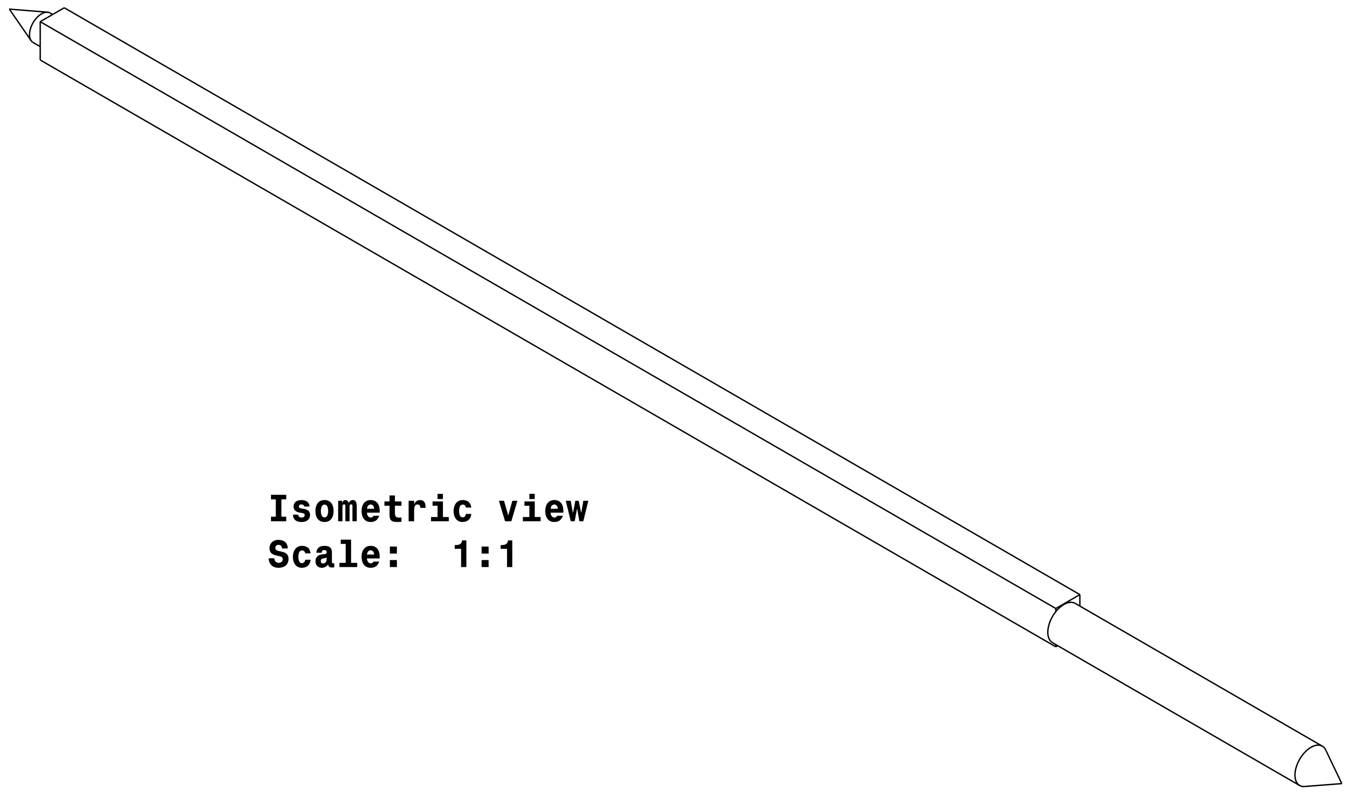

Isometric view
Scale: 1:1

Material: water-filled copper heat pipe

MATERIAL	INITIAL STATE	FINAL STATE
Copper		

ISO GPS STANDARDS

ISO 2768-fH	Ra 1.6 (✓)	ISO 13715 +0.05 -0.05

NOTE: UNLESS OTHERWISE MENTIONED, APPLICABLE ISO GPS STANDARDS ARE THOSE PRIOR TO 2010-08-01 REGARDLESS OF THE DRAWING DATE

MASS 34.9 g

DESIGNATION
Heat Copper Pipe

DESIGNED	M.GALKA	FORMAT	A3
CHECKED			
RELEASED		SCALE	1:1
APPROVED			

DESIGNED 2018-11-30

EQUIPMENT CODE LHBTUEL_ LHCb_TRACKING_SYSTEM_UT_Electronics

REFERENCES Doc No: ST0995768_02
LHBTUEL_0005

INDEX

LABEL NOT VALID FOR EXECUTION

QAC -

SHEET 1/1

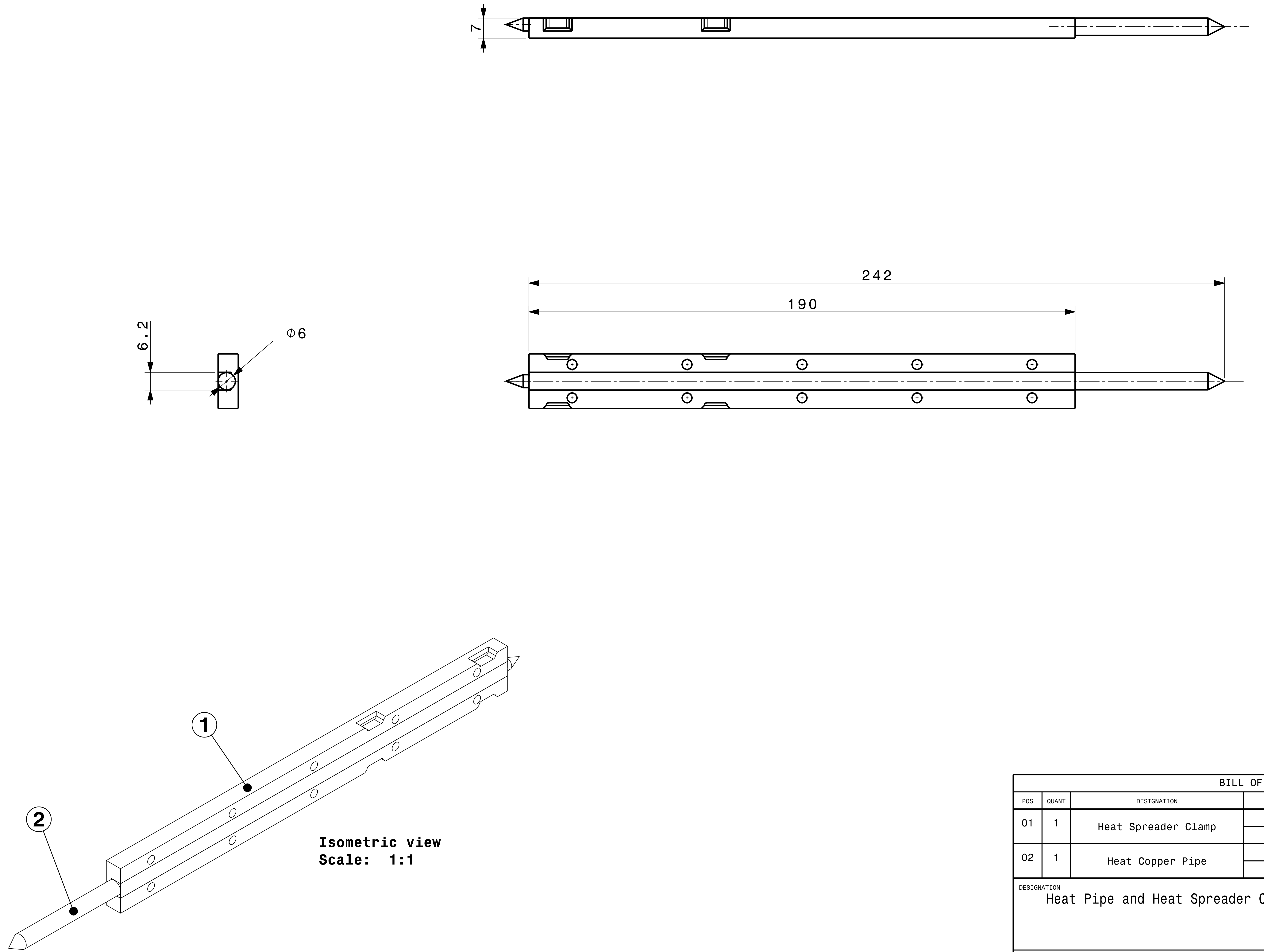

BILL OF MATERIALS					
POS	QUANT	DESIGNATION	REFERENCE	MATERIAL	EDH SCEM
01	1	Heat Spreader Clamp	LHBTUEL_0004 ST0986152	Aluminum	
02	1	Heat Copper Pipe	LHBTUEL_0005 ST0995768	Copper	

DESIGNATION
Heat Pipe and Heat Spreader Clamp

DESIGNED	M.GALKA	FORMAT A2
CHECKED		
RELEASED		SCALE 1:1
APPROVED		

DESIGNED 2018-11-30

EQUIPMENT CODE LHBTUEL_ LHCb_TRACKING_SYSTEM_UT_Electronics

REFERENCES Doc No: ST1000197_02

LHBTUEL_0006

INDEX | LABEL: NOT VALID FOR EXECUTION | QAC: - | SHEET: 1/1

ORGANISATION EUROPEENNE POUR
LA RECHERCHE NUCLEAIRE
EUROPEAN ORGANIZATION FOR NUCLEAR RESEARCH
GENEVE

TB v2.0 A2:Landscape

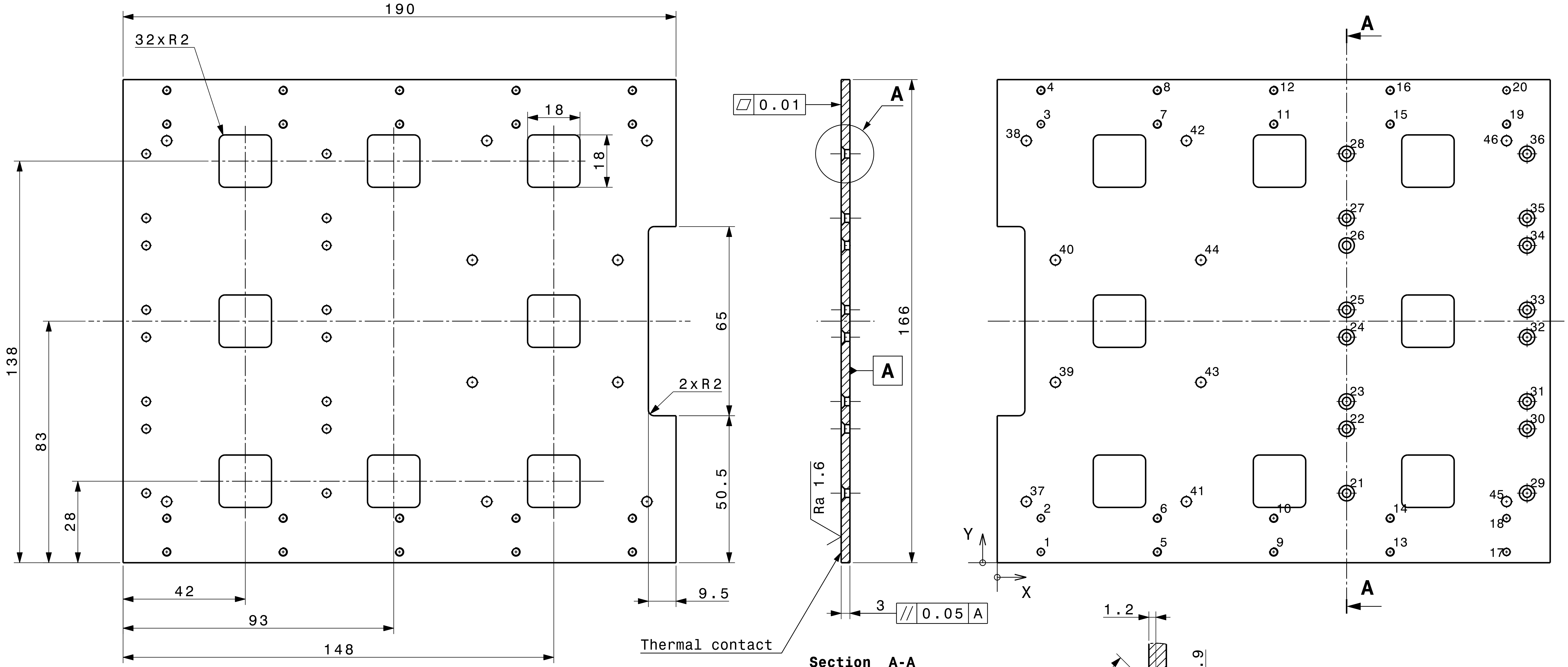

Section A-A
Scale: 1:1

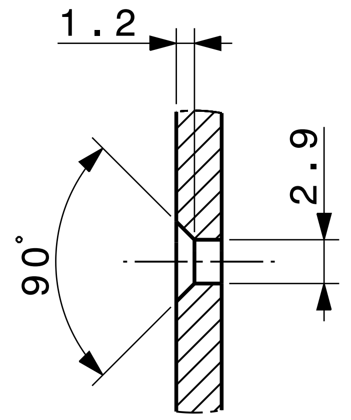

Detail A
Scale: 2:1

Applies to holes 21-36

Material: Aluminium alloy 6082 - T6

Holes Dimension Table			
REF.	X	Y	Diameter
1	15	3.7	M3
2	15	15.3	
3	15	150.7	
4	15	162.3	
5	55	3.7	
6	55	15.3	
7	55	150.7	
8	55	162.3	
9	95	3.7	
10	95	15.3	

Holes Dimension Table			
REF.	X	Y	Diameter
21	120.06	23.9	2.9 See detail A
22	120.06	46	
23	120.06	55.4	
24	120.06	77.5	
25	120.06	86.9	
26	120.06	109	
27	120.06	118.4	
28	120.06	140.5	
29	182.06	23.9	
30	182.06	46	

Holes Dimension Table			
REF.	X	Y	Diameter
11	95	150.7	M3
12	95	162.3	
13	135	3.7	
14	135	15.3	
15	135	150.7	
16	135	162.3	
17	175	3.7	
18	175	15.3	
19	175	150.7	
20	175	162.3	

Holes Dimension Table			
REF.	X	Y	Diameter
31	182.06	55.4	2.9 See detail A
32	182.06	77.5	
33	182.06	86.9	
34	182.06	109	
35	182.06	118.4	
36	182.06	140.5	
37	10	21	3.4
38	10	145	
39	20	62	
40	20	104	

Holes Dimension Table			
REF.	X	Y	Diameter
41	65	21	3.4
42	65	145	
43	70	62	
44	70	104	
45	175	21	
46	175	145	

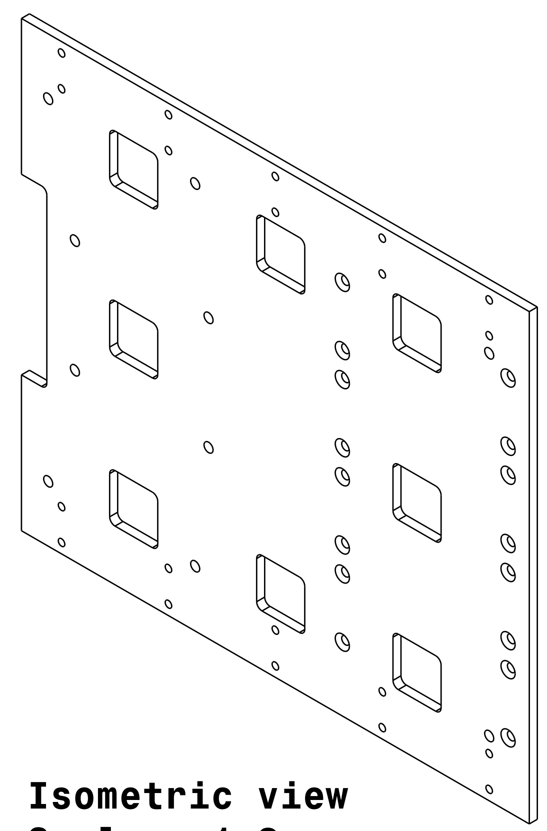

Isometric view
Scale: 1:2

MATERIAL	INITIAL STATE	FINAL STATE
Aluminum		

ISO GPS STANDARDS

ISO 2768-fH | Ra 3.2 | ISO 13715 +0.05 -0.05

NOTE: UNLESS OTHERWISE MENTIONED, APPLICABLE ISO GPS STANDARDS ARE THOSE PRIOR TO 2010-08-01 REGARDLESS OF THE DRAWING DATE

MASS 227 g

DESIGNATION: DCB Heat Spreader

DESIGNED	M.GALKA	FORMAT	A2
CHECKED			
RELEASED		SCALE	1:1
APPROVED			

DESIGNED 2018-11-30

EQUIPMENT CODE LHBTUEL_ LHCb_TRACKING_SYSTEM_UT_Electronics

REFERENCES: LHBTUEL_0007 — Doc No: ST0984423_02 — INDEX — LABEL: NOT VALID FOR EXECUTION — QAC: - — SHEET: 1/1

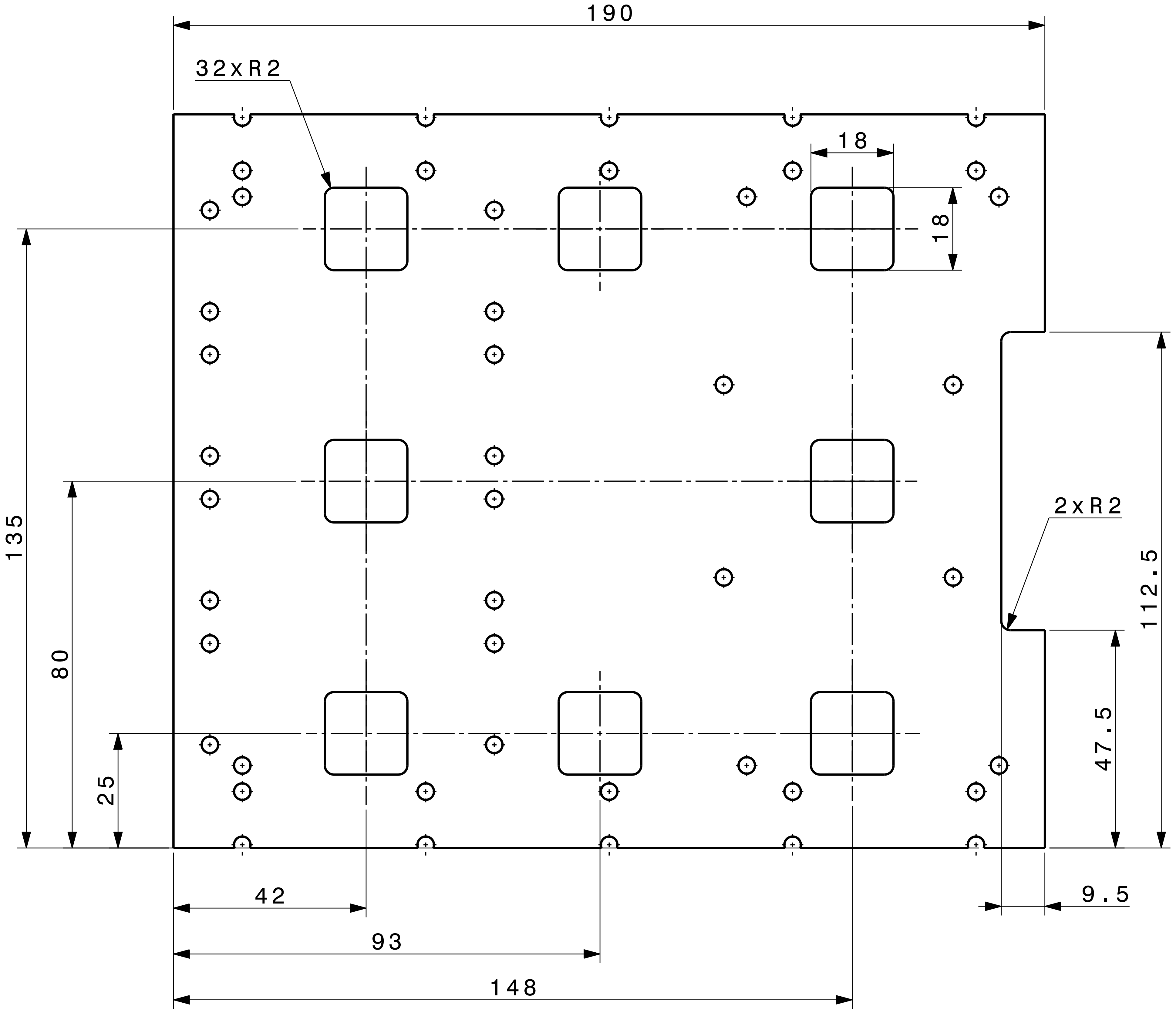

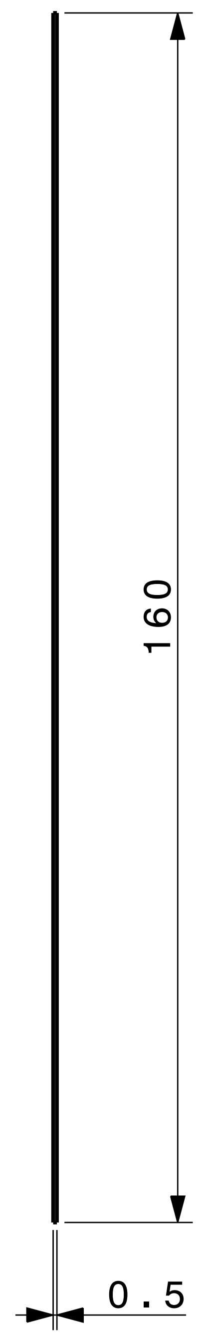

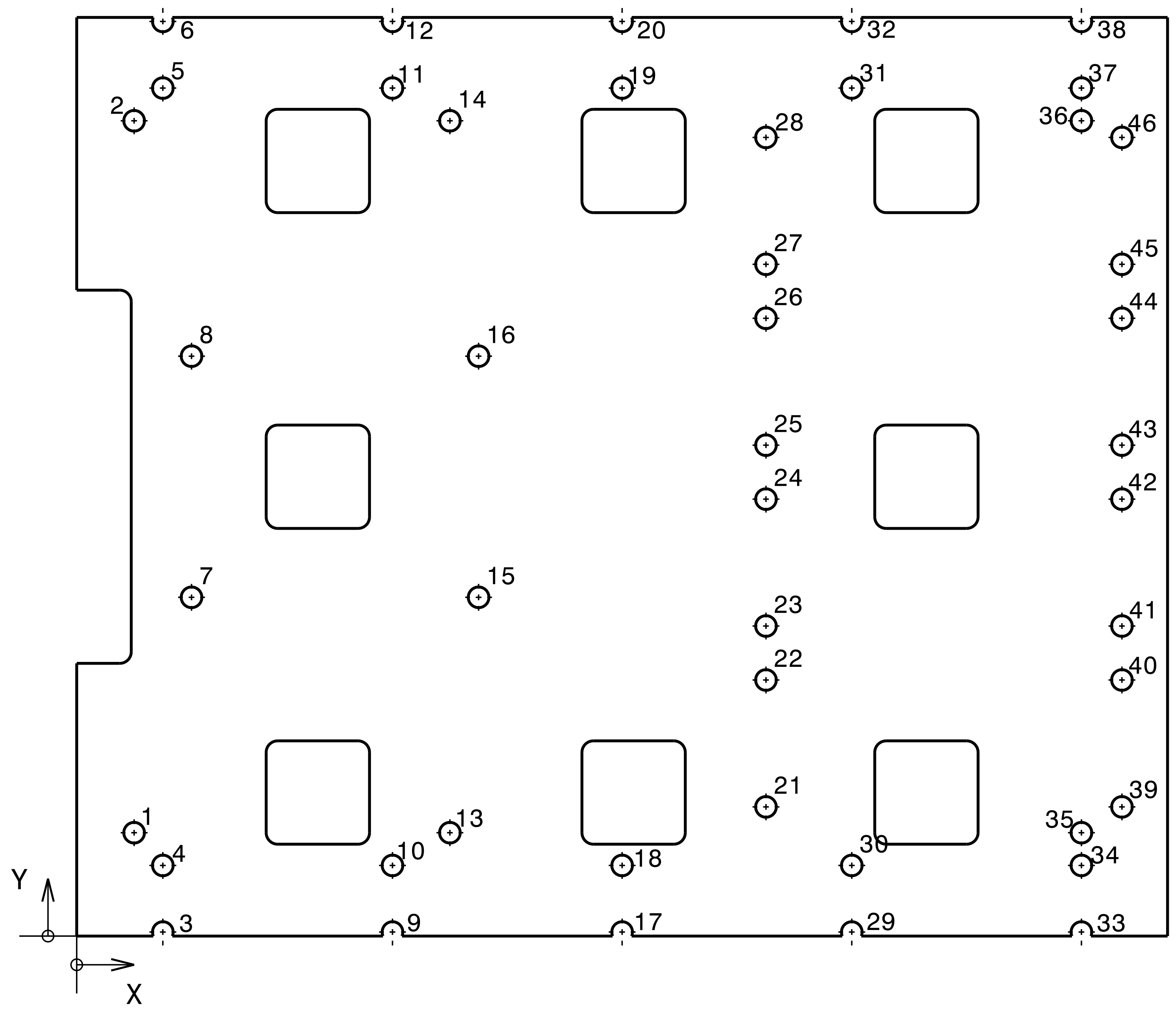

Hole Dimension Table			
REF.	X	Y	Diameter
1	10	18	3.6
2	10	142	3.6
3	15	0.7	3.6
4	15	12.3	3.6
5	15	147.7	3.6
6	15	159.3	3.6
7	20	59	3.6
8	20	101	3.6
9	55	0.7	3.6
10	55	12.3	3.6

Hole Dimension Table			
REF.	X	Y	Diameter
11	55	147.7	3.6
12	55	159.3	3.6
13	65	18	3.6
14	65	142	3.6
15	70	59	3.6
16	70	101	3.6
17	95	0.7	3.6
18	95	12.3	3.6
19	95	147.7	3.6
20	95	159.3	3.6

Hole Dimension Table			
REF.	X	Y	Diameter
21	120.06	22.5	3.6
22	120.06	44.6	3.6
23	120.06	54	3.6
24	120.06	76.1	3.6
25	120.06	85.5	3.6
26	120.06	107.6	3.6
27	120.06	117	3.6
28	120.06	139.1	3.6
29	135	0.7	3.6
30	135	12.3	3.6

Hole Dimension Table			
REF.	X	Y	Diameter
31	135	147.7	3.6
32	135	159.3	3.6
33	175	0.7	3.6
34	175	12.3	3.6
35	175	18	3.6
36	175	142	3.6
37	175	147.7	3.6
38	175	159.3	3.6
39	182.06	22.5	3.6
40	182.06	44.6	3.6

Hole Dimension Table			
REF.	X	Y	Diameter
41	182.06	54	3.6
42	182.06	76.1	3.6
43	182.06	85.5	3.6
44	182.06	107.6	3.6
45	182.06	117	3.6
46	182.06	139.1	3.6

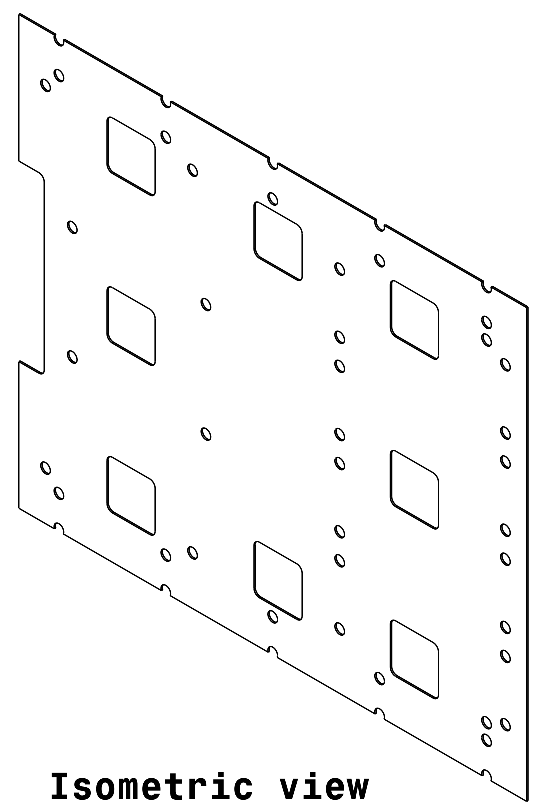

Isometric view
Scale: 1:2

Material: Bergquist VO Ultra Soft Gap Pad, or
Farnell 189-3443, or
Digi-Key Gap Pad VO Ultra Soft.

ISO GPS STANDARDS

ISO 2768-fH | Ra 3.2 | ISO 13715 +0.05 -0.05

NOTE: UNLESS OTHERWISE MENTIONED, APPLICABLE ISO GPS STANDARDS ARE THOSE PRIOR TO 2010-08-01 REGARDLESS OF THE DRAWING DATE

DESIGNATION: Gap Filler HS-DCB

DESIGNED: M.GALKA
CHECKED
RELEASED
APPROVED

FORMAT: A2
SCALE: 1:1

DESIGNED 2018-11-30

EQUIPMENT CODE LHBTUEL_ LHCb_TRACKING_SYSTEM_UT_Electronics

REFERENCES: LHBTUEL_0008 — Doc No: ST1003580_02
INDEX
LABEL: NOT VALID FOR EXECUTION
QAC: -
SHEET: 1/1

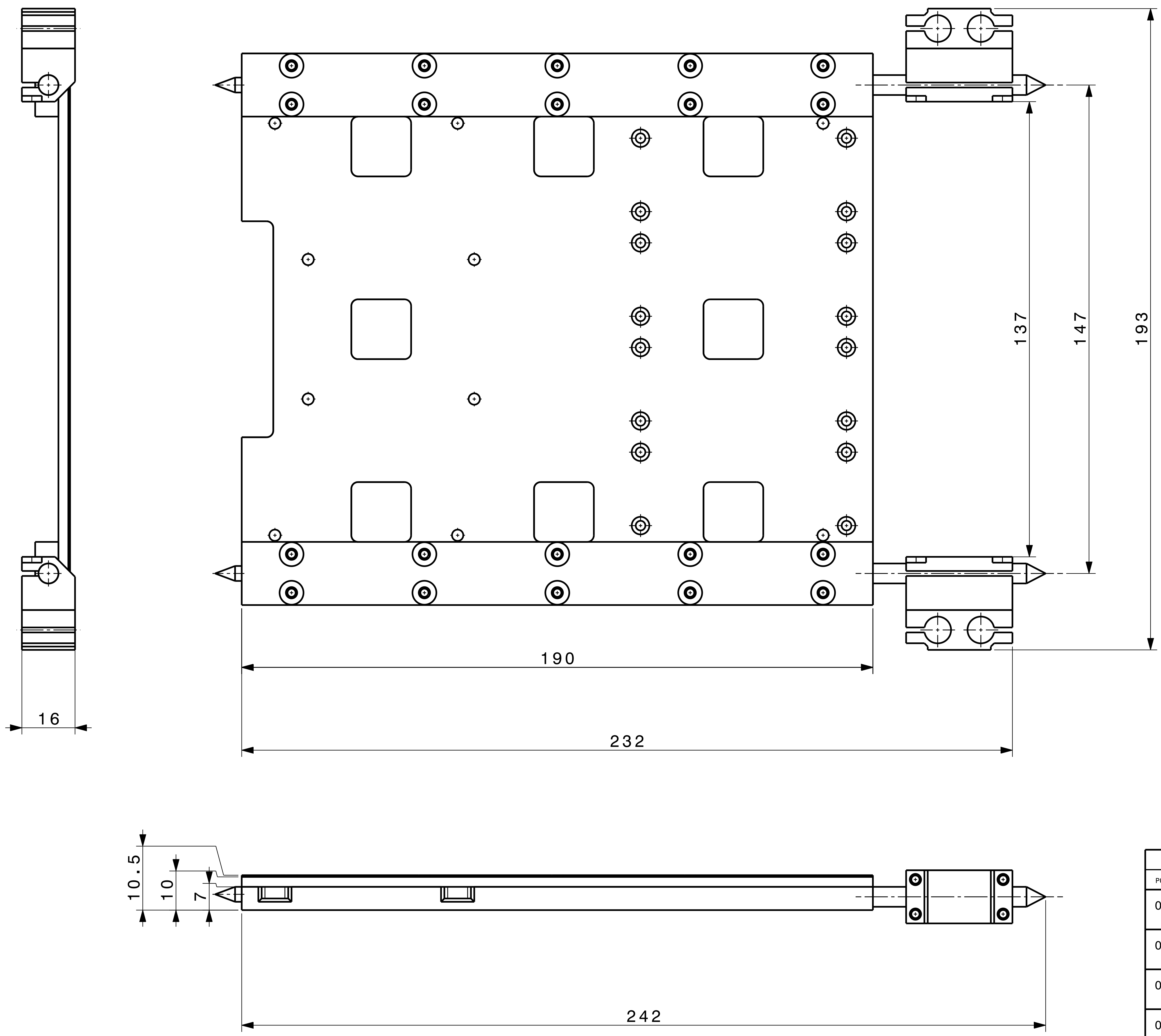

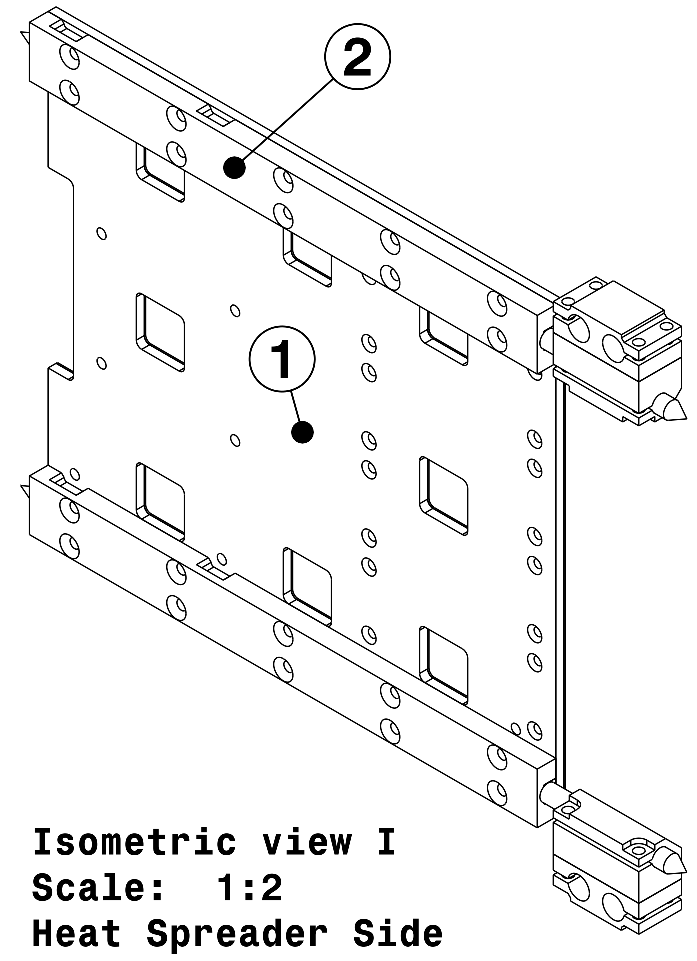

Isometric view I
Scale: 1:2
Heat Spreader Side

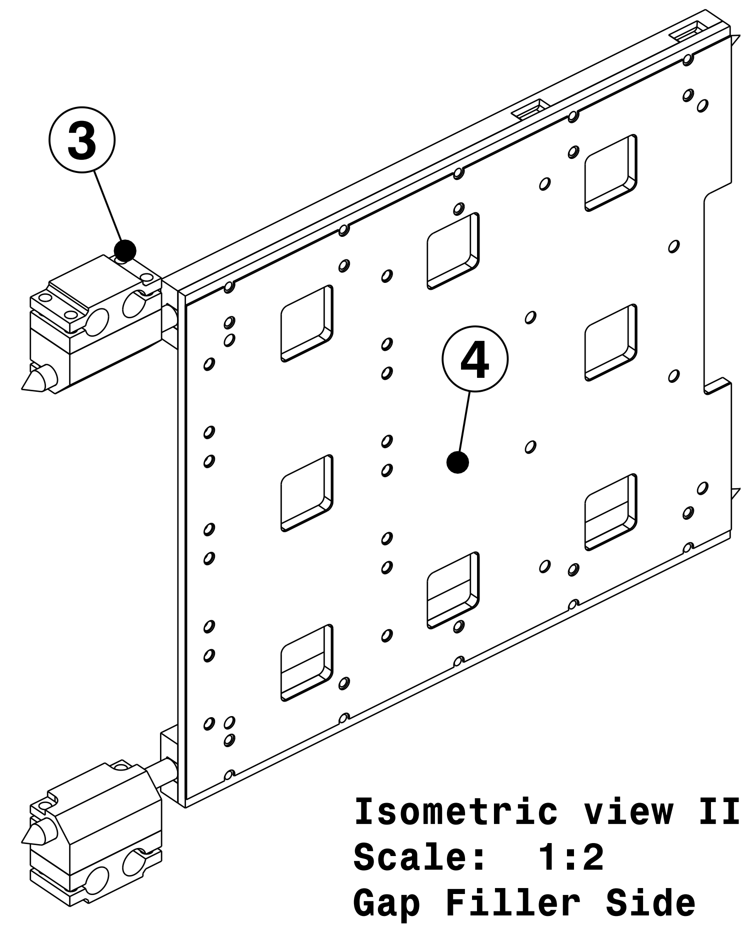

Isometric view II
Scale: 1:2
Gap Filler Side

BILL OF MATERIALS

POS	QUANT	DESIGNATION	REFERENCE	MATERIAL	EDH SCEM
01	1	DCB Heat Spreader	LHBTUEL_0007 ST0984423	Aluminum	
02	2	Heat Pipe and Heat Spreader Clamp	LHBTUEL_0006 ST1000197		
03	2	Water Pipe to Heat Pipe Interface	LHBTUEL_0003 ST1000445		
04	1	Gap Filler HS-DCB	LHBTUEL_0008 ST1003580		

DESIGNATION

DCB Cooling Interface

DESIGNED	M.GALKA	FORMAT	A2
CHECKED			
RELEASED		SCALE	1:1
APPROVED			

DESIGNED 2018-11-30

EQUIPMENT CODE LHBTUEL_ LHCb_TRACKING_SYSTEM_UT_Electronics

REFERENCES Doc No: ST1000799_02

LHBTUEL_0009

INDEX

LABEL NOT VALID FOR EXECUTION

QAC -

SHEET 1/1

CERN

ORGANISATION EUROPEENNE POUR
LA RECHERCHE NUCLEAIRE
EUROPEAN ORGANIZATION FOR NUCLEAR RESEARCH
GENEVE

TB v2.0 A2:Landscape

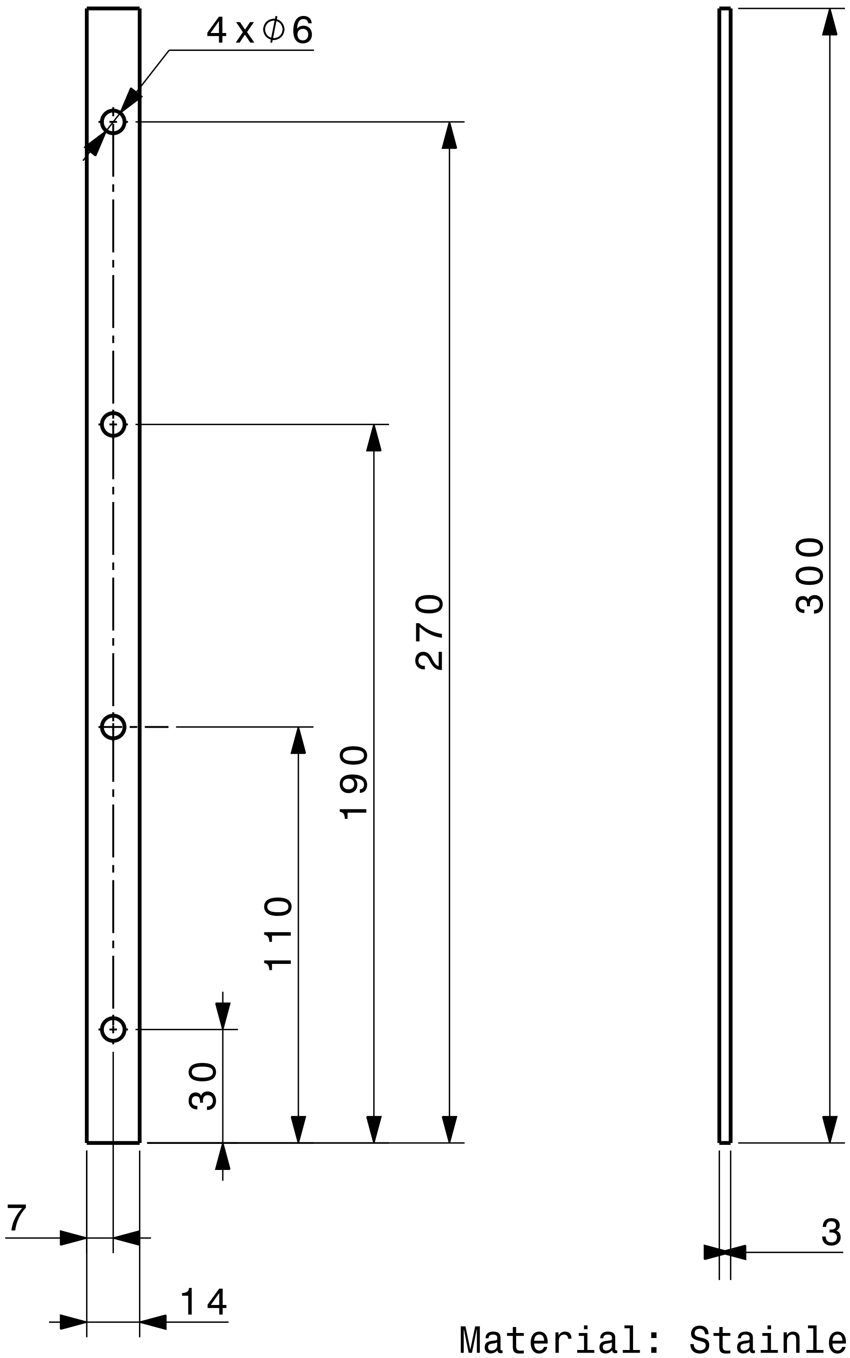

Material: Stainless Steel 316L

MATERIAL	INITIAL STATE	FINAL STATE
Stainless Steel		

ISO GPS STANDARDS

ISO 2768-fH	Ra 3.2 (✓)	ISO 13715 +0.05 -0.05 +0.05 -0.05

NOTE: UNLESS OTHERWISE MENTIONED, APPLICABLE ISO GPS STANDARDS ARE THOSE PRIOR TO 2010-08-01 REGARDLESS OF THE DRAWING DATE

MASS 98.1 g

DESIGNATION
Wall Part_1 - Pathfinder

DESIGNED	M.GALKA	FORMAT A4	
CHECKED			
RELEASED		SCALE 1:2	
APPROVED			
DESIGNED 2018-11-30			

EQUIPMENT CODE LHBTUEL_ LHCb_TRACKING_SYSTEM_UT_Electronics

REFERENCES	INDEX	LABEL	QAC	SHEET
Doc No: ST1063126_02 LHBTUEL_0010		NOT VALID FOR EXECUTION	-	1/1

ORGANISATION EUROPEENNE POUR LA RECHERCHE NUCLEAIRE
EUROPEAN ORGANIZATION FOR NUCLEAR RESEARCH
GENEVE

CERN

TB v2.0 A4:Portrait

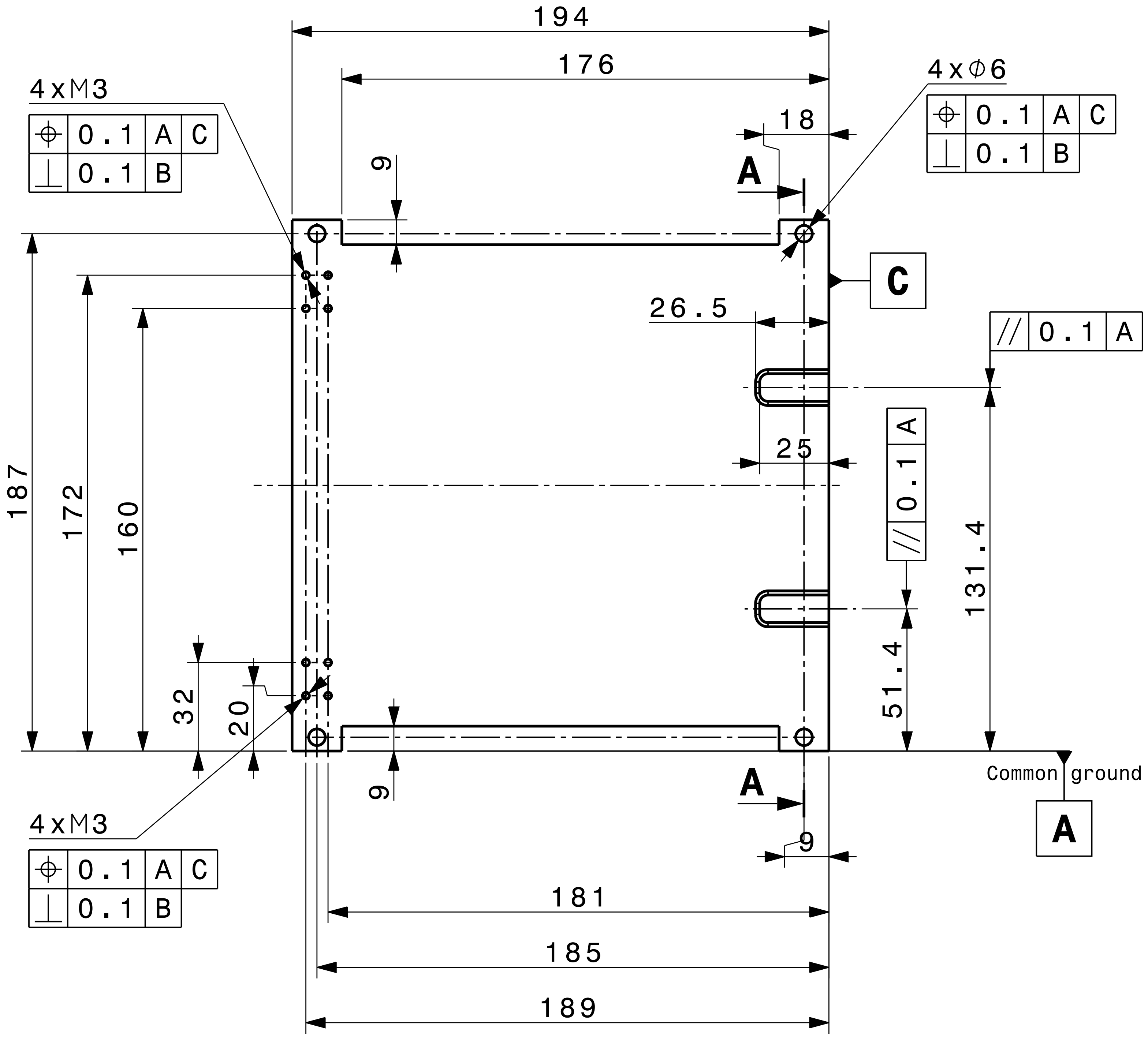

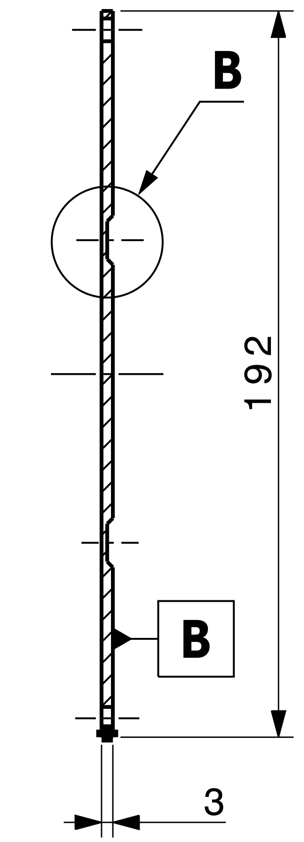

Section: A-A
Scale: 1:2

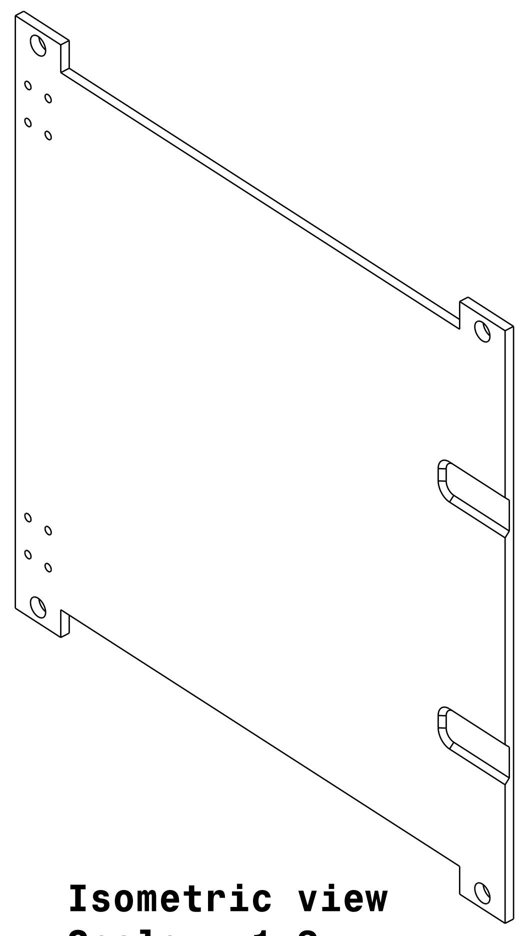

Isometric view
Scale: 1:2

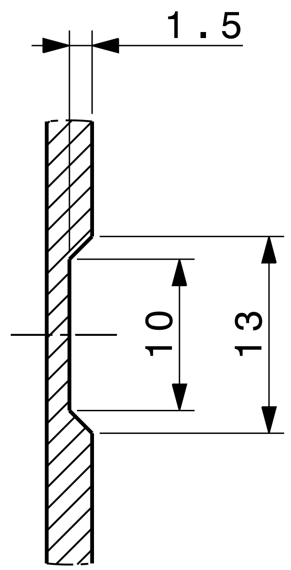

Detail B
Scale: 2:1

Material: Stainless Steel 316L

MATERIAL	INITIAL STATE	FINAL STATE
Stainless Steel		

ISO GPS STANDARDS		
ISO 2768-fH	Ra 3.2	ISO 13715 +0.05 -0.05

NOTE: UNLESS OTHERWISE MENTIONED, APPLICABLE ISO GPS STANDARDS ARE THOSE PRIOR TO 2010-08-01 REGARDLESS OF THE DRAWING DATE

MASS 815 g

DESIGNATION			
Wall Part_2 - Pathfinder	DESIGNED	M.GALKA	FORMAT A3
	CHECKED		
	RELEASED		SCALE 1:2
	APPROVED		
EQUIPMENT CODE LHBTUEL_ LHCb_TRACKING_SYSTEM_UT_Electronics	DESIGNED 2018-11-30		

REFERENCES	INDEX	LABEL	QAC	SHEET
Doc No: ST1063127_02 LHBTUEL_0011		NOT VALID FOR EXECUTION	-	1/1

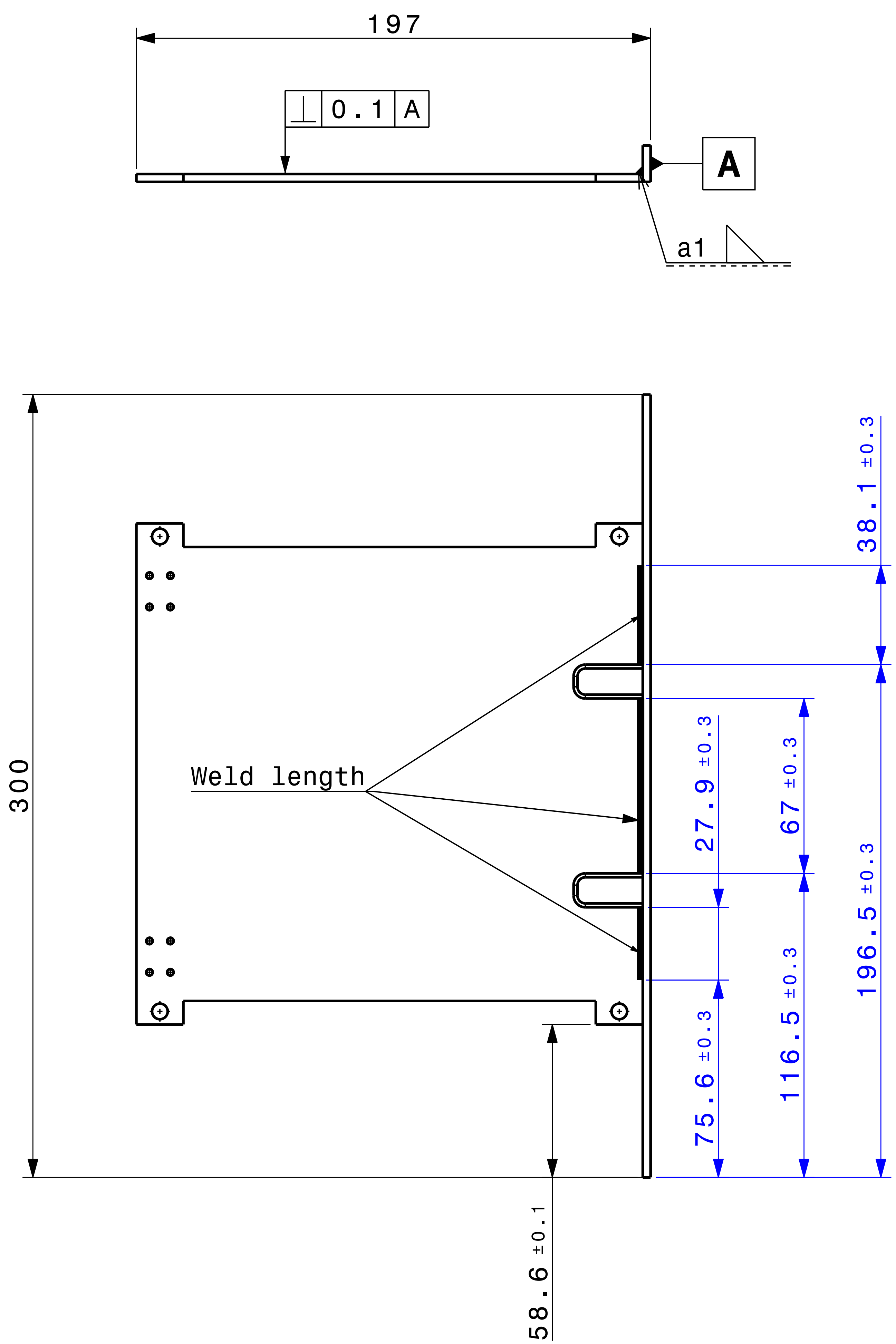

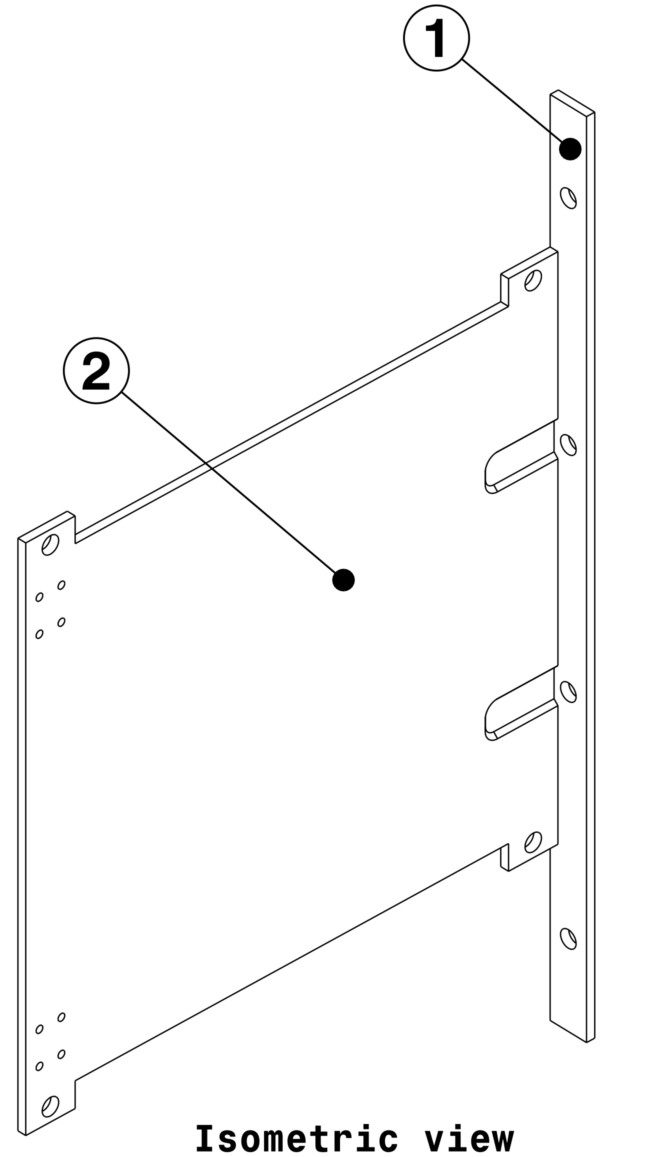

Isometric view
Scale: 1:2

Material: Stainless Steel 316L

BILL OF MATERIALS

POS	QUANT	DESIGNATION	REFERENCE	MATERIAL	EDH SCEM
01	1	Wall Part_1 - Pathfinder	LHBTUEL_0010 ST1063126	Stainless Steel	
02	1	Wall Part_2 - Pathfinder	LHBTUEL_0011 ST1063127	Stainless Steel	

DESIGNATION: Wall - Pathfinder	DESIGNED	M.GALKA	FORMAT A3
	CHECKED		
	RELEASED		SCALE 1:2
	APPROVED		
EQUIPMENT CODE LHBTUEL_ LHCb_TRACKING_SYSTEM_UT_Electronics	DESIGNED 2018-11-30		
REFERENCES: LHBTUEL_0012 (Doc No: ST1063144_02)	INDEX	LABEL: NOT VALID FOR EXECUTION	QAC: - / SHEET: 1/1

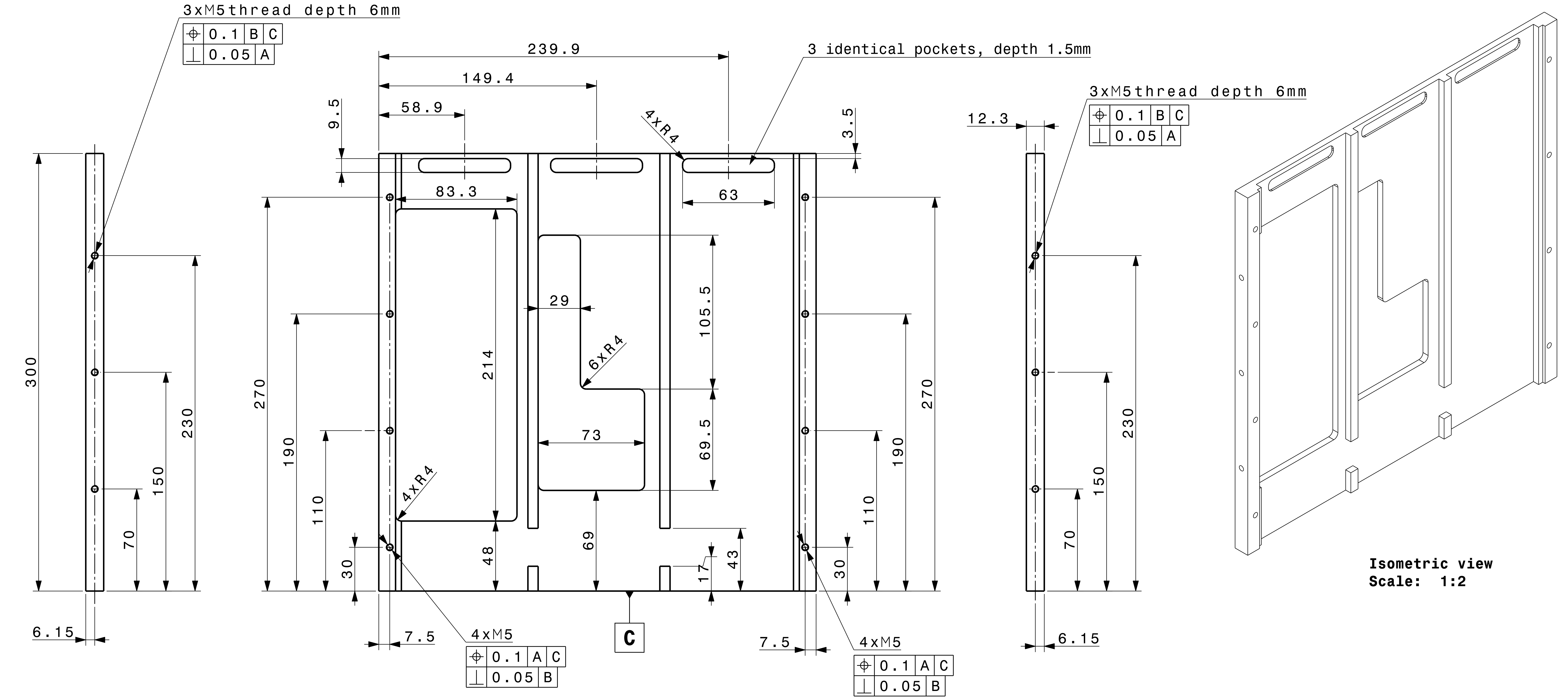

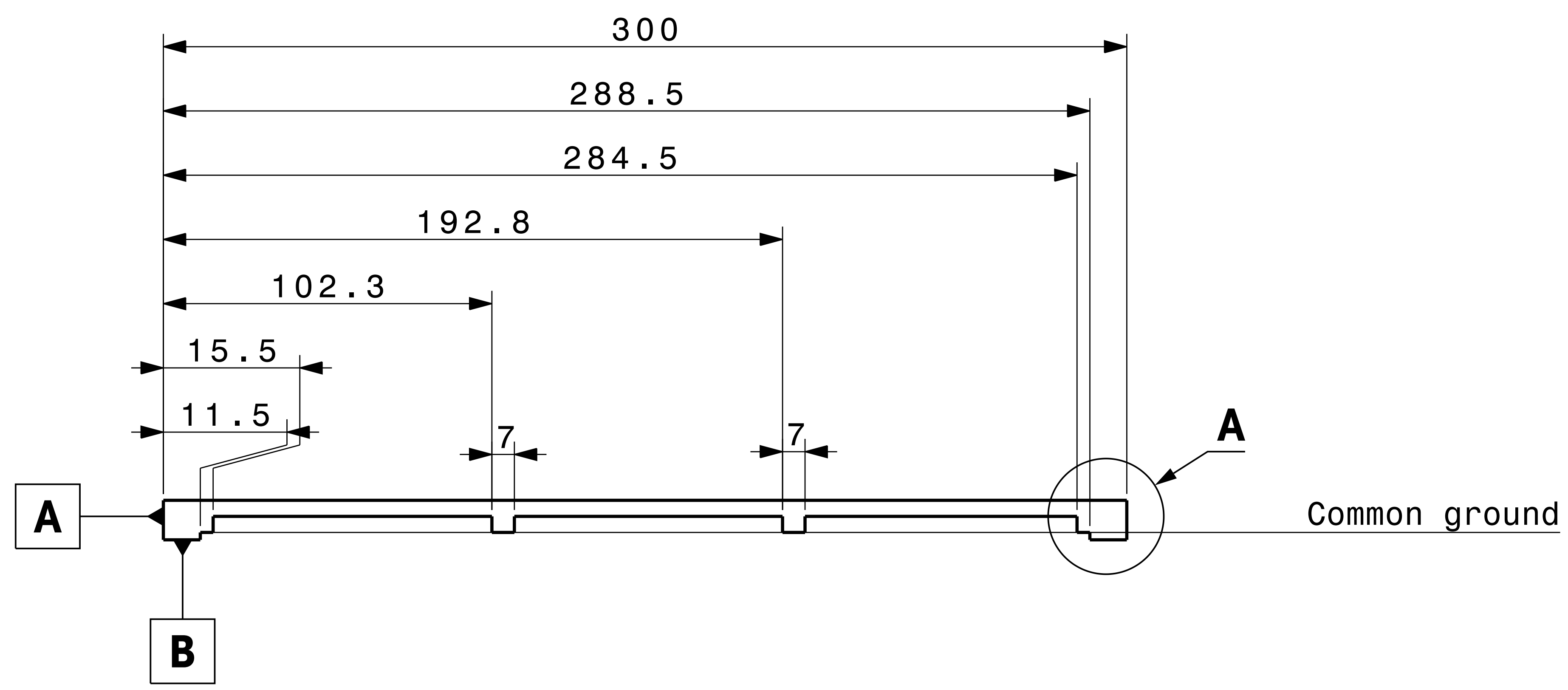

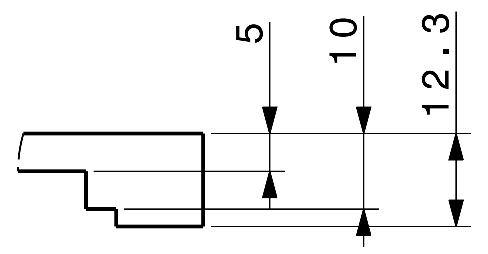

Detail A
Scale: 1:1

Material: Aluminium alloy 6082 - T6

MATERIAL	INITIAL STATE	FINAL STATE
Aluminum		

ISO GPS STANDARDS

ISO 2768-fH | Ra 3.2 | ISO 13715 +0.05 -0.05

NOTE: UNLESS OTHERWISE MENTIONED, APPLICABLE ISO GPS STANDARDS ARE THOSE PRIOR TO 2010-08-01 REGARDLESS OF THE DRAWING DATE

MASS 1.06 kg

DESIGNATION Base Plate - Pathfinder

DESIGNED	M.GALKA	FORMAT	A2
CHECKED			
RELEASED		SCALE	1:2
APPROVED			

DESIGNED 2018-11-30

EQUIPMENT CODE LHBTUEL_ LHCb_TRACKING_SYSTEM_UT_Electronics

REFERENCES Doc No: ST1061437_02

LHBTUEL_0013

INDEX

LABEL NOT VALID FOR EXECUTION

QAC -

SHEET 1/1

ORGANISATION EUROPEENNE POUR LA RECHERCHE NUCLEAIRE
EUROPEAN ORGANIZATION FOR NUCLEAR RESEARCH
GENEVE

TB v2.0 A2:Landscape


2xM3Thread depth 6mm
⌖ 0.1 A B
⊥ 0.1 C
See Detail B
(11x22.67)=249.37
B
200
188
D
2xM5Thread depth 6mm
⌖ 0.1 B C
⊥ 0.1 A
A
257.17
232
2xM3Thread depth 6mm
⌖ 0.1 A B
⊥ 0.1 C
30.45
13
8
70.5
179
186
196.5
3.5
21
24.25
34.65
160.25
170.65
250.9
261.3
12xΦ3thread depth 6mm
⌖ 0.1 A B
⊥ 0.1 C
Common ground
13
7
9
15
Section A-A
Scale: 1:2
5
6
12
3
3
15
Detail D
Scale: 2:1
282
276
274
8
6
C
10
12
15
Detail C
Scale: 2:1
Isometric view II
Scale: 1:2
Detail A
Scale: 2:1
5
6
12
3.5
12
15
Detail B
Scale 2:1
3.5
13
22.67
3
21
6.67
12
12
1.8
2
2
Isometric view I
Scale: 1:2
Material: Aluminium alloy 6082 - T6
MATERIAL
Aluminum
INITIAL STATE
FINAL STATE
ISO GPS STANDARDS
ISO 2768-fH
Ra 3.2
ISO 13715
NOTE: UNLESS OTHERWISE MENTIONED, APPLICABLE ISO GPS STANDARDS ARE THOSE PRIOR TO 2010-08-01 REGARDLESS OF THE DRAWING DATE
MASS 643 g
DESIGNATION
DCB Card Guide - Pathfinder
DESIGNED M.GALKA
CHECKED
RELEASED
APPROVED
FORMAT A1
SCALE 1:2
DESIGNED 2018-11-30
EQUIPMENT CODE LHBTUEL_ LHCb_TRACKING_SYSTEM_UT_Electronics
REFERENCES
Doc No: ST1061442_02
INDEX
LABEL
LHBTUEL_0014
NOT VALID FOR EXECUTION
QAC -
SHEET 1/1
ORGANISATION EUROPEENNE POUR LA RECHERCHE NUCLEAIRE
EUROPEAN ORGANIZATION FOR NUCLEAR RESEARCH
GENEVE

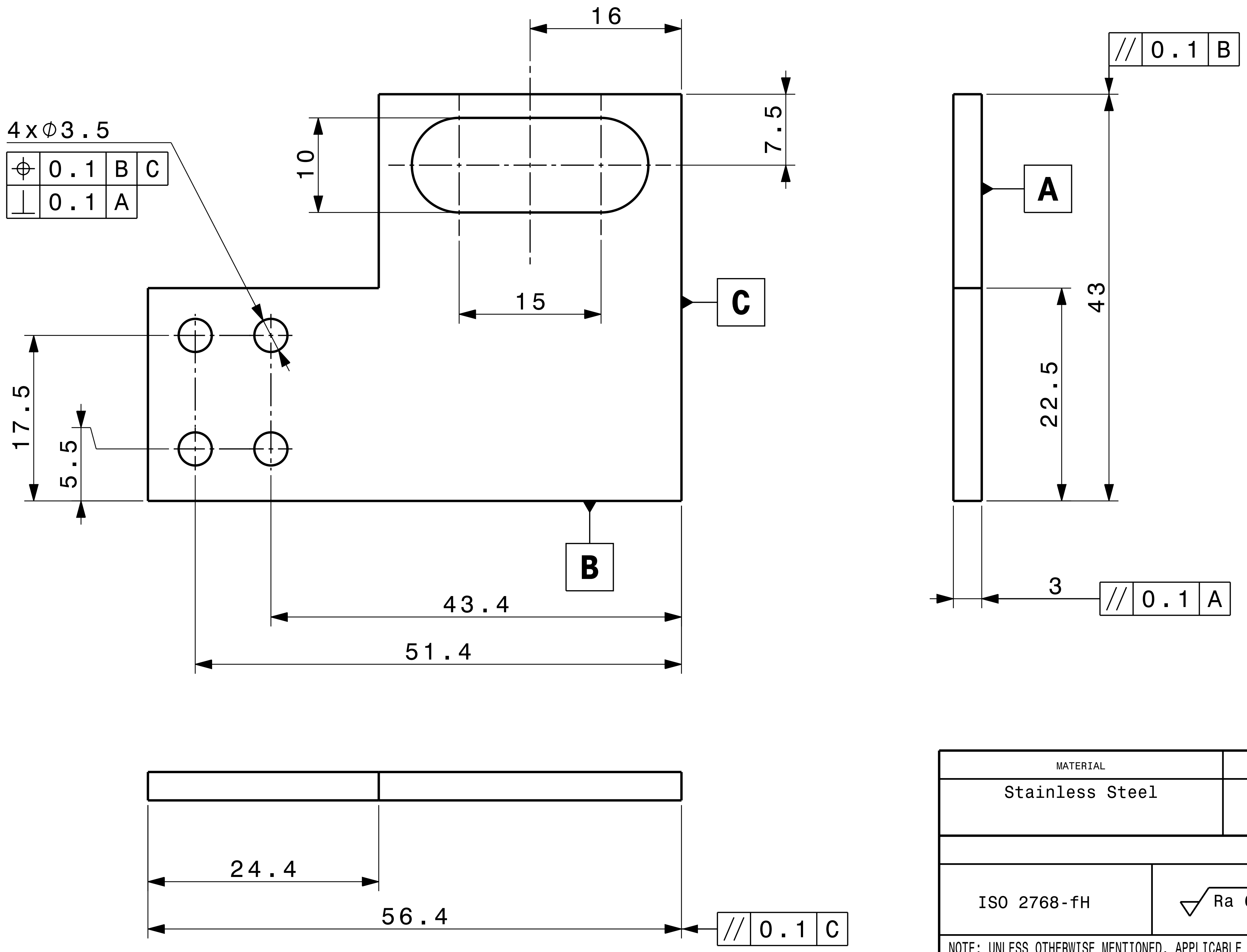

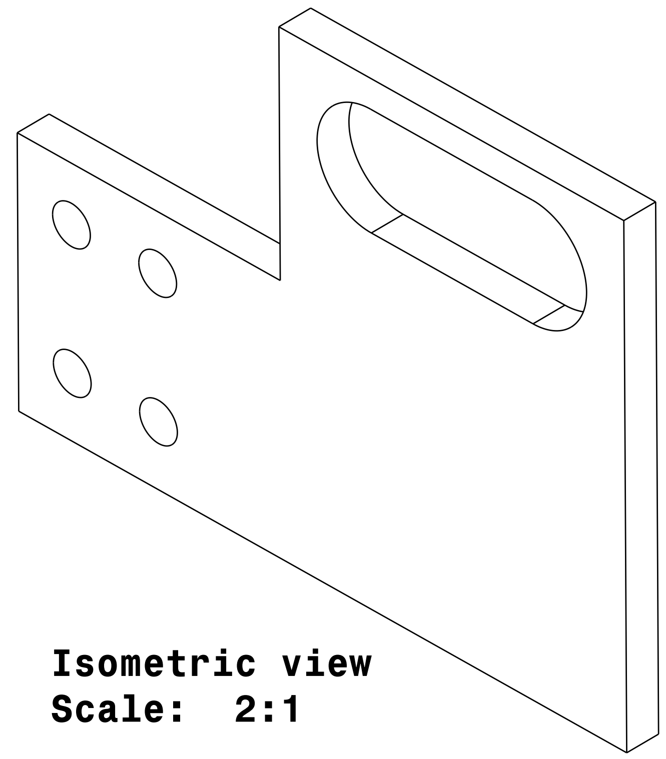

Isometric view
Scale: 2:1

Material: Stainless Steel 316L

MATERIAL	INITIAL STATE	FINAL STATE
Stainless Steel		

ISO GPS STANDARDS

ISO 2768-fH | Ra 6.3 | ISO 13715 +0.05 -0.05 +0.05 -0.05

NOTE: UNLESS OTHERWISE MENTIONED, APPLICABLE ISO GPS STANDARDS ARE THOSE PRIOR TO 2010-08-01 REGARDLESS OF THE DRAWING DATE

MASS 39.8 g

DESIGNATION Water Pipe Support Wall

DESIGNED	M.GALKA	FORMAT	A3
CHECKED			
RELEASED		SCALE	2:1
APPROVED			

DESIGNED 2018-11-30

EQUIPMENT CODE LHBTUEL_ LHCb_TRACKING_SYSTEM_UT_Electronics

REFERENCES	INDEX	LABEL	QAC	SHEET
Doc No: ST1073444_02 LHBTUEL_0015		NOT VALID FOR EXECUTION	-	1/1

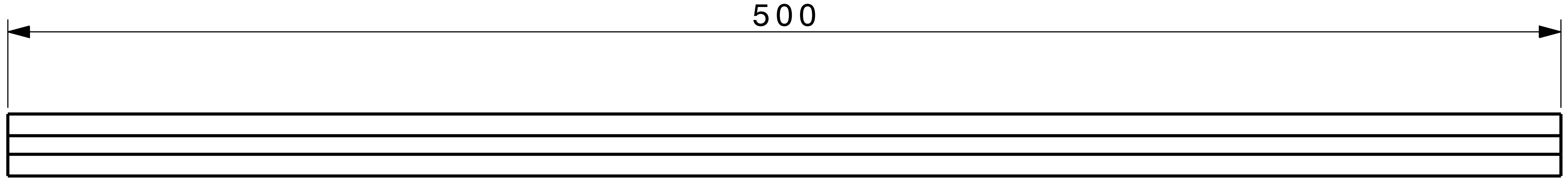

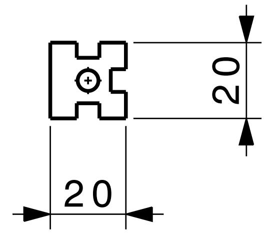

Material: Bosh Profile 20x20 3S

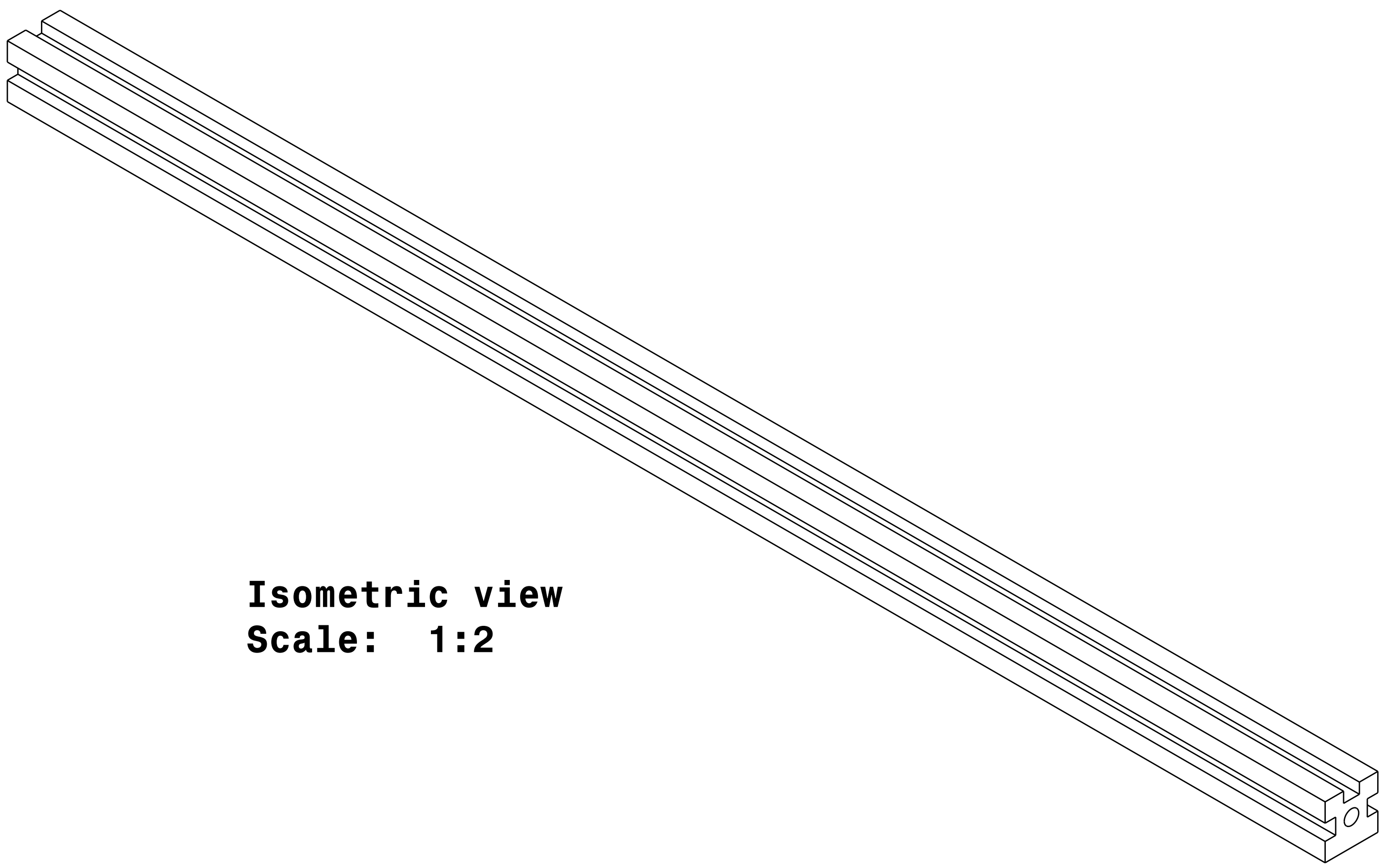

Isometric view
Scale: 1:2

MATERIAL	INITIAL STATE	FINAL STATE
Aluminum		

ISO GPS STANDARDS		
ISO 2768-mK	Ra 6.3	ISO 13715 +0.05 -0.05 +0.05 -0.05

NOTE: UNLESS OTHERWISE MENTIONED, APPLICABLE ISO GPS STANDARDS ARE THOSE PRIOR TO 2010-08-01 REGARDLESS OF THE DRAWING DATE

MASS 411 g

DESIGNATION			
Bottom Stand Profile	DESIGNED	M.GALKA	FORMAT A3
	CHECKED		
	RELEASED		SCALE 1:2
	APPROVED		
EQUIPMENT CODE LHBTUEL_ LHCb_TRACKING_SYSTEM_UT_Electronics	DESIGNED 2018-11-30		

REFERENCES Doc No: ST1062258_02	INDEX	LABEL	QAC	SHEET
LHBTUEL_0016		NOT VALID FOR EXECUTION	-	1/1

ORGANISATION EUROPEENNE POUR LA RECHERCHE NUCLEAIRE
EUROPEAN ORGANIZATION FOR NUCLEAR RESEARCH
GENEVE

CERN

TB v2.0 A3:Landscape

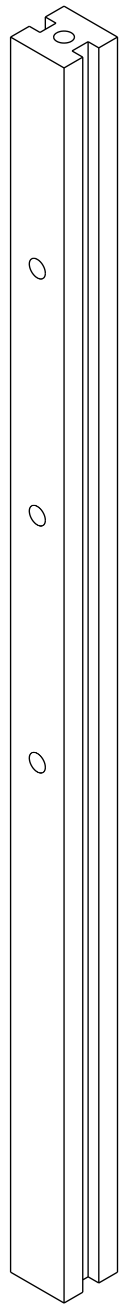

Isometric view
Scale: 1:2

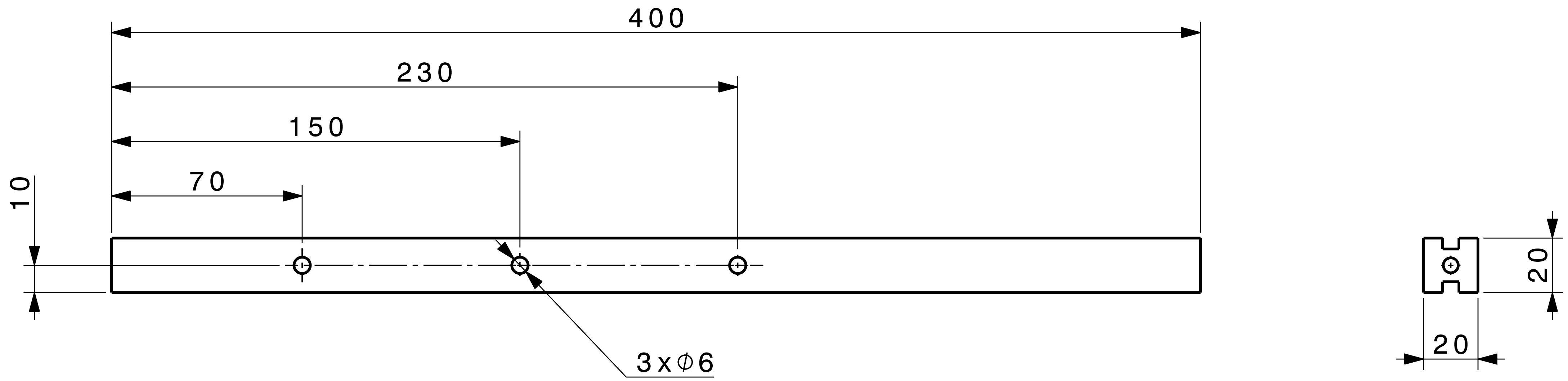

Material: Bosh Profile 20x20 2S

MATERIAL	INITIAL STATE	FINAL STATE
Aluminum		

ISO GPS STANDARDS

ISO 2768-mK | Ra 6.3 | ISO 13715 +0.05 -0.05 | +0.05 -0.05

NOTE: UNLESS OTHERWISE MENTIONED, APPLICABLE ISO GPS STANDARDS ARE THOSE PRIOR TO 2010-08-01 REGARDLESS OF THE DRAWING DATE

MASS 351 g

DESIGNATION Vertical Baseplate Profile

DESIGNED	M.GALKA	FORMAT	A3
CHECKED			
RELEASED		SCALE	1:2
APPROVED			

DESIGNED 2018-11-30

EQUIPMENT CODE LHBTUEL_ LHCb_TRACKING_SYSTEM_UT_Electronics

REFERENCES	INDEX	LABEL	QAC	SHEET
Doc No: ST1062259_02 LHBTUEL_0017		NOT VALID FOR EXECUTION	-	1/1

ORGANISATION EUROPEENNE POUR LA RECHERCHE NUCLEAIRE
EUROPEAN ORGANIZATION FOR NUCLEAR RESEARCH
GENEVE

CERN

TB v2.0 A3:Landscape

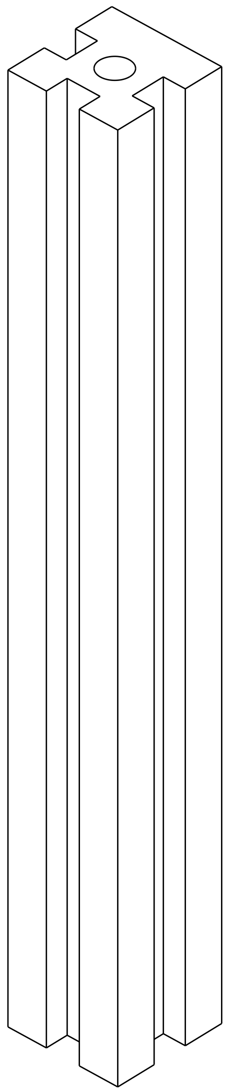

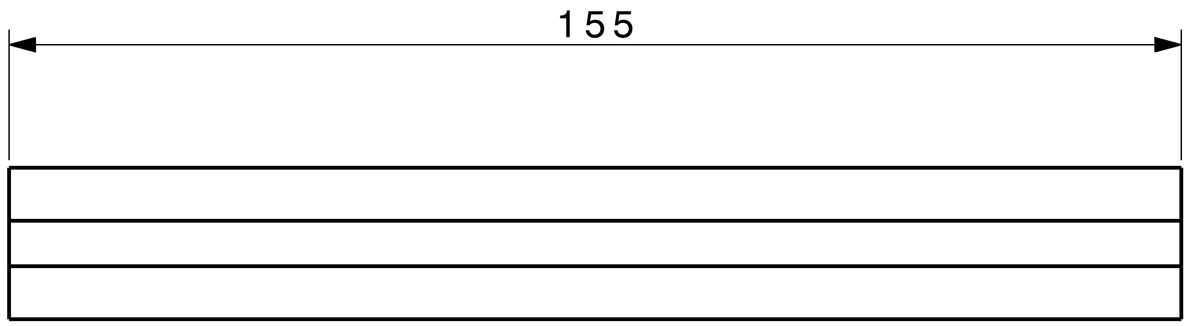

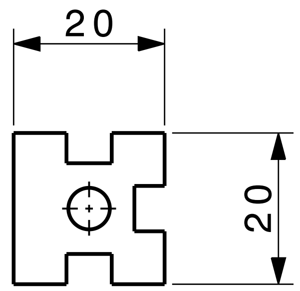

Material: Bosh Profile 20x20 3S

Isometric view
Scale: 1:1

MATERIAL	INITIAL STATE	FINAL STATE
Aluminum		

ISO GPS STANDARDS

ISO 2768-mK | Ra 6.3 | ISO 13715 +0.05 -0.05 | +0.05 -0.05

NOTE: UNLESS OTHERWISE MENTIONED, APPLICABLE ISO GPS STANDARDS ARE THOSE PRIOR TO 2010-08-01 REGARDLESS OF THE DRAWING DATE

MASS 127 g

DESIGNATION
Vertical COMET Profile

DESIGNED	M.GALKA	FORMAT	A3
CHECKED			
RELEASED		SCALE	1:1
APPROVED			

DESIGNED 2018-11-30

EQUIPMENT CODE LHBTUEL_ LHCb_TRACKING_SYSTEM_UT_Electronics

REFERENCES	Doc No: ST1062260_02	INDEX	LABEL	QAC	SHEET
LHBTUEL_0018			NOT VALID FOR EXECUTION	-	1/1

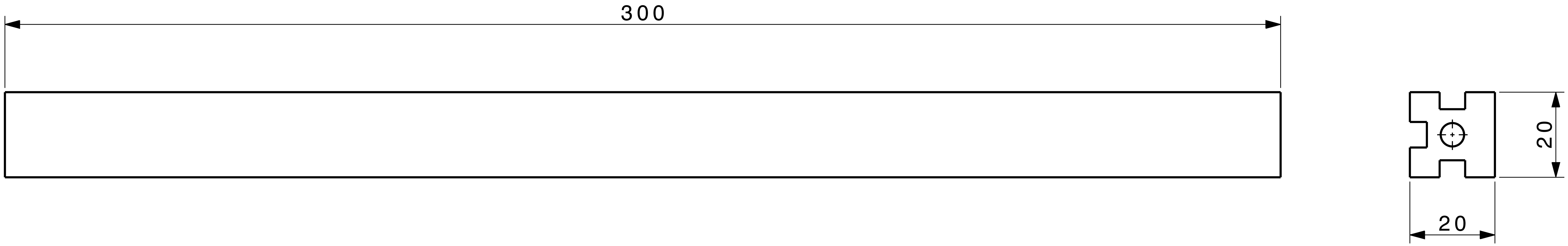

Material: Bosh Profile 20x20 3S

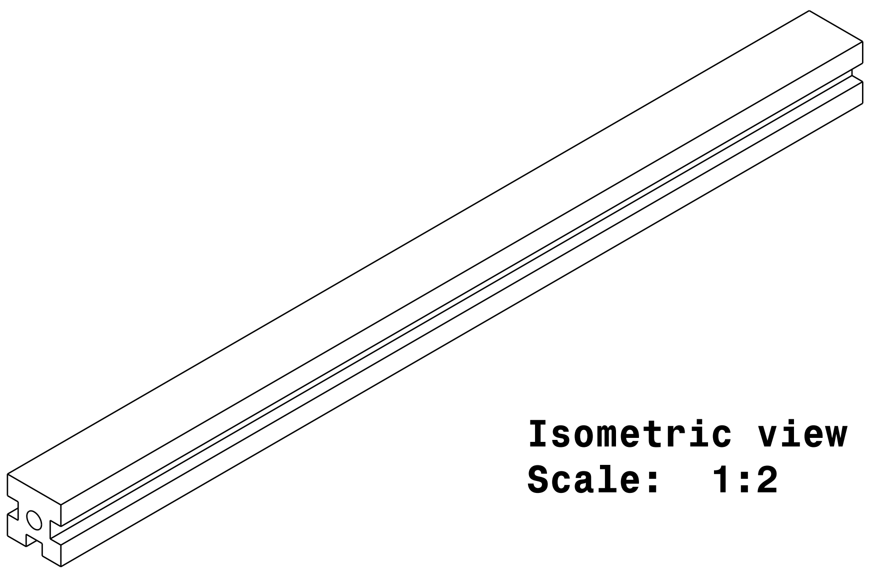

Isometric view
Scale: 1:2

MATERIAL	INITIAL STATE	FINAL STATE
Aluminum		

ISO GPS STANDARDS

ISO 2768-mK | Ra 6.3 | ISO 13715 +0.05 -0.05

NOTE: UNLESS OTHERWISE MENTIONED, APPLICABLE ISO GPS STANDARDS ARE THOSE PRIOR TO 2010-08-01 REGARDLESS OF THE DRAWING DATE

MASS 246 g

DESIGNATION Horizontal COMET Profile

DESIGNED	M.GALKA	FORMAT A3
CHECKED		
RELEASED		SCALE 1:1
APPROVED		

DESIGNED 2018-11-30

EQUIPMENT CODE LHBTUEL_ LHCb_TRACKING_SYSTEM_UT_Electronics

REFERENCES Doc No: ST1062261_02

LHBTUEL_0019

INDEX | LABEL NOT VALID FOR EXECUTION | QAC - | SHEET 1/1

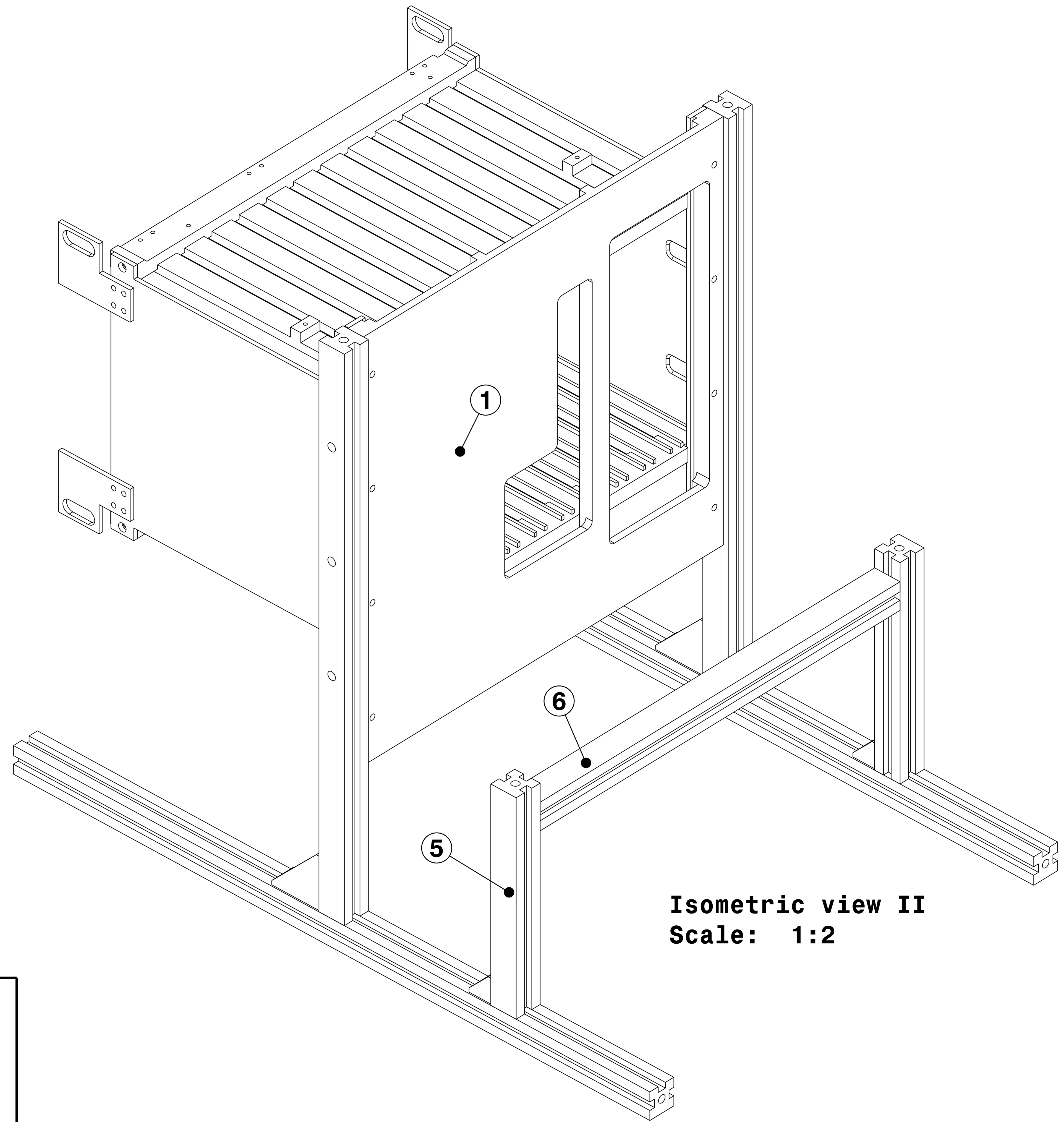

Isometric view II
Scale: 1:2

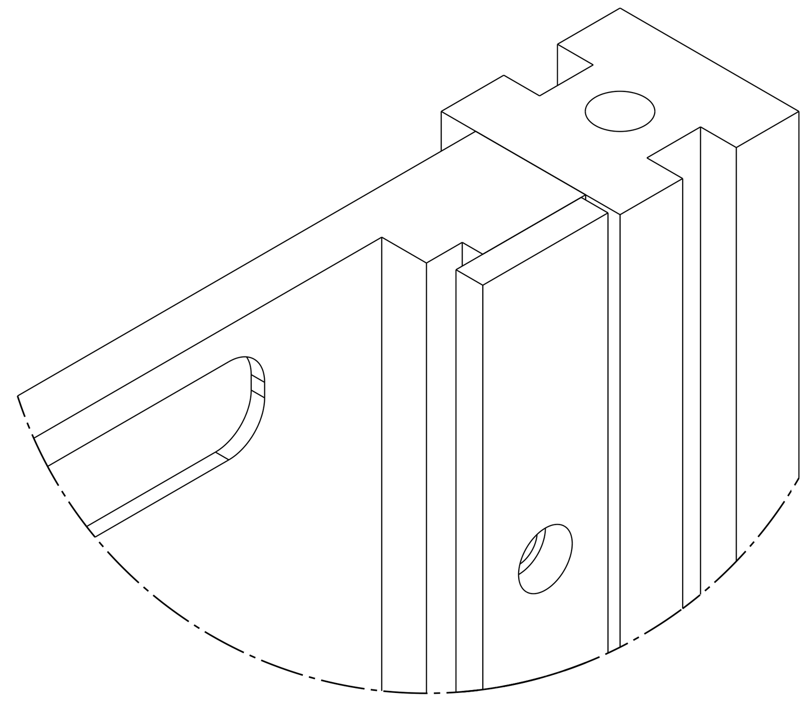

Detail A
Scale: 2:1

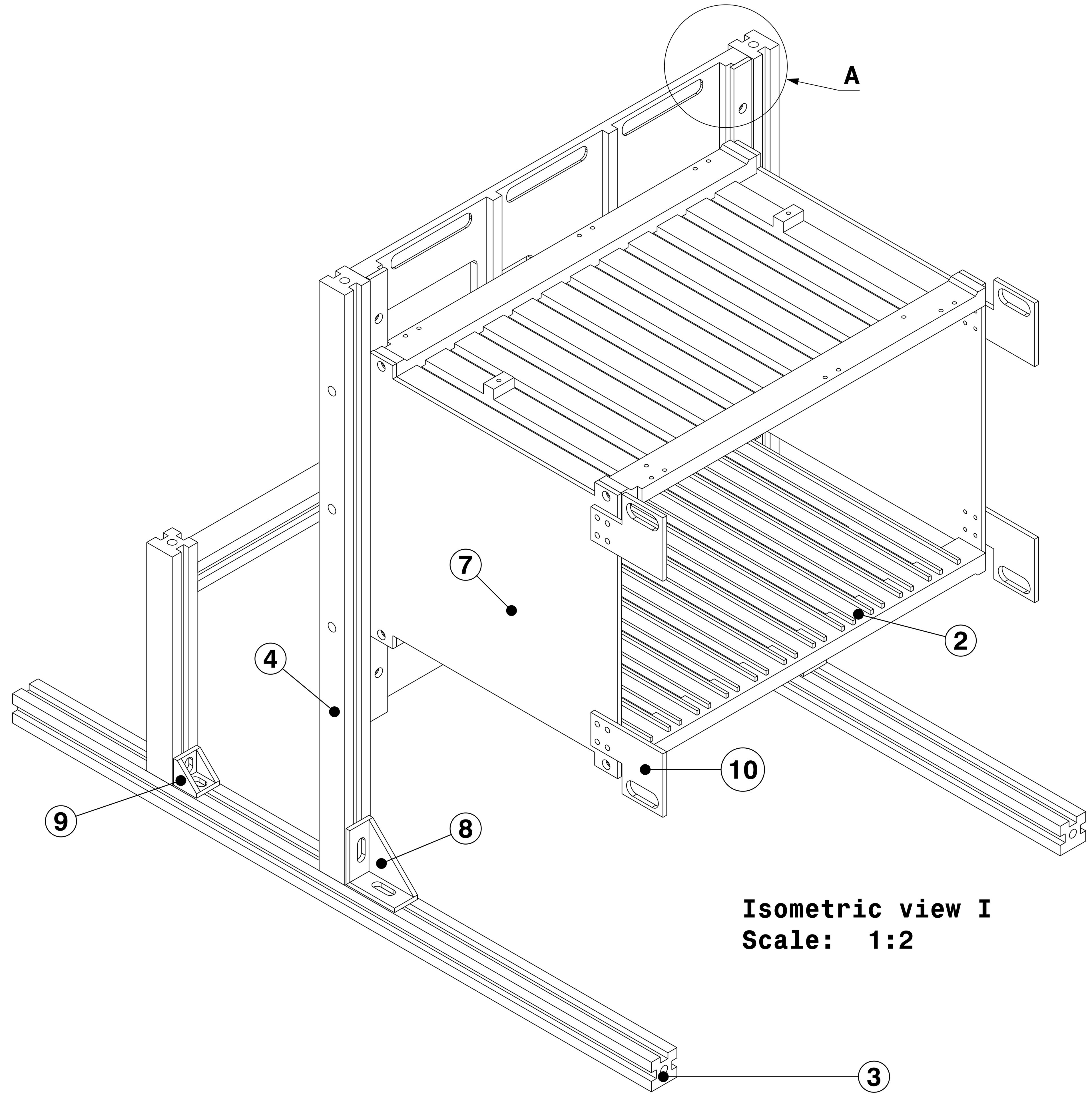

Isometric view I
Scale: 1:2

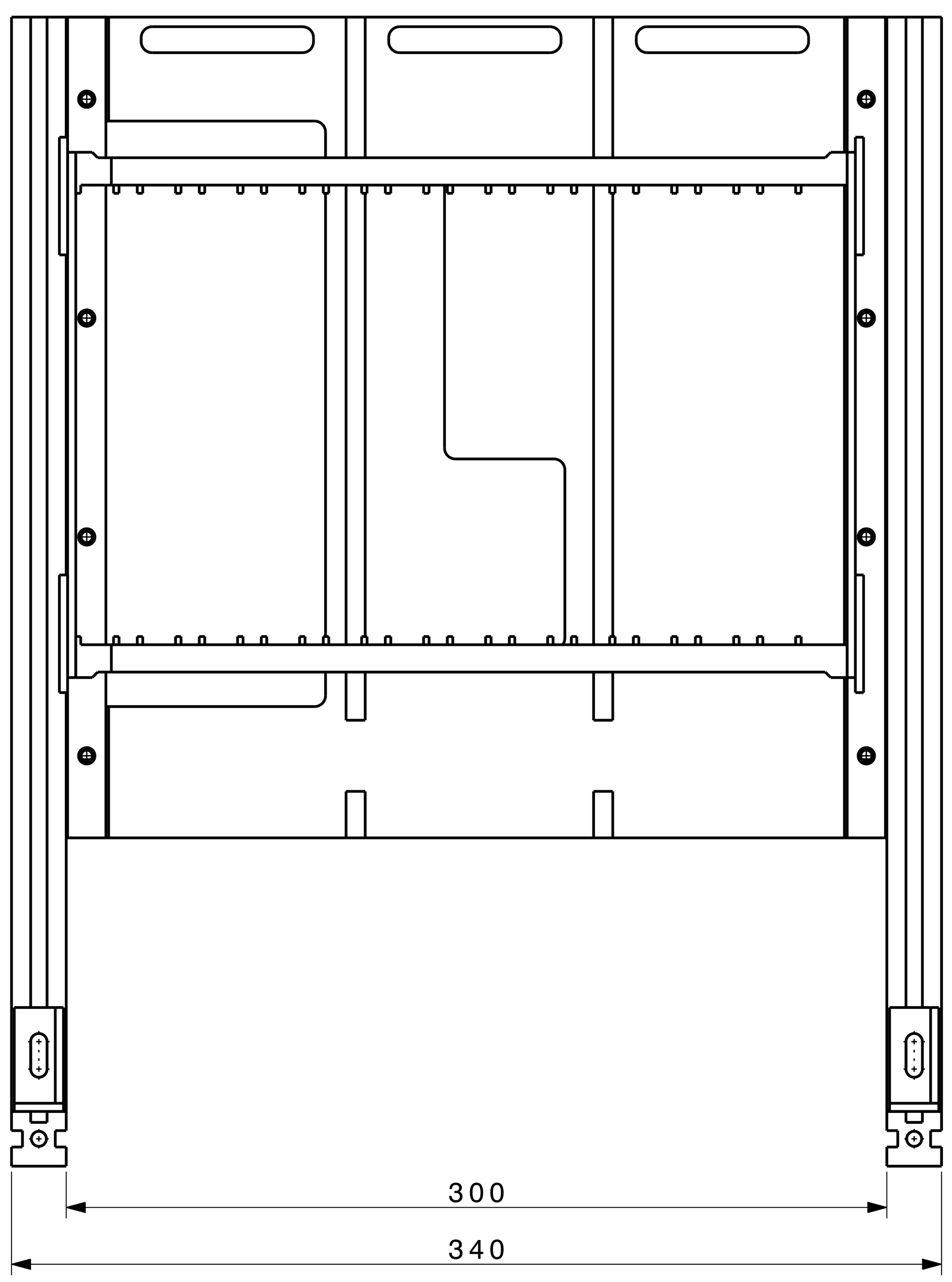

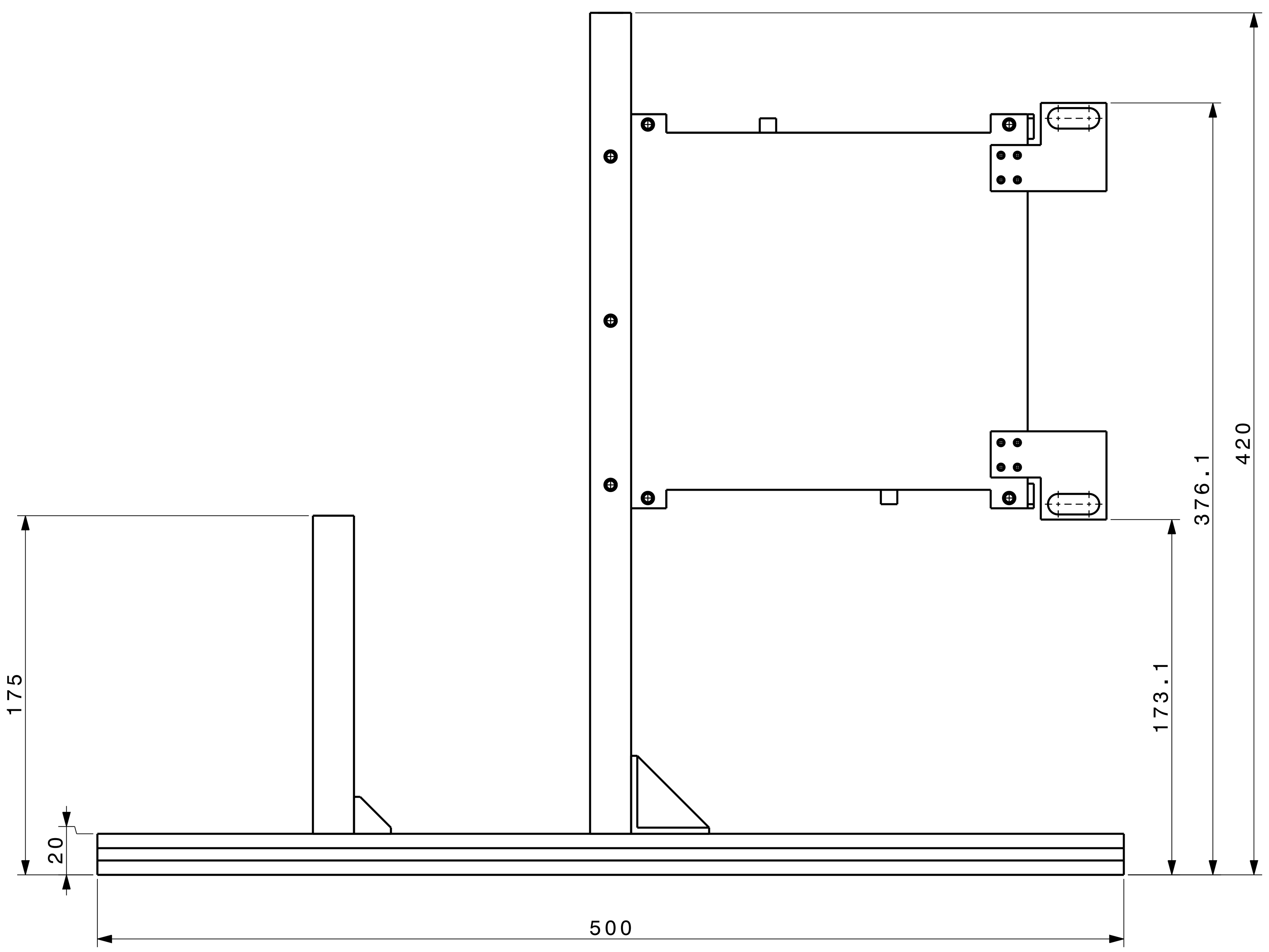

BILL OF MATERIALS					
POS	QUANT	DESIGNATION	REFERENCE	MATERIAL	EDH SCEM
01	1	Base Plate - Pathfinder	LHBTUEL_0013 ST1061437	Aluminum	
02	2	DCB Card Guide - Pathfinder	LHBTUEL_0014 ST1061442	Aluminum	
03	2	Bottom Stand Profile	LHBTUEL_0016 ST1062258	Aluminum	
04	2	Vertical Baseplate Profile	LHBTUEL_0017 ST1062259	Aluminum	
05	2	Vertical COMET Profile	LHBTUEL_0018 ST1062260	Aluminum	
06	1	Horizontal COMET Profile	LHBTUEL_0019 ST1062261	Aluminum	
07	2	Wall - Pathfinder	LHBTUEL_0012 ST1063144		
08	2	Gusset 20x40	ST1063146		
09	2	Gusset 20x20	ST1063147		
10	4	Water Pipe Support Wall	LHBTUEL_0015 ST1073444	Stainless Steel	

DESIGNATION: Pathfinder Support	DESIGNED	M.GALKA	FORMAT A1
	CHECKED		
	RELEASED		SCALE 1:2
	APPROVED		
EQUIPMENT CODE LHBTUEL_ LHCb_TRACKING_SYSTEM_UT_Electronics	DESIGNED 2018-11-30		
CERN	REFERENCES Doc No: ST1062268_02 — LHBTUEL_0020	INDEX	LABEL: NOT VALID FOR EXECUTION	QAC: -	SHEET 1/1

ORGANISATION EUROPEENNE POUR
LA RECHERCHE NUCLEAIRE
EUROPEAN ORGANIZATION FOR NUCLEAR RESEARCH
GENEVE

TB v2.0 A1:Landscape

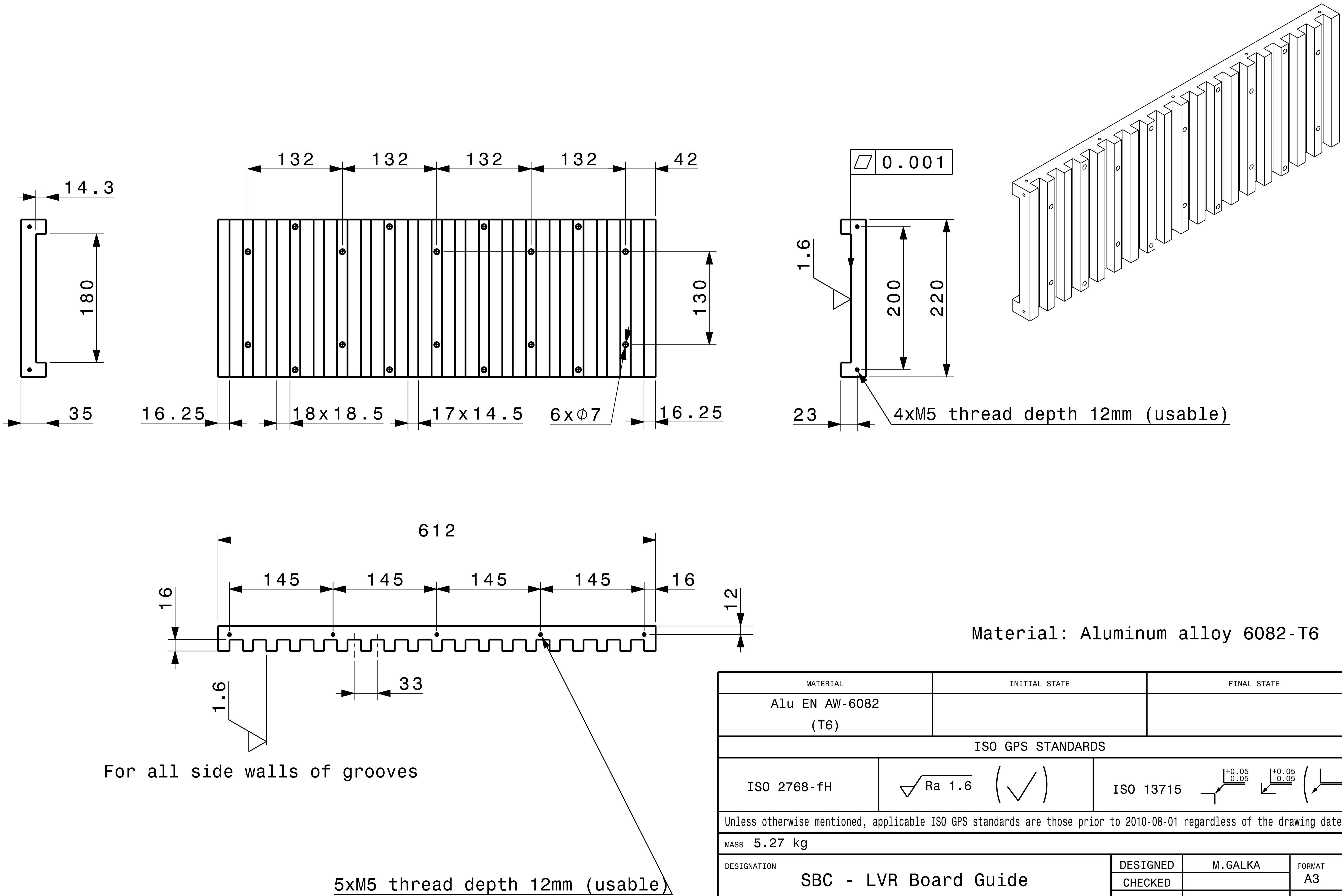

MATERIAL	INITIAL STATE	FINAL STATE
Alu EN AW-6082 (T6)		

ISO GPS STANDARDS

ISO 2768-fH | Ra 1.6 | ISO 13715 +0.05 -0.05 +0.05 -0.05

Unless otherwise mentioned, applicable ISO GPS standards are those prior to 2010-08-01 regardless of the drawing date

MASS 5.27 kg

DESIGNATION
SBC - LVR Board Guide

EQUIPMENT CODE

DESIGNED	M.GALKA	FORMAT A3
CHECKED		
RELEASED		SCALE 1:1
APPROVED		

DESIGNED 2019-06-02

REFERENCES Doc No: ST0910865_02 | INDEX | LABEL NOT VALID FOR EXECUTION | QAC | SHEET 1/1

ORGANISATION EUROPEENNE POUR LA RECHERCHE NUCLEAIRE
EUROPEAN ORGANIZATION FOR NUCLEAR RESEARCH
GENEVE

TB v2.0 A3:Landscape

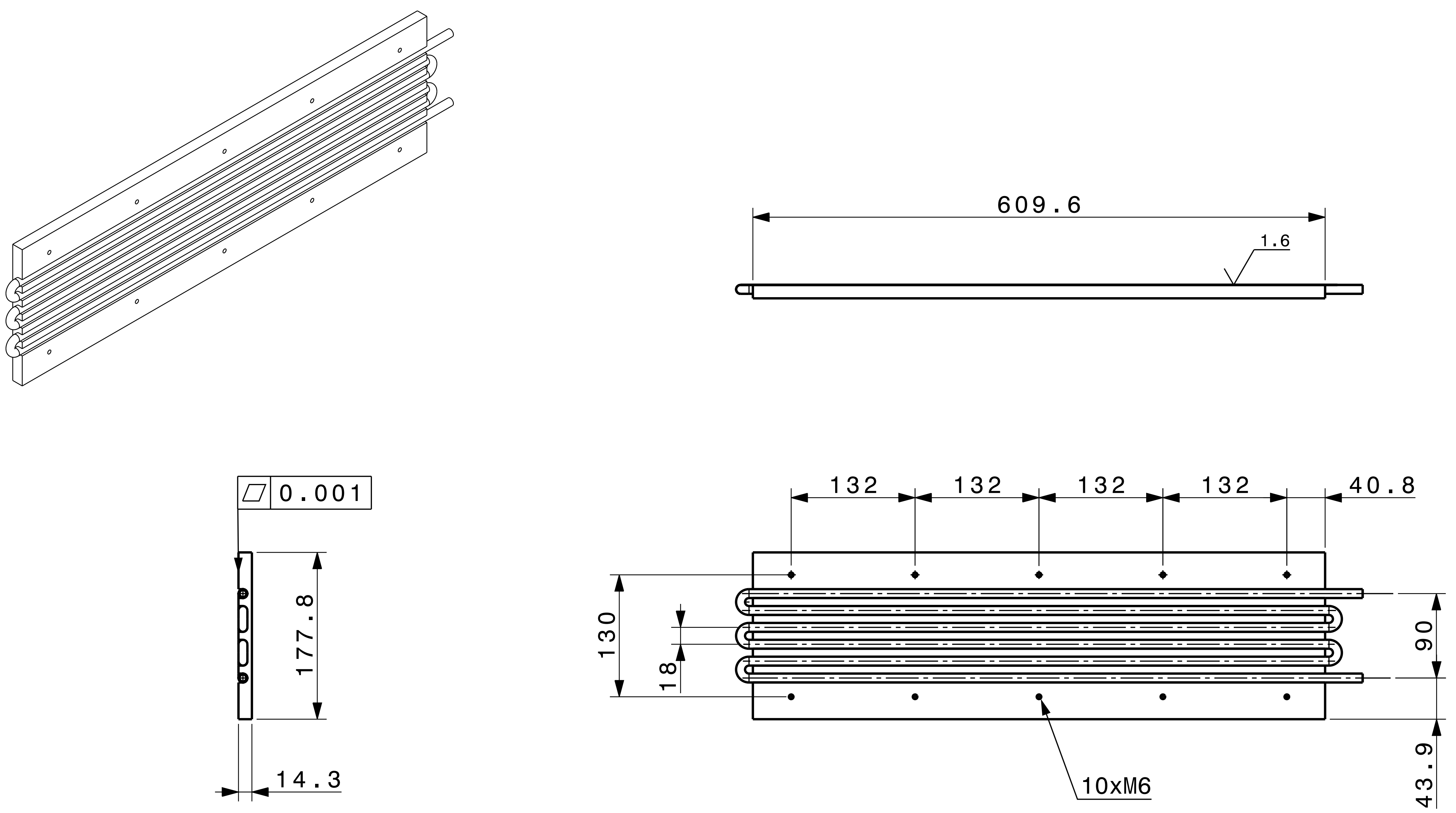

We buy this cold plate from a supplier.
We need to make ten M6 threaded holes in it
as shown on drawing.

BILL OF MATERIALS

POS	QUANT	DESIGNATION	REFERENCE	MATERIAL	EDH SCEM
01	1	SBC - Cold Plate - Al_Slab	ST0912582		
02	1	SBC - Cold Plate - Copper Pipe 3/8 inch	ST0912584		

DESIGNATION: SBC - Cold Plate	DESIGNED	M.GALKA	FORMAT A3
	CHECKED		
	RELEASED		SCALE 1:5
	APPROVED		
EQUIPMENT CODE	DESIGNED 2019-06-02		
REFERENCES Doc No: ST0912817_02	INDEX	LABEL NOT VALID FOR EXECUTION	QAC / SHEET 1/1

ORGANISATION EUROPEENNE POUR LA RECHERCHE NUCLEAIRE
EUROPEAN ORGANIZATION FOR NUCLEAR RESEARCH
GENEVE

TB v2.0 A3:Landscape

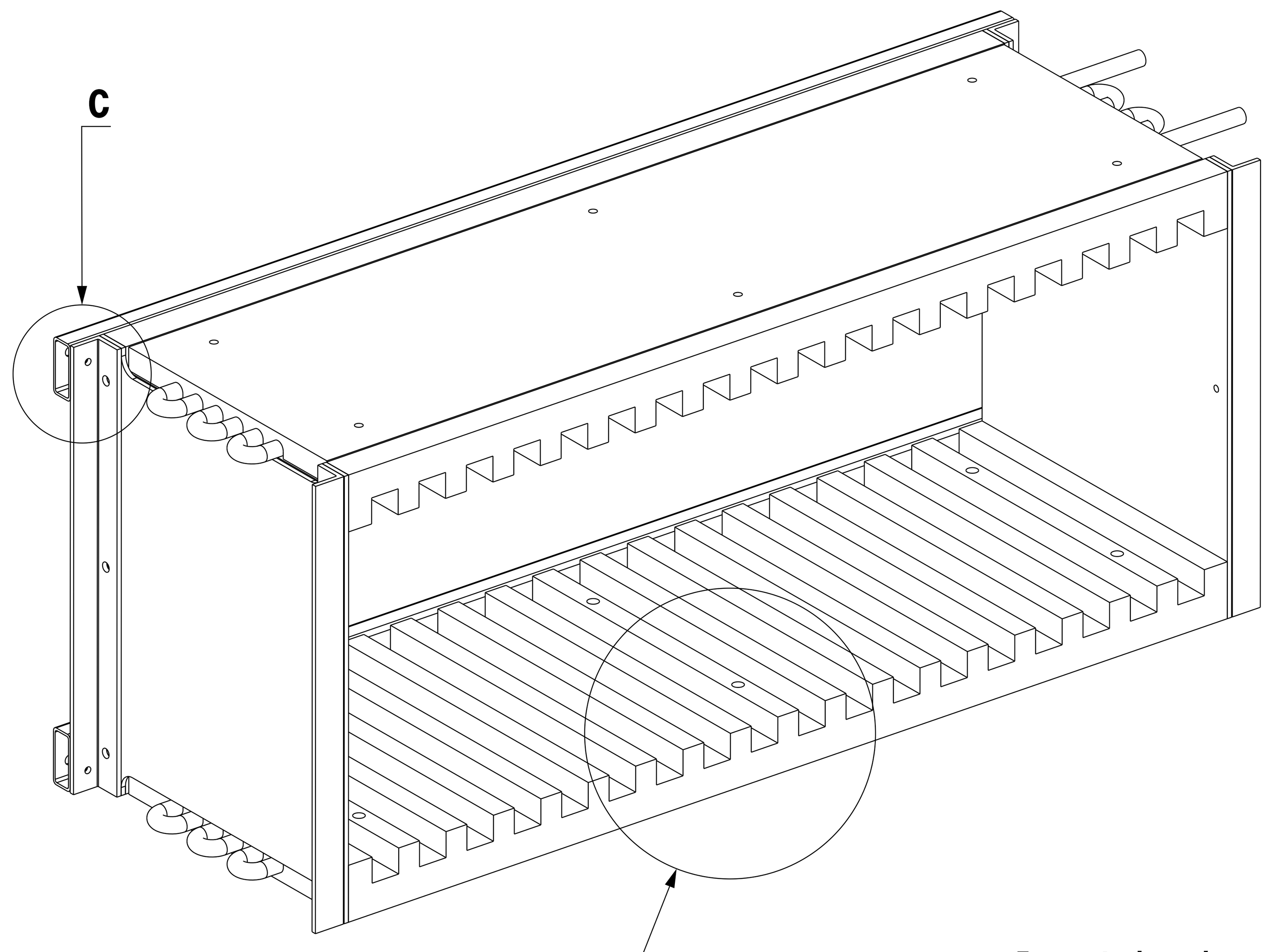

Isometric view
Scale: 1:3

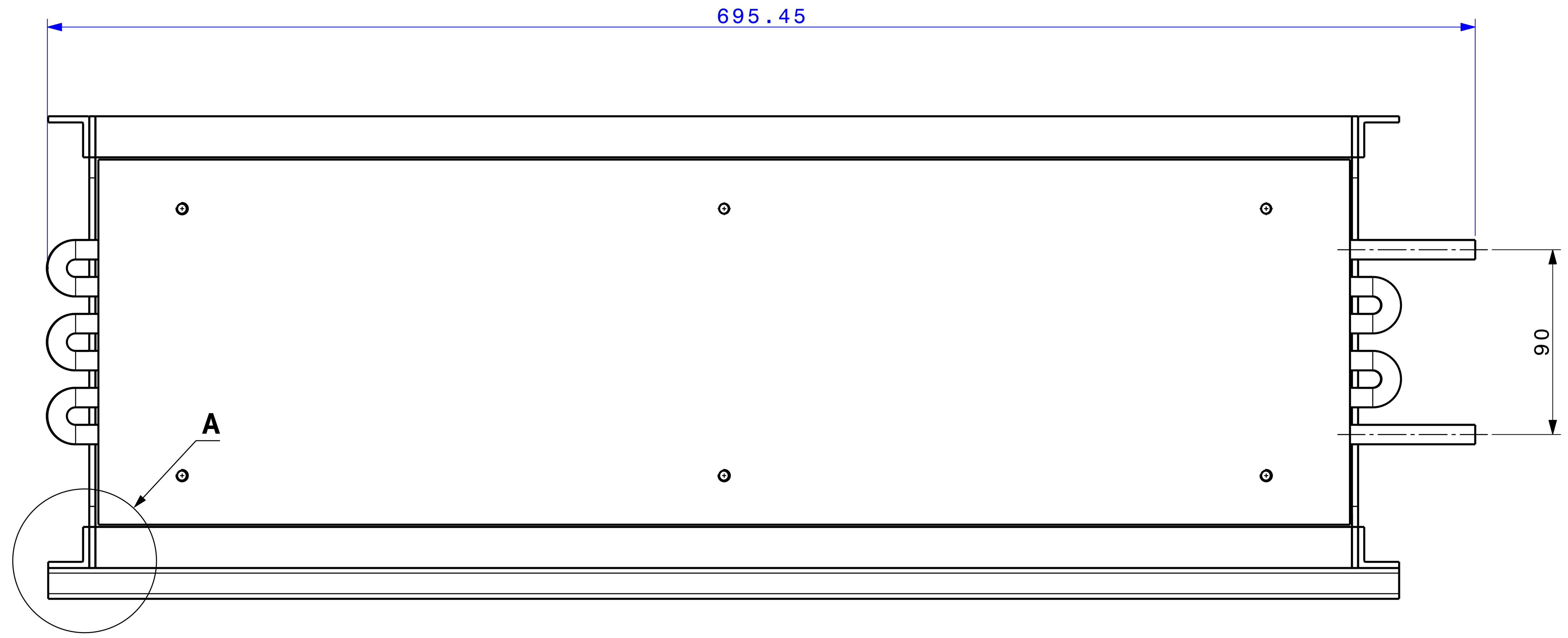

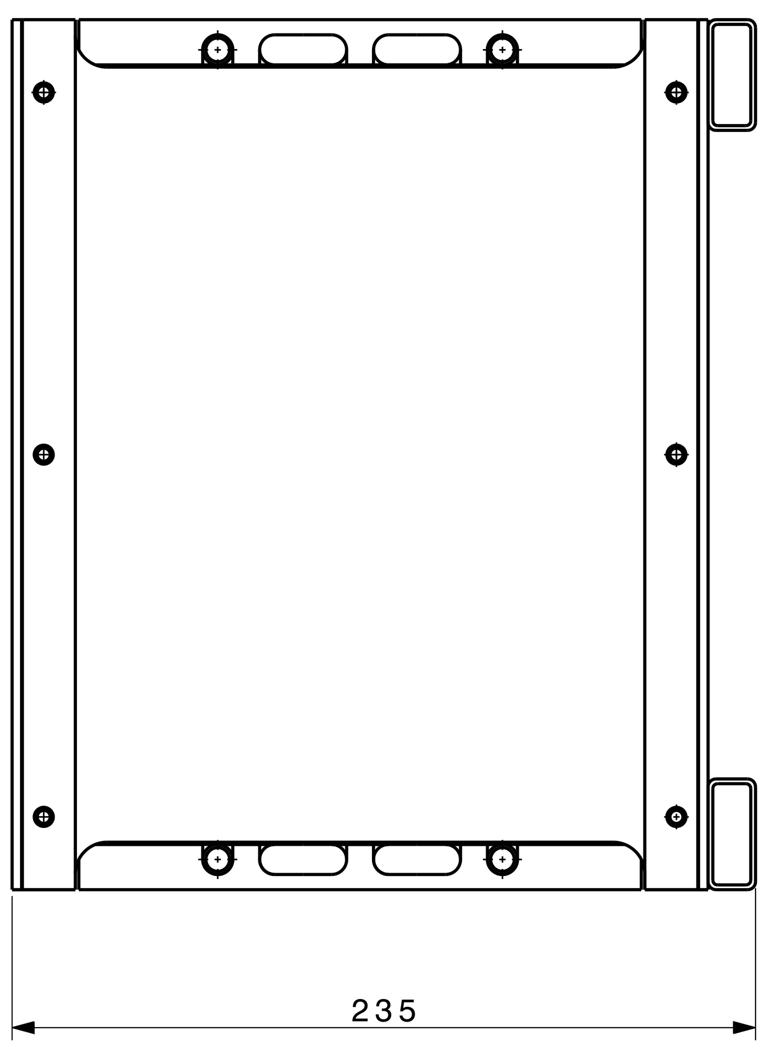

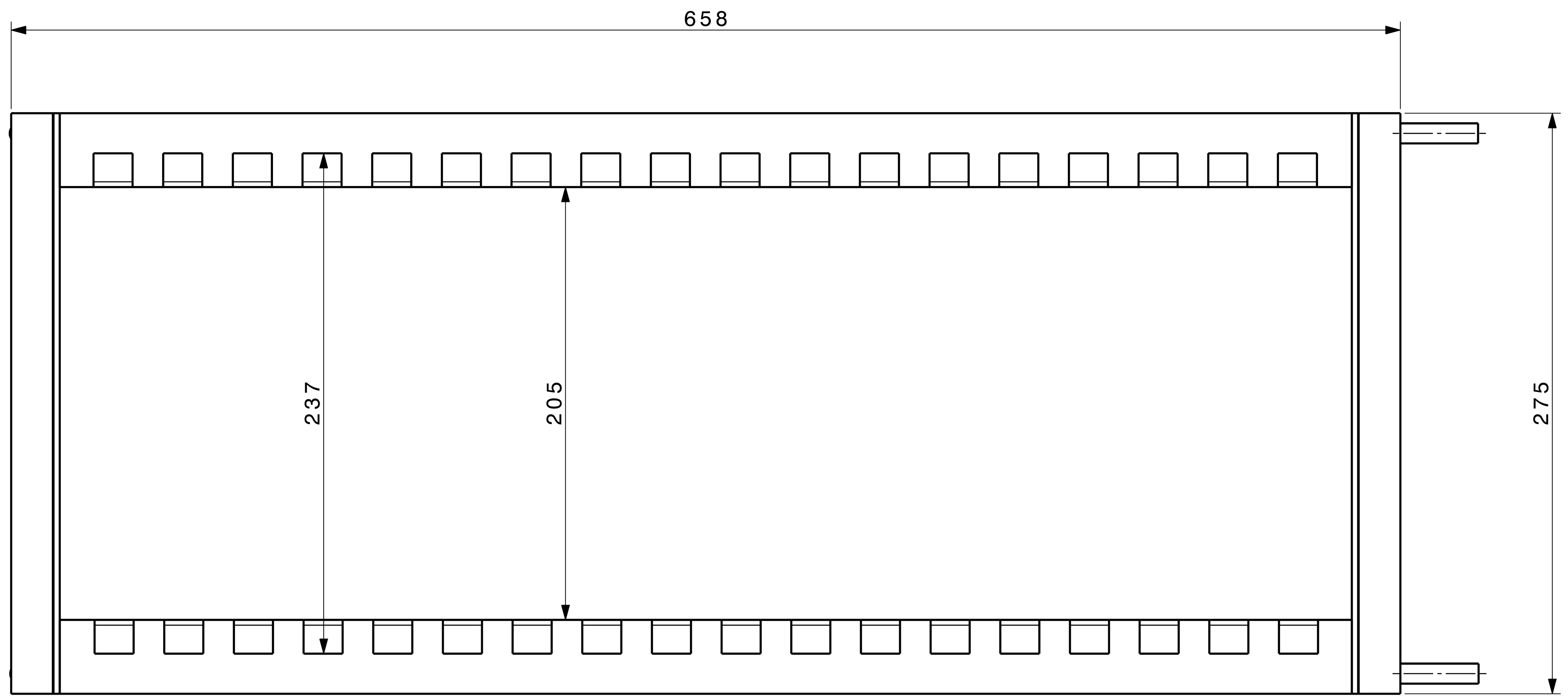

Hexagon socket
head cap screws:
1. M6x30mm – 12pcs.
2. M5x25mm – 10pcs.
3. M5x20mm – 4pcs.
4. M5x12mm – 8pcs.
5. M5x6mm – 4pcs.

Weight: 20.974kg
Quantity: 20

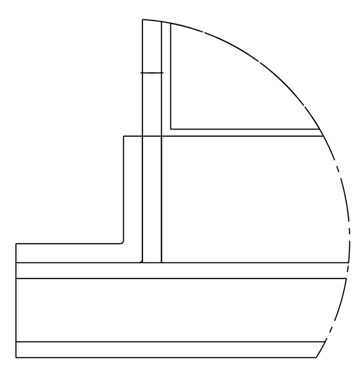

A
1:1

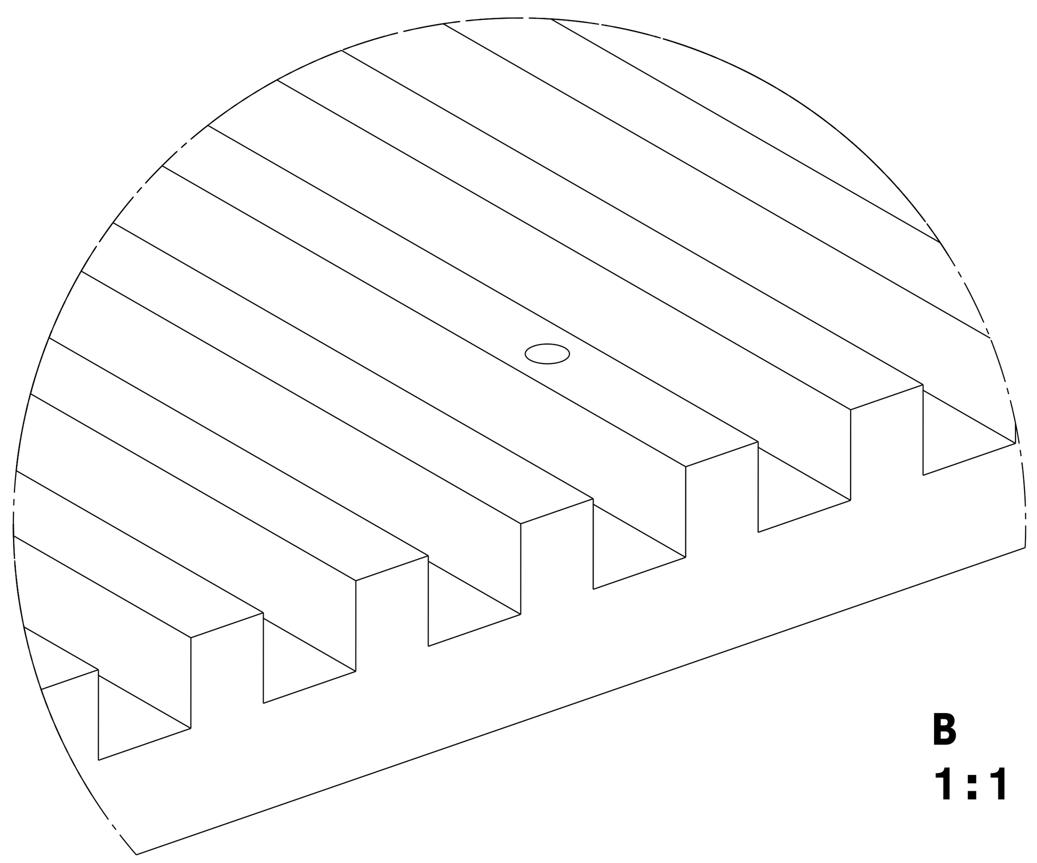

B
1:1

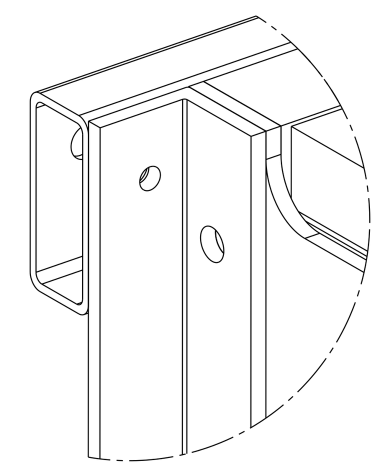

C
1:1

QUA	DESCRIPTION	POS	MAT.	OBSERVATIONS	REF.CERN
2	O-Profile	6		ST0913365	
2	L-Profile Back	5		ST0913193	
2	L-Profile Front	4		ST0913165	
2	Side Wall	3		ST0912983	
2	Cold Plate	2		ST0912817	
2	Board Guide Plate	1		ST0910865	

ENS/ASS — S.ENS/S.ASS

SBC Crate	SCALE 1:2	DRAWN: M. Galka 2017-11-22
		CONTROLLED
		RELEASED
		APPROVED
		CAD Document Number: ST0913387_02
		REPLACES

NON VALABLE POUR EXECUTION
NOT VALID FOR EXECUTION

QAC: -

SIZE: 1 IND.

DESSIN, RUGOSITE, TOLERANCES SELON NORMES ISO
DRAWING, RUGOSITY, TOLERANCES ACCORDING TO ISO STANDARDS

PROJECTION

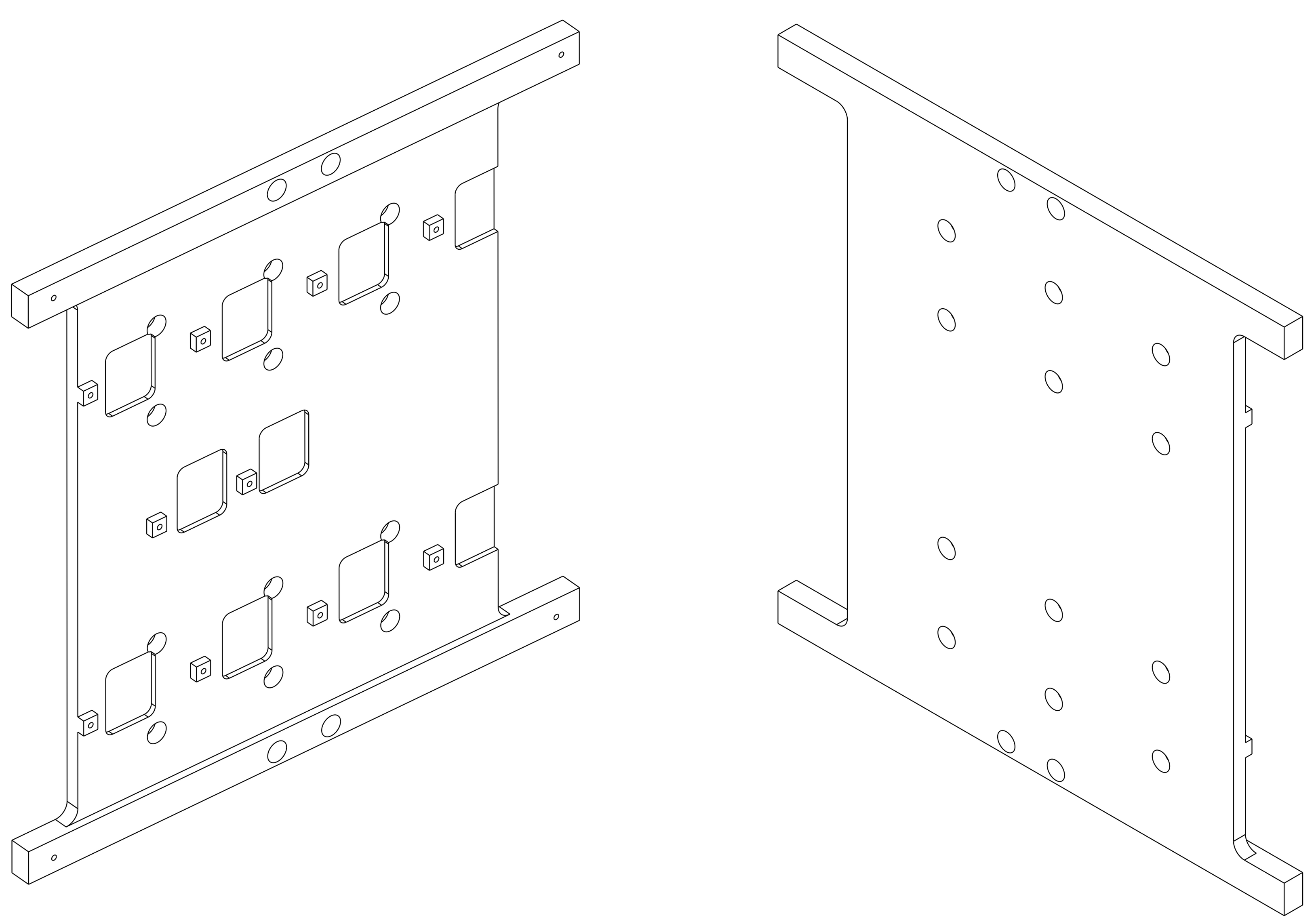

Detail A
Scale: 4:1

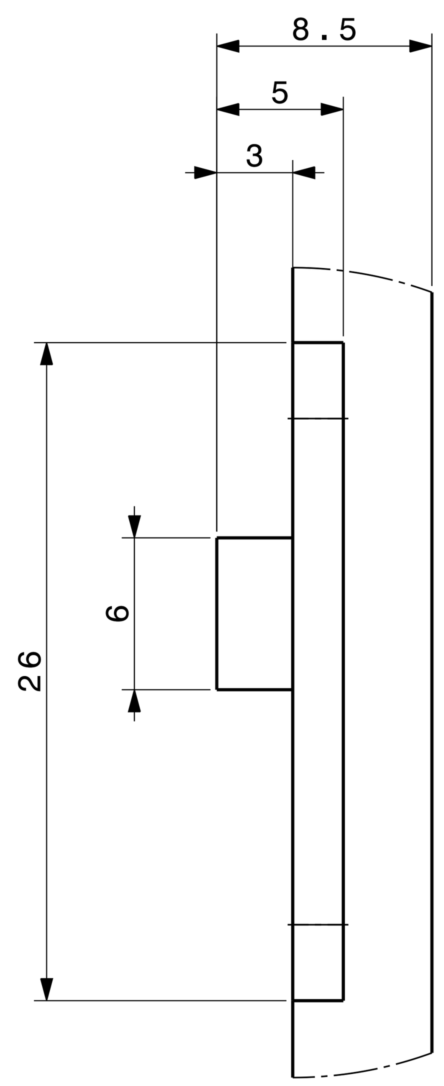

Hole Dimension Table			
REF.	X	Y	Diameter
1	10.78	5.78	M2.5
2	10.78	229.22	M2.5
3	26.37	183.32	M2.5
4	26.37	51.63	M2.5
5	55.57	117.54	M2.5
6	74.12	51.63	M2.5
7	74.12	183.32	M2.5
8	93.67	117.54	M2.5
9	123.52	51.63	M2.5
10	123.52	183.32	M2.5

Hole Dimension Table			
REF.	X	Y	Diameter
11	172.8	51.62	M2.5
12	172.8	183.32	M2.5
13	223.49	5.78	M2.5
14	225.78	229.22	M2.5
15	56.8	33.23	8
16	56.8	68.8	8
17	56.8	160.05	8
18	56.8	195.61	8
19	105.26	5.4	8
20	105.26	229.6	8

Hole Dimension Table			
REF.	X	Y	Diameter
21	106.23	33.23	8
22	106.23	68.8	8
23	106.23	160.05	8
24	106.23	195.61	8
25	128.12	5.4	8
26	128.12	229.6	8
27	155.65	33.23	8
28	155.65	68.8	8
29	155.65	160.05	8
30	155.65	195.61	8

All pockets (8x) are the same 21mm (x) by 26mm (y), with 3mm radius in corners and they are 2mm deep. See detail A.

All square stand-offs ("islands") (10x) are the same 6mm(x)by 6mm (y).
Center of the square coincides with center of the respective threaded hole.
Applies to holes 3 to 12 form hole dimension table.
See detail A.

Thread depth for all threaded holes is 6mm.

Material: Aluminium alloy 6082 - T6

MATERIAL	INITIAL STATE	FINAL STATE
Aluminum		

ISO GPS STANDARDS

ISO 2768-mK | Ra 3.2 | ISO 13715

NOTE: UNLESS OTHERWISE MENTIONED, APPLICABLE ISO GPS STANDARDS ARE THOSE PRIOR TO 2010-08-01 REGARDLESS OF THE DRAWING DATE

MASS 652 g

DESIGNATION: LVR Heat Sink

DESIGNED	M.GALKA	FORMAT	A1
CHECKED		SCALE	1:1
RELEASED			
APPROVED			

DESIGNED 2019-02-13

EQUIPMENT CODE

REFERENCES — Doc No: ST1091384_02 — INDEX — LABEL: NOT VALID FOR EXECUTION — QAC — SHEET 1/1